UNIVERSIDADE ESTADUAL DE MARINGÁ
CENTRO DE CIÊNCIAS BIOLÓGICAS
DEPARTAMENTO DE BIOLOGIA
PROGRAMA DE PÓS-GRADUAÇÃO EM ECOLOGIA DE
AMBIENTES AQUÁTICOS CONTINENTAIS

GABRIEL DE CARVALHO DEPRÁ

Relações filogenéticas em Geophagini (Acanthopterygii, Cichlidae), utilizando caracteres miológicos

Maringá
2019

GABRIEL DE CARVALHO DEPRÁ

Relações filogenéticas em Geophagini (Acanthopterygii, Cichlidae), utilizando caracteres miológicos

Tese apresentada ao Programa de Pós-Graduação em Ecologia de Ambientes Aquáticos Continentais do Departamento de Biologia, Centro de Ciências Biológicas da Universidade Estadual de Maringá, como requisito parcial para a obtenção do título de Doutor em Ciências.
Área de concentração: Ciências Ambientais

Orientador: Prof. Dr. Weferson Júnio da Graça
Coorientadora: Dr.ª Carla Pavanelli

Maringá
2019

"Dados Internacionais de Catalogação-na-Publicação (CIP)"
(Biblioteca Setorial - UEM. Nupélia, Maringá, PR, Brasil)

D424r

Deprá, Gabriel de Carvalho, 1988-
Relações filogenéticas em Geophagini (Acanthopterygii, Cichlidae), utilizando caracteres miológicos / Gabriel de Carvalho Deprá. -- Maringá, 2019.
234 f. : il. color.

Tese (doutorado em Ecologia de Ambientes Aquáticos Continentais)--Universidade Estadual de Maringá, Dep. de Biologia, 2019.
Orientador: Prof. Dr. Weferson Júnio da Graça.
Coorientadora: Dr.ª Carla Simone Pavanelli.

1. Geophagini (Acanthopterygii, Cichlidae) "cará" - Filogenia - América do Sul. 2. Geophagini (Acanthopterygii, Cichlidae) "cará" - Morfologia - Musculatura esquelética - América do Sul. 3. Peixes de água doce - Filogenia - América do Sul. I. Universidade Estadual de Maringá. Departamento de Biologia. Programa de Pós-Graduação em Ecologia de Ambientes Aquáticos Continentais.

CDD 23. ed. -597.74138098

Maria Salete Ribelatto Arita CRB 9/858
João Fábio Hildebrandt CRB 9/1140

GABRIEL DE CARVALHO DEPRÁ

Relações filogenéticas em Geophagini (Acanthopterygii, Cichlidae), utilizando caracteres miológicos

Tese apresentada ao Programa de Pós-Graduação em Ecologia de Ambientes Aquáticos Continentais do Departamento de Biologia, Centro de Ciências Biológicas da Universidade Estadual de Maringá, como requisito parcial para a obtenção do título de Doutor em Ciências e aprovada pela Comissão Julgadora composta pelos membros:

COMISSÃO JULGADORA

Prof. Dr. Weferson Júnio da Graça
Nupélia/Universidade Estadual de Maringá (Presidente)

Dr. Luiz Antonio Wanderley Peixoto
Universidade de São Paulo (Pós-Doutorando, USP)

Prof. Dr. Fernando Camargo Jerep
Universidade Estadual de Londrina (UEL)

Dr.ª Renata Rúbia Ota
Universidade Estadual de Maringá (Pós-Doutoranda, PEA/UEM)

Dr.ª Anielly Galego de Oliveira
Universidade Estadual de Maringá (Pós-Doutoranda, PEA/UEM)

Aprovada em: 20 de março de 2019.
Local de defesa: Anfiteatro Prof. "Keshiyu Nakatani", Nupélia, Bloco G-90, *campus* da Universidade Estadual de Maringá.

AGRADECIMENTOS

Tornar-me um candidato ao título de doutor foi um processo árduo e, em grande parte, solitário. Contudo, eu não teria chegado sequer à metade do caminho se não estivesse bem acompanhado. Para mim, não se tratou apenas de ter com quem dividir minhas angústias, alguém para aplacar minha ansiedade. Também não me bastaria ter um objetivo, sonhar com as possibilidades que podem surgir depois da conquista do diploma. Precisei ser feliz o tempo todo para enfrentar o desafio da pós-graduação, e isso só me foi possível porque conheço a amizade e o amor, principalmente da família. Isso me restaurou a força quando senti que ela estava me faltando, e daí nasceu a alegria necessária para pensar, ter ideias e colocá-las em prática. Portanto, os merecedores dos meus agradecimentos mais especiais são todos aqueles com quem vivi momentos calorosos de riso, carinho, euforia e todo tipo de sentimento bom que alimenta o espírito. Não por acaso, são justamente essas as pessoas que mais me ajudaram com os probleminhas do dia-a-dia. Listar nomes é até desnecessário, quando todos sabem quem são e quão importantes eu os considero. Mesmo assim, a homenagem é justa.

Agradeço aos meus pais, Tomires e Marco. Aos meus irmãos, Igor e Lucas. E a todo o restante da família, que é sempre um porto seguro quando o cansaço ameaça me derrubar.

Aos amigos do Museu, Renata “Rubs” Ota (já vale para o Hugo Message também!), Carlos “Charlinho” Oliveira, Fagner de Souza e Hugmar Pains Silva, que já estavam ali desde o começo e são grandes amigos até hoje. Gabriela “Bilinha” Nardi e Iago Penido, que chegaram depois, mas sempre são parceiros para tudo. Augusto “Bigode” Frota, Helen “Gremlen” Proença, Filipe “Nego” Azevedo, Rianne “Carol” de Oliveira, Renan “Chups” dos Reis e Renzy. Também os agregados frequentes, Toé, Gabi Navarro e Gisele Arruda. Agradeço também a vários outros amigos, de quem gosto muito, que conheci no Nupélia ou mesmo durante a graduação, especialmente à Anielly e ao Daniel (“Zidane”) e à Fani.

Também aos professores, principalmente ao Weferson e à Carla, responsáveis pela minha orientação há muito tempo, e ao Claudio Zawadzki. Considero todos pela amizade, acima da hierarquia. Não posso deixar de lembrar, ainda, o Zé Birindelli e o Aléssio Datovo, que me ensinaram muito sobre anatomia de peixes.

Ainda, aos pesquisadores que se propuseram à importante tarefa de participar da banca.

À Salete, bibliotecária do Nupélia, pelo carinho e disposição para me fornecer sempre cópias das mais raras referências que se possa imaginar. Ao Celso Ikedo por me ajudar a aprender um pouco de fotografia.

Ao Conselho Nacional de Desenvolvimento Científico e Tecnológico (CNPq), pela concessão da bolsa e taxa de bancada.

As demais pessoas que merecem agradecimentos são especificamente reconhecidas nos "Acknowledgements" dos artigos apresentados aqui.

Há vários outros nomes que poderiam ser mencionados aqui. No entanto, mesmo que eles não apareçam, tenho certeza de que serei perdoado, pois aqueles que sabem da importância que têm em minha vida não ficarão ofendidos por não constarem desta lista.

Muito obrigado!

When taxonomists study current living species, they examine an evolutionary cross section of time in that they view only the most recent but continuing species with a long diverging history behind them. The apparent discreteness of species or groups at the current moment is partly due to their previous divergence.

Kardong

All ~~animals~~ "*cichlids"* are equal, but some ~~animals~~ "*cichlids"* are more equal than others.

George Orwell

Relações filogenéticas em Geophagini (Acanthopterygii, Cichlidae), utilizando caracteres miológicos

RESUMO

Apesar de diversos estudos terem tratado da descrição de caracteres morfológicos em Cichlidae, geralmente para fins de inferência filogenética, muito pouco se estudou sobre sua musculatura. Descreveu-se, pela primeira vez, a musculatura estriada completa de uma espécie de ciclídeo, *Geophagus sveni* Lucinda, Lucena & Assis, com ilustrações de todos os músculos e um protocolo para a dissecção de exemplares. Comparou-se a musculatura esquelética de pelo menos uma espécie de cada gênero da tribo Geophagini, dentre outros ciclídeos, e descreveram-se 98 caracteres com o propósito de analisar sua relação com a filogenia do grupo. Essa matriz de caracteres foi empregada para produzir duas análises filogenéticas sem restrição, uma com pesagem e outra sem pesagem. Mapearam-se os caracteres miológicos sobre uma hipótese filogenética pré-existente, para a compreensão da correlação entre os caracteres e as especializações tróficas de cada táxon. Conclui-se que os Geophagini especializados em peneirar o substrato (*winnowers*) tendem a apresentar algumas adaptações convergentes, manifestadas na forma e no grau de desenvolvimento de músculos como *adductor mandibulae*, *levator arcus palatini*, *dilatator operculi*, *adductor branchialis 1* e *obliqui ventrales 1–2*. Este estudo possibilita futuras investigações acerca das funções dos músculos estriados em peixes e seu papel nos processos de irradiação adaptativa, *i.e.*, diversificação funcional.

Palavras-chave: Cichlinae. Convergência adaptativa. Evolução de caracteres. Mapeamento de caracteres. Morfologia. Musculatura esquelética. Músculo estriado.

Phylogenetic relationships in Geophagini (Acanthopterygii, Cichlidae), using myological characters

ABSTRACT

Although several studies have dealt with the description of morphological characters in Cichlidae, usually aiming for phylogenetic inference, little attention has been given to their musculature. The complete striated musculature of a cichlid species, *Geophagus sveni* Lucinda, Lucena & Assis, was described for the first time, with illustrations of all muscles and a protocol for the dissection of specimens. The striated musculature of at least of species of each genus in tribe Geophagini, among other cichlids, was compared, and 98 characters were described with the purpose of analysing their relation with the group's phylogeny. This character matrix was employed to produce two unconstrained phylogenetic analyses, one weighted and the other unweighted. The myological characters were mapped upon a pre-existing phylogenetic hypothesis, for understanding the correlation among the characters and trophic specialisations of each taxon. The conclusion is that Geophagini specialised in sifting substrate (winnowers) tend to present a few convergent adaptations, manifested in the shape and degree of development of muscles such as *adductor mandibulae*, *levator arcus palatini*, *dilatator operculi*, *adductor branchialis 1* and *obliqui ventrales 1–2*. This study facilitates future investigations on the functions of the striated muscles in fishes and their role in the processes of adaptive radiation, *i.e.*, functional diversification.

***Keywords*:** Adaptive convergence. Character evolution. Character mapping. Cichlinae. Morphology. Skeletal musculature. Striated muscle.

Tese elaborada e formatada conforme as normas da publicação científica *Zoological Journal of the Linnean Society*. Disponível em: https://academic.oup.com/zoolinnean/pages/General_Instructions.

SUMMARY

1 INTRODUCTION

1.1 Theoretical foundation

In this conceptual framework, we aim to expose first our opinion on the importance of phylogeny, then the reasons why we are cautious about the phylogenetic signal of morphological characters, but advocate their analysis under the light of molecular phylogenies. Subsequently, we provide a brief summary of the developments in cichlid and geophagine systematics that occurred in the last decades. Finally, we discuss patterns of morphological character evolution under the light of molecular analyses in previous analyses.

1.1.1 Why is phylogenetics important and what should we expect from it?

While alpha taxonomy concerns diagnosing and naming species, beta taxonomy concerns the classification of species in higher taxonomic levels. Modern classification relies on phylogenetic hypotheses, because it understands that all taxa must be monophyletic. In other words, if taxon 1 includes species A and B, but not C, then A and B share an ancestor that is not shared with C, and both are equally distant from C in an evolutionary sense. Phylogenetics is not strictly necessary for alpha taxonomy (although species-delimitation tests based on molecular phylogenetic analyses are becoming increasingly important), because other methods of classification could work just as well or even better in the sense of facilitating the comparisons between species already described. In fact, phylogenetic hypotheses frequently delimit clades based on characters of difficult visualisation, confusing the identification of supraspecific taxa. One could reasonably argue that it makes more sense to recognise artificial groups based on non-synapomorphic, but easily observable characters. For instance, one can compare the straightforward classification system proposed by Eigenmann (1917) for the Characidae with the hypothesis of, *e.g.*, Betancur-R. *et al*. (2018). Additionally, phylogenetic classifications are in constant change. If phylogeny can make classification more difficult and less stable, then why should we use it?

Species descriptions and taxonomic revisions are readily understood as vital for almost any biological study focused on the species, population, community or ecosystem level. For instance, if one aims to determine the behaviour of a species, they have to be

sure of analysing only individuals that in fact belong to that species. If one seeks to determine the species turnover across a landscape, too, it is necessary to know the differences between species. Alpha taxonomy is also crucial to conservation efforts. On the other hand, most biological studies can do without beta taxonomy. In particular, the classification based on shared ancestry is of little importance to most studies. However, the same is not true for studies that concern, *e.g.*, the evolution and historical biogeography of organisms and the phylogenetic diversity of a community. To understand, *e.g.*, the evolution of the avian wing, we must understand the relationships between birds and non-avian dinosaurs.

However, the applicability of phylogenetics to other kinds of studies depends on the accuracy of phylogenetic hypotheses. If the different clades of mammalians bearing a patagium were recovered as monophyletic in a phylogenetic analysis, we would be forced to conclude that gliding represents a unique innovation within Mammalia. However, we know that the patagium appeared several times in mammalian evolution, making it a frequently repeated case of convergent evolution (in Diapsida as well). When dealing with similar character states occurring within clades of a more recent origin, it is much more difficult to determine if they are convergences or synapomorphies. That means, if close-related taxa show a similar character state, it is hard to know if this state was developed independently or inherited from the common ancestor, with subsequent reversion in other close-related taxa.

The stevardiines illustrate well this problem, as several of them bear some kind of modified caudal-fin scales. Weitzman & Menezes (1998) considered those species to form a monophyletic unit, to which the presence of any kind of modified caudal-fin scale would be an unreversed synapomorphy. According to this hypothesis, all of the very divergent shapes exhibited by the modified scales in the different genera would have had evolved by modification of the same ancestral specialised scale. Several molecular phylogenies showed that not to be the case (Oliveira *et al*., 2011; Thomaz *et al*., 2015; Betancur-R. *et al*., 2018). Instead, those hypotheses suggest that modified scales have appeared several times in stevardiine evolution – or, at least, have been lost a few times, which is unlikely because the scales assume very different shapes in each tribe. Those modified scales, however rare in Characiformes, are also present in the cheirodontines *Compsura* and *Saccoderma*.

At times, correct conclusions emerge from false premises. Darwin recognised the power of natural selection to guide evolutionary changes, even though he thought that all

inherited characters represented a mixture between the conditions provided by the parental organisms, which would eventually lead to the disappearance of the advantageous trait, unless it emerged repeated times in the same population as a consequence of some obscure influence of the environment. More frequently, however, wrong premises lead to wrong conclusions. Thus, if we start with a completely wrong topology, how can we derive correct character reconstructions from it and understand how the phenotypic characters managed to guarantee the evolutionary success of the studied group? How can we begin to understand how the current distribution of the species reflects past geological changes and vicariant events?

Deciding, however, which of the available phylogenetic hypotheses is a closer representation of the real tree of life may be a very difficult task. Many papers deal with how to interpret and select characters for phylogenetic analyses and how to perform the computational analyses (syntheses are found in, *e.g.*, Amorim, 2002; San Mauro & Agorreta, 2010). Still, for some groups of organisms there are several published phylogenetic hypotheses, which are overwhelmingly incongruent. We will probably never be sure to have found the true phylogeny of a group, but perhaps we can reasonably reject some of the hypotheses. The following sections will deal with that problem. For now, let us look into the possibilities that may emerge from character mapping and reconstruction, one of the possible applications of phylogenetics, once we have a satisfactory topology to start with.

Consider the following questions: Was the body plan of the ancestral animals symmetric? How many times did ratites lose flight? How many times did *Agama* lizards develop sexual dimorphism and polygyny, and how do those characters correlate? We can answer them by mapping the evolution of morphological characters onto phylogenetic trees, at least in cases in which unambiguous optimisations are possible (Harshman *et al*., 2008; Philippe *et al.*, 2009; Leaché *et al*., 2014). By doing so, we can begin to ask deeper questions. For instance, given that body elongation followed by limb loss is common in Squamata (Whiting *et al*., 2003), but not in, *e.g.*, Mammalia, are there more genetic mechanisms capable of producing this pattern in Squamata or is elongation much more likely to improve fitness in this group than in Mammalia? What about the same comparison between Trichomycteridae and Loricariidae? If it is true that in *Bachia* lizards the number of digits reversed from a smaller to a larger number (Kohlsdorf & Wagner, 2006), how does it translate into genetic mechanisms? Those kinds of questions cannot be answered without phylogenetic analyses, and particularly not without

phenotypic studies. However, molecular data are becoming increasingly more important for stablishing robust hypotheses of relationships, as I will stress in the next sections.

1.1.2 The relevance of molecular and morphological analyses

To Hillis (1987), the advantages of molecular methods are the size of the data set (which has increased exponentially in the last decades), its applicability to analyses at any depth (*i.e.*, to resolve ancient, intermediate or recent cladogeneses), and the certainty that the characters observed are strictly inheritable. In comparison, the advantages of morphological methods would be the applicability to museum specimens (*e.g.*, formaldehyde-fixed) and fossils, the use of ontogenetic information and low costs. Recent molecular phylogenetic analyses have shown that the lack of tissue samples and the costs are no longer important issues. Ontogeny and any other kind of inheritable phenotypic information is a consequence of the genotype, and therefore it seems better to infer phylogenies from DNA, because it means to explore variation directly from its ultimate source. Alternatively, employing morphological characters means to propose primary homologies that can result from completely different genetic mechanisms.

As for fossils, it is evident that they are always a problem in phylogenetic analyses, since they fail to preserve many of the structures from which phylogeneticists interpret characters. That is unfortunate because, as pointed out by Wiens (2004), over 99% of the species that ever existed on Earth are now extinct, and fossils are necessary to calibrate molecular clock models. We explore other shortfalls of morphological datasets, not treated by Hillis (1987), in the next three sections.

1.1.2.1 Character interpretation

To illustrate how morphological characters can be misleading or interpretative when it comes to coding character states for phylogeny reconstruction, we can think about the presence or absence of a structure. For instance, this structure can be a paired fin. Although paired fins appear in the fossil record before the origin of the Gnathostomata (Zhu *et al.*, 2012), they are absent from many groups of more recent origin, which can be thought of as a reversal to the ancestral condition, when only morphological data is considered (binary character). However, there are many ways of losing a fin. Thus, to interpret the secondary absence of a fin as primarily homologous for two species may be

misleading when we have no genetic information to explain such loss. That is to say, morphological homoplasies are frequently difficult to detect *a priori* when no other type of data is available. Of course, parsimony analyses have the power to detect homoplasies, but only if the data set comprises a large number of informative characters.

Osteological studies of cichlids contribute a few more examples. Several authors (*e.g.*, Cichocki, 1976; Oliver, 1984; Stiassny, 1991; Casciotta & Arratia, 1993; Kullander, 1998; López-Fernández *et al*., 2005) have investigated the infraorbital bones of cichlids for possible characters. Because no cichlid has more than seven ossicles (including those called lachrymals and the dermosphenotic), there is a general agreement that this is the ancestral state, and different total numbers of ossicles represent fusions and losses. Only the first or both the first and the second infraorbital bones (*i.e.*, the lachrymals) are plate-like. Thus, when only one plate-like bone is present, authors usually agree that it represents a fusion of the two lachrymals. In some cases, authors are confident enough to identify all of the ossicles, advancing explicit hypotheses of loss or fusion. However, some taxa present difficulties. For instance, Stiassny (1991, Fig. 1.13c-d) depicted the infraorbital series of *Etroplus* as having a lachrymal identical to that of most Neotropical cichlids, followed by six tubular ossicles, and the infraorbital series of *Tylochromis* as having four separate tubular ossicles, one of which seems to be the fusion of three ossicles (because two pores are present within the ossicle, except the ones at the extremities). The lachrymal of *Tylochromis*, featuring five pores, therein interpreted as the fusion of lachrymals 1 and 2, could be reinterpreted as a single lachrymal with an additional pore, when compared to *Etroplus* and Neotropical cichlids in general. Otherwise, we would have to assume that the long ossicle with two pores has gained an additional pore, or that *Tylochromis* has eight bones in the infraorbital series, of which the two lachrymals are fused, as are three of the tubular ossicles. In sum, one cannot be certain about the real homology between ossicles, pores and canals, because they all have very different shapes, relative lengths and directions among taxa.

If determining homologies among infraorbital bones in different species may be hard, serially homologous structures that appear in large numbers (*e.g.*, scales, rays) are even more complicate. For instance, Lippitsch's (1993) character 41 discretises a continuous character, according to the number of scale series between lateral line and the midventral scale series. There is no means of determining which scale series are homologous, otherwise the character could be coded in a completely different manner (*e.g.*, series H1 and H2 triplicate, series H3 duplicate). Thus, several genetic and

developmental mechanisms that may be involved in the increase in the number of scale series may be confused under the same character state. Likewise, the dorsal-fin spines/dorsal-fin rays ratio may be altered by an increase/decrease in the length of the spiny/soft portion of the fin, or by the transformation of the spines in rays and vice-versa.

Moreover, there is no reason to presume that increases or decreases in meristic characters always obey a gradual pattern (*e.g.*, is it more likely that the number of teeth in the maxilla increases from 7 to 10 or from 7 to 20?). Reductive characters related to miniaturisation are also a problem. Losses of specific bones, reduction in the number of lateralis pores, rays, scales *etc.*, and changes in body proportions tend to make dwarf taxa 'attract' each other in morphological phylogenetic analyses, as well as non-dwarf taxa that occasionally converge to similar conditions. Characters based on the proportions of structures are probably correlated with other characters (modular evolution, pleiotropy). Including characters that are not independent from one another will, in practice, artificially add weight to those characters. Characters describing shapes may be tremendously subjective as well. For instance, should I express the length of the ascending process of the maxilla relative to SL or to HL? Another characteristic of morphological studies that is arguably problematic is related to the fact that some structures appear to be more variable (*e.g.*, subject to a larger amount of developmental processes). If a disproportional number of characters are described based on a single structure, this structure will have an abnormal weight in the analysis (*e.g.* see the amount of characters related to squamation in López-Fernández *et al*., 2005).

Another issue related to morphological character interpretation is that phenotype is a consequence of a series of ontogenetic processes, not a property inherited as such. Sereno (2007:570) stated that "in summary, in its most basic sense a phylogenetic character is here defined as a *heritable*, organismal feature (*i.e.*, an observable condition) expressed as an *independent* variable" (my italics). However, in my view no morphological character is a unit of inheritance nor independent from other morphological characters. The development of any structure or property of a structure is strictly dependent on the existence of other structures, therefore dependent on previous ontogenetic processes and, ultimately, on underlying genetic mechanisms. For instance, the presence of ectopterygoid teeth obviously depends on the existence of the ectopterygoid itself, but it may depend as well on numerous other factors that are impossible to identify at the present.

Consider, hypothetically, that along the generations between specimen A, which bears ectopterygoid teeth, and its ancestor B, which does not, ten mutations in different portions of the genome were strictly necessary to make the ectopterygoid teeth be expressed for the first time in the evolution of the group. Most will interpreted the teeth as inheritable, because they can observe that the teeth are present throughout generations. However, parental organisms do not really pass teeth forward to their offspring. Instead, they transfer DNA sequences to the next generation, and the interaction between those sequences may result in the production of teeth. Even if the ten aforementioned hypothetical DNA sequences were transferred artificially to an individual C of the same family, but not descending from B, the ectopterygoid teeth might not be expressed, given that C might have accumulated other mutations that prevent those teeth from developing. Likewise, if a descendant of A suffers an additional mutation in one of those ten sequences, it might not express ectopterygoid teeth too. In sum, morphological structures and their shapes are the complex outcome of simple changes in DNA (not to mention the environmental influences, which are not inheritable, except through epigenetic factors).

Thus, we can describe the inheritability of a morphological character as follows. Any structure or property of a structure of a specimen X has a statistical probability of being identical to the corresponding structure or property in its ancestor Y or in its descendant Z that is inversely proportional to the number of generations between Y and X or X and Z. The observable differences that may exist when we compare ancestor and descendant, though, may be subtle or drastic, *i.e.*, we must not assume gradual evolutionary changes *a priori*. Thus, the presence of, *e.g.*, identical incisive teeth in two fish species may be indicative of a close relationship, but one cannot assume *a priori* that a tooth with gradually decreasing cusps has a higher probability of evolving from a tooth with a large central cusp than from an incisive or a molar tooth. In fact, it is not the tooth itself that is evolving, but the DNA sequences that lead to the production of the tooth.

As for independence, the genetic information is not partitioned according to the morphological structures they affect. There is no such thing as ‘the set of genes that together encrypt instructions for making the lachrymal and only the lachrymal’, including a ‘gene responsible for determining the shape of the anterodorsal margin of the lachrymal and nothing else’. In fact, the hypothetical character statement ‘lachrymal, anterodorsal margin, shape: concave (0), convex (1)’ derives from an observation that, although reproducible, presupposes a biological mechanism whose existence is not supported. That mechanism is a genetic transformation that influences the shape of the anterodorsal

margin of the lachrymal, but has no developmental correlation with any other character described in the analysis. In reality, however, many morphological traits seem to be pleiotropic or to evolve in modules.

Hawkins (2000) observed:

> However, many might argue that the construction of a morphological cladistic data matrix can only be a subjective process, guided by biological knowledge or insight, and that inconsistency is therefore to be expected. Primary homology assessment is subjective, imprecise and intuitive. To what extent must it remain so? I believe that the theoretical framework informing character conceptualisation has not yet been fully explored, and that better guidelines are required. Until there is a clarification of theory inconsistency will remain.

I think 'clarification of theory' means understanding genetic and ontogenetic processes behind morphology. More specifically, knowing the time and order of the genic expression, and the effects of each gene at each developmental stage would reveal how morphological structures come to existence. Thus, a character such as 'number of lateral-line scales' could be translated into 'time of expression of gene X' or 'effect of gene Y when expressed prior to gene Z'. Evidently, gathering all that information may prove impossible. Moreover, we would still be relying on phenotypic evidence, as the timing of genic expression is also a consequence of the DNA sequences. Again, DNA sequences are the ultimate inheritable units, thus they seem to be less likely to bear false phylogenetic signal.

Taking the tail example from Maddison (1993), we can discuss the genetic basis for the colour character. If there are only two possible colours, red and blue, then how can one state turn into the other? First, we should be sure whether those colours are strictly 'inherited' or influenced by the environment or behaviour. Frequently, that is not possible. But let's take it as true, the colour is inherited. If we analyse the chemical formula of the two pigments, verifying that one is slightly different from the other, and that the two pigments cannot appear in the same individual, then we can conclude with some confidence that a gene responsible for producing the pigment has undergone mutation, producing a pigment of a different colour. However, if both pigments are present at least in one of the species (say, red in the tail, blue in the wing), then we should probably conclude that the genes for producing both pigments may be present in more than one species, and the difference in the distribution of pigments throughout the body

is a matter of gene expression. However, because we are hardly able to test those hypotheses, we must simply code the characters as we see them. That means we assume a large risk of not representing the truth about the character.

For instance, say we have three species: A, B and C, in which A is sister to B and C. Species A has only one gene coding for pigment (red), and has the body entirely red. Species B and C are united by a synapomorphy, which is the duplication of the gene that codes for red pigment in A. Both copies of this gene suffered mutations after the duplication, but in species B they continued coding for red pigment. In C, on the other hand, one of the copies of the gene suffered a mutation that affected the resulting pigment colour, changing it to blue. While B is entirely red (as A), C has a red body and a blue tail, because the "blue paralogue" is expressed in the tail. In fact, in species B, too, the orthologue of the "blue paralogue" is expressed, but it results in the same red colour as the body. Back to coding, the intuitive thing to do is: "Character 1. Tail colour: [0] red; [1] blue". Depending on the other taxa analysed, this character could be uninformative or it could contribute to cluster species A and B, or state 1 could result in an autapomorphy of C. There is no scenario in which such coding results in B and C as sisters. A realistic approach (impossible to reach with the tools we have), is to code as this: "Character 1. Number of paralogues of pigment gene: [0] one; [1] two"; Character 2. Colour of the pigment coded by paralogue 2: [0] red; [1] blue"; "Character 3: Paralogue expressed in the tail: [0] paralogue 2; [1] paralogue 1". In this scenario, character 3 would be uninformative. Character 1 would be a synapomorphy of B and C, and character 2 would be an autapomorphy of C. However, given that we know which gene is involved in this example, why not to use the information from it?

In short, there are many different ways to interpret phenotypic characters in a phylogenetic context. Each one presupposes hypothetical genetic mechanisms, which we are not able to test. Given that DNA is the ultimate source of inheritance, is much simpler to interpret differences in DNA sequences than in morphological structures. That leads us to the next issue.

1.1.2.2 Information/parsimony trade-off

In the example illustrated in Fig. 1, the hypothetical structure (which may be thought of as a laminar bone or a scale, for instance) has different shapes in species a, b, c and d. In species a and b, the hypothetical structure shows a longer vertical axis, while in species c

and d its maximum width is similar to the maximum height. In a, b and d, the structure is broader at the bottom, while in c it is as wide in the top as it is in the bottom. In a, the sides of the structure are concave, while in b, c and d, they are straight.

There are several ways to interpret those shape descriptions in order to code character states from this hypothetical structure. It is undeniable that all interpretations presuppose genetic mechanisms by which the shape of the structure can change evolutionarily. Because those mechanisms are unknown, the intuition of the morphologist will decide which hypotheses of character transformation seem more plausible. For instance, one could code all those differences under the same character, as four different states, diminishing considerably its amount of information. The assumption behind this decision would be that we have no idea of which pairs of shapes have a higher probability of turning into each other during evolution, because the genetic mechanisms acting upon each variable in question (*i.e.* top width/bottom width ratio, maximum height/maximum width ratio, side shape) may be too complex. This point of view, if applied to all structures, is likely to result in a topology dominated by polytomies, which despite being frustrating is not necessarily a wrong hypothesis, but rather a reflexion of a data set with little phylogenetic signal.

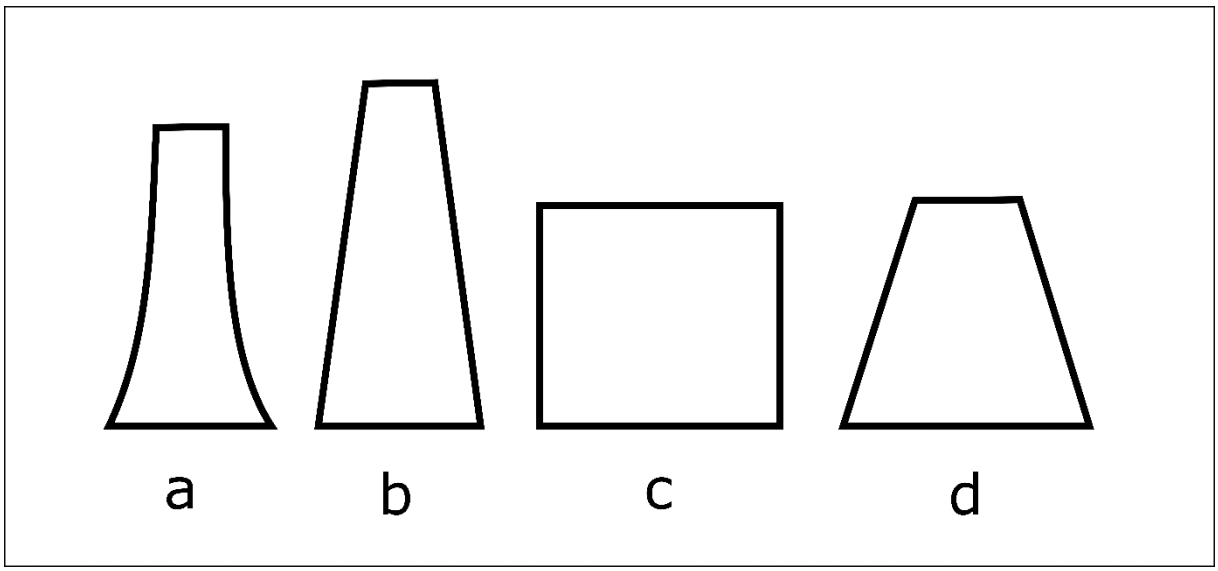

Figure 1. Schematic representation of a hypothetical structure that is homologous in species a, b, c and d.

Alternatively, one could translate each of the aforementioned variables into a different character. That implies assuming there is a genetic mechanism working on elongation/shortening of the vertical axis of the hypothetical structure, another mechanism affecting the width at the top extremity, and yet another one affecting the degree of concavity of its side. This interpretation would result in a more informative matrix in the sense that, the outgroup being identical to any of the four species with respect to our hypothetical structure, the topology derived exclusively from that structure would be a completely resolved one. On the other hand, this form of character coding would be intrinsically less parsimonious, given that there are too many unsupported assumptions. In other words, finding the tree with the least steps is not the only way to achieve the most parsimonious phylogenetic hypothesis, because when suggesting primary homologies one should avoid postulating mechanisms for which there is no evidence.

In summary, there appears to be a trade-off between finding parsimonious hypotheses and recovering well-resolved phylogenies when employing morphological data.

1.1.2.3 Adaptive convergence

Highly homoplastic characters, which are common both in molecular and morphological data sets, add noise to the phylogenetic analyses and mask the phylogenetic signal present in other, less plastic characters. Adaptive convergence commonly misleads morphological phylogenetic reconstructions, because there are relatively fewer paths in morphological evolution to achieve an adaptive peak. That is, organisms living in the same environment and exploring similar niches are likely to evolve similar tools, especially when they share a recent phylogenetic history (*e.g.*, species belonging to the same family). Thus, many terrestrial predators (extinct and extant) developed canine teeth and claws; many herbivores developed flat, multicuspidate teeth or molar specialised to macerate vegetable matter; flying vertebrates usually have extremely light bones and so on. To illustrate this argument with fishes, I suggest comparing the relationships of *Cichla* Bloch & Schneider and *Crenicichla* Heckel as recovered by Kullander (1998), López-Fernández *et al*. (2005; morphological analysis) and Ilves *et al.* (2017), as well as the relationships of the Stevardiinae in Weitzman & Menezes (1998), Menezes & Weitzman (2009) and Thomaz *et al.* (2015).

On the other hand, few cases are reported in which adaptive convergence drives molecular (exon) evolution in a way that homoplastic characters are likely to mislead phylogenetic reconstruction (*e.g.*, Bull *et al*., 1997; Castoe *et al*., 2008; Castoe *et al*., 2009; Castoe *et al*., 2010). Even in these cases, phylogenetic analyses featuring a larger dataset can dilute the importance of these convergent characters and recover a more accurate hypothesis (compare Castoe *et al.*, 2008, with Wiens *et al.*, 2012, and Pyron *et al.*, 2013). Moreover, I could not find any examples of such a convergence in nuclear genes, only in viral and mitochondrial ones.

It is true that, in the context of a morphological analysis, one can reinterpret primary homologies after recovering a preliminary topology. However, that practice is relevant only when comparing the result with phylogenies derived from other data sets. It works like follows: after a primary analysis revealing a homoplasy, the phylogeneticist can take a closer look at the homoplastic character, detecting differences not previously noticed, at a finer degree of detail. For instance, in a phylogeny of the amniotes one could code species A and B as having a patagium. After a first analysis, A and B are recovered as not closely related. The phylogeneticist then reanalyses the character and notices that in A the patagium includes the tail, while in B, it does not. Immediately, the homoplasy hypothesis is dismissed: in reality, A and B present two independently derived character states, only superficially similar. However, the characters supporting this first topology in which A and B are not sisters may well have been poorly interpreted as well. And, because they may represent adaptive convergences among the groups analysed, they might have erroneously influenced the topology by clustering species with similar niches. Additionally, the difference between the patagium of A and B may be due to different degrees of development of that structure, even if they are, in fact, homologous.

Thus, in the example given above, the hypothetical loss of the fin may have occurred by several genetic pathways. Different mutations in the same gene may have caused that loss in both species, as well as mutations in two different genes. However, it is unlikely that the same mutations have caused the fin loss in both species. In a morphological phylogenetic analysis, where one has no reason to code a different character state for the fin loss in each species *a priori*, this character will have a strong tendency to cluster the two species. That is mainly because morphological data sets are small. In a molecular analysis, even if the responsible gene happens to be sequenced, and even if it has the same sequence in both species by convergence, the whole data set, being large enough, will point to a better hypothesis.

1.1.2.4 Morphological vs. molecular characters: a conclusion

In sum, we conclude that molecular data are far better to recover phylogenies than are morphological data. Then why to use the latter? Because the phenotype is the interface between the genotype and the forces of natural selection. Only by studying the phenotype can we understand the scenario that led to the diversification of a group. For instance, it is consensus that, by any measure, the Ostariophysi are the dominant group in most tropical freshwaters worldwide. Morphology is necessary to explain this fact – as it was to identify it, in the first place. Only by recognizing phenotypic peculiarities (*e.g.*, the Weberian apparatus) of different lineages can we recognize adaptation, the key to understand how the evolution of a group works.

1.1.3 Composition and relationships of Cichlidae

Cichlidae is amongst the most diverse fresh-water fish families in the world. It comprises 1723 valid species (Fricke *et al*., 2020) distributed in most of the tropical portion of the Americas, Cuba and Hispaniola, Africa and a few localities in the Middle East, Madagascar and Sri Lanka and India (Kullander, 2003). Stiassny (1981) and other authors have long established the monophyly of cichlid fishes, although their affinities with other Acanthomorpha diverge among different phylogenetic hypotheses. Kaufman & Liem (1982) considered the cichlids to be part of the Labriformes, along with Labridae, Scaridae, Odacidae, Embiotocidae and Pomacentridae, all of which share a set of gill-arch specializations (see summary in Wiley & Johnson, 2010). Posterior morphological analyses suggested that Pholidichthyidae nests within this putative clade (Springer & Orrell, 2004). Alternatively, Betancur-R. *et al*. (2013) found Cichlidae and Pholidichthyidae (as sister groups), Embiotocidae and Pomacentridae to nest in different clades within Ovalentariae, whereas Labridae, Odacidae and Scaridae form the order Labriformes within Percomorpharia. Considering that the study of Betancur-R. *et al*. (2013) employed a very large molecular dataset, and that none of the putative synapomorphies of Labriformes *sensu* Kaufman & Liem (1982) is exclusive to the group, the most recent hypothesis seems the best one available.

Thus, we currently consider cichlids to be sister to *Pholidichthys* (Pholidichthyiformes: Pholidichthyidae; Betancur-R. *et al*., 2013), which includes two

eel-like species from Western Pacific Ocean north to Australia. Sister to Cichlidae and Pholidichthyidae is Polycentridae, which includes only four genera and a few species restricted to portions of South America and Africa. Those three families are, in turn, sister to Atherinomorphae, a large clade comprising Atheriniformes, Cyprinodontiformes and Beloniformes. The Atherinomorphae include many marine as well as freshwater species, thus having a wide distribution, even in North America. However, they are still mostly absent from the Eurasian continent. Cichlids, much like the aplocheiloids (Cyprinodontiformes), are mainly restricted to the areas that formerly comprised the Gondwana supercontinent, and to Middle America. However, the estimated age of the cichlid lineage is approximately the same as that of Atherinomorphae (Betancur-R. *et al*., 2013, Fig. 8), suggesting that cichlids have a much lower ability to disperse through marine environments.

As well as the relationships between Cichlidae and other acanthomorph families, the intrarelationships of cichlids have been subject of incongruence between different analyses. To Cichocki (1976), Ptychochrominae is sister to all other cichlids; the second clade to diverge is *Paratilapia*, followed by Etroplinae, which is sister to a trichotomy between Pseudocrenilabrinae, *Cichla* and the remaining Cichlinae. Oliver (1984), too, found a similar sequence of divergence: Ptychochrominae, *Paratilapia* and Etroplinae. However, he found a trichotomy between *Cichla*, *Heterochromis* and a clade including the remaining Neotropical and Afrotropical cichlids. Stiassny (1991) found Ptychochrominae to be sister to other cichlids, but the relationships between other subfamilies was not resolved. Kullander (1998) considered *Ptychochromis* to be part of Etroplinae, which he recognised as sister to Pseudocrenilabrinae. The two subfamilies he found to be sister to Cichlinae, but with *Heterochromis* nested within the latter. All of the aforementioned studies are based on morphology. The molecular analysis by Friedman *et al*. (2013) recovered Etroplinae as sister to all other cichlids. Ptychochrominae was the second subfamily to diverge, and the other two (Cichlinae and Pseudocrenilabrinae) are sister to each other.

On the other hand, there is considerable agreement as to relationships among the tribes of Cichlinae. Kullander (1998) and Ilves *et al*. (2017) agree that Cichlasomatini is sister to Heroini and that both clades are monophyletic (except for the position of *Acaronia* Myers); Cichlini and Retroculini diverged early in Cichlinae evolution; and Geophagini includes species with or without an epibranchial 1 lobe, as well as with different body sizes and shapes. The main aspect in which some morphological and molecular analyses

disagree is the position of *Crenicichla* Heckel (including *Teleocichla* Kullander). To Kullander (1998), it nests within Cichlinae (= Cichlini), following Stiassny (1987). To Ilves *et al*. (2017), it nests deeply within Geophagini, which is at least partially congruent with some morphological hypotheses (see the next section). Other aspect is the position of the small tribes Astronotini, Chaetobranchini and Retroculini. To Ilves *et al*. (2017), Chaetobranchini is the sister to Geophagini, and those tribes are sister to Astronotini, while Retroculini is sister to Cichlini. To Kullander (1998), Astronotini and Chaetobranchini are a clade (called Astronotinae therein), which is sister to Geophagini and the clade formed by Cichlasomatini and Heroini, while Retroculini is sister to all other Neotropical cichlids (which would include *Heterochromis* Regan).

1.1.3.1 Composition and relationships of Geophagini

It took about a century, after Haseman (1911) turned available the family-rank name Geophaginae, to reach a modern concept of what a geophagine cichlid is. Since the work of Heckel (1840), subsequent authors have reasonably associated with *Geophagus* other genera bearing an epibranchial 1 lobe (*e.g.*, Regan, 1906), but only much later Kullander (1983) suggested a close relationship with genera without an obvious lobe, such as *Crenicara* Steindachner and *Taeniacara* Myers. It is worth to mention that the reported presence of a lobe in *Saraca* Steindachner (1875) (= *Biotoecus* Eigenmann & Kennedy) and *Acarichthys* Eigenmann (1912) was erroneous, thus early associations of those genera with geophagines is partly accidental. Additionally, several studies (*e.g.*, Kullander, 1998; López-Fernández *et al*., 2005; Ilves *et al*., 2017) proved the initial trend to include *Retroculus* Eigenmann & Bray among geophagines to be inconsistent.

Kullander (1998) was the first to employ a reasonably large morphological dataset in order to test the monophyly of subgroups of Cichlinae, incorporating many interesting characters previously described by other authors (Cichocki, 1976; Oliver, 1984; Stiassny, 1987; Casciotta & Arratia, 1993) and adding a number of previously undescribed ones. His results confirm the position of *Acarichthys*, *Biotoecus*, *Crenicara*, *Dicrossus* Steindachner, *Guianacara* Kullander & Nijssen and *Taeniacara* among the geophagines, despite lacking a well-developed lobe (a rudimentary one is present in *Crenicara* and *Dicrossus*). At the same time, Farias *et al*. (1998) published the first molecular study to investigate the relationships within Cichlinae and recovered, also for the first time, a close relationship between *Crenicichla* and *Teleocichla* and the geophagines, although with

feeble evidence (only one marker). A series of subsequent papers (Farias *et al*., 1999; Farias *et al*., 2000; Farias *et al*., 2001) counted with more taxa and corroborated that hypothesis and, otherwise, the composition of the geophagine clade of Kullander (1998). In other words, those studies formed the base for a modern concept of Geophagini, although with a small dataset (relatively few taxa and a maximum of three molecular markers employed).

The hypothesized position of crenicichlines (*Crenicichla* and *Teleocichla*) among geophagines seemed not intuitive and openly challenged the importance of the morphological characters pointed out as synapomorphic for *Crenicichla* and *Cichla* (Stiassny, 1987; Kullander, 1998), although Kullander (1983) had already stated that *Cichla* presents more ancestral character states than crenicichlines and should not be considered as closely related to them. The subsequent paper by López-Fernández *et al*. (2005) greatly contributed to settle the apparent dispute between previous molecular and morphological studies. In their strictly morphological analysis, they employed the largest number of characters so far (136, *vs*. 91 in Kullander, 1998), and focused on resolving the geophagine relationships. This resulted in the crenicichlines not deeply nested within Geophagini, but sister to them, showing that molecular and morphological data are more congruent than previous works suggested. Additionally, López-Fernández *et al*. (2005) presented an analysis concatenating the morphological characters with sequences from a few molecular markers, now recovering crenicichlines deeply nested within Geophagini.

In the same period, Landim (2001; 2006) produced two morphological studies that remain unpublished, one on the relationships of Geophagini, and the other being the most complete morphological analysis on Cichlidae relationships to date. The first analysis counted on very few non-geophagine taxa and 80 characters and resulted in the exclusion of *Crenicichla* from Geophagini and the clustering of most small-sized geophagines in one clade and all large-sized ones in the other. The second analysis included 114 terminal taxa and 287 characters, and recovered Retroculini as sister to Geophagini, the latter with *Crenicichla* nested deep within. An odd result of Landim (2006) was the inclusion of *Nannacara anomala* Regan in Geophagini. Other analyses recovered *Nannacara* Regan within Cichlasomatini (*e.g.*, Kullander, 1998; Ilves *et al*., 2017). Deprá (2014), also in an unpublished study, analysed 121 characters (12 of them continuous) in 35 terminal taxa. The resulting topology clustered large-sized geophagines, with smaller species as successive sister groups. An exception was *Apistogramma*, which was found as sister of *Satanoperca*, which agrees with Ilves *et al*. (2017) (it is important to notice that several

geophagine genera, including *Taeniacara*, were not sampled by Deprá, 2014, who focused on the relationships between *Satanoperca* species).

The greatest contributions to the understanding of the Geophagini relationships, the molecular studies by López-Fernández *et al*. (2010) and, more importantly, Ilves *et al*. (2017), came after the study of Landim (2006). Although using the same markers as López-Fernández *et al*. (2005), the work of López-Fernández *et al*. (2010) sampled virtually all Cichlinae genera and sustained the position of crenicichlines among geophagines. Ilves *et al*. (2017) confirmed this hypothesis as well, this time employing hundreds of exons to build their phylogenetic tree, apparently the best available to date.

Given the position of crenicichlines within Geophagini as solved, Ilves *et al*. (2017) contributed to consolidate a few subclades, which could be treated as subtribes, but I prefer to maintain the informal names. Despite the utterly contrasting body shape, *Crenicichla* (including *Teleocichla*, from here forth considered its junior synonym) and the clade formed by *Acarichthys* and *Biotoecus* are members of crenicichlines. López-Fernández *et al*. (2010) had already recovered this clade, although with low support. Studies employing only morphological characters completely differed from this result, recovering *Acarichthys* as sister to *Guianacara*, *Biotoecus* as sister to *Crenicara* and *Dicrossus*, and *Crenicichla* as sister either to *Cichla* or to Geophagini (Kullander, 1998; López-Fernández, 2005). The concatenate analysis by López-Fernández *et al*. (2005) recovered *Crenicichla* as sister to *Biotoecus*, but not closely related to *Acarichthys*. By including morphological data from *Mazarunia* Kullander, López-Fernández (2012) published the only phylogeny with concatenate morphological data in which crenicichlines are monophyletic.

Another clade recovered with high support by both Ilves *et al*. (2017) and López-Fernández *et al*. (2010) is apistogrammines, encompassing *Satanoperca* as sister to *Taeniacara* and *Apistogramma* (which includes its junior synonym *Apistogrammoides*). López-Fernández *et al*. (2005) recovered apistogrammines as monophyletic as well, but only in the concatenated analysis. Their strictly morphological analysis resulted in the clustering of all small-sized geophagines and in the placement of *Satanoperca* in a polytomy with other large-bodied geophagines (on the other hand, it supported the sisterhood between *Apistogramma* and *Taeniacara*, which was also the opinion of Kullander, 1998). López-Fernández *et al*. (2012) also recovered apistogrammines as monophyletic.

Guianacarines from López-Fernández *et al*. (2010), López-Fernández *et al.* (2012) and Ilves *et al*. (2017) encompasses *Guianacara* and *Mazarunia*, differing from previous analyses, which recovered *Guianacara* as sister to *Acarichthys* (*e.g.*, Kullander, 1998). The next group are the biotodomines (designated herein), which are equivalent to geophagines plus mikrogeophagines of Ilves *et al*. (2017). The reason for rejecting their previously settled names is that mikrogeophagines are polyphyletic and geophagines is an informal name always employed in the literature as a synonym for the tribe Geophagini. López-Fernández *et al*. (2010) recovered biotodomines as composed of *Gymnogeophagus* as sister to *Geophagus* and the "*Geophagus*" *steindachneri* species group. Although recovering the same group, Ilves *et al*. (2017) found a much smaller support for the relationships among clades within biotodomines. On the other hand, they recovered the clade formed by *Mikrogeophagus* and the "*Geophagus*" *brasiliensis* species complex, and *Biotodoma* as sister to the remaining biotodomines.

The last group found by Ilves *et al*. (2017) within Geophagini are the crenicaratines, composed only of *Crenicara* and *Dicrossus*, a clade already recovered in all previous analyses. In sum, we recognize five informal groups, phylogenetically arranged as follows: geophagines are sister to crenicaratines, and this clade is sister to the clade formed by guianacarines as sister to apistogrammines and crenicichlines.

1.2 What to do with morphological characters?

We have already seen that mapping morphological characters on a topology derived from an independent data set such as the genome may improve our understanding of their evolution (*e.g.* Borchiellini *et al*., 2004; Kergoat *et al*., 2005; Vargas & Madriñán, 2012; Wedin *et al*., 2009). Also, I have said that morphological characters are essential to understand the evolution of any organism, as the phenotype is the interface between genes and natural selection. But which kinds of questions may be answered by character mapping? One possible answer is: questions related to adaptive morphology.

One of the most remarkable features of cichlids is their many documented adaptive radiations. Adaptive radiations mean that an ancestral species diversifies to occupy several niches, thus presenting adaptations to an array of different life styles. When two or more adaptive radiations occurred in the same family, their corresponding species may develop similar morphological traits to deal with similar problems. That is, predators, plankton feeders, winnowers, grazer and so on may be so similar among

themselves that they look like monophyletic. On the other hand, adaptations may be rather different. Thus, a first question emerges: what are the probabilities that two species of the same family, which converge to a similar feeding habit, develop similar morphological traits to deal with food intake and processing?

Character mapping can also help solving the problem of identifying morphological adaptations that are not understood yet. While some of them may seem obvious, such as numerous, long gill rakers in planktivores, large mouths in piscivores, teeth forming a rasping edge in species that scrape rocks for algae etc., we cannot identify promptly which parts of a specialist can be considered as adaptive in some cases. Instead of speculating how each part of the organism could possibly work to enhance fitness relative to its particular speciality, a better way of identify adaptive traits is to look for them in species that converged to the same habits. In fact, that can be done by reanalysing published data.

Kullander (1998), in his analysis of cichlid fishes (mainly Neotropical), included four piscivorous genera, *viz*. *Acaronia*, *Caquetaia*, *Cichla* and *Crenicichla* (although not all *Crenicichla* species are strictly piscivorous). In Appendix 1, I provide a .tnt file in which the data from Kullander (1998) is forced to reconstruct the topology from Ilves *et al*. (2017). By mapping the characters by Kullander (1998) upon the topology of Ilves *et al*. (2017), only *Cichla* and *Crenicichla* among the aforementioned genera present a considerable number of convergent character state. These are the shape of the gill rakers (character 16[0]), the direction of the urohyal spine (25[1]; also shared with *Chaetobranchus*), the insertion of Baudelot's ligament (29[1]; also shared with *Astronotus*), the shape of vomer (32[1]), the presence of a long distal-post-cleithrum spine (49[2]), a large amount of vertebrae, of which the abdominal ones are more numerous (67[3]; also shared with *Satanoperca*) and the rounded pelvic fin (86[0]; also shared with *Retroculus*). *Cichla* and *Crenicichla* also share with *Acaronia* a similar maxillary process of the palatine (51[1]), which is, however, present in a few non-piscivorous genera.

None of the aforementioned character states is obviously related to piscivory. However, the fact that all of them are present (almost) only in piscivores makes us think that they are related directly or indirectly to that feeding habit. The larger amount of abdominal vertebrae, for instance, may allow the abdominal cavity to accommodate large prey. The presence of a longer abdominal cavity in *Satanoperca*, certainly not related to the necessity of fitting the prey size, may correlate to the size of other structures, such as the swim bladder. Because *Satanoperca* feeds by plunging its snout into the substrate,

perhaps a longer swimbladder would help displacing the gravity centre posteriorly, making the anterior portion of the body heavier and lowering the snout. That hypothesis is supported by the fact that *Geophagus*, although not presenting a long abdominal cavity, presents extensions of the swim bladder into the caudal region.

This kind of reasoning is certainly speculative. However, speculation is built upon evidence and may inspire testable hypotheses. If we did the alternative way, *i.e.*, analysing each of the structures present in an organism assuming its adaptiveness to the organism's life style, we would have much more trouble to explain how each structure is adaptive in that case. This exercise is obviously complicated by the fact that many phenotypical features are pleiotropic, *i.e.*, they are not selected by their adaptiveness *per se*, but for the gain in fitness provided by other characters, to which they are pleiotropically connected.

With all that in mind, the objective of this thesis, presented in the form of two articles, is to investigate the skeletal musculature of geophagine cichlids. The first article is a complete description of the skeletal musculature of one of their representatives, *Geophagus sveni* Lucinda, Lucena & Assis. It is intended to serve as an atlas, a reference for all future works on cichlid musculature, featuring a protocol for the myological dissection of specimens. The second article deals with the relationship between morphological characters and the phylogeny of Geophagini. In the first article, few considerations are made regarding adaptive morphology, a subject further developed in the second article, in which a comparison with other cichlids, representing a wide array of specialisations, is possible.

REFERENCES

Amorim, D. S. 2002. Fundamentos de sistemática filogenética. Holos.

Betancur-R., R., R. E. Broughton, E. O. Wiley, K. Carpenter, J. A. López, C. Li *et al*. 2013. The tree of life and a new classification of bony fishes. PLoS Currents, ecurrents.tol.53ba26640df0ccaee75bb165c8c26288

Betancur-R. R., D. Arcila, R. P. Vari, L. C. Hughes, C. Oliveira, M. H. Sabaj & G. Ortí. 2018. Phylogenomic incongruence, hypothesis testing, and taxonomic sampling: the monophyly of characiform fishes. *Evolution*, 73(2): 329–345.

Borchiellini, C., C. Chombard, M. Manuel, E. Alivon, J. Vacelet & N. Boury-Esnault. 2004. Molecular phylogeny of Demospongiae: implications for classification and scenarios of character evolution. *Molecular Phylogenetics and Evolution*, 32: 823–837.

Bull, J. J., M. R. Badgett, H. A. Wichman, J. P. Huelsenbeck, D. M. Hillis, A. Gulati *et al*. 1997. Exceptional convergent evolution in a virus. *Genetics*, 147: 1497–1507.

Casciotta, J. R. & G. Arratia. 1993. Tertiary cichlid fishes from Argentina and reassessment of the phylogeny of New World cichlids. Kaupia, (2): 195–240.

Castoe, T. A., Z. J. Jiang, W. Gu, Z. O. Wang & D. D. Pollock. 2008. Adaptive evolutional and functional redesign of core metabolic proteins in snakes. *PLoS ONE*, 3(5): e2201

Castoe, T. A., A. P. Jason de Koning, H.-M. Kim, W. Gu, B. P. Noonan, G. Naylor *et al*. 2009. Evidence for an ancient adaptive episode of convergent molecular evolution. *PNAS*, 106(22): 8986–8991.

Castoe, T. A. A. P. Jason de Koning & D. D. Pollock. 2010. Adaptive molecular convergence: Molecular evolution *versus* molecular Phylogenetics. *Communicative and Integrative Biology*, 3(1): 67–69.

Cichocki, F. P. 1976. Cladistic history of cichlid fishes and reproductive strategies of the American genera *Acarichthys*, *Biotodoma* and *Geophagus*. Unpublished D. Phil. Thesis, The University of Michigan.

Deprá, G. C. 2014. Estudo das relações filogenéticas em *Satanoperca* Günther, 1862 (Perciformes: Cichlidae). Unpublished Masters dissertation, Universidade Estadual de Maringá.

Eigenmann, C. H. 1912. The freshwater fishes of British Guiana, including a study of the ecological grouping of species, and the relation of the fauna of the plateau to that of the lowlands. *Memoirs of the Carnegie Museum*, 5(1): 1–578.

Eigenmann C. H. 1917. The American Characidae. Part 1. *Memoirs of the Museum of Comparative Zoology*, 43(1): 1–102.

Farias, I. P., G. Ortí & A. Meyer. 2000. Total evidence: Molecules, morphology, and the phylogenetics of cichlid fishes. *Journal of Experimental Zoology*, 288: 76–92.

Farias, I. P., G. Ortí, I. Sampaio, H. Schneider & A. Meyer. 1999. Mitochondrial DNA phylogeny of the family Cichlidae: Monophyly and fast molecular evolution of the Neotropical assemblage. *Journal of Molecular Evolution*, 48: 703–711.

Farias, I. P., G. Ortí, I. Sampaio, H. Schneider & A. Meyer. 2001. The Cytochrome *b* gene as a phylogenetic marker: The limits of resolution for analyzing relationships among cichlid fishes. *Journal of Molecular Evolution*, 53: 89–103.

Farias, I. P., H. Schneider & Sampaio, I. 1998. Molecular phylogeny of Neotropical cichlids: The relationships of cichlasomines and heroines. Pp. 499–508. In: Malabarba LR, Reis RE, Vari RP, Lucena ZM, Lucena CAS, eds. *Phylogeny and classification of Neotropical fishes*. Porto Alegre: Edipucrs.

Fricke R., W. N. Eschmeyer & J. D. Fong. 2020. *Eschmeyer's catalog of fishes: species by family/subfamily*. (http://researcharchive.calacademy.org/research/ichthyology/catalog/SpeciesByFamily.asp). Electronic version accessed 29 Jan 2020.

Friedman, M., B. P. Keck, A. Dornburg, R. I. Eytan, C. H. Martin, C. D. Hulsey *et al*. 2013. Molecular and fossil evidence place the origin of cichlid fishes long after Gondwanan rifting.

Harshman, J. E. L. Braun, M. J. Braun, C. J. Huddleston, R. C. K. Bowie, J. L. Chojnowski *et al*. 2008. Phylogenomic evidence for multiple losses of flight in ratite birds. *PNAS*, 105(36): 13462–13467.

Haseman, J. D. 1911. Descriptions of some new species of fishes and miscellaneous notes on others obtained during the expedition of the Carnegie Museum to central South America. *Annals of the Carnegie Museum*, 7(3–4): 315–328.

Hawkins, J. A. 2000. A survey of primary homology assessment: Different botanists perceive and define characters in different ways. Pp. 22–53. In: Scotland, R. & Pennington, T. (Eds.). *Homology and systematics: coding characters for phylogenetic analysis*. London: Taylor and Francis.

Heckel, J. J. 1840. Johann Natterer's neue Flussfische Brasilien's nach den Beobachtungen und Mittheilungen des Entdeckers beschrieben (Erste Abtheilung, Die Labroiden). *Annalen des Wiener Museums der Naturgeschichte,* 2: 325–471.

Hillis, D. M. 1987. Molecular *versus* morphological approaches to Systematics. *Annual Review of Ecology and Systematics*, 18: 23–42.

Ilves, K. L., D. Torti & H. López-Fernández. 2017. Exon-based phylogenomics strengthens the phylogeny of Neotropical cichlids and identifies remaining conflicting clades (Cichliformes: Cichlidae: Cichlinae). *Molecular Phylogenetics and Evolution* 118: 232–243.

Kaufman, L. S., K. F. Liem. 1982. Fishes of the suborder Labroidei (Pisces: Perciformes): Phylogeny, ecology, and evolutionary significance. *Breviora*, (472): 1–19.

Kergoat, G. J., A. Delobel, G. Fédière, B. Le Rü, J.-F. Silvain. 2005. Both host-plant phylogeny and chemistry have shaped the African seed-beetle radiation. *Molecular Phylogenetics and Evolution*, 35: 602–611.

Kohlsdorf, T. & G. P. Wagner. 2006. Evidence for the reversibility of digit loss: a phylogenetic study of limb evolution in *Bachia* (Gymnophthalmidae: Squamata). Evolution, 60(9): 1896–1912.

Kullander, S. O. 1983. Taxonomic studies on the percoid freshwater fish family Cichlidae in South America. Part II. Review of the South American Cichlidae. Pp. 297–440. Stockolm: Naturhistoriska Riksmuseet.

Kullander, S. O. 1998. A phylogeny and classification of the South American Cichlidae (Teleostei: Perciformes). Pp. 461–498. In: Malabarba LR, Reis RE, Vari RP, Lucena ZM, Lucena CAS, eds. *Phylogeny and classification of Neotropical fishes*. Porto Alegre: Edipucrs.

Kullander, S. O. 2003. Family Cichlidae. Pp. 609–659. In: Reis, R. E., S. O. Kullander & C. J. Ferraris, Jr. Check list of the freshwater fishes of South and Central America. Porto Alegre: Edipucrs.

Landim, M. I. 2001. Relações filogenéticas na subfamília Geophaginae Haseman (Perciformes, Cichlidae). Unpublished Masters dissertation, Universidade Federal do Rio de Janeiro.

Landim, M. I. P. F. 2006. Relações filogenéticas na família Cichlidae Bonaparte, 1840 (Teleostei: Perciformes). Unpublished D. Phil. Thesis, Universidade de São Paulo.

Leaché, A. D., P. Wagner, C. W. Linkem, W. Böhme, T. J. Papenfuss, R. A. Chong *et al*. 2014. A hybrid phylogenetic-phylogenomic approach for species tree estimation in African *Agama* lizards with implications to biogeography, character evolution, and diversification. *Molecular Phylogenetics and Evolution*, 79: 215–230.

Lippitsch, E. 1993. A phyletic study on lacustrine haplochromine fishes (Perciformes, Cichlidae) of East Africa, based on scale and squamation characters. *Journal of Fish Biology*, 42: 903–946.

López-Fernández, H., R. L. Honeycutt, M. L. J. Stiassny & K. O. Winemiller. 2005. Morphology, molecules, and character congruence in the phylogeny of South American geophagine cichlids (Perciformes, Labroidei). *Zoologica Scripta*, 34(6): 627–651.

López-Fernández, H., D. Taphorn, E. A. Liverpool. 2012. Phylogenetic diagnosis and expanded description of the genus *Mazarunia* Kullander, 1990 (Teleostei: Cichlidae) from the upper Mazaruni River, Guyana, with description of two new species. *Neotropical Ichthyology*, 10(3): 465–486.

López-Fernández, H., K. O. Winemiller, R. L. Honeycutt. 2010. Multilocus phylogeny and rapid radiations in Neotropical cichlid fishes (Perciformes: Cichlidae: Cichlinae). *Molecular Phylogenetics and Evolution*, 55: 1070–1086.

Maddison, W. P. Missing data *versus* missing characters in phylogenetic analysis. *Systematic Biology*, 42(4): 675–581.

Menezes, N. A. & S. H. Weitzman. 2009. Systematics of the Neotropical fish subfamily Glandulocaudinae (Teleostei: Characiformes: Characidae). *Neotropical Ichthyology*, 7(3): 295–370.

Oliveira, C., G. S. Avelino, K. T. Abe, T. C. Mariguela, R. C. Benine, G. Ortí *et al*. 2011. Phylogenetic relationships within the speciose family Characidae (Teleostei: Ostariophysi: Characiformes) based on multilocus analysis and extensive ingroup sampling. *BMC Evolutionary Biology*, (11): 275.

Oliver, M. K. 1984. Systematics of African cichlid fishes: determination of the most primitive taxon, and studies on the haplochromines of Lake Malawi. Unpublished D. Phil. Thesis, Yale University.

Philippe, H., R. Derelle, P. Lopez, K. Pick, C. Borchiellini, N. Boury-Esnault *et al*. 2009. Phylogenomics revives traditional views on deep animal relationships. *Current Biology*, 19: 706–712.

Pyron, R. A., F. T. Burbrink & J. J. Wiens. 2013. A phylogeny and revised classification of Squamata, including 4161 species of lizards and snakes. *BMC Evolutionary Biology*, 13: 93.

Regan, C. T. 1906. A revision of the South-American cichlid genera *Retroculus*, *Geophagus*, *Heterogramma*, and *Biotoecus*. *Annals and Magazine of Natural History (Series 7)*, 17(97): 49–66.

San Mauro, D. & A. Agorreta. 2010. Molecular systematics: a synthesis of the common methods and the state of knowledge. *Cellular & Molecular Biology Letters*, 15: 311–341.

Sereno, P. C. 2007. Logical basis for morphological characters in Phylogenetics. *Cladistics*, 23: 565–587.

Springer, V. G. & T. M. Orrell. 2004. Appendix: phylogenetic analysis of 147 families of acanthomorph fishes based primarily on dorsal gill-arch muscles and skeleton. In: Springer, V. G. & G. D. Johnson. Study of the dorsal gill-arch musculature of teleostome fishes, with special reference to the Actinopterygii. *Bulletin of the Biological Society of Washington*, 11: 236–260.

Steindachner, F. 1875. Beiträge der Kenntniss der Chromiden des Amazonenstromes. *Sitzungsberichte der Kaiserlichen Akademie der Wissenschaften. Mathematisch-Naturwissenschaftliche Classe*, 71(1): 61–137.

Stiassny, M. L. J. 1981. Phylogenetic *versus* convergent relationship between piscivorous cichlid fishes from lakes Malawi and Tanganyika. *Bulletin of the British Museum of Natural History (Zoology)*, 40(3): 67–101.

Stiassny, M. L. J. 1987. Cichlid familial intrarelationships and the placement of the Neotropical genus *Cichla* (Perciformes, Labroidei). *Journal of Natural History*, 21: 1311–1331.

Stiassny, M. L. J. 1991. Phylogenetic intrarelationships of the family Cichlidae: an overview. Pp. 1–35. In: Keenleyside MHA, ed. *Cichlid fishes: Behaviour, ecology and evolution*. London: Chapman & Hall.

Thomaz, A. T., D. Arcila, G. Ortí & L. R. Malabarba. 2015. Molecular phylogeny of the subfamily Stevardiinae Gill, 1858 (Characiformes: Characidae): classification and the evolution of reproductive traits. *BMC Evolutionary Biology*, (15): 146.

Vargas, O. M. & S. Madriñán. 2012. Preliminary phylogeny of *Diplostephium* (Asteraceae): Speciation rate and character evolution. *Lundellia*, 15: 1–15.

Wedin, M., E. Wiklund, P. M. Jørgensen & S. Ekman. 2009. Slippery when wet: Phylogeny and character evolution in the gelatinous cyanobacterial lichens (Peltigerales, Ascomycetes). *Molecular Phylogenetics and Evolution*, 53: 862–871.

Weitzman, S. H. & N. A. Menezes. 1998. Relationships of the tribes and genera of the Glandulocaudinae (Ostariophysi: Characiformes: Characidae) with a description of a new genus, *Chrysobrycon*. Pp. 171–192. In: Malabarba, L. R., R. E. Reis, R. P. Vari, Z. M. S. Lucena & C. A. S. Lucena. Phylogeny and classification of Neotropical fishes. Porto Alegre: Edipucrs. 603 p.

Whiting, A. S., A. M. Bauer & J. W. Sites, Jr. 2003. Phylogenetic relationships and limb loss in sub-Saharan African scincine lizards (Squamata: Scincidae). *Molecular Phylogenetics and Evolution*, 29: 582–598.

Wiens, J. J. 2004. The role of morphological data in phylogeny reconstruction. *Systematic Biology*, 53(4): 653–661.

Wiens, J. J., C. R. Hutter, D. G. Mulcahy, B. P. Noonan, T. M. Townsend, J. W. Sites, Jr. *et al*. 2012. Resolving the phylogeny of lizards and snakes (Squamata) with extensive sampling of genes and species. *Biology Letters*, 8: 1043–1046.

Wiley, E. O. & G. D. Johnson. 2010. A teleost classification based on monophyletic groups. Pp. 123–182. In: Nelson, J. S., H.-P. Schulze & M. V. H. Nelson. *Origin and phylogenetic interrelationships of teleosts*. Munich: Verlag Dr. Friedrich Pfeil.

Zhu, M., X. Yu, B. Choo, J. Wang & L. Jia. 2012. An antiarch placoderm shows that pelvic girdles arose at the root of jawed vertebrates. *Biology Letters*, 8: 453–456.

2 SKELETAL MUSCULATURE OF *GEOPHAGUS SVENI* LUCINDA, LUCENA & ASSIS (CICHLIFORMES: CICHLIDAE), A SPECIALISED WINNOWER, WITH A PROTOCOL FOR MYOLOGICAL DISSECTION IN CICHLIDS

ABSTRACT

Cichlids, one of the largest freshwater fish families, are best known for having undergone remarkable adaptive radiations. Winnowing (or substrate sifting), the capacity to use the branchial basket to sort food items hidden in the substrate from non-edible particles, is one of the most interesting feeding habits resulting from that diversification process. Many aspects of winnowing are not yet understood. Although the literature bears information on the skeletal morphology of winnowers, little is known about their skeletal musculature. In fact, studies on the skeletal musculature of fishes are rare, in comparison to other morphological works. Regarding cichlids, the only in-depth investigation of the musculature focused on a single African species, *Haplochromis elegans*, not including post-cranial muscles. Herein we provide the first complete description of the skeletal muscles of a cichlid, and perhaps the first of any kind of fish. We analysed a Neotropical species, *Geophagus sveni*, which is a specialised winnower belonging to tribe Geophagini. We provide a protocol for the dissection of specimens and photographs of all muscles studied, and discuss the differences observed in comparison with previous works.

Key words: Adaptive morphology - Cichlinae - Eartheater - Evolution - Geophagini - Myology - Striated muscle - Substrate sifter.

2.1 Introduction

Cichlids are one of the richest families of freshwater fish, with 2283 species (Fricke *et al*., 2020). Better known for the amazing, well-studied adaptive radiations undergone by its African representatives (subfamily Pseudocrenilabrinae) in the great rift valley lakes (a summary of the ecological and evolutionary studies on African cichlids is found in, *e.g.*, Keenleyside, 1991), the family also includes many representatives in South and Central Americas, as well as a few others in Madagascar, Middle East and in the Indian subcontinent (Stiassny, 1991). Cichlids of the Americas (subfamily Cichlinae) have diversified to a degree comparable to that seen in African cichlids, although much less attention has been given to their ecology. In South America, the most impressive adaptive radiation was that undergone by tribe Geophagini, which exhibits very diversified body shapes and feeding habits (López-Fernández *et al*., 2013), while in Central America tribe Heroini accounts for virtually the whole cichlid diversity (Říčan et al., 2013; 2016).

At the core of cichlid adaptive radiations is a functional morphology capable of evolving many specialisations while retaining incredible versatility (Liem, 1991; Yamaoka, 1991). The many trophic specialisations repeatedly evolved by cichlids result from the shape plasticity of teeth, skull, head muscles, gill rakers etc.; their versatility, in turn, relies in the great mobility of the skull (including pharyngeal jaws), associated with a rich repertoire of movements that can be explored regardless of morphological specialisations (Liem, 1991). For instance, although the tridimensional configuration of the orobranchial cavity is partly determined by skull shape and correlates with the various modes of food intake (*viz*. ram feeding, suction feeding and biting), it can be widely regulated by oral opening and protrusion, as well as the lifting or depression of the orobranchial floor (Liem, 1991). Likewise, the same repertoire of movements of the

pharyngeal jaws can serve different purposes in different species (*e.g.*, shred, crush, pile).

Still, morphological specialisations do exist, and must be explained in terms of a gain in fitness as they correlate to various feeding habits. One of the most remarkable feeding habits shown by cichlids consists in taking in the mouth food mixed with substrate, and subsequently ejecting the non-edible particles while keeping the food items (*e.g.*, López-Fernández *et al*., 2014; Weller *et al*., 2016). This behaviour, also found in a few other fish families, is called winnowing or substrate-sifting (Drucker & Jensen, 1991). Although it is understood that the gill rakers act like a sieve (*e.g.*, Yamaoka, 1991), the mechanism by which the particles are sorted from larger, non-edible items is not fully understood, and no study has extensively explored the morphological traits that can be interpreted as adaptations to winnowing. López-Fernández *et al*. (2014) compared the efficiency of winnowers and non-winnowers at recovering buried arthropods in aquarium, but it is not clear how winnower morphology may provide a gain in fitness. In fact, a thorough list of species capable of winnowing is not available at the present, although López-Fernández *et al*. (2014) mention several taxa. Among South American Cichlinae, winnowing is best developed in *Retroculus* and in some large-bodied species of Geophagini, which are particularly interesting to us, as the behaviour seems to have evolved independently several times within the tribe.

The tribe Geophagini, as presently understood (Ilves *et al*., 2017), comprises 16 valid genera and two undescribed ones included in *Geophagus sensu lato* (Kullander, 1998), although the inclusion of *Apistogrammoides* and *Teleocichla* in *Apistogramma* and *Crenicichla*, respectively, seems unavoidable. Therefore, we can reasonably state that Geophagini includes 16 natural genera, distributed in a few lineages. Ilves *et al*. (2017) name those lineages as follows: crenicichlines, apistogrammines, guianacarines,

geophagines, mikrogeophagines and crenicaratines. However, because their mikrogeophagines do not represent a monophyletic unit, and because the term geophagines is widely employed in the literature as an informal synonym of Geophagini, we refer to both groups as a single lineage herein called “biotodomines”, so that Geophagini includes five lineages.

While the crenicaratines include only dwarf species, with relatively short snouts and shallow bodies, and the biotodomines include medium- to large-sized species with relatively long snouts and deep bodies, other lineages are more heterogeneous. The guianacarines include both *Guianacara*, which resembles biotodomines, and *Mazarunia*, which has a more generalised body shape reminiscent of Cichlasomatini. Apistogrammines include the dwarf cichlids of genera *Apistogramma* (including *Apistogrammoides*) and *Taeniacara*, but also the biotodomine-like *Satanoperca*. Crenicichlines are the most morphologically diverse assemblage, including the slender-bodied dwarf cichlids of genus *Biotoecus*; the large-bodied, biotodomine-like Acarichthys; and *Crenicichla* (including *Teleocichla*), which encompasses species of different body sizes, but always with shallow, sub-cylindrical bodies.

In terms of feeding habits, all biotodomines and *Acarichthys*, *Guianacara* and *Satanoperca* are clearly orobranchial winnowers (herein defined as winnowers that eject non-edible particles both through the gills and back through the mouth; personal observation). Winnowing is most likely absent in *Crenicichla*, and it is uncertain whether *Mazarunia* presents some variation of this behaviour, but all remaining Geophagini perform, at least, oral winnowing (defined herein as the type of winnowing in which non-edible particles are ejected only through the mouth). Species known to be orobranchial winnowers agree to a large extent to the morphology exhibited by suction feeders, according to Liem (1991:138–139): “very large epaxial muscles and high

supraoccipital crests, deep palatopterygoid arches [= suspensorium] offering expansive surfaces for the *levator* and *adductor arcus palatini* [= *adductor hyomandibulae*] and *adductor mandibulae* muscles and long ascending processes for jaw protrusion". It seems fair, thus, to regard winnowers as specialised suction feeders.

In order to shed some light on the subject of how winnowers gain efficiency in feeding on benthic invertebrates, when compared to generalised suction feeders, we must recognise their typical morphological traits. A first step is to investigate the skeleton, teeth and gill raker morphology, and there is already plenty of information of those structures in the literature. However, although studies on the osteology of Neotropical cichlids are abundant and account for the whole skeleton (*e.g.*, Kullander, 1983, 1986; 1989; 1998), studies involving aspects of their myology are still rare and limited to one or a few muscles, mainly the *adductor mandibulae* and other superficial head muscles (*e.g.*, Cichocki, 1976; Dutta, 1987; Arbour & López-Fernández, 2018). In comparison, there is much more information on the skeletal muscles of African cichlids (*e.g.*, Baerends & Baerends-Van Roon, 1950; Stiassny, 1981; Aerts, 1982), the most important study being that of Anker (1978), which accounts for all head muscles. Baerends & Baerends-Van Roon (1950) briefly account for the postcranial ones. Still, even those studies fail to contemplate winnowers.

Given its importance to food processing in fish, we postulate the muscular system as one of the key morphological determinants in cichlid adaptive radiations, which agrees with Liem's (1991) observation that muscle shape correlates with the different modes of food intake. In our view, thus, to understand better how winnowing works and how it became such a widespread behaviour among geophagines, it is necessary to investigate how it relates to muscles. Considering the current lack of a complete, well-illustrated work on the muscles of Neotropical cichlids, our objective is

to describe and depict the whole striated musculature of *Geophagus sveni* Lucinda, Lucena & Assis. It will serve as a step stone for an ongoing phylogenetic study of the Geophagini focused on skeletal muscles and their functioning, but also help to reveal myological characters that might explain gain in winnowing efficiency. We opted for using *G. sveni* as a study model because this species belongs to the type genus of the tribe (of which all species seem to be winnowers), is easy to analyse due to the medium body size, and has been extensively analysed in other works involving DNA sequencing, colour-pattern variation and ontogeny, brain gross morphology, parasites, diet, invasiveness etc. (Moretto *et al*., 2008; Zago *et al*., 2013; Gois *et al*., 2015; A. B. da Silva *et al.*, unpubl. data; R. C. Oliveira & W. J. da Graça, unpubl. data), constituting a well-studied species. Another objective of our paper is to provide a protocol for myological dissection of cichlids, also applicable to other fish families.

2.2 Materials and methods

We based our study on a single specimen of *Geophagus sveni*, prepared for myological study as in Datovo & Bockmann (2010). We dissected the specimen as in the protocol described in Supplementary File 1, and photographed the successive stages in order to evidence the shape and relative positions of all striated muscles. The names of the bones and *lateralis* pores follow Kullander (1983); of the muscles, Winterbottom (1974a), except in the cases mentioned under the descriptions.

We present a list of all muscles analysed, with their origin and insertion sites, in Table 1, following the same order as Winterbottom (1974a). Subsequently, we describe the shape and other important information on individual muscles, comparing each of them with the description provided by Anker (1978) for *Haplochromis elegans* Trewavas or with that by Baerends & Baerends-Van Roon (1950) for *Pseudocrenilabrus philander*

(Weber). We discuss homology issues for each muscle when pertinent. We found no swimbladder musculature nor subcutaneous musculature neither in *Geophagus sveni* nor in any other, comparative cichlids. We deliberately neglected muscles associated to branchial filaments because they are hardly observable without histological preparations (but see comments under the description of the *adductor branchialis 1*). Because the limits of some of the neurocranial bones are unclear, we occasionally placed a "(?)" after the name of a bone, indicating that we are not sure if it is the exact attachment site of a muscle.

2.3 Results

We recognised 97 muscles in *Geophagus sveni*, counting serial muscles serving the fin rays as one of each kind, as well as the *epaxialis* and *hypaxialis* muscles, and excluding from the count the muscle parts, even in those cases in which the parts are differentiated enough to be treated as separate muscles. The list of muscles analysed, with respective figures, is given in Table 1. A list of synonyms found in selected papers is presented in Table 2.

Table 1. Complete list of the striated muscles found in *Geophagus sveni*, with origin and insertion sites, and figures that illustrate each muscle. Muscles that are treated as absent in *G. sveni* are included to facilitate comparison with Winterbottom (1974a), who has reported them for other groups of fishes. An exception is *pars post-temporalis* of *levator operculi*, which we first recognised in *Satanoperca* sp.

Muscle	Origin	Insertion
Muscles of the cheek		
Adductor mandibulae		
Pars malaris (Figs. 1–2)	preopercular *lateralis* canal; ventral arm of hyomandibula	base of maxillary head's medial face; base of ventral process of anguloarticular; *segmentum mandibularis* tendon
Pars rictalis (Figs. 1–2)	preopercle; quadrate	dentary coronoid process; anguloarticular primordial process
Pars stegalis (Figs. 2–3)	metapterygoid body and external face of metapterygoid *calyx*; ventral arm of hyomandibula; connective tissue between preopercle and metapterygoid; symplectic	*pars rictalis*; coronomeckelian
Segmentum mandibularis (Fig. 2)	medial side of quadrate (including head); preopercle	dentary coronoid process and ventral arm, well posterior to *intermandibularis*; ventral process of anguloarticular

Levator arcus palatini (Figs. 1, 3)	posteroventral portion of sphenotic	dorsal portion of hyomandibula; internal face of metapterygoid *calyx*
Dilatator operculi (Figs. 1, 3)	posterodorsal portion of sphenotic; ventral portion of pterotic; head of hyomandibula	anterodorsal corner of opercle (tendinous tissue inserts on opercular anterodorsal process)
Levator operculi (Figs. 1, 4)	posteroventral portion of pterotic	dorsomedial portion of opercle, dorsal to the opercular shelf
Pars post-temporalis	absent (see text)	absent (see text)
Adductor hyomandibulae		
Pars primordialis (Figs. 4–6)	exoccipital (?)	medial face of hyomandibula, dorsally to opercular condyle
Pars parasphenoidalis pterygoidea (Figs. 1, 3–5)	ventral wing of parasphenoid	medial face of metapterygoid body; dorsal portion of endopterygoid
Pars parasphenoidalis hyomandibularis (Fig. 4)	parasphenoid, near its limits with prootic and sphenotic	medial face of anterodorsal expansion of hyomandibula

Adductor operculi (Fig. 4–6)	exoccipital (?)	medial face of opercle, on the dorsal face of anterior portion of opercular shelf and medial process that projects from the shelf
Muscles of the ventral surface of the head		
Intermandibularis (Figs. 2, 7)	anterior portion of medial face of dentary	antimere
Protractor hyoidei (Figs. 7–8)	anterior portion of medial face of dentary	middle portion of lateral face of anterior ceratohyal, between branchiostegal rays 1–2
Hyohyoideus inferioris	absent	absent
Hyohyoideus abductor 1 (Fig. 8)	anteromedial side of the interdigitations between anterior ceratohyal and ventral hypohyal	central portion of branchiostegal ray 1
Hyohyoideus abductor 2 (Fig. 8)	anteromedial side of the anterior portion of anterior ceratohyal	central portion of branchiostegal ray 2
Hyohyoideus abductor 3 (Fig. 8)	posterior rim of the branchiostegal ray 1	central portion of branchiostegal ray 2
Hyohyoideus abductor 4 (Fig. 8)	posterior rim of the branchiostegal ray 1	central portion of branchiostegal ray 3
Hyohyoideus abductor 5 (Fig. 8)	posterior rim of the branchiostegal ray 1	central portion of branchiostegal ray 4

Hyohyoideus adductor		
Pars dorsalis (Figs. 4, 8)	posteroventral margin of opercle; dorsal portion and process of subopercle; membrane between subopercle and preopercle	branchiostegal ray 1 (also connecting remaining branchiostegal rays)
Pars ventralis proximalis (Fig. 8)	ventrolateral side of the interdigitations between anterior ceratohyal and ventral hypohyal (ventral to origin of *hyohyoideus abductor 1*)	external side of contralateral branchiostegal ray 1, close to its proximal extremity
Pars ventralis distalis (Fig. 8)	ventrolateral side of the interdigitations between anterior ceratohyal and ventral hypohyal (ventral to origin of *hyohyoideus abductor 1*); raphe between the muscle and its antimere	external side of contralateral branchiostegal ray 1, along most of its length, except the proximal portion
Pars marginalis	absent	absent
Muscles serving the dorsal parts of the branchial arches		
Levator externus 1 (Figs. 5, 9–12)	sphenotic process of prootic	posterior rim of external face of epibranchial 1
Levator externus 2 (Figs. 5, 11–12)	sphenotic process of prootic	posterior rim of external face of epibranchial 2

Levator externus 3 (Figs. 5, 10, 13)	sphenotic process of prootic	uncinate process of epibranchial 3
Levator externus 4 (Figs. 5, 10, 13)	sphenotic process of prootic	uncinate process of epibranchial 4; *levator externus 5*
Levator externus 5 (Figs. 5, 9–11)	fossa on dorsal portion of prootic	raphe on proximal portion of *obliquus posterior 2*; cleithrum (see description)
Levator internus 1 (Figs. 5, 9–11)	sphenotic process of prootic	connective tissue that envelopes the dorsomedial corner of pharyngobranchial 2; cartilage on tip of epibranchial 1 uncinate process; body of pharyngobranchial 1
Levator internus 2 (Figs. 9, 14)	sphenotic process of prootic	lateral portion of pharyngobranchial 3, adjacent to the articulation with epibranchial 3
Levator posterior (Figs. 5–6, 9–10)	exoccipital (?), on posterior rim of the fossa that contains the *adductor operculi*	posterior face of epibranchial 4, close to the ventrolateral extremity of the bone
Obliquus dorsalis 3–4 (Figs. 9–10, 13–15)	pharyngobranchial 3, lateral to neurocraniad articulation facet	ventral face of the anterodorsal expansion of the epibranchial 4; uncinate process of epibranchial 3

Obliquus posterior 1 (Fig. 10)	epibranchial 4 uncinate process; levator posterior	base of ceratobranchial 5 posterolateral process; *obliquus posterior 2*
Obliquus posterior 2 (Figs. 10, 15)	raphe on distal portion of *levator externus 5*; *levator externus 4* tendon; internal face of process of the extremity of the epibranchial 4 that articulates with ceratobranchial 4	base of ceratobranchial 5 posterolateral process; raphe with *obliquus posterior 3*
Obliquus posterior 3 (Figs. 9–10, 15)	dorsal face of the anterodorsal expansion of the epibranchial 4	base of ceratobranchial 5 posterolateral process
Obliquus posterior 4 (Fig. 10)	epibranchial 4, posteroventrally to the extremity that articulates with the upper tooth-plate 4	posterior margin of ceratobranchial 5
Adductor branchialis 1 (Figs. 5, 12)	both faces of process on posteroventral margin of epibranchial 1 lobe	ceratobranchial 1; cartilage between ceratobranchial 1 and epibranchial 1; base of dorsalmost external branchial filaments of 1st arch
Adductor branchialis 2 (Figs. 5, 12)	ventral face of lateral wing of epibranchial 2	ceratobranchial 2; cartilage between ceratobranchial 2 and epibranchial 2

Adductor branchialis 3 (Figs. 5, 13)	ventral face of lateral process of epibranchial 3	ceratobranchial 3; cartilage between ceratobranchial 3 and epibranchial 3; possibly to base of dorsalmost external branchial filaments of 3rd arch
Adductor branchialis 4 (Figs. 5, 13)	ventral margin of epibranchial 4	ceratobranchial 4; cartilage between ceratobranchial 4 and epibranchial 4
Adductor branchialis 5 (Figs. 5, 10)	process of the extremity of the epibranchial 4 that articulates with ceratobranchial 4	process of the posterolateral extremity of ceratobranchial 5
Transversus pharyngobranchialis 2 (Figs. 9, 11, 14–15)	parasphenoid; anterior face of pharyngobranchial 3	lateral portion of anterior face of pharyngobranchial 2
Transversus pharyngobranchialis 2a (9, 11, 14B,C, 15)	lateral portion of anterior face of pharyngobranchial 2	antimere
Transversus epibranchialis 2 (Figs. 9–10, 14A, 15)	antimere; connective tissue covering neurocraniad pharyngobranchial 3 articulation facet	dorsal portion of anterior expansion of epibranchial 2
Transversus pharyngobranchialis 3 (Figs. 9, 14B,F, 15)	pharyngobranchial 3, posterolaterally to the neurocraniad articulation facet	antimere

Transversus epibranchialis 4 (Figs. 9, 15)	connective tissue between epibranchial 4 and upper tooth-plate 4	antimere
Retractor dorsalis (Figs. 6, 9–10, 14)	vertebral centra 1–3 and hypapophysis of 3rd vertebra	posterior portion of pharyngobranchial 3
Rectus pharyngobranchialis 2–3, n. nov. (Fig. 14A, E, F)	anterolateral margin of pharyngobranchial 3	posterior face of pharyngobranchial 2
Circumpharyngobranchialis		
Pars lateralis (Fig. 14A, C–F)	posterolateral corner of upper tooth-plate 4	anterolateral side of pharyngobranchial 2, close to the base of the teeth
Pars medialis (Fig. 14E)	posterolateral corner of upper tooth-plate 4	anteromedial corner of pharyngobranchial 3
Muscles serving the ventral parts of the branchial arches		
Sphincter oesophagi (Figs. 9–10, 16)	gut	posterior portion of pharyngobranchial 3; ceratobranchial 5; connective tissue between upper tooth-plate 4 and ceratobranchial 5
Obliquus ventralis 1		
Pars abductoris rectus (Figs. 16, 17A)	lateral portion of hypobranchial 1	blunt process at tip of ceratobranchial 1

Pars addcutoris obliquus (Figs. 16, 17A)	central portion of dorsal face of hypobranchial 1	cartilage at tip of ceratobranchial 1
Pars adductoris transversus (Figs. 16, 17A)	basibranchials 1–2; antimere	cartilage at tip of ceratobranchial 1
Obliquus ventralis 2		
Pars abductoris rectus (Fig. 17B)	lateral portion of hypobranchial 2	blunt process at tip of ceratobranchial 2
Pars adductoris obliquus (Figs. 16, 17B–C)	basibranchial 1; rostral and cross ligamentous systems	blunt process at tip of ceratobranchial 2
Pars adductoris transversus (Fig. 17C)	posterior face of hypobranchial 2; antimere; possibly basibranchial 3	cartilage at tip of ceratobranchial 2
Obliquus ventralis 3		
Pars abductoris rectus (Fig. 17D)	ventrolateral face of hypobranchial 3	body of ceratobranchial 3
Pars adductoris (Figs. 16, 17D)	semi-circular ligamentous system; medial face of hypobranchial 3	body of ceratobranchial 3
Transversus ventralis 4 (Figs. 16, 17D)	ceratobranchial 5 keel; antimere	medial face of ceratobranchial 4
Rectus ventralis 4		

Pars medialis (Fig. 17D)	semi-circular ligamentous system	medial face of medial keel of ceratobranchial 4
Pars lateralis (Figs. 16, 17D)	semi-circular ligamentous system; *obliquus ventralis 3, pars adductoris*	lateral face of medial keel of ceratobranchial 4
Rectus communis (Figs. 5, 16)	dorsal keel and spine of urohyal	lateral face of ceratobranchial 5; lateral face of *pharyngoclavicularis externus*
Muscles between the pectoral girdle and the skull, hyoid, and branchial arches		
Sternohyoideus (Figs. 5, 18)	ventral portion of lateral wing of cleithrum; *hypaxialis*	entire surface of urohyal
Pharyngoclavicularis externus		
Pars anterior (Figs. 5, 18)	ventralmost portion of medial wing of cleithrum, reaching the angle with lateral wing	anterolateral face of ceratobranchial 5; branchial groove of ceratobranchial 4
Pars posterior (Figs. 5, 16, 18)	dorsal to origin of *pars anterior*, not reaching the angle with lateral wing of cleithrum	anterolateral face of ceratobranchial 5, posteriorly to insertion of *pars anterior*
Pharyngoclavicularis internus (Figs. 5, 16, 18)	medial rim of cleithrum	body of ceratobranchial 5, close to its anterolateral margin; posterior portion of ceratobranchial 5 keel
Protractor pectoralis (Figs. 5, 6B, 18)	lateral process of exoccipital (?)	anterior face of the dorsal portion of cleithrum

Levator pectoralis (Figs. 1, 5, 6B, 18)	exoccipital, pterotic and epiotic (?)	proximal extrascapular; post-temporal; supracleithrum; cleithrum; Baudelot's ligament; *hypaxialis*
Muscles of the pectoral fin		
Abductor superficialis		
Pars radii pectorales ventrales (Fig. 18)	posterior face of lateral wing of cleithrum	ventralmost pectoral-fin rays
Pars radii pectorales mesiales (Fig. 19A)	posterior face of lateral wing of cleithrum	8th pectoral-fin ray
Pars radii pectorales dorsales (Fig. 19A)	posterior face of lateral wing of cleithrum	2nd–7th pectoral-fin rays
Abductor profundus (Fig. 19B)	coracoid; ventral tip of posterior face of lateral wing of cleithrum	all dorsal-fin rays, except 1st
Arrector ventralis (Figs. 18–19)	posterior face of lateral wing of cleithrum	1st pectoral-fin ray
Adductor superficialis		
Pars medialis (Fig. 20)	posterior face of dorsal portion of medial wing of cleithrum and medial face of dorsal portion of	ventral pectoral-fin rays

	cleithrum, from immediately ventral to Baudelot's ligament to posterior to *pharyngoclavicularis internus*	
Pars lateralis (Fig. 21)	most of posterior face of medial wing of cleithrum (ventrally limited by *arrector dorsalis*)	3rd–4th pectoral-fin rays
Adductor profundus (Fig. 20)	posterior face of ventral portion of medial wing of cleithrum; lateral face of basipterygium; coracoid	all pectoral-fin rays
Adductor radialis (Fig. 21)	radials 1–3	three ventralmost pectoral-fin rays
Arrector dorsalis (Figs. 20–21)	ventral portion of posterior face of medial wing of cleithrum	2nd pectoral-fin ray
Coracoradialis	absent (or fused to *abductor profundus*)	absent (or fused to *abductor profundus*)
Muscles of the pelvic fin		
Abductor superficialis pelvicus (Fig. 22A)	lateral margin of ventromedial process of basipterygium; *hypaxialis*	ventral basal process of pelvic-fin spine and of all pelvic-fin soft rays
Abductor profundus pelvicus (Fig. 22A)	ventral face of body of basipterygium; lateral margin of ventromedial process of basipterygium	pelvic-fin soft rays

Arrector ventralis pelvicus (Fig. 22A)	medial face of ventrolateral keel of basipterygium; medial face of *arrector dorsalis pelvicus*	ventral portion of pelvic-fin spine, close to its base
Adductor superficialis pelvicus		
Pars dorsalis (Fig. 22B)	medial rim of basipterygium	ventral basal process of pelvic-fin soft rays 1–4
Pars ventralis (Fig. 22B)	medial rim of basipterygium	ventral basal process of pelvic-fin spine
Adductor profundus pelvicus (Fig. 22B)	dorsal face of body of basipterygium	proximal tip of pelvic-fin soft rays 1–4
Arrector dorsalis pelvicus (Fig. 22)	lateral faces of ventrolateral and dorsolateral keels of basipterygium	lateral face of pelvic-fin spine base
Extensor proprius (Fig. 22B)	*adductor superficialis pelvicus*; *adductor profundus pelvicus*	laterodorsal face of pelvic-fin soft rays 4–5
Muscles of the dorsal fin		
Erectores dorsales (Figs. 23A, 24)	dorsal-fin proximal pterygiophores	anteriorly to base of lateral process of dorsal-fin spines and soft rays
Depressores dorsales (Figs. 23A, 24)	dorsal-fin proximal pterygiophores	posterior process of dorsal-fin spines and soft rays

Inclinatores dorsales (Fig. 23B)	skin; *epaxialis*	lateral face of lateral process of dorsal-fin spines and soft rays; ventral face of lateral wing of dorsal-fin distal pterygiophores
Muscles of the anal fin		
Erectores anales (Figs. 23A, 25)	anal-fin proximal pterygiophores	anteriorly to base of lateral process of anal-fin spines and soft rays
Depressores anales (Figs. 23A, 25)	anal-fin proximal pterygiophores	posterior process of anal-fin spines and soft rays
Inclinatores anales (Fig. 23B)	skin; *hypaxialis*	lateral face of lateral process of anal-fin spines and soft rays; dorsal face of lateral wing of anal-fin distal pterygiophores
Carinal muscles		
Supracarinalis anterior (Fig. 24A)	supraoccipital crest	supra-neural; first haemal spine; first dorsal-fin proximal pterygiophore
Supracarinalis medius	absent	absent
Supracarinalis posterior (Figs. 26, 27C)	last dorsal-fin distal pterygiophore; *epaxialis*	two posteriormost dorsal procurrent caudal-fin rays

Infracarinalis anterior (Fig. 27B)	ventral portion of cleithrum; *hypaxialis* musculature	lateral process of basipterygium; pelvic-fin
Infracarinalis medius (Fig. 27B)	first anal-fin distal pterygiophore; *hypaxialis*	ischiatic process of basipterygium; *hypaxialis*
Infracarinalis posterior (Figs. 26, 27D)	last anal-fin distal pterygiophore; *hypaxialis*	two posteriormost ventral procurrent caudal-fin rays
Muscles of the caudal fin		
Interradiales (Fig. 26)	see description	see description
Hypochordal longitudinalis (Fig. 26A–B)	horizontal myoseptum; parhypural; hypurals 2–3	dorsalmost (unbranched) principal caudal-fin ray and the four branched rays immediately ventral to it, slightly distally to their bases; the remaining three dorsal-lobe branched rays, on their bases
Flexor dorsalis		
Pars anterioris (Fig. 26)	two posteriormost vertebral centra bearing a well-developed neural spine	lateral process on base of ventralmost dorsal-lobe principal caudal-fin ray
Pars posterioris (Fig. 26)	posteriormost well-developed neural spine; posteriormost well-developed centrum; uroneural	lateral process on bases of all dorsal-lobe principal caudal-fin rays

Flexor dorsalis superior (Fig. 26)	distal portion of last well-developed neural spine; epurals	posteriormost dorsal procurrent caudal-fin ray
Flexor ventralis (Fig. 26A)	horizontal myoseptum; first to third posteriormost haemal arches and respective centra; parhypural; hypurals 1–2	all principal caudal-fin rays
Flexor ventralis inferior (Fig. 26)	first and second posteriormost haemal spines	posteriormost ventral procurrent caudal-fin ray
Flexor ventralis externus	absent	absent
Adductor dorsalis	absent	absent
Proximalis	absent	absent
Body muscles		
Epaxialis (Figs. 24A, 27)	see description	see description
Lateralis superficialis (Fig. 23B)	see description	see description
Hypaxialis obliquus superioris (Fig. 23B)	see description	see description
Hypaxialis obliquus inferioris (Fig. 23B)	see description	see description
Spinalis	see *supracarinalis anterior*	see *supracarinalis anterior*

Muscles of the eye		
Obliquus inferior (Figs. 6C, 28)	posterior wing of mesethmoid	ventral face of eyeball
Obliquus superior (Figs. 6C, 28)	anterior myodome (mesethmoid)	dorsal face of eyeball
Rectus externus (Figs. 6C, 28)	1st vertebra; basioccipital	posterior (ossified) face of eyeball
Rectus inferior (Figs. 6C, 28)	basiphenoid	ventral face of eyeball
Rectus internus		
Pars dorsalis (Figs. 6C, 28)	basiphenoid	anterior (ossified) face of eyeball
Pars ventralis (Figs. 6C, 28)	posterior myodome (parasphenoid; basioccipital)	anterior (ossified) face of eyeball
Rectus superior (Figs. 6C, 28)	anterior opening of posterior myodome (parasphenoid)	dorsal face of eyeball

Table 2. List of synonyms of the muscles described herein, extracted from selected references. Question marks indicate that the correspondence is uncertain. See text for further explanations.

Muscle (this paper)	Synonym	Reference
Muscles of the cheek		

Adductor mandibulae, *pars malaris*	*Adductor mandibulae* A_1	Anker (1978:238)
		Stiassny (1981)
	AM1	Arbour & López-Fernández (2018)
	Pars rictalis	Weller *et al*. (2016)
Adductor mandibulae, *pars rictalis*	*Adductor mandibulae* A_2	Anker (1978:238)
		Stiassny (1981)
	AM2	Arbour & López-Fernández (2018)
	Pars malaris	Weller *et al*. (2016)
Adductor mandibulae, *pars stegalis*	*Adductor mandibulae* A_3	Anker (1978:239)
		Stiassny (1981)
	AM3	Arbour & López-Fernández (2018)
Adductor mandibulae, *segmentum mandibularis*	*Adductor mandibulae* A_ω	Anker (1978:241)
		Stiassny (1981)
Adductor hyomandibulae	*Adductor arcus palatini*; *Adductor operculi*	Anker (1978:241–245)
	(portion inserting on hyomandibula)	

Adductor operculi	*Adductor operculi* (portion inserting on the opercle)	Anker (1978:244–245)
Muscles of the ventral surface of the head		
Protractor hyoidei	*Geniohyoideus*	Anker (1978:246–248)
Hyohyoidei abductores	*Hyohyoideus ventralis*, *pars rostralis*	Anker (1978:248)
Hyohyoideus adductor	*Hyohyoideus ventralis*, *pars caudalis*; *Hyohyoideus dorsalis*; *Hyohyoideus marginalis* (absent)	Anker (1978:248–250)
Muscles serving the dorsal parts of the branchial arches		
Levator externus 4	*Levator externus 4* (part; although other authors do not mention an insertion on epibranchial 4)	Anker(1978:254) Springer & Johnson (2004)
Levator externus 5	*Levator externus 4* (or the major part)	Anker (1978:254) Springer & Johnson (2004)
Levator internus 1	*Levator internus medialis*	Anker (1978:256)
Levator internus 2	*Levator internus lateralis*	Anker (1978:256)

Obliquus dorsalis 3–4	*Obliquus dorsalis*	Anker (1978:256)
Obliquus posterior 1	*Levator externus 4* (part) (?)	Anker (1978)
Obliquus posterior 2	*Levator externus 4* (part) (?)	Anker (1978)
Obliquus posterior 3	*Obliquus posterior* (?)	Anker (1978:254, Fig. 12A)
Obliquus posterior 4	*Sphincter oesophagi* (part) (?)	Anker (1978)
Adductor branchialis 1	First branchial *adductor*; *interbranchial abductor*	Cichocki (1976, Fig. 1.17)
Transversus pharyngobranchialis 2	*Cranio-pharyngobranchialis 2*	Anker (1978:258)
Transversus pharyngobranchialis 2a	*Transversus pharyngobranchialis 2*	Anker (1978:258)
Transversus pharyngobranchialis 3	*Transversus pharyngobranchialis 4*, ventral section	Anker (1978:257)
Transversus pharyngobranchialis 4	*Transversus pharyngobranchialis 4*, dorsal section	Anker (1978:257)
Circumpharyngobranchialis	Subepithelial muscular tissue (part)	Anker (1978:261, Fig. 14)
Muscles serving the ventral parts of the branchial arches		
Sphincter oesophagi, ceratobranchial section	*Transversus ventralis 5* (?)	Winterbottom (1974a)

Rectus communis	*Pharyngohyoideus*	Anker (1978:266, Fig. 10)
Muscles between the pectoral girdle and the skull, hyoid, and branchial arches		
Pharyngoclavicularis externus, *pars anterior*	*Pharyngocleithralis externus*, ventral section	Anker (1978:266, Fig. 10)
Pharyngoclavicularis externus, *pars posterior*	*Pharyngocleithralis externus*, dorsal section	Anker (1978:266–267, Fig. 10).
Pharyngoclavicularis internus	*Pharyngocleithralis internus*	Anker (1978:267)
Adductor superficialis, *pars medialis*	*Adductor superficialis*	Baerends & Baerends-Van Roon (1950:15, Fig. 5d)
Adductor superficialis, *pars lateralis*	*Arrector dorsalis* (part)	Baerends & Baerends-Van Roon (1950:16, Fig. 5e)
Arrector dorsalis	*Arrector dorsalis* (part)	Baerends & Baerends-Van Roon (1950:16, Fig. 5e)
Carinal muscles		
Supracarinalis posterior	*Flexor dorsalis superior* (part)	Baerends & Baerends-Van Roon (1950, Fig. 4)
Infracarinalis posterior	*Flexor ventralis inferior* (part)	Baerends & Baerends-Van Roon (1950, Fig. 4)
Flexor dorsalis, *pars anterioris*	*Proximalis* (?)	Winterbottom (1974a:293)

2.3.1 Muscles of the cheek

***Adductor mandibulae*.** We recognize four parts of the *adductor mandibulae*, of which the *segmentum mandibularis* is topologically distant from the other three, lying on the medial face of the lower jaw. The other parts (*i.e.*, *malaris*, *rictalis* and *stegalis*), form a roughly triangular pack that occupies the cheek, covering the bones of the suspensorium, thus lying ventrally to the eye, posteroventrally to the lachrymal, anterior to the vertical arm of the preopercle and dorsal to its horizontal arm. Those three parts, although clearly distinct from each other towards their insertion, merge to some degree near their origins. Terminology follows Datovo & Vari (2014).

Pars malaris. The *pars malaris* lies on the dorsal portion of the *adductor mandibulae* pack and has the shape of an elongate triangle ventrally inclined towards its insertion (Fig. 1). It originates as a thin sheet of fibres (dorsally, as an aponeurosis), due to the distal portion of the *levator arcus palatini*, which lies medially to the *pars malaris*. In lateral view, the fibres converge uniformly into the insertion tendon, tapering towards it. In medial view, the *pars malaris* appears to divide into two poorly distinct sections, the ventral one having a pearl glow anteriorly, suggestive of tendinous tissue (Fig. 2). Thus, the maxillary tendon begins in the middle of the medial face of the *pars malaris*. The proximal portion of the tendon, as well as the portion that inserts on the maxilla, is round in cross section, while the portion that inserts on the lower jaw is flat (laterally compressed). This latter portion runs laterally to the *segmentum mandibularis* tendon and medially to the *pars stegalis* tendon. In *Haplochromis elegans*, an aponeurotic sheet immediately ventral to the eyeball partially divides the *pars malaris* in an anterior and a posterior section (Anker, 1978:238). That division is absent from *Geophagus sveni* (Fig. 1).

Pars rictalis. The *pars rictalis* lies ventral to the *pars malaris* and has approximately a quadrilateral shape, in which the posterior side is much deeper than the anterior one (Fig. 1). It is also a sheet-like muscle, and has a slight dorsomedial concavity that fits the *pars malaris*. The dorsal fibres are more ventrally inclined towards the insertion, while the ventral fibres are slightly dorsally inclined. The origin is muscular. The insertion is ventrally muscular (to anguloarticular) and dorsally tendinous (to dentary) (Figs. 1–2).

Pars stegalis. The *pars stegalis* lies medial to the *pars rictalis* and to the proximal portion of the *pars malaris* (Figs. 2–3). It is shaped approximately as *pars rictalis*, but even deeper proximally. Its tendon lies lateral to the *segmentum mandibularis* and, although inserting on a different site than the *pars rictalis*, adheres to the latter laterally by connective tissue. In fact, the whole *pars stegalis* attaches to the *pars rictalis*, making the limits between the two parts confused. The fibres homogeneously converge into the tendon, which is proximally deep, sheet-like, but becomes cord-like after passing the anguloarticular primordial process. In *Geophagus sveni* there seems to be no clear division of *pars stegalis* into sections, as suggested by Anker (1978:239) for *Haplochromis elegans*. Moreover, we observed that the ventral portion of *pars stegalis* origin includes the connective tissue between preopercle and metapterygoid, the symplectic and the quadrate (*vs*. the rostral edge of the preopercular crescent in *H. elegans*).

Segmentum mandibularis. The *segmentum mandibularis* has a delicate appearance, being somewhat translucent (Fig. 2). It is medial to the *pars stegalis* tendon and its fibres diverge anterodorsally or anteroventrally towards the insertion, forming two almost indistinguishable sections (equivalent to *pars coronalis* and *pars mentalis* of Datovo & Vari, 2014). A sheet of connective tissue, called here an aponeurotic system, covers the entire *segmentum*

mandibularis. Its tendon runs medial to the medial head of the quadrate and spreads towards the origin into an aponeurotic sheet. The dorsal margin of the fibre bunch seems to be largely formed by tendinous tissue. In *Geophagus sveni*, the insertion of the *segmentum mandibularis* falls distinctly short from the *intermandibularis*, whereas in *Haplochromis elegans* the two muscles are adjacent (Anker, 1978:241, Fig. 5).

***Levator arcus palatini*.** The *levator arcus palatini* has an irregular shape (Figs. 1, 3). Its insertion site is approximately vertical. The dorsalmost fibres – which slightly hide the anteroventral portion of the *dilatator operculi* – run only a short distance from sphenotic to hyomandibula, thus having an oblique orientation. Fibres that originate more ventrally, which are longer, have a vertical orientation. An aponeurotic sheet covers part of the anterodorsal face of the muscle, but not the anterolateral face as in *Haplochromis elegans* (Anker, 1978:241, Figs. 1–2). Additionally, the insertion is completely muscular in *G. sveni*.

***Dilatator operculi*.** Approximately triangular (Figs. 1, 3). An anteroventral section runs from sphenotic to base of anterodorsal process of opercle, its fibres obliquely descending posteriad. A posterodorsal section runs between pterotic and the anterodorsal process of opercle, its fibres being more vertical. Posteriormost fibres are contiguous with tendinous tissue (most evident in the fibres originating between clst2 and clst3). Its attachments are otherwise completely muscular. The insertion area lies ventral to the middle of the origin area, due to the skull shape (*vs*. ventral to the posterior extremity of the origin area in *Haplochromis elegans*, *cf.* Anker, 1978, Fig. 1). Additionally, the *levator arcus palatini* hides a relatively small portion of the *dilatator operculi* in *Geophagus sveni* (*vs*. a larger portion in *H. elegans*, *cf.* Anker, 1978, Figs. 1–2).

***Levator operculi*.** The origin of this fan-like muscle is compact, but its insertion site is extensive, spanning almost the whole area of the medial face of the opercle that lies dorsally to the opercular shelf (Figs. 1, 4). Its attachments are completely muscular, except for a few medial fibres that originate tendinously. In *Geophagus sveni*, the posteriormost fibres insert distantly from the fibres of the *hyohyoideus adductor*, *pars dorsalis*, instead of adjacent to it (and merging into a same sheet of connective tissue) in *Haplochromis elegans* (*cf.* Anker, 1978:244, Fig. 4).

Pars post-temporalis. We found this part only in *Satanoperca* Günther and in one undescribed species of *Teleocichla*, thus we will described and illustrate it in future paper on phylogeny myological variation among cichlids. Not previously reported in the literature.

***Adductor hyomandibulae*.** Terminology follows Datovo & Rizzato (2018). This muscle originates and inserts muscularly. We recognize three parts. *Pars primordialis*, which corresponds to the portion of *adductor operculi* that inserts on hyomandibula in Anker (1978:244–245) is barely distinguishable from our *adductor operculi*, and originates quite far from the other two parts. Although Anker (1978:241–242) recognized a difference in shape and fibre direction between the anterior and posterior portions of his *adductor arcus palatini* (which corresponds to our *pars parasphenoidalis pterygoidea* and *pars parasphenoidalis hyomandibularis*, separated by the pseudobranchial fissure *sensu* Datovo & Castro, 2012) in *Haplochromis elegans*, he did not consider it to be divided in parts. The main difference, though, is that in *Geophagus sveni* no fibres of the *adductor hyomandibulae* insert on the palatine, which occurs in *H. elegans*.

Pars primordialis. See "*adductor operculi*" below.

Pars parasphenoidalis pterygoidea. Although we recognize no sections to this part, its anterior and posterior portions are somewhat different in shape and fibre orientation (Figs. 1, 3–5). The portion that originates anteriorly to the ventral process of the parasphenoid keel is similar to an arched awning, with uniform thickness, its fibres being approximately transverse and attaching to the endopterygoid (Figs. 3–5). The portion arising from the process is much deeper (Fig. 4). Its fibres fan out to insert from the anterior portion of metapterygoid (anteroventrally), to the posterior portion of metapterygoid (posteroventrally), to the dorsal portion of metapterygoid (posterodorsally). This portion has a posterior concavity that fits a pseudobranch (not illustrated), which is ventral to *pars parasphenoidalis hyomandibularis*. The fibres of the *pars parasphenoidalis pterygoidea* insert obliquely and extensively, as in *levator operculi*.

Pars parasphenoidalis hyomandibularis. The *parasphenoidalis hyomandibularis* is small, and its fibres, short (Fig. 4). Although tightly attached to the *pars parasphenoidalis pterygoidea* by connective tissue, the direction of its fibres is quite distinct and it is possible to tear them apart by dissection.

***Adductor operculi*.** At the origin, the *adductor operculi* is fused to the *adductor hyomandibulae, pars primordialis*, although the muscles diverge distally, inserting on different bones. The muscle originates broadly and abruptly thins, becoming cylindrical (Figs. 4–6). Thus, it has the appearance of a tree root and the base of the trunk. The origin is completely muscular and the insertion is almost completely so, except for the portion that inserts on the process of the opercular shelf, which presents tendinous tissue. The *adductor*

hyomandibulae, pars primordialis is much smaller and half-hidden by *adductor operculi* in medial view.

2.3.2 Muscles of the ventral surface of the head

***Intermandibularis*.** The *intermandibularis* has the aspect of a tape, spanning between the contralateral dentaries (Figs. 2, 7). All fibres run in a transversal sense. The attachment is muscular. It lies dorsally to the origin of the *protractor hyoidei*, anterodorsal and anteroventral sections (*geniohyoideus*, rostral part, of Anker, 1978) and ventrally to the origin of the *protractor hyoidei*, lateral section (*geniohyoideus*, lateral part, of Anker, 1978). Differently from *Haplochromis elegans* (see Anker, 1978, Fig. 5), in *Geophagus sveni* the attachment of the *intermandibularis* to the dentary is much anterior to the insertion of the *adductor mandibulae*, *segmentum mandibularis* (Fig. 2).

***Protractor hyoidei*.** We consider the *protractor hyoidei* to be a paired muscle, and recognize four sections (Figs. 7–8; we opted not for considering them as parts because they merge distally, preventing us from recognizing their limits). We call posterior section the one in which the contralateral halves are completely separate (*geniohyoideus*, caudal part, plus distal half of lateral part of Anker, 1978:246–248). The anterior (proximal) end of this section is a transversal raphe on which the fibres of the other three sections insert. The posterior (distal) end, which corresponds to the insertion of the muscle, is muscular. The lateral section (proximal half of *geniohyoideus*, lateral part, of Anker, 1978), which is very narrow, originates dorsally to the *intermandibularis*, as a long, tape-like tendon. The anteroventral and anterodorsal sections (both constituting what Anker, 1978, treated as *geniohyoideus*, rostral part) are separate from their antimeres only by the sagittal raphe. The anterodorsal section originates as a sheet-like tendon, ventrally to the *intermandibularis*, close to the sagittal plane.

The anteroventral section originates muscularly, also ventral to the *intermandibularis*, but somewhat distant from the sagittal plane. The fibres of the anteroventral section diverge anteriorly (*i.e.*, towards origin), while the fibres of the remaining sections are parallel to the sagittal plane. Anker (1978, Fig. 8A) recognized an incipient division of his *geniohyoideus*, rostral part, into a medial and a lateral section. However, we believe that partial division not be homologous with the division seen in *Geophagus sveni* because of the different relative positions between the anteroventral and anterodorsal sections.

Hyohyoidei abductores. We identified five individual *hyohyoidei abductores*, all of which are tape-like, with homogeneously oriented fibres, whose insertions appear to be through a very short tendon each (Fig. 8). The *hyohyoidei abductores 3–5* originate tendinously, while *hyohyoidei abductores 1–2* originate muscularly. Anker (1978:248) recognised only four of such muscles (under the designation of *musculus hyohyoideus ventralis, pars rostralis*), one for each of the first four branchiostegal rays.

***Hyohyoideus adductor*.** The *hyohyoideus adductor* is a very thin, translucent, membranous muscle, which connects the medial side of the opercle with the branchiostegal rays from either side (Fig. 8). We recognize three parts, based on topological isolation, different fibre directions and thickness. We recognized no part corresponding to the *musculus hyohyoideus marginalis* of Anker (1978:248–250, Figs. 4, 7). We also rejected his interpretation of the so-called *musculus hyohyoideus* complex, preferring a nomenclature more consistent with that of Winterbottom (1974a), concerned with the functional aspect of the muscles (see below).

Pars dorsalis. Connects the medial side of the opercle, to which the fibres attach parallely, to branchiostegal ray 1, also connecting the remaining branchiostegal rays (Figs. 4, 8). This part

is much thinner than the other parts and runs externally to *hyohyoidei abductores 2–5*. Differs from the *musculus hyohyoideus dorsalis* of Anker (1978:250, Fig. 4B) only in the origin, which is far from the insertion of the *levator operculi* (*vs*. close to it in *Haplochromis elegans*).

Pars ventralis proximalis. Connects branchiostegal ray 1 to contralateral hyoid arch (Fig. 8). It originates as a tape-like tendon, which is paired and contiguous with the raphe between contralateral halves of *pars ventralis distalis*. The *pars ventralis proximalis* is tape-shaped itself and thicker than the other parts. Its fibres are parallel and overlap externally the *hyohyoideus abductor 1*. They also cross the contralateral *pars ventralis proximalis*, the one inserting on the left side running external (ventral) to the one inserting on the right side (in accordance with Anker, 1978:249). To Anker (1978:248–249), the muscle corresponding to our *hyohyoideus adductor*, *pars ventralis proximalis* plus *pars ventralis distalis* is his *hyohyoideus ventralis*, *pars caudalis* (his *pars rostralis* corresponding to our *hyohyoidei abductores*). According to his illustration (Anker, 1978, Fig. 7), in *Haplochromis elegans* there is no separation between what we call the *pars ventralis proximalis* and *pars ventralis distalis*.

Pars ventralis distalis. We consider this part to be paired, because there is a raphe separating the contralateral halves (Fig. 8). Posteriorly, the *pars ventralis distalis* connects the contralateral branchiostegal rays 1, and its fibres are arched, but approximately transversal. Anteriorly, the fibres become oblique to the raphe. The raphe bifurcates anteriorly, forming the contralateral tendons through which the *pars ventralis distalis* and *pars ventralis proximalis* originate from the contralateral hyoid arch. Fibres of the *pars ventralis distalis* converge upon those tendons, so the fibres of the left side cross and run externally to those of

the right side, as in *pars ventralis proximalis*. This part is of intermediate thickness when compared to the other parts and externally overlaps the distal portion of *hyohyoideus abductor 1*.

2.3.3 Muscles serving the dorsal parts of the branchial arches

***Levator externus 1*.** This muscle has a conical shape (broader towards insertion), although slightly anteroposteriorly compressed and tapering more abruptly towards its tendinous origin (Figs. 5, 9–12). The insertion is muscular, and fibres are homogeneously disposed. Differs from the *levator externus 1* of *Haplochromis elegans* by having a completely tendinous origin, *vs*. partially muscular (Anker, 1978:254). The same is true for *levator externus 2*.

***Levator externus 2*.** Same shape as *levator externus 1*, but slightly thicker (Figs. 5, 11–12).

***Levator externus 3*.** The proximal three fourths or so are conical, more anteroposteriorly flattened than *levatores externi 1–2*, and wider (Fig. 5, 10, 13). The distal fourth tapers very abruptly, ending in a short tendon. The origin is tendinous as well, and fibres are homogeneously disposed. Differs from the *levator externus 3* of *Haplochromis elegans* by the insertion site: in *H. elegans*, it inserts on the ligament between epibranchials 3 and 4 (Anker, 1978:254), while in *Geophagus sveni* it inserts on the uncinate process of the epibranchial 3, opposite to the side to which the ligament attaches.

***Levator externus 4*.** The *levator externus 4*, as we understand, is a thin, cord-like muscle, which originates and inserts tendinously (Fig. 5, 10, 13). The *levator externus 4* of Springer & Johnson (2004), Anker (1978:254) and other authors correspond to the union of our *levatores externi 4–5* (see below).

***Levator externus 5*.** The homology of this muscle is uncertain. It may well be a part of the *levator externus 4*, which would be partially in agreement with Springer & Johnson (2004), as well as with Anker (1978:254), although none of those authors reported this muscle to have more than one insertion site (*viz*. the epibranchial 4 and the ceratobranchial 5 via *obliquus posterior 2*). If it is correct to assume that our *levator externus 5* is merely a part of the *levator externus 4*, this much more developed part (*i.e.*, our *levator externus 5*) would have shifted its insertion site from epibranchial 4 to the raphe shared with *obliquus posterior 2*, effectively inserting on ceratobranchial 5 (Figs. 5, 9–11). Because the raphe between *levator externus 5* and *obliquus posterior 2* is contiguous with a tendon that inserts on cleithrum (Figs. 10), immediately ventral to *protractor pectoralis*, we also considered the possibility that the *levator externus 5* developed from a part of the *protractor pectoralis*, to which the *obliquus posterior 2* attached later in the evolution, changing its function. However, this last hypothesis seems less parsimonious, because we have no examples of related groups with a *protractor pectoralis* divided in two parts or originating adjacent to the *levator externi* and *interni*. Moreover, Springer & Johnson (2004) provided several examples in which the *obliquus posterior* attaches to the *levator externus 4* through a raphe. In the case of *Amphistichus* (Embiotocidae), illustrated by Springer & Johnson (2004; Plate 162.1B), the *levator externus 4* appears not to be clearly divided in two parts, but still there is a bunch of fibres inserting on epibranchial 4, while most of the fibres run to the raphe with *obliquus posterior*. The origin of *levator externus 5* is muscular.

***Levator internus 1*.** This muscle is shaped approximately as *levatores externi 1–2*, but much broader (Figs. 5, 9–11). The origin and insertion are muscular, except for the insertion on pharyngobranchial 1, which is through a thin strap of connective tissue. Fibres are

homogeneously disposed. Differs from the *levator internus 1* of *Haplochromis elegans* by the insertion site, clearly mostly on pharyngobranchial 2, with no fibres inserting on pharyngobranchial 3 (*vs*. on pharyngobranchial 3, possibly with a few fibres inserting on pharyngobranchial 2, but not on pharyngobranchial 1 nor in the cartilage on tip of epibranchial 1 uncinate process; *cf.* Anker, 1978:256).

***Levator internus 2*.** Cylindrical, all fibres homogeneously oriented (Fig. 9, 14). In dorsal view, the *obliquus dorsalis 3–4* completely hides the distal portion of *levator internus 2*. Origin and insertion muscular.

***Levator posterior*.** Fusiform, origin and insertion muscular, fibres homogeneously oriented (Figs. 5–6, 9–10). Anteroposteriorly flattened.

***Obliquus dorsalis 3–4*.** In dorsal view, the origin of the *obliquus dorsalis 3–4* is approximately triangular, following the shape of the articulation facet of the *pharyngobranchial 3,* and is mostly parallel to the sagittal plane (Figs. 9–10, 13, 15). The portion of the insertion that lies on the anterodorsal expansion of the epibranchial 4 lies approximately perpendicular to the sagittal plane. The small bunch of fibres that inserts on the epibranchial 3 tapers towards its uncinate process. Its middle portion overlaps dorsally the distal portion of the *levator internus 2*. The *transversus epibranchialis 2* overlaps the anterior portion of the *obliquus dorsalis 3–4*. Both the origin and the insertion are muscular, and the fibres are homogeneously oriented.

***Obliquus posterior 1*.** In posterior view, the shape is similar to a triangle, tapering towards the insertion (Fig. 10). It arises from the epibranchial 4 muscularly, and connects to the *levator*

posterior through a feeble sheet of connective tissue. It inserts on the ceratobranchial 5 process as a long, tape-like tendon, and ventromedially connects to the *obliquus posterior 2* by thin connective tissue. Topologically, it lies ventromedial to the *levator posterior*, ventrolateral to the *obliquus posterior 2*, posteroventral to the *levator externus 5*, and dorsal to the *adductor branchialis 5*. Fibres fan out homogeneously towards origin. Anker (1978:235–236) suggested that the distal portion of what he considered to be the *levator externus 4* may be a part of the *obliquus posterior*, which is coherent with the interpretation of Springer & Johnson (2004) and our own. Probably Anker (1978) considered both *obliqui posteriores 1–2* to be part of his *levator externus 4*. On the other hand, we observed that only *obliquus ventralis 2* shares a raphe with the posteriormost *levator externus*.

***Obliquus posterior 2*.** This muscle has approximately the shape of an obliquely cut cone, such that the deeper side points anterodorsally (Fig. 10, 15). The *obliquus posterior* is bipennate, thus through the middle of this deeper side runs a tendinous structure dividing the muscle in two portions with fibres of either side converging towards insertion. The insertion in the ceratobranchial 5 is by a long tendon. Connected to *obliquus posterior 3* by a raphe. See *levator externus 5* for further detail.

***Obliquus posterior 3*.** Flat, triangular muscle, which originates and inserts muscularly (Figs. 9–10, 15). Connected to *obliquus posterior 2* by a raphe. Fibres fan out from insertion to origin. Probably corresponds to the *musculus obliquus posterior* of Anker (1978:254, Fig. 12A).

***Obliquus posterior 4*.** Sheet-like, approximately rectangular. Its proximal portion lies anteroventrally to the *obliquus posterior 3* (Fig. 10). Fibres are mostly parallel. Anker (1978) possibly considered it as part of the *sphincter oesophagi*.

***Adductor branchialis 1*.** Because this muscle inserts both on the ceratobranchial 1 and on the base of some branchial filaments, it would seem that the *adductor branchialis 1* is fused to the gill-filament muscle 1 (*sensu* Springer & Johnson, 2004). This was the interpretation of Cichocki (1976). However, the gill-filament muscle 1 is present as a different structure, originating on the connective tissue linking the ceratobranchial 1 external gill rakers. The gill-filament muscle 1 consists of a feeble sheet of fibres perpendicular to the ceratobranchial 1, apparently running along most of the posterior margin of that bone, although it is difficult to distinguish it from the surrounding connective tissue at some stretches. The *adductor branchialis 1*, on the other hand, is a thick, much more developed muscle, whose numerous fibres fan out towards the insertion sites (Figs. 5, 12). There is no clear separation between the anteroventral fibres, which insert on ceratobranchial 1, and the posterodorsal fibres, which insert on the gill filaments, contrary to what Cichocki (1976, Fig. 1.17) suggests. Origin and insertion muscular. Considerably shorter, but more massive than the homologue in *Haplochromis elegans* (*cf*. Anker, 1978, Fig. 10).

***Adductor branchialis 2*.** Slightly more developed than *adductor branchialis 1* (Figs. 5, 12). Dorsal portion somewhat crescent-shaped, but fibres are approximately parallel. Origin and insertion muscular.

***Adductor branchialis 3*.** Slightly less developed than *adductor branchialis 2* (Figs. 5, 13). Shaped approximately as a semicircle. Fibres approximately parallel, except posterior ones, which apparently diverge to attach to gill filaments. Origin and insertion muscular.

***Adductor branchialis 4*.** Slightly less developed than *adductor branchialis 3* (Figs. 5, 13). Somewhat rectangular, with parallel fibres. Origin and insertion muscular.

***Adductor branchialis 5*.** Roughly fusiform (Figs. 5, 10). Originates as a thick, flat tendon. Inserts muscularly. Differs from the homologue in *Haplochromis elegans* by the muscular insertion (*vs*. aponeurotic; Anker, 1978:259).

***Transversus pharyngobranchialis 2*.** Somewhat flat in an anteroposterior direction muscle tapers slightly towards insertion (Figs. 11, 14; see also Figs. 9, 15). Fibres are nearly parallel. Both attachments muscular. Its distal portion is mostly dorsal to the proximal portion of *transversus pharyngobranchialis 2a*, but a portion of it partially hides the latter in frontal view.

***Transversus pharyngobranchialis 2a*.** Approximately drop-shaped in anterior view, tapering towards sagittal plane (Fig. 11, 14C). Proximally flat in an anteroposterior direction. Distally broadening in an anteroposterior sense (Figs. 9, 14B, 15). Origin muscular, insertion on a raphe shared with the antimere. Differs from the homologue in *Haplochromis elegans* because the antimeres are completely separate by a raphe (*vs*. raphe present only in a ventrocaudal section; Anker, 1978:258).

***Transversus epibranchialis 2*.** Roughly cylindrical, arched over the medial tip of the epibranchial 2 (Figs. 9–10, 15). Insertion muscular, immediately anteromedial to the ligament between epibranchials 1–2. Origin by tendinous tissue merging into connective tissue that envelopes the articulation facet of the pharyngobranchial 3 (Fig. 14A). Fibres parallel. Differs from the *transversus epibranchialis 2* of *Haplochromis elegans* by not being divided into parts and by not attaching to or passing over pharyngobranchial 2 (*cf.* Anker, 1978:258).

***Transversus pharyngobranchialis 3*.** Usually considered to form a single muscle with *transversus epibranchialis 4* (called *transversus pharyngobranchialis 3–epibranchialis 4*), in *Geophagus sveni* it seems completely separate from the latter, thence we treat them as two distinct muscles (Fig. 9, 14B,F, 15). The muscle is cord-like, somewhat flattened in an anteroposterior direction. The origin is muscular, and there is no apparent division between the antimeres (there is no raphe, and the fibres seem to continue from one side to the other). Fibres parallel.

***Transversus epibranchialis 4*.** The muscle is cord-like, somewhat flattened in an anteroposterior direction (Fig. 9, 15). The origin is tendinous, and there is no apparent division between the antimeres (there is no raphe, and the fibres seem to continue from one side to the other). Fibres parallel. The ventral portion of the muscle loosely attaches to the pharyngobranchial 3. Corresponds to the dorsal section of the *musculus transversus epibranchialis 4* of Anker (1978:257).

***Retractor dorsalis*.** The *retractor dorsalis* has the shape of a strongly compressed cone (Fig. 6). At the origin, it is narrowly separate from its antimere (more so anteriorly, where the eye muscle *rectus externus* occupies the space between the contralateral muscles; Fig. 6A–B).

Immediately distal to the origin, the antimeres contact each other, but do not fuse. More distally, however, they taper and become separate by a space about half the width of the insertion site, which is oval, with the long axis in a dorsomedial-ventrolateral direction (Figs. 9–10, 14). The fibres originating from the vertebral centra 1 and 2 lie ventral to the respective parapophyses, while some fibres inserting on the vertebral centrum 3 reach a point immediately posterior to the respective parapophysis (Fig. 6C). Only the basal fourth of the hypapophysis of third vertebra contributes to the origin of the *retractor dorsalis*. Nearly all fibres spanning the entire distance from origin to insertion originate from the first vertebra. The fibres arising from the second vertebra converge into those from the first vertebra close to the insertion. Those arising from the third vertebra converge into the preceding ones more proximally. We distinguished no clear sections, but upon handling, the fibres attached to the different vertebrae tend to become separate from each other (Fig. 6C). Origin muscular. Insertion partly muscular, but ventrally encompassing some aponeurotic tissue (Fig. 14, especially Fig. 14B). Differs from the homologue in *Haplochromis elegans* mainly by lacking fibres originating on the neurocranium and by the fibres originating muscularly from the basal fourth oh hypapophysis of third vertebra (*vs*. some of the fibres originating on exoccipital and fibres attaching aponeurotically to the whole anterior margin of the hypapophysis; *cf*. Anker, 1978:259–260, Fig. 11).

***Rectus pharyngobranchialis 2–3*, n. nov.** Cylindrical, with parallel fibres (Fig. 14A,E,F). The *rectus pharyngobranchialis 2–3* may derive from the *circumpharyngobranchialis*, as suggested for the *transversus pharyngobranchialis 2a* by Springer & Johnson (2004:7). It originates muscularly from the pharyngobranchial 3 immediately anteriorly to the insertion of *levator internus 2* and anteromedially to the epibranchiad 3 articulation facet. It inserts, also muscularly, on the posterior face of pharyngobranchial 2, somewhat lateral to the middle of

the bone. Apparently, previous authors have not described this muscle before, nor used this name. We need further study in order to determine its homology. One can only see *rectus pharyngobranchialis 2–3* in dorsal view after the removal of the epibranchial 2 and of the *transversus epibranchialis 2*.

***Circumpharyngobranchialis*.** Springer and Johnson (2004) proposed the name *circumpharyngobranchialis* to the 'subepithelial muscular tissue' of Anker (1978:261, Fig. 14). Springer & Johnson (2004, Plate 159C), as well as ourselves, diverge from Anker (1978) in considering the fibres running along the sagittal plane between the contralateral pharyngobranchial 3 as belonging to the *sphincter oesophagi*, instead as to the *circumpharyngobranchialis* (see below). In *Geophagus sveni* (Fig. 14A, C–F), we observed the same two parts described by Springer & Johnson (2004:190, Plate 159C).

Pars lateralis. The *pars lateralis* is much bulkier and more easily distinguishable from the surrounding dermis (Fig. 14A, C–F). However, the fibres are less tightly packed than those of other branchial muscles are. Both attachments are muscular. The fibres are parallel to each other, but when at rest form an arch around lateral border of pharyngobranchial 3. One can see the *pars lateralis* between the epibranchials in lateral view, after the removal of the dermis.

Pars medialis. The *pars medialis* passes laterally to the pharyngobranchial 3 and across the space between pharyngobranchials 2–3 (Fig. 14E). It is difficult to distinguish from the surrounding connective tissue, which seems to intermingle with the fibres. Both attachments are muscular. The *pars medialis* is somewhat confused with the proximal portion of the *rectus pharyngobranchialis 2–3*, which is the reason why we believe the latter may have a common

origin with *circumpharyngobranchialis*. However, the fibres of the *rectus pharyngobranchialis 2–3* are much more tightly packed and uniform. The *pars medialis* is only visible ventrally, after the separation of the dorsal and ventral portions of the gill arches.

2.3.4 Muscles serving the ventral parts of the branchial arches

***Sphincter oesophagi*.** The superficial fibres of the *sphincter oesophagi* are circular close to the gut (Figs. 9–10, 16). Anteriorly, the dorsal portion of the fibre rings become gradually convex (in dorsal view). Close to pharyngobranchial 3, some rings become open and the tips of the most superficial fibres point in an anteromedial direction. The tips of the anteriormost fibres finally converge between the contralateral *retractores dorsales* and attach to the pharyngobranchial 3 or pass through the space between the contralateral pharyngobranchials 3. This portion, which passes along the medial faces of the contralateral pharyngobranchials 3 and inserts on the medial tips of contralateral pharyngobranchials 2, we call pharyngobranchial section. The fibres in the lateral side of the *sphincter oesophagi* also have tips free from fibre rings, which are either anterodorsally or anteroventrally directed, attaching, respectively, to the pharyngobranchial 3 and to the ceratobranchial 5. The connective tissue between the upper tooth-plate 4 and the ceratobranchial 5 is another site of attachment to the *sphincter oesophagi*. The ceratobranchial section of the *sphincter oesophagi*, running between the contralateral ceratobranchials 5 looks slightly separate from the remainder of the muscle for being more bulky; having transversally-oriented fibres, not taking part in fibre rings; and having a raphe along its sagittal plane. This may be an evidence that this portion corresponds to *transversus ventralis 5*.

***Obliquus ventralis 1*.** The *obliqui ventrales* usually are cord-like muscles connecting a ceratobranchial to a hypobranchial of the same arch (Winterbottom, 1974a). In *Geophagus*

sveni, as in other cichlids preliminarily analysed for a forthcoming paper on geophagine myology and phylogeny, those muscles are much more complex, made up of more than one part, some of which are compatible with the definitions of *transversi ventrales* and *recti ventrales* (Figs. 16, 17A). Because the parts of the *obliquus ventralis 1* are not always distinct from one another and not always present in all comparative species analysed, we interpret them as derived from the same muscle (we were not able to determine their innervation). The same applies to other *obliqui ventrales*. The *obliquus ventralis 1* of *G. sveni* has three distinct parts, as follows, none of which seems to be equivalent to the dorsal section described by Anker (1978:263–265, Fig. 16).

Pars abductoris rectus. Cylindrical, with both the origin and the insertion muscular (Figs. 16, 17A). Lies laterally to the other two parts. Corresponds to the anterolateral fibres of the *obliquus ventralis 1*, originating immediately posteriorly to the hypobranchial 1–dorsal hypohyal ligament, as depicted by Anker (1978, Fig. 15) for *Haplochromis elegans*. In *Geophagus sveni*, though, this part is more distinctly separate from the rest of the muscle fibres.

Pars adductoris obliquus. Somewhat triangular, its fibres fanning out towards origin (Figs. 16, 17A). Partially hidden posteromedially by *pars adductoris transversus*. Origin and insertion muscular. Apparently corresponds to a portion of the ventral section of the *obliquus ventralis 1* of Anker (1978:263–265, Figs. 15–16).

Pars adductoris transversus. This part has a roughly rectangular main section, which links the ceratobranchial 1 with the hypobranchial 2 (Figs. 16, 17A). Its fibres are not quite transversal, but directed somewhat posteriorly towards insertion. The posterior section is cord-like, and

runs transversally between the contralateral ceratobranchials 1, with no apparent raphe in the sagittal plane. The posterior section slightly hides the main section in ventral view. On the left side of the specimen, an anterior section, also cord-like, links the ceratobranchial 1 with the basibranchial 1. Origin and insertion muscular. Apparently corresponds to a portion of the ventral section of the *obliquus ventralis 1* of Anker (1978:263–265, Figs. 15–16).

***Obliquus ventralis 2*.** The large *obliquus ventralis 2* also consists of three parts, as follows (Figs. 16, 17B–C).

Pars abductoris rectus. Approximately cylindrical, as corresponding part of *obliquus ventralis 1* (Fig. 17B). Somewhat confused with *pars adductoris obliquus* medially, and largely hidden by it in ventral view. Origin and insertion muscular. Possibly corresponds to the lateralmost fibres of the *obliquus ventralis 2* depicted by Anker (1978, Fig. 15).

Pars adductoris obliquus. Approximately triangular, with the fibres fanning out towards origin (Figs. 16, 17B–C). Originating from and dorsally continuous with an aponeurotic sheet connecting hypobranchials 2 and 3 and basibranchial 1, which corresponds to rostral and cross ligamentous systems of Anker (1978:262, Figs. 15–16). This sheet has a longitudinally oval anterior opening immediately posterior to its attachment to basibranchial 1, making the contralateral *pars adductoris obliqui* anteriorly separate. More posteriorly, bunches of fibres from either side cross their counterparts close to their origin. This crossing between fibres of contralateral muscles seem to be a rare condition among cichlids, otherwise observed in few muscles of some Geophagini. Winterbottom (1974b, Fig. 94), however, illustrates a somewhat similar condition in the *transversi ventrales 4* and *5* of *Pervagor melanocephalus* (Bleeker, 1853) (Monacanthidae). The insertion of *pars adductoris obliquus* is muscular. Origin

partially muscular, mainly by aponeurotic sheet. Corresponds to the ventral section of the *obliquus ventralis 2* of Anker (1978:256, Figs. 15–16). Differs from the homologue in *Haplochromis elegans* mainly by the following characters: (1) In *Geophagus sveni*, the rostral ligamentous system attaches to the basibranchial 1 (*vs*. to hypobranchials 1); (2) In *G. sveni*, the fibres cover the complete ventral face of the rostral ligamentous system, thus reaching the basibranchial 1 (*vs.* fibres leaving most of the rostral ligamentous system exposed, thus lying far from its anterior attachment); (3) In *G. sveni*, the fibres from the contralateral *pars abductores obliqui* either meet at the sagittal plane or cross each other (*vs*. contralateral fibres not in contact or crossing each other).

Pars adductoris transversus. Completely hidden by *pars adductoris obliquus* in ventral view. Originates from the hypobranchial 2 (Fig. 17C). The fibres joining the antimere apparently do it by a raphe. Origin and insertion muscular. Corresponds to the dorsal section described by Anker (1978:265).

***Obliquus ventralis 3*.** Although the limit between the two parts is distinguishable mostly by the direction of the fibres, we treat them as different because their position relative to the branchial skeleton suggests antagonistic functions.

Pars abductoris rectus. The fibres fan out slightly towards the origin, but are overall more horizontal than the fibres of *pars adductoris* (Fig. 17D). The origin of the *pars abductoris rectus reaches* about the middle of the ventral process of the hypobranchial 3. Origin and insertion muscular.

Pars adductoris. Approximately triangular, the fibres fan out towards insertion (Figs. 16, 17D). Most fibres originate muscularly from the hypobranchial 3, extending almost to the tip of its ventral process. A smaller portion of them rises directly from the semi-circular ligamentous system. The insertion is muscular. Corresponds to the parts described by Anker (1978:265), differing by reaching the tip of the hypobranchial 3 ventral process.

***Transversus ventralis 4*.** The *transversus ventralis 4* has the origin and insertion sites much longer than the fibres themselves (Figs. 16, 17D). The origin site occupies the whole ceratobranchial 5 keel, and the insertion site occupies almost the entire anterior half of ceratobranchial 4. There are an anterior and a posterior section. The anterior section comprises the largest part of the muscle, and inserts solely on the medial face of the medial keel of ceratobranchial 4. Its fibres are transversal in direction, and some encounter their antimeres without an apparent raphe. The posterior section inserts on ventral face of ceratobranchial 4, and its fibres are obliquely oriented, pointing more posteriorly towards the origin. The ceratobranchial 4 tooth plates largely attach to this muscle.

***Rectus ventralis 4*.** The two parts differ in fibre direction, origin and insertion, as follows.

Pars medialis. The *pars medialis* has a narrow, triangular shape, its long axis approximately longitudinal (Fig. 17D). It is a bipennate muscle, whose lateral fibres diverge from the sagittal plane towards the insertion, while the medial fibres are approximately parallel to the same plane. The insertion is muscular and the origin in directly from the semi-circular ligamentous system.

Pars lateralis. Also somewhat triangular, but broader than *pars medialis*. The fibres fan out towards origin. The insertion is entirely muscular, and most of the fibres seem to originate from within the *obliquus ventralis 3, pars adductoris* (Figs. 16, 17D).

***Rectus communis*.** Cord-like, originates as a single bunch of fibres and bifurcates at one-third the distance to the insertion, each branch running laterally to the distal portion of the *pharyngoclavicularis externus* and inserting immediately posterior to it (Figs. 5, 16). Shortly posterior to the bifurcation, a narrow, approximately longitudinal aponeurosis almost completely bisects the bunch of fibres in each side. From this point on, the dorsal rim of the muscle reveals a tendinous tissue, which continues to the insertion, which is itself completely tendinous. The distal portion of the *rectus communis* tightly attaches medially to the *pharyngoclavicularis externus* by connective tissue. The origin is muscular, and the fibres are parallel to each other. Apparently differs from its homologue in *Haplochromis elegans* by the aponeurosis almost bisecting the muscle close to the bifurcation point (*vs*. completely bisecting) and by the tendinous tissue apparently along most of the dorsal margin of the muscle (*vs*. mainly close to the insertion).

2.3.5 Muscles between the pectoral girdle and the skull, hyoid, and branchial arches

***Sternohyoideus*.** The *sternohyoideus* (Figs. 5, 18) arises muscularly from the cleithrum, immediately lateral to the proximal portion of the *pharyngoclavicularis externus*, although very few of the medialmost fibres are medial to it (originating aponeuroticly). The shape of the *sternohyoideus* origin site is dorsolaterally oblique, in anterior view. The fibres are homogeneously oriented, and we recognize no sections. The insertion site, which is entirely muscular, encompasses almost the entire surface of the urohyal, except the head and the narrow distal edges of the urohyal wings. There is, thus, only a narrow space between the

insertion of the *sternohyoideus* and the origin of the *rectus communis*. When we remove the proximal portion of the *sternohyoideus*, we can see a distinct scar on the cleithrum. Apparently differs from its homologue in *Haplochromis elegans* (*cf.* Anker, 1978, Fig. 9A) by the origin site much ventral to the origin of the posteriormost *pharyngoclavicularis externus* fibres (*vs*. at the same horizontal).

***Pharyngoclavicularis externus*.** Sheet-like. The two portions differ in their origin site and shape of distal portion, as follows (Figs. 5, 10, 16, 18). Corresponds to the *musculus pharyngocleithralis externus* of Anker (1978:266–267, Fig. 10).

Pars anterior. Originates muscularly at the angle between medial and lateral wings of cleithrum, and the fibres gradually give place to an aponeurotic complex that attaches to ceratobranchial 5 both medially and laterally to the *rectus communis* (Figs. 5, 18), and to the ceratobranchial 4 immediately posterior to the insertion of *transversus ventralis 4* (Fig. 5).

Pars posterior. Originates partly muscularly, partly aponeurotically, from the rim and from the lateral face of medial wing of cleithrum, but not close to the angle with lateral wing (Figs. 5, 16, 18). It then runs completely muscularly to the insertion site. Fibres are parallel.

***Pharyngoclavicularis internus*.** Strap-like. Distally, most fibres ultimately converge into a long tendon, which inserts on the base of the ceratobranchial 5 keel (Figs. 5, 16, 18). The dorsal fibres, on the other hand, either attach muscularly to the body of ceratobranchial 5 or through an aponeurotic complex. To the origin site, the fibres attach mostly muscularly, although some of them appear to attach by a very short strap of aponeurotic tissue. The origin of the *pharyngoclavicularis internus* is distant from that of the *pharyngoclavicularis externus*,

but the insertions are adjacent. Differs from its homologue in *Haplochromis elegans* by the extensive insertion (*vs*. insertion by a single tendon).

***Protractor pectoralis*.** The *protractor pectoralis* tapers from insertion to origin (Figs. 5, 6B, 18). Almost the entire proximal half is predominantly tendinous. The distal half is anteroventrally compressed. The ventral margin of the insertion site is horizontal (seen in anterior view). Fibres are homogeneously distributed. The insertion is completely muscular in *Geophagus sveni*, whereas Anker (1978:245) states that in *Haplochromis elegans* it is mainly muscular. Moreover, the insertion area in *H. elegans* is oval (Anker, 1978:245, Fig. 17), and the muscle is more longitudinal than vertical (*vs*. at a 45° angle with the longitudinal axis), due to a different neurocranial shape.

***Levator pectoralis*.** The *levator pectoralis* is a bulky muscle (Figs. 1, 5, 6B, 18). The origin site of the *levator pectoralis* is approximately oval in a transversal sense. The fibres fan out towards the several insertion sites. The anteroventral fibres originate completely muscularly and run parallely to their muscular insertions. The fibres in the midlateral section of the muscle are involved in an aponeurotic tissue proximally and fan out towards a muscular insertion. More dorsally, the fibres run in irregular directions, some of which longitudinal, others oblique; their attachments are completely muscular. In *Geophagus sveni*, the ventral margin of the *levator pectoralis* is oriented in an anterodorsal-posteroventral direction, due to the more ventral position of the cleithrum in relation to the neurocranium, whereas in *Haplochromis elegans* (which has a more dorsally positioned cleithrum) the ventral margin of the muscle is longitudinal (Anker, 1978:245–246, Fig. 10A). Moreover, Anker (1978:246) states that the ventralmost insertion site of the *levator pectoralis* in *H. elegans* lies in the "connective tissue around the attachment of Baudelot's ligament to the pectoral element",

whereas in *G. sveni* the ventralmost fibres insert directly on the *hypaxialis*, ventral to Baudelot's ligament, and partially merge with the latter.

2.3.6 Muscles of the pectoral fin

***Abductor superficialis*.** Consists of three sheet-like parts, which differ in shape and insertion site (Figs. 18–19).

Pars radii pectorales ventrales. Broad, triangular (Fig. 18). Fibres are unusually spaced proximally. Distally, dorsal fibres overlay ventral ones. Origin muscular, insertion aponeurotic. In lateral view, almost completely hides the other two parts. Corresponds to outer layer of the *musculus abductor superficialis* of Baerends & Baerends-Van Roon (1950:15, Fig. 5A). Differs from its homologue in *Pseudocrenilabrus philander* by being less elongate.

Pars radii pectorales mesiales. Also triangular, but less deep than preceding part (Fig. 19A). Its proximal portion is medial to the ventral portion of *pars radii pectorales ventrales*, and thicker than the proximal portion of the other parts. Origin muscular, insertion aponeurotic, divided in several attachments. The *pars radii pectorales mesiales*, along with the *pars radii pectorales dorsales*, corresponds to the inner layer of the *musculus abductor superficialis* of Baerends & Baerends-Van Roon (1950:15, Fig. 5A).

Pars radii pectorales dorsales. Triangular (Fig. 19A). Proximal portion also thicker than that of *pars radii pectorales ventrales*. Origin muscular, insertion aponeurotic, divided in several attachments.

***Abductor profundus*.** Approximately club-shaped, but, contrary to *abductor superficialis*, the broadest portion is the distal one (Fig. 19B). Proximal portion is shallow. Origin muscular, insertion aponeurotic. If the *coracoradialis* is present, we must interpret it as fused to the *abductor profundus,* which occupies the same location usually occupied by *coracoradialis*.

***Arrector ventralis*.** Medial to *abductor superficialis,* anteromedial to *abductor profundus* (Figs. 18–19). A long muscle, broader proximally than distally. Origin muscular, insertion aponeurotic. Differs from its homologue in *Pseudocrenilabrus philander* by having a more ventral origin, which results in an angle of about 45° between the dorsalmost fibres of the *arrector ventralis* and the first pectoral-fin ray (*vs*. fibres aligned with ray). Concurrently, the distal portion of the *arrector ventralis* of *Geophagus sveni* forms an almost 90° angle with the dorsalmost fibres of the *abductor superficialis, pars radii pectorales ventrales* (*vs*. about 60°).

***Adductor superficialis*.** Consists of two approximately sheet-like parts, which are very distinct distally, but not so proximally, except because *pars lateralis* has a much wider origin site (Figs. 20–21). The *adductor medialis* of Winterbottom (1974a, Fig. 36) occupies a position similar to that of the ventral portion of the *adductor superficialis*, *pars lateralis* of *Geophagus sveni*. However, Winterbottom (1974a) states, "In most, if not all cases, the [*adductor superficialis*] muscle 'crosses over' itself. The more dorsomedial fibres serve the more dorsal rays. Owing to this 'cross over', the two extreme fibre directions are right angles to each other, with a complete gradation of direction between them". Thus, the two parts we ascribe to the *adductor superficialis* are homologous to the same muscle as described by Winterbottom (1974a), although he did not recognize distinct parts. The *adductor medialis,* on the other hand, is absent in *G. sveni*.

Pars medialis. Long, roughly rectangular or trapezoidal (Fig. 20). The fibres are approximately parallel, despite the insertion being by a narrow tendon that emerges from an aponeurotic sheet, which receives all fibres. Origin muscular.

Pars lateralis. Very deep, roughly triangular (Fig. 21). As in *abductor superficialis*, *pars ventralis*, the fibres fan out towards the origin, and are proximally separate from each other. The tendons by which this part inserts on the pectoral-fin rays cross each other, *i.e.*, tendons emerging from more dorsal fibres insert on more ventral rays and vice-versa. Ventrally, the *pars lateralis* is nearly fused to, and difficult to distinguish from the *arrector dorsalis*. Corresponds to most of the *arrector dorsalis* (dorsally) of Baerends & Baerends-Van Roon (1950:16, Fig. 5e).

***Adductor profundus*.** Approximately rectangular, but with anteroventral margin rounded, bulky in the middle (Fig. 20). Almost completely exposed in medial view, only hidden by *adductor superficialis* distally. The muscle has several sections somewhat distinct from each other, one for each pectoral-fin ray in which the muscle inserts. Fibres are mostly parallel to each other. Origin muscular, insertion by thick, short tendons, one for each ray.

***Adductor radialis*.** Somewhat compressed, stripe-like (Fig. 21). Completely hidden by *adductores superficialis* and *profundus*, except by a small ventral portion. Origin muscular, insertion by a narrow strip of connective tissue.

***Arrector dorsalis*.** Nearly fused to, and largely hidden in medial view by the *adductor superficialis, pars lateralis* (Figs. 20–21). Distinguishable from it by the insertion by a longer tendon, which inserts dorsally on the second pectoral-fin ray, instead of medially.

Corresponds to the ventralmost fibres of the *arrector dorsalis* of Baerends & Baerends-Van Roon (1950:16, Fig. 5e), while most of their *arrector dorsalis* corresponds to our *adductor superficialis, pars lateralis*. Differs from its homologue in *Pseudocrenilabrus philander* by having a more ventral origin.

***Coracoradialis*.** Apparently absent, but possibly fused to *abductor profundus*.

2.3.7 Muscles of the pelvic fin

***Abductor superficialis pelvicus*.** Bulky, approximately square (Fig. 22A). Fibres inserting on the tip of ventral basal process of pelvic-fin spine fan out towards origin. Remaining fibres run parallely on both sides. Origin muscular (though a raphe may be present at the junction with *hypaxialis*), insertion by a thick strip of tendinous connective tissue. Differs from its homologue in *Pseudocrenilabrus philander* (compare with Baerends & Baerends-Van Roon, 1950, Fig. 6A) by being much shorter and somewhat squarish, and by not touching its antimere (*vs*. long, nearly reaching the anterior tip of basipterygium, and anteriorly pointed; touching its antimere all along its

***Abductor profundus pelvicus*.** Bulky, shaped as a long triangle in ventral view (Fig. 22A). In ventral view, only posteromedial portion is visible. The *abductor profundus pelvicus* consists of two poorly defined sections (one medial, one lateral), in which the fibres are nearly parallel. The *hypaxialis* hides much of the proximal portion *abductor profundus pelvicus*. The *abductor superficialis pelvicus* hides much of the laterodistal portion. Origin muscular, insertion by a mass of fibrous connective tissue.

***Arrector ventralis pelvicus*.** Long, approximately triangular (Fig. 22A). Distal portion visible laterally to *abductor superficialis pelvicus*. Consists of three poorly defined sections (lateral, central and medial), of which the central one presents some tendinous tissue in its distal half. Origin muscular, insertion tendinous. Differs from its homologue in *Pseudocrenilabrus philander* (compare with Baerends & Baerends-Van Roon, 1950, Fig. 6b) by being much bulkier proximally.

***Adductor superficialis pelvicus*.** In dorsal view, almost completely hidden by *extensor proprius* (Fig. 22B). In turn, the *adductor superficialis pelvicus* hides most of the medial portion of the *adductor profundus pelvicus*, and fits a concavity formed by the lateral portion of the latter. Divided in two parts, as follows. Differs from its homologue in *Pseudocrenilabrus philander* (compare with Baerends & Baerends-Van Roon, 1950, Fig. 6e) by being divided in two parts.

Pars dorsalis. Long, approximately fusiform (Fig. 22B). Hides some of the medial half of *pars ventralis* in dorsal view. Roughly divided in four sections, one for each ray it serves. Origin muscular, insertion by short tendons.

Pars ventralis. We opted not for considering this part as a section of the preceding *pars dorsalis* because its fibres are clearly separate from the latter (Fig. 22B). Long, tape-like. Origin muscular, insertion by short tendons.

***Adductor profundus pelvicus*.** Long, trapezoidal, massive (Fig. 22B). Origin muscular, insertion by very short tendons.

***Arrector dorsalis pelvicus*.** Drop shaped. Most fibres (*i.e.*, those that make up the ventral portion of the muscle) run in a longitudinal direction (Fig. 22). The dorsalmost fibres run in an anterodorsal-posteroventral direction. Origin muscular, insertion tendinous. Differs from its homologue in *Pseudocrenilabrus philander* (compare with Baerends & Baerends-Van Roon, 1950, Fig. 6c) by being shorter, not reaching the tip of the basipterygium.

***Extensor proprius*.** Long, more bulky at the middle (Fig. 22B). Origin muscular, insertion tendinous.

2.3.8 Muscles of the dorsal fin

***Erectores dorsales*.** The *erectores dorsales* are long muscles, each one originating muscularly and inserting by a single short tendon (Figs. 23A, 24). The origin of the anteriormost *erector dorsalis* reaches almost the tip of the respective pterygiophore. Posteriorly, the *erectores dorsales* of the spiny dorsal fin become progressively shorter, so that from the sixth on they occupy only half of the pterygiophore (Fig. 23A). Along the soft dorsal fin, the *erectores dorsales* are about as long as those along the spiny dorsal fin, but they fall closer to the tip of the respective pterygiophore, because the posteriormost pterygiophores are shorter than the anterior ones. The *erectores dorsales* from the spiny dorsal fin differ from those of the soft dorsal fin in that they originate from the anterior half of the same pterygiophore supporting the spine on which they insert. Thus, they are separate from the respective *depressores dorsales* by the lateral wing of the proximal pterygiophore from which both originate. The *erectores dorsales* from the soft dorsal originate from the posterior half of the pterygiophore immediately anterior. They run obliquely towards the insertion, passing laterally to the lateral wing of the pterygiophore. The proximal portion of each of the posteriormost *erector dorsalis* is partially hidden by the immediately anterior *depressor dorsalis*.

***Depressores dorsales*.** As the *erectores*, the *depressores dorsales* are long, originate muscularly and insert by a short tendon (Figs. 23A, 24). All of them are approximately as long as the respective *erectores*, but much more slender (except those at the posterior end of the dorsal fin, which are about as wide). The *depressores dorsales* from the spiny dorsal fin originate from the posterior half of the pterygiophore that supports the spines on which they insert, as happens to the *erectores dorsales* from this region. In the soft dorsal fin, the *depressores* originate from the anterior half of the same pterygiophore supporting the rays on which they insert. More posteriorly, the origin site of some *depressores* include the posterior half of the anterior pterygiophores as well.

***Inclinatores dorsales*.** The *inclinatores dorsales* form a single muscular wall, and it is difficult to distinguish the units (Fig. 23B). The fibres attaching to the distal pterygiophores are approximately vertical, slightly inclined posteriorly. The fibres inserting on fin rays are inclined at an angle of about 45°. Origin muscular, insertion on rays by very short tendons.

2.3.9 Muscles of the anal fin

***Erectores anales*.** Similar to the *erectores dorsales*, but similar in width to the *depressores anales*, instead of being much wider (Figs. 23A, 25). The origin of *erectores anales* serving the spiny anal fin reach the caudal swim-bladder expansion, and the first *erector* seems to fuse with the *hypaxialis*.

***Depressores anales*.** Similar to the *depressores dorsales*, but similar in width to the *erectores anales*, instead of being much more slender (Figs. 23A, 25). In addition, most of the

depressores from the soft anal fin take their origin on the pterygiophore that precedes the one supporting the ray on which they insert.

***Inclinatores anales*.** Similar to *inclinatores dorsales* (Fig. 23B).

2.3.10 Carinal muscles

***Supracarinalis anterior*.** Much compressed. Fibres approximately longitudinal. Origin and insertion muscular (Fig. 24A).

***Supracarinalis medius*.** The *supracarinalis medius* is present in fishes with two separate dorsal fins, thus absent from cichlids (Winterbottom, 1974a).

***Supracarinalis posterior*.** Posterodorsal portion bulky, with the fibres inclined dorsad and converging into the two tendons, which attach to the two posterior procurrent rays of caudal fin (Figs. 26, 27C). Partially corresponds to *flexor dorsalis superior* of Baerends & Baerends-Van Roon (1950, Fig. 4).

***Infracarinalis anterior*.** Not clearly distinguishable from *hypaxialis*. Myocommata ill defined (Fig. 27B).

***Infracarinalis medius*.** Not clearly distinguishable from *hypaxialis*. Myocommata well defined. Attachment to ischiatic process includes some tendinous tissue (Fig. 27B).

***Infracarinalis posterior*.** Similar to *supracarinalis posterior* (Figs. 26, 27D). Partially corresponds to *flexor ventralis inferior* of Baerends & Baerends-Van Roon (1950, Fig. 4).

2.3.11 Muscles of the caudal fin

***Interradiales*.** Between every pair of caudal-fin rays from posteriormost dorsal procurrent caudal-fin ray to ventralmost principal caudal-fin ray (Fig. 26). Interestingly, there is no *interradialis* between the ventralmost principal caudal-fin ray and the adjacent procurrent ray, which is the posteriormost insertion site of *infracarinalis posterior* and the insertion of the *flexor ventralis inferior*. In the dorsal portion of the caudal fin, the ray on which the *supracarinalis posterior* and the *flexor dorsalis superior* insert (*viz*. the posteriormost procurrent ray) is also the dorsalmost ray to which an *interradialis* attaches.

***Hypochordal longitudinalis*.** Triangular (Fig. 26A–B). The dorsal portion of the muscle consists of thick tendinous tissue, which branches to serve each of the rays in which it inserts individually. In the drawing by Baerends & Baerends-Van Roon (1950, Fig. 4), the *hypochordal longitudinalis* appears to originate dorsally to the vertebrae. However, we believe that it is just a matter of not removing the *flexor ventralis*.

***Flexor dorsalis*.** Divided in two portions, as follows (Fig. 26). The drawing by Baerends & Baerends-Van Roon (1950, Fig. 4) shows that the *pars anterioris* is clearly absent in *Pseudocrenilabrus philander*, and the *flexor dorsalis* seems to mirror the shape of the *flexor ventralis*, differently from *Geophagus sveni*.

Pars anterioris. Long, running immediately dorsal to last three vertebral centra (Fig. 26). At about mid-length, all fibres converge into a very long, depressed, tape-like tendon, which goes onto the insertion site. Origin muscular.

Pars posterior. Triangular (Fig. 26). Fibres roughly divided into sections, one for each ray to which they attach. Origin muscular, insertion by short tendons not clearly separate from one another.

***Flexor dorsalis superior*.** Very elongate, located at the thin space between *supracarinalis posterior* and *flexor dorsalis* (Fig. 26). Origin muscular, insertion by tendon. The drawing by Baerends & Baerends-Van Roon (1950, Fig. 4) shows a *flexor dorsalis superior* whose dorsal portion seems to be homologous to the posterior portion of our *supracarinalis posterior*, although it agrees in shape with the *flexor dorsalis superior* shown by Winterbottom (1974a, Fig. 50).

***Flexor ventralis*.** Triangular, similar to *flexor dorsalis, pars posterioris*, but slightly larger (Fig. 26A).

***Flexor ventralis inferior*.** Similar to *flexor dorsalis superior* (Fig. 26). The drawing by Baerends & Baerends-Van Roon (1950, Fig. 4) shows a *flexor ventralis inferior* whose dorsal portion seems to be homologous to the posterior portion of our *infracarinalis posterior*, although it agrees in shape with the *flexor ventralis inferior* shown by Winterbottom (1974a, Fig. 50).

***Flexor ventralis externus*.** We interpret this muscle as absent in *Geophagus sveni* instead of fused to *flexor ventralis* because the latter has no aponeurotic sheet as described by Winterbottom (1974a:292, Figs. 49–50).

***Adductor dorsalis*.** We found in *G. sveni* no muscle remotely similar to the *adductor dorsalis* described by Winterbottom (1974a:293, Fig. 51).

***Proximalis*.** The *proximalis*, as described by Winterbottom (1974a:293) is similar in position to the *flexor dorsalis*, *pars anterioris*. The latter may be homologous to the *proximalis* of Atherinomorphae. However, testing this hypothesis is beyond the scope of this study, and we prefer to consider the *proximalis* as absent until more evidence is available.

2.3.12 Body muscles

We observed no clear limit between the so-called body muscles, and based the following descriptions solely on the topology of the muscle masses and on the direction of the fibres.

***Epaxialis*.** In dorsal view, the anterior extremity of the *epaxialis* (*i.e.*, the portion covering the dorsal face of the neurocranium) is triangular, ending medially to clf_2 (Fig. 27). The ventrolateral fibres (emerging from the frontal) run in an anteroventral-posterodorsal direction. The dorsomedial fibres (emerging from supraoccipital crest) run in an anterodorsal-posteroventral direction. The postorbital section of the *epaxialis* (Fig. 24A) lies between the dorsal process of the post-temporal and the frontal-pterotic ridge. Fibres constituting the postorbital section, emerging from the post-temporal, are approximately vertical, while those emerging from the frontal-pterotic ridge are approximately horizontal. The medial face of the portion of the *epaxialis* flanking the dorsal-fin pterygiophores is free (*i.e.*, the muscle is not attached to any bones or to any other muscle masses), except close to the vertebral centra, where the contralateral *epaxialis* join each other. The angle of the myocommata lie slightly ventral to the caudal-peduncle dorsal profile (Fig. 23B). Dorsally, the myocommata are nearly

parallel to the dorsal-fin base, and the fibres are approximately longitudinal. Ventrally, the fibres seem to run in an anteroventral-posterodorsal direction.

***Lateralis superficialis*.** We only distinguish the *lateralis superficialis* by the direction of the fibres, which are longitudinal, contrasting with the neighbouring fibres of the *epaxialis* and of the *hypaxialis* (Fig. 23B). Apparently, the *lateralis superficialis* is extremely thin, poorly developed. We were not able to define the anterior and posterior limits of this muscle, but its centre lies along the epicentrals (*sensu* Patterson & Johnson, 1995)

***Hypaxialis*.** We were not able to verify any distinction between the *hypaxialis obliquus superioris* and *inferioris* (Fig. 23B). Therefore, we treat them as a single muscle, simply the *hypaxialis*. Indeed, no clear limit appears to exist between the *hypaxialis* and the *epaxialis*. The dorsalmost fibres of the *hypaxialis* run in anterodorsal-posteroventral direction. More ventrally, the fibres are approximately longitudinal. The *hypaxialis* is largely free from the pectoral girdle. However, it attaches to the occipital region of the neurocranium, and largely to the medial face of the dorsal portion of the cleithrum. It also spans from the ventral half of the distal extrascapular to the ventral portion of the cleithrum. A small coracoid section links the distal post-cleithrum with the medial face of the coracoid. An elliptical hiatus surrounds the pelvic-fin base.

***Spinalis*.** Winterbottom (1974a) stated that the *spinalis* might represent the ventral portion of the *supracarinalis anterior*. Because there is only one muscle mass between the neurocranium and the first dorsal-fin pterygiophore, we consider the *spinalis* to be either fused to the *supracarinalis anterior* or absent.

2.3.13 Muscles of the eye

***Obliquus inferior*.** Very flat both proximally and distally (Figs. 6C, 28). Median portion somewhat less flat. At the insertion, completely overlaps the *rectus inferior*. Origin and insertion muscular. Fibres parallel.

***Obliquus superior*.** Somewhat flat proximally, and very flat distally, but its median portion is round in cross-section (Figs. 6C, 28). Originates anteroventrally from the *obliquus inferior*, and crosses the proximal portion of the latter. Thus, the *obliquus superior* hides the origin site of the *obliquus inferior*. At the insertion, it partially overlaps the *rectus superior*. Origin and insertion muscular. Fibres parallel.

***Rectus externus*.** Emerges from the ventrolateral face of 1st vertebra, narrowly separate from the antimere, but soon encounters the latter, although the contralateral muscles never fuse to each other (Figs. 6C, 28). The *rectus externus* describes a semicircle ventrally, entering the posterior opening of the posterior myodome at about one third of its length, and then running through the entire myodome. After leaving the anterior opening of the myodome, it bends laterally at a 90° angle and inserts on the eyeball. Origin and insertion muscular. In lateral view, hides most of the *rectus superior* and the proximal portion of *rectus inferior*.

***Rectus inferior*.** Originates medial to *rectus externus* and to *rectus superior*, posterolateral to *rectus internus, pars dorsalis*, and ventral to the optic nerve (Figs. 6C, 28). Runs anteroventrally towards its insertion, which is completely overlapped by *obliquus inferior*. Proximally cylindrical. Origin and insertion muscular.

***Rectus internus*.** The medialmost of the eye muscles, and anteromedial to optic nerve (Figs. 6C, 28). Presents two clearly distinct parts, which differ mainly in the origin site.

Pars dorsalis. The shorter of the two parts, originating within the orbit, from the basiphenoid (Fig. 6C). Tape-like throughout, it runs longitudinally (medially to the eyeball) from origin to anterior portion of orbit, where it bends laterally to insert on the anterior portion of eyeball (Fig. 28).

Pars ventralis. Longer than *pars dorsalis*, given its much posterior origin, at posterior extremity of posterior myodome, close to its opening (Fig. 6C). Tape-like throughout, bending medially as it enters the orbit, then passing medial to the eye towards anterior portion of orbit, then bending again laterally to insert on the anterior portion of eyeball (Fig. 28).

***Rectus superior*.** Flat both proximally and distally, but subcylindrical close to its origin, it runs anterodorsally from its origin at the floor of anterior opening of posterior myodome to its insertion on dorsal portion of eyeball (Figs. 6C, 28).

2.4 Discussion

2.4.1 Comparisons with previous articles on cichlid myology

The present paper is the first complete description of the striated muscles of a cichlid species and, apparently, the first regarding any fish group. However, Anker's (1978) extensive work on the head muscles of *Haplochromis elegans* provides a robust base for comparison between Afrotropical and Neotropical cichlids. The most obvious characters present in *Geophagus sveni*, which diverge from *H. elegans*, include the shape of the *adductor mandibulae, pars*

malaris and *rictalis*; shape and fibre orientation of the *levator arcus palatini*, *dilatator operculi* and *levator operculi* (those three muscles strongly reflect the shape of the neurocranium); presence of the *adductor hyomandibulae*, *pars parasphenoidalis* (*hyomandibularis* and *pterygoidea*); presence of the anteroventral and anterodorsal sections of the *protractor hyoidei*; hypertrophied *levator externus 5*, separate from the *levator externus 4*; *levator internus 1* insertion; proportions of the *adductor branchialis 1*; *transversus epibranchialis 2* in only one part, not reaching the antimere muscularly; separate *transversus pharyngobranchialis 3* and *transversus epibranchialis 4*; *retractor dorsalis* less developed, not originating from the neurocranium; presence of a *rectus pharyngobranchialis 2–3*; larger and more complex *obliqui ventrales 1–2*; more extensive *pharyngoclavicularis internus* insertion; and more vertical *protractor pectoralis* and *levator pectoralis*, also as a result of neurocranial shape.

As other species in *Geophagus*, *G. sveni* is a specialised substrate sifter. Although several African cichlids are known to sift substrate (López-Fernández *et al.*, 2014), we found no information in the literature about this behaviour in *Haplochromis elegans*. Thus, we can hypothesize that some of the myological differences between the two species correlate with this difference in behaviour. Weller *et al*. (2016) noticed that the shape of the *adductor mandibulae*, *pars malaris* and *rictalis* of geophagine substrate sifters is different from that of other cichlids, especially because the *pars malaris* is relatively less deep and the *pars rictalis* is much deeper. It is not clear, however, how this character relates to the feeding behaviour of substrate sifters. We understand the different shape of the *levator arcus palatini*, *dilatator operculi*, *levator operculi*, *protractor pectoralis* and *levator pectoralis* as correlated to changes in the neurocranial proportions, given that substrate sifters in the subfamily Cichlinae exhibit a consistent head-shape pattern including a long snout with low-positioned mouth and a deep head with high-positioned eye (López-Fernández *et al*., 2014).

The shape and degree of development of the *obliqui ventrales 1–2* seems to be a promising clue regarding the myological adaptations that allow geophagines to sift substrate efficiently. As seen in Fig. 16, the rakers and pseudo-rakers (*sensu* Greenwood, 1973), allied to deep, blade-like ceratobranchials, form the branchial sieve of geophagine substrate sifters. However, this sieve is not static, because the size of the interspaces varies with the distance between gill arches. This is important because the size of the substrate and food particles varies among microhabitats. Thus, we believe that an efficient substrate sifting depends on the fish's ability to control actively the distance between the gill arches. Without a specialised musculature to do so, the water flowing against the gills would probably force the arches to open. A future paper by us (Deprá *et al*., unpubl. data) will investigate further this subject, in order to reveal other adaptations common to geophagine substrate sifters.

The post-cranial musculature of *Geophagus sveni* also showed some differences in comparison with the African cichlid *Pseudocrenilabrus philander* (*cf*. Baerends & Baerends-Van Roon, 1950). The main characters present in *G. sveni*, which differed from those of *P. philander*, were the less elongate *abductor superficialis*, *pars radii pectorales ventrales*; more ventral origin of the *arrector dorsalis* and of the *adductor superficialis*, *pars lateralis*; much smaller *abductor superficialis pelvicus*; bulkier *arrector ventralis pelvicus*; shorter *arrector dorsalis pelvicus*; the presence of a *flexor dorsalis*, *pars anterioris*; the *flexores dorsalis* and *ventralis* mirroring each other in shape.

We found an interesting character in the musculature of the eye of *Geophagus sveni*, *viz*. the origin of the *rectus externus*, which lies on the first vertebra and on the posterior portion of the neurocranium, and a posterior opening of the myodome, apparently previously unreported for acanthomorph fishes (Anker, 1978, did not analyse the eye musculature of *Haplochromis elegans*). The only report on such character that we could find in the literature is that of Mayden (1989), who considered it as synapomorphic for a clade of leuciscids

(Cypriniformes). This posteriorly displaced origin of the *rectus externus*, also present in other cichlids analysed for our work in progress on the phylogeny of geophagines, would suggest that this muscle is longer in cichlids than in most other fishes. However, a comparison with Oliva & Skořepa (1968a, 1968b) shows us that in fishes with a close myodome the *rectus externus* may have a similar length. Thus, we hypothesize that the open myodome in cichlids may compensate the relatively short post-orbital region of the head.

2.4.2 Nomenclatural issues

We used a different nomenclature for a few muscles, in comparison to other authors. The names *adductor operculi* and *adductor hyomandibulae* were employed in accordance to Datovo & Rizzato (2018), although it is quite odd that *pars primordialis* of the latter originates and inserts at very distant sites in comparison with the other two parts of the same muscle, while being almost indistinguishable from *adductor operculi* proximally. In fact, a poor differentiation between *adductor operculi* and *adductor hyomandibulae* is ancestral in Actinopterygii, and a more developed *adductor hyomandibulae*, whose origin advances more and more onto the parasphenoid, appeared later in the evolution of the group (Winterbottom, 1974a; Datovo & Rizzato, 2018). It is possible that at some point a median portion of the muscle, which would connect *pars primordialis* with the other two parts observed herein, has been lost. That hypothesis is coherent with the morphology of the *adductor hyomandibulae* (= *adductor arcus palatini*) of Characiformes described in Castro & Vari (2012:92, Figs. 5–6). However, it is also plausible that our *pars primordialis* is in reality a part of *adductor operculi* that has changed its insertion to the hyomandibula, occupying the vacant spot left by the change of the insertion of *adductor hyomandibulae* from the dorsal portion of the hyomandibulae to a more ventral position.

To Winterbottom (1974), Anker (1978) and Springer & Johnson (2004), only *levatores externi 1–4* are present in cichlids. The *levator externus 4*, which is by far the most massive of the *levatores externi*, would not insert on epibranchial 4, as expected, but on a raphe shared with the *obliquus posterior*, ultimately transmitting its force to the ceratobranchial 5. However, because we observed the presence of a separate, slender muscle inserting exclusively on the uncinate process of the epibranchial 4, we opted for naming it *levator externus 4*. We name *levator externus 5* the bulkier muscle, which other authors named *levator externus 4*. Although Springer & Johnson (2004) employed this name only for a muscle present in sarcopterygians, which is certainly not homologous to our *levator externus 5*, for now we consider it a better alternative than treating both our *levatores externi 4–5* as two parts of a single muscle, or proposing a completely new name for our *levator externus 5*.

To Cichocki (1976:86, character 33), the dorsal portion of our *adductor branchialis 1* represents the *interbranchialis abductor*, in accordance with the nomenclature used by Winterbottom (1974a). However, we found that the gill-arch muscle (= *interbranchialis abductor*) is present, but only along the ceratobranchial (Fig. 12), unless the epibranchial portion is fused to the *adductor branchialis 1*. We base our interpretation on the fact that the *adductor branchialis 1* is much thicker and more developed than the gill-arch muscle. If we are correct, the *adductor branchialis 1* (whose primary function is, of course, to shorten the angle between epibranchial 1 and ceratobranchial 1) acquired in cichlids a second function, *i.e.*, to pull outwards the external row of gill filaments. Nonetheless, the actual distribution of this character, as well as its functional importance, remain unknown.

Anker (1978:254) did not attempt to distinguish between the *obliqui posteriores*. His illustrations are not clear about the arrangement of these muscles, thus a comparison with *Geophagus sveni* is not possible. However, our observations are in total agreement to those of

Springer & Johnson (2004, Plate 159C), thus we follow their nomenclature for *obliqui posteriores 1–4*.

As far as we know, previous authors have not used the name *rectus pharyngobranchialis 2–3*. A name such as *rectus dorsalis* is not suitable, because Winterbottom (1974a:259) defined the *recti dorsales* as spanning between an epibranchial and the epibranchial immediately anterior to it. We opted for not considering the *rectus pharyngobranchialis 2–3* as a part of the *circumpharyngobranchialis* because it is anatomically and probably functionally distinct from the latter.

Some of the nomenclatural disagreements between our work and that of Baerends & Baerends-Van Roon (1950) are probably due to the fact that the latter is anterior to Winterbottom (1974a), thus not encompassing his synonymy proposals. The muscle named *arrector dorsalis* by Baerends & Baerends-Van Roon (1950:16, Fig. 5e) is clearly a composite of our *arrector dorsalis* and our *adductor superficialis*, *pars lateralis*. The *flexor dorsalis superior* and the *flexor ventralis inferior* of Baerends & Baerends-Van Roon (1950:13, Fig. 4), which appear to include a portion of our *supracarinalis posterior* and *infracarinalis posterior*, nonetheless agree in shape with the *flexor dorsalis superior* and the *flexor ventralis inferior* of Winterbottom (1974a). Thus, we are not certain if this is a matter of different interpretation or if different character states are present in *Geophagus sveni* and *Pseudocrenilabrus philander*.

2.5 Conclusion

Our results show there is a considerable variation in cichlid skeletal musculature, which could bare information on their phylogenetic relationships and, more importantly, shed light on the evolution of their adaptive morphology. In particular, the specialised ventral branchial muscles present in *Geophagus sveni* apparently explain part of the functioning of the

winnowing behaviour. The existence of nomenclatural conflicts between our study and previous ones reflects the importance of investigating the homology of anatomic complexes.

REFERENCES

Aerts P. 1982. Development of the *musculus levator externus IV* and the *musculus obliquus posterior* in *Haplochromis elegans* Trewavas, 1933 (Teleostei:Cichlidae): a discussion on the shift hypothesis. *Journal of Morphology* 173: 225–235.

Anker GC. 1978. The morphology of the head-muscles of a generalized *Haplochromis* species: *H. elegans* Trewavas 1933 (Pisces, Cichlidae). *Netherlands Journal of Zoology* 28: 234–271.

Arbour J, López-Fernández H. 2018. Intrinsic constraints on the diversification of Neotropical cichlid *adductor mandibulae* size. *The Anatomical Record* 301: 216–226.

Baerends GP, Baerends-van Roon JM. 1950. An introduction to the study of the ethology of cichlid fishes. *Behaviour. Supplement* 1: 1–242.

Cichocki FP. 1976. Cladistic history of cichlid fishes and reproductive strategies of the American genera *Acarichthys*, *Biotodoma* and *Geophagus*. Unpublished D. Phil. Thesis, The University of Michigan.

Datovo A, Bockmann FA. 2010. Dorsolateral head muscles of the catfish families Nematogenyidae and Trichomycteridae (Siluriformes: Loricarioidei): comparative anatomy and phylogenetic analysis. *Neotropical Ichthyology* 8: 193–246.

Datovo A, Castro RMC. 2012. Anatomy and evolution of the mandibular, hyopalatine, and opercular muscles in characiform fishes (Teleostei: Ostariophysi). *Zoology* 115: 84–116.

Datovo A, Rizzato PP. 2018. Evolution of the facial musculature in basal ray-finned fishes. *Frontiers in Zoology* 15: 40.

Datovo A, Vari RP. 2014. The *adductor mandibulae* muscle complex in lower teleostean fishes (Osteichthyes: Actinopterygii): comparative anatomy, synonymy, and phylogenetic implications. *Zoological Journal of the Linnean Society* 171: 554–622.

Drucker EG, Jensen JS. 1991. Functional analysis of a specialized prey processing behavior: winnowing by surfperches (Teleostei: Embiotocidae). *Journal of Morphology* 210: 267–287.

Dutta HM. 1987. Osteology, myology and feeding mechanism of *Astronotus ocellatus* (Pisces, Perciformes). *Zoomorphology* 106: 369–381.

Fricke R, Eschmeyer WN, Fong JD. 2020. *Eschmeyer's catalog of fishes: species by family/subfamily*. (http://researcharchive.calacademy.org/research/ichthyology/catalog/SpeciesByFamily.asp). Electronic version accessed 29 jan 2020.

Gois KS, Pelicice FM, Gomes LC, Agostinho AA. 2015. Invasion of an Amazonian cichlid in the Upper Paraná River: facilitation by dams and decline of a phylogenetically related species. *Hydrobiologia* 746: 401–413.

Greenwood PH. 1973. A revision of the *Haplochromis* and related species (Pisces: Cichlidae) from Lake George, Uganda. *Bulletin of the British Museum of Natural History (Zoology)* 25: 141–242.

Ilves KL, Torti D, López-Fernández H. 2017. Exon-based phylogenomics strengthens the phylogeny of Neotropical cichlids and identifies remaining conflicting clades (Cichliformes: Cichlidae: Cichlinae). *Molecular Phylogenetics and Evolution* 118: 232–243.

Keenleyside MHA, ed. 1991. *Cichlid fishes: Behaviour, ecology and evolution*. London: Chapman & Hall.

Kullander SO. 1983. *A review of the South American cichlid genus* Cichlasoma. Stockholm: Swedish Museum of Natural History.

Kullander SO. 1983. *Cichlid fishes of the Amazon River drainage of Peru*. Stockholm: Swedish Museum of Natural History.

Kullander SO. 1989. *Biotoecus* Eigenmann and Kennedy (Teleostei: Cichlidae): description of a new species from the Orinoco basin and revised generic diagnosis. *Journal of Natural History* 23: 225–260.

Kullander SO. 1998. A phylogeny and classification of the South American Cichlidae (Teleostei: Perciformes). In: Malabarba LR, Reis RE, Vari RP, Lucena ZM, Lucena CAS, eds. *Phylogeny and classification of Neotropical fishes*. Porto Alegre: Edipucrs, 461–498.

Liem KF. 1991. Functional morphology. In: Keenleyside MHA, ed. *Cichlid fishes: Behaviour, ecology and evolution*. London: Chapman & Hall, 129–150.

López-Fernández H, Arbour J, Willis S, Watkins C, Honeycutt RL, Winemiller KO. 2014. Morphology and efficiency of a specialized foraging behavior, sediment sifting, in Neotropical cichlids. *PLoS One* 9: e89832.

López-Fernández H, Arbour J, Winemiller KO, Honeycutt RL. 2013. Testing for ancient adaptive radiations in Neotropical cichlid fishes. *Evolution* 67: 1321–1337.

Mayden RL. 1989. Phylogenetic studies of North American minnows, with emphasis on the genus *Cyprinella* (Teleostei: Cypriniformes). *University of Kansas Museum of Natural History, Miscellaneous Publications* 80: 1–189.

Moretto EM, Marciano FT, Velludo MR, Fenerich-Verani N, Espíndola ELG, Rocha O. 2008. The recent occurrence, establishment and potential impact of *Geophagus proximus* (Cichlidae: Perciformes) in the Tietê River reservoirs: an Amazonian fish species introduced in the Paraná basin (Brazil). *Biodiversity and Conservation* 17: 3013–3025.

Oliva O, Skořepa V. 1968a. The myodome in barbel, *Barbus barbus* (Linnaeus) and tench, *Tinca tinca* (Linnaeus). *Věstník Československé Společnosti Zoologické* 32: 227–231.

Oliva O, Skořepa V. 1968b. The myodome in bream, *Abramis brama* (Linnaeus). *Věstník Československé Společnosti Zoologické* 32: 181–184.

Patterson C, Johnson GD. 1995. The intermuscular bones and ligaments of teleostean fishes. *Smithsonian Contributions to Zoology* 559: 1–83.

Říčan O, Piálek L, Dragová K, Novák J. 2016. Diversity and evolution of the Middle American cichlid fishes (Teleostei: Cichlidae) with revised classification. *Vertebrate Zoology* 66: 1–102.

Říčan O, Piálek L, Zardoya R, Doadrio I, Zrzavý. 2013. Biogeography of the Mesoamerican Cichlidae (Teleostei: Heroini): colonization through the GAARlandia land bridge and early diversification. *Journal of Biogeography* 40: 579–593.

Springer VG, Johnson GD. 2004. Study of the dorsal gill-arch musculature of the teleostome fishes, with special reference to the Actinopterygii. *Bulletin of the Biological Society of Washington* 11: 1–260.

Stiassny MLJ. 1981. Phylogenetic *versus* convergent relationship between piscivorous cichlid fishes from lakes Malawi and Tanganyika. *Bulletin of the British Museum of Natural History (Zoology)* 40: 67–101.

Stiassny MLJ. 1991. Phylogenetic intrarelationships of the family Cichlidae: an overview. In: Keenleyside MHA, ed. *Cichlid fishes: Behaviour, ecology and evolution*. London: Chapman & Hall, 1–35.

Weller HI, McMahan CD, Westneat MW. 2016. Dirt-sifting devilfish: winnowing in the geophagine cichlid *Satanoperca daemon* and evolutionary implications. *Zoomorphology* 136: 45–59.

Winterbottom R. 1974a. A descriptive synonymy of the striated muscles of the Teleostei. *Proceedings of the Academy of Natural Sciences of Philadelphia* 125: 225–317.

Winterbottom R. 194b. The familial phylogeny of the Tetraodontiformes (Acanthopterygii: Pisces) as evidenced by their comparative myology. *Smithsonian Contributions to Zoology* 155: 1–201.

Yamaoka K. 1991. Feeding relationships. In: Keenleyside MHA, ed. *Cichlid fishes: Behaviour, ecology and evolution*. London: Chapman & Hall, 151–172.

Zago AC, Franceschini L, Zocoller-Seno MC, Veríssimo-Silveira R, Maia AAD, Ikefuti CV, Silva RJ. 2013. The helminth community of *Geophagus proximus* (Perciformes: Cichlidae) from a tributary of the Paraná River, Ilha Solteira Reservoir, São Paulo State, Brazil. *Journal of Helminthology* 97: 203–211.

SUPPLEMENTARY MATERIAL CAPTIONS

Supplementary File 1. Protocol for the dissection of specimens for myological study.

FIGURE CAPTIONS

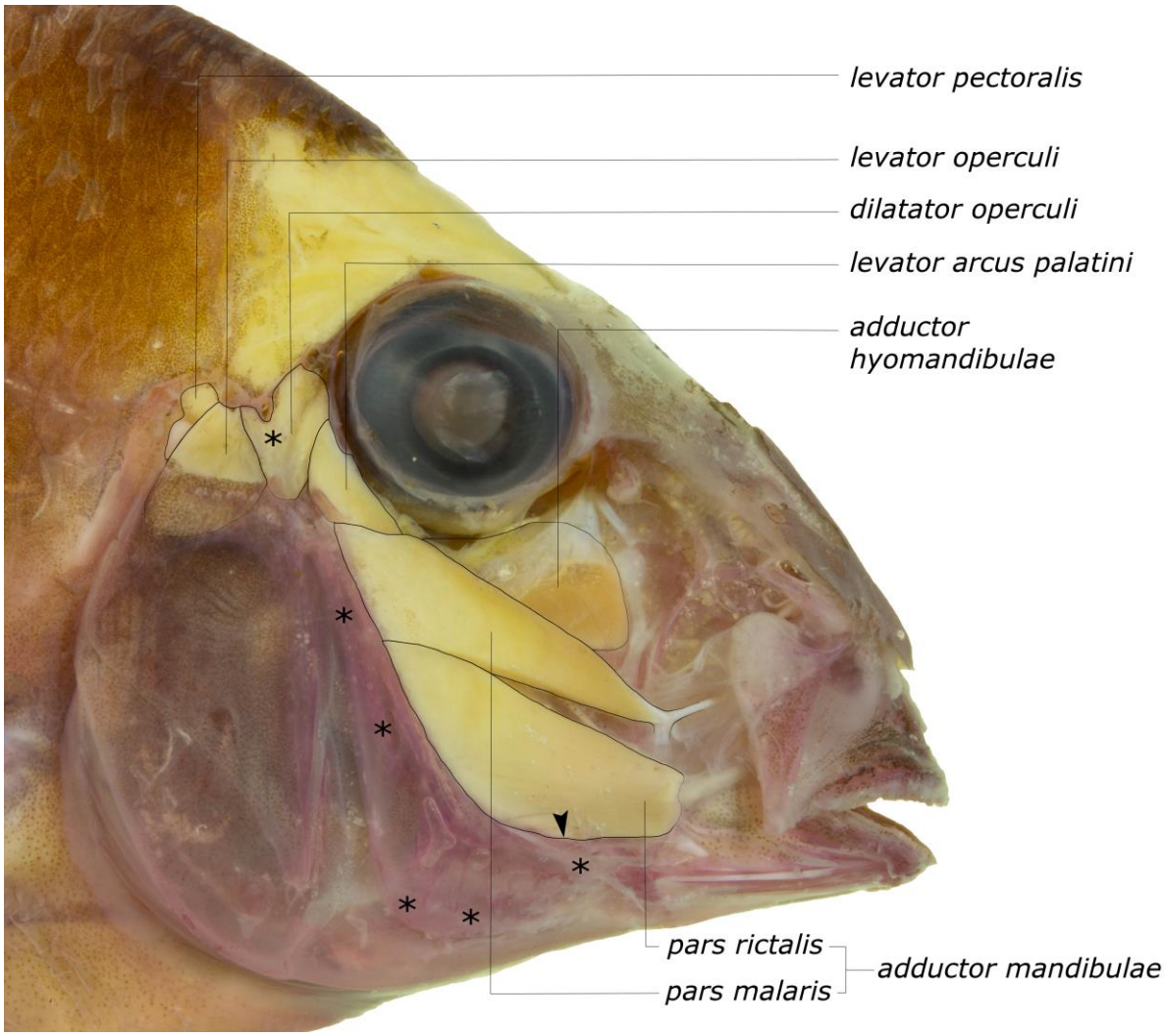

Fig. 1. Dissection stage 1A (see Supplementary File 1 for explanation). Right lateral view of head, with superficial muscles exposed. Asterisks indicate the position of the preopercular *lateralis* pores. Arrowhead indicates the anteriormost point where fibres of *adductor mandibulae, pars rictalis* originate.

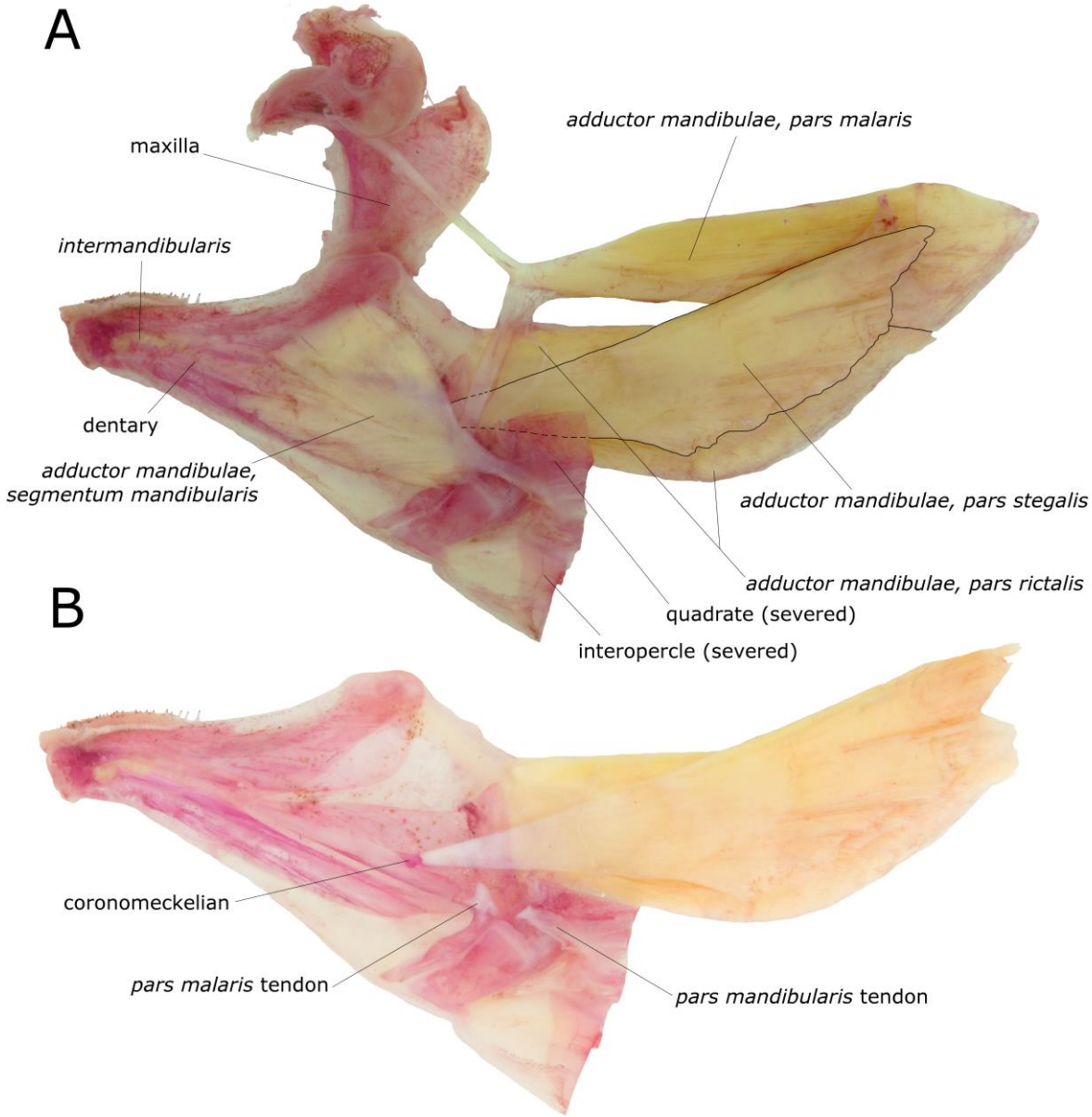

Fig. 2. Attachments of the *adductor mandibulae* to the jaws. (A) Dissection stage 2A (see Supplementary File 1 for explanation). Medial view of right lower jaw and maxilla and associate muscles. (B) Dissection stage 2B. Medial view of right lower jaw, evidencing the insertion tendons of the *adductor mandibulae*, *pars malaris* and *stegalis*.

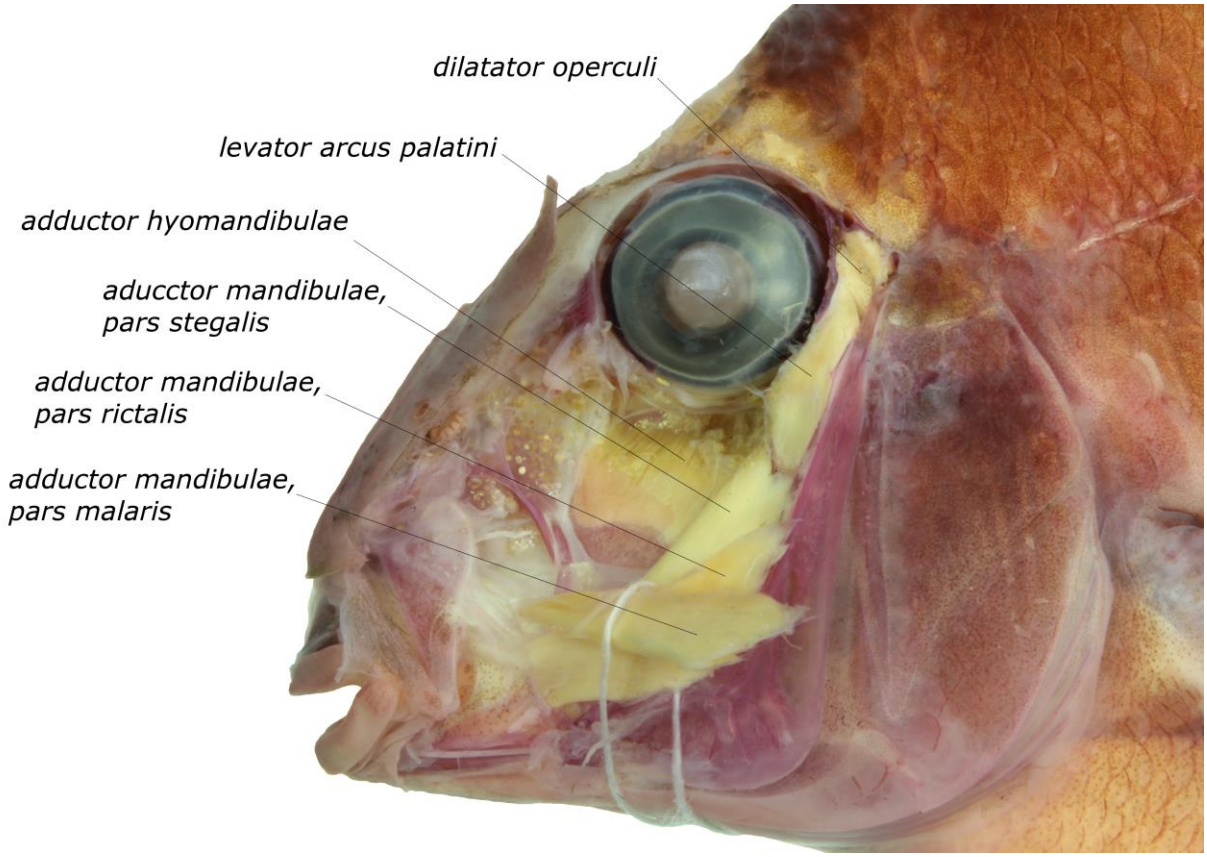

Fig. 3. Dissection stage 1B (see Supplementary File 1 for explanation). Left lateral view of head, evidencing origin of *adductor mandibulae*, *pars stegalis* and insertion of *levator arcus palatini*.

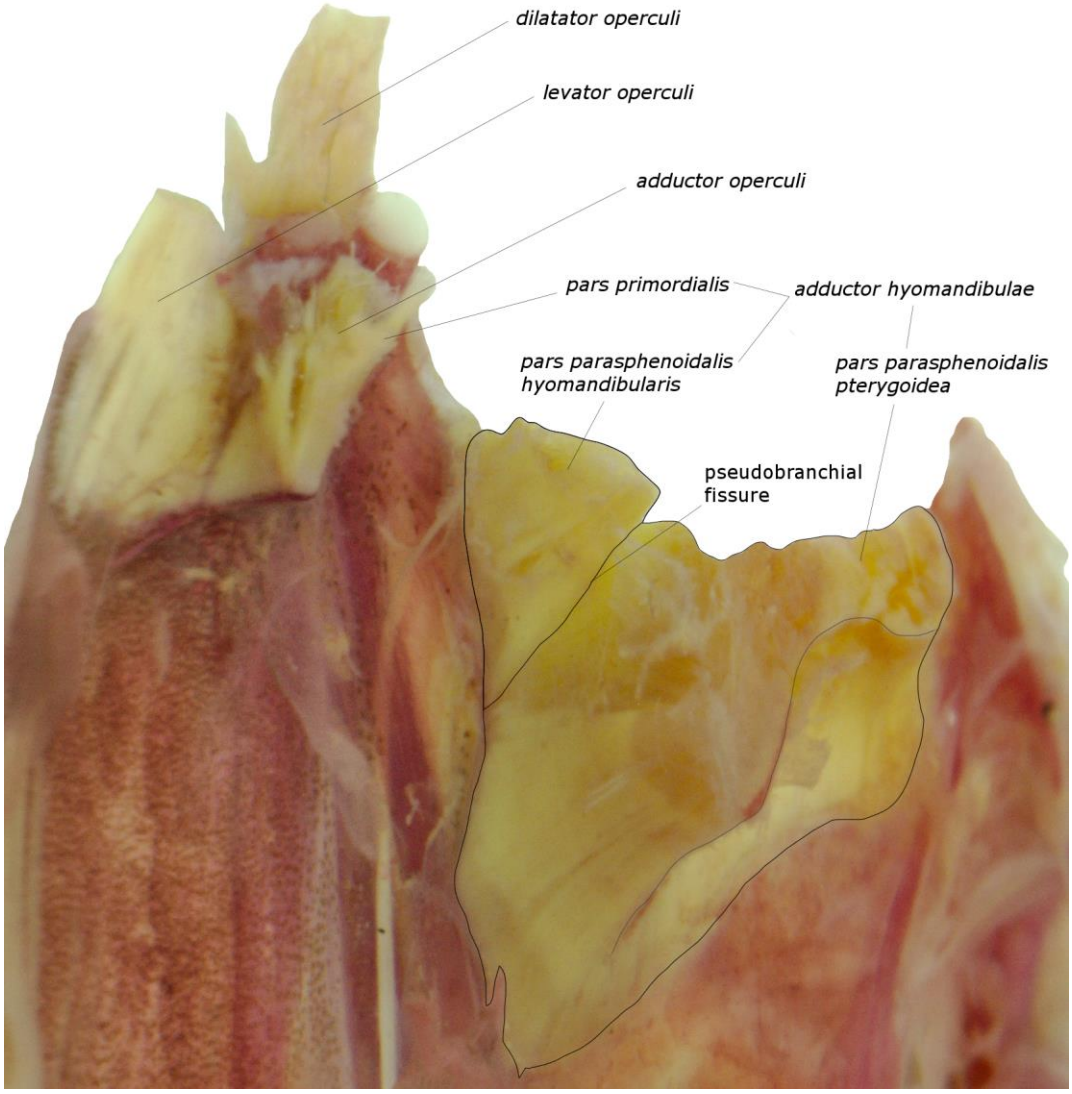

Fig. 4. Dissection stage 3 (see Supplementary File 1 for explanation). Left suspensorium in posteromedial view, evidencing the three parts of the *adductor hyomandibulae*. The fibres seen in the bottom left represent the dorsal portion of the *hyohyoidei adductores, pars dorsalis*.

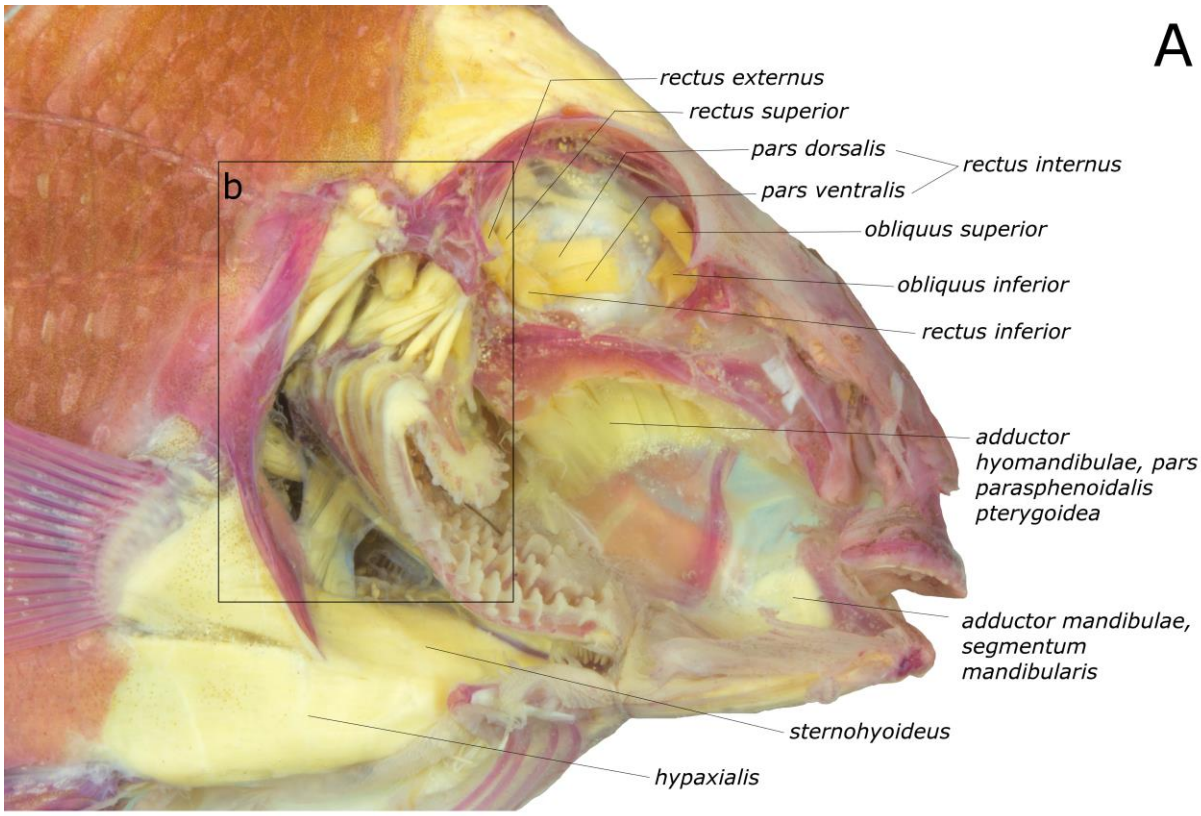
A
b
rectus externus
rectus superior
pars dorsalis
pars ventralis
rectus internus
obliquus superior
obliquus inferior
rectus inferior
adductor hyomandibulae, pars parasphenoidalis pterygoidea
adductor mandibulae, segmentum mandibularis
sternohyoideus
hypaxialis

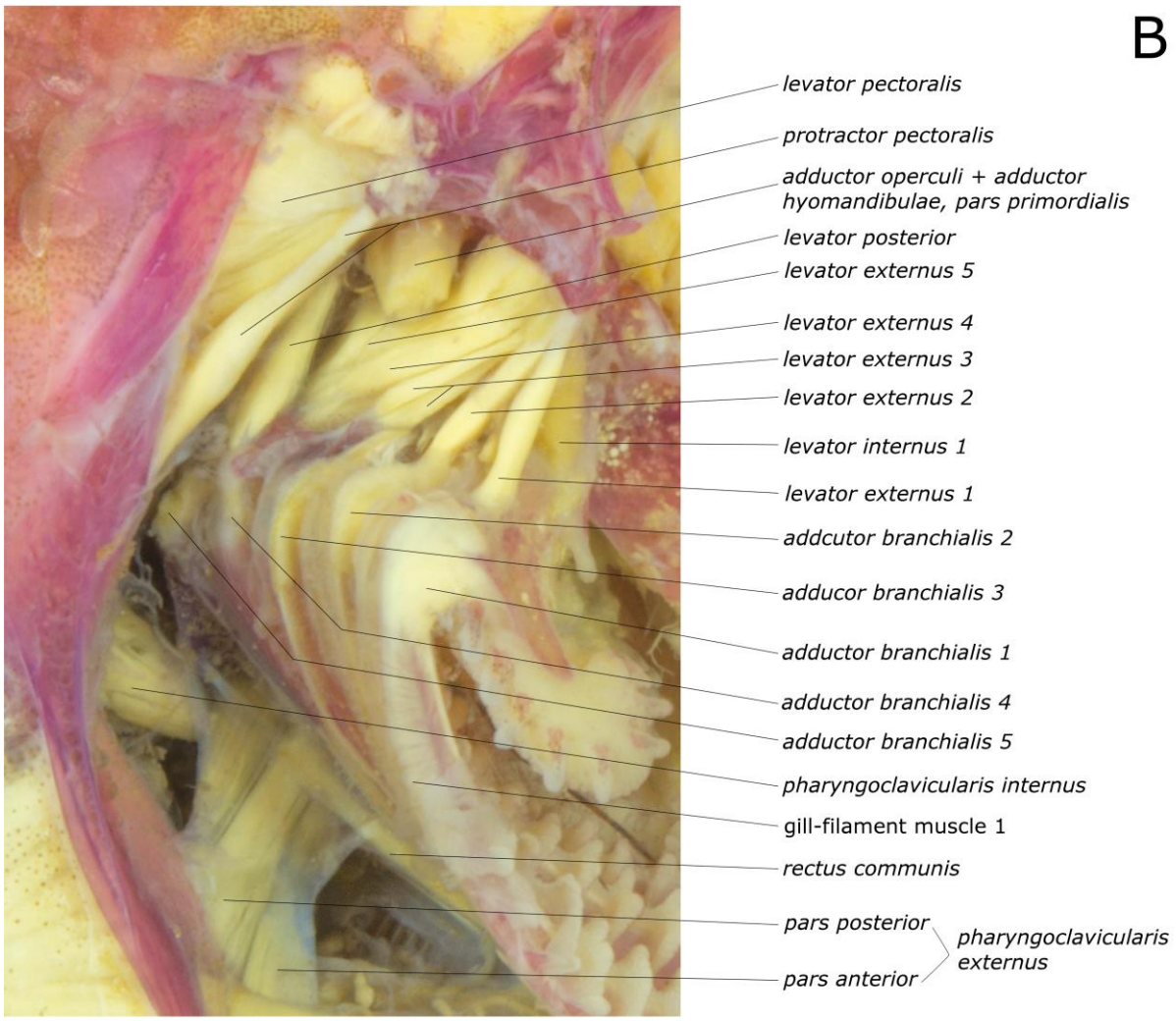
B
levator pectoralis
protractor pectoralis
adductor operculi + adductor hyomandibulae, pars primordialis
levator posterior
levator externus 5
levator externus 4
levator externus 3
levator externus 2
levator internus 1
levator externus 1
addcutor branchialis 2
adducor branchialis 3
adductor branchialis 1
adductor branchialis 4
adductor branchialis 5
pharyngoclavicularis internus
gill-filament muscle 1
rectus communis
pars posterior
pars anterior
pharyngoclavicularis externus

Fig. 5. Dissection stage 3 (see Supplementary File 1 for explanation). (A) Right lateral view of the head, exposing profound musculature. (B) Close-up of the muscles linking the branchial arches, neurocranium and pectoral fin.

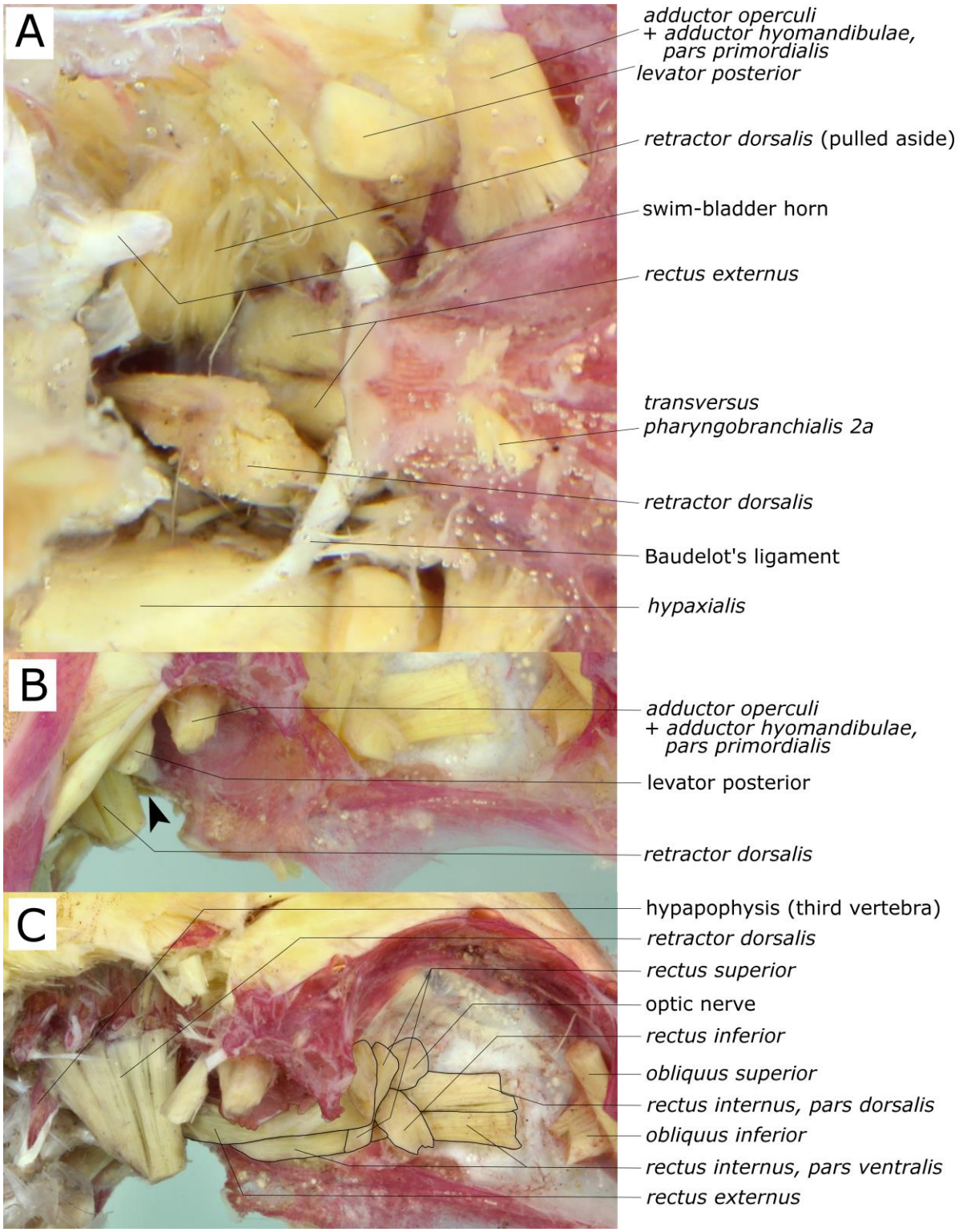

Fig. 6. *Retractor dorsalis* and eye muscles. (A) Dissection stage 6A, before the removal of the ribs (see Supplementary File 1 for explanation). Anteroventral view of posteroventral region of neurocranium and anterior vertebrae, with associated muscles (anterior to the right). (B) Dissection stage 4A. Lateral view of posteroventral region of head, part of the shoulder girdle and associated muscles (anterior to the right). Arrowhead indicates a small portion of the *rectus externus*, which is visible without dissection of the neurocranium. (C) Dissection stage 7. Lateral view of orbit and posteroventral region of head and associated muscles. We pulled aside the anterior portion of the swimbladder, in order to expose the hypapophysis of 3rd vertebra.

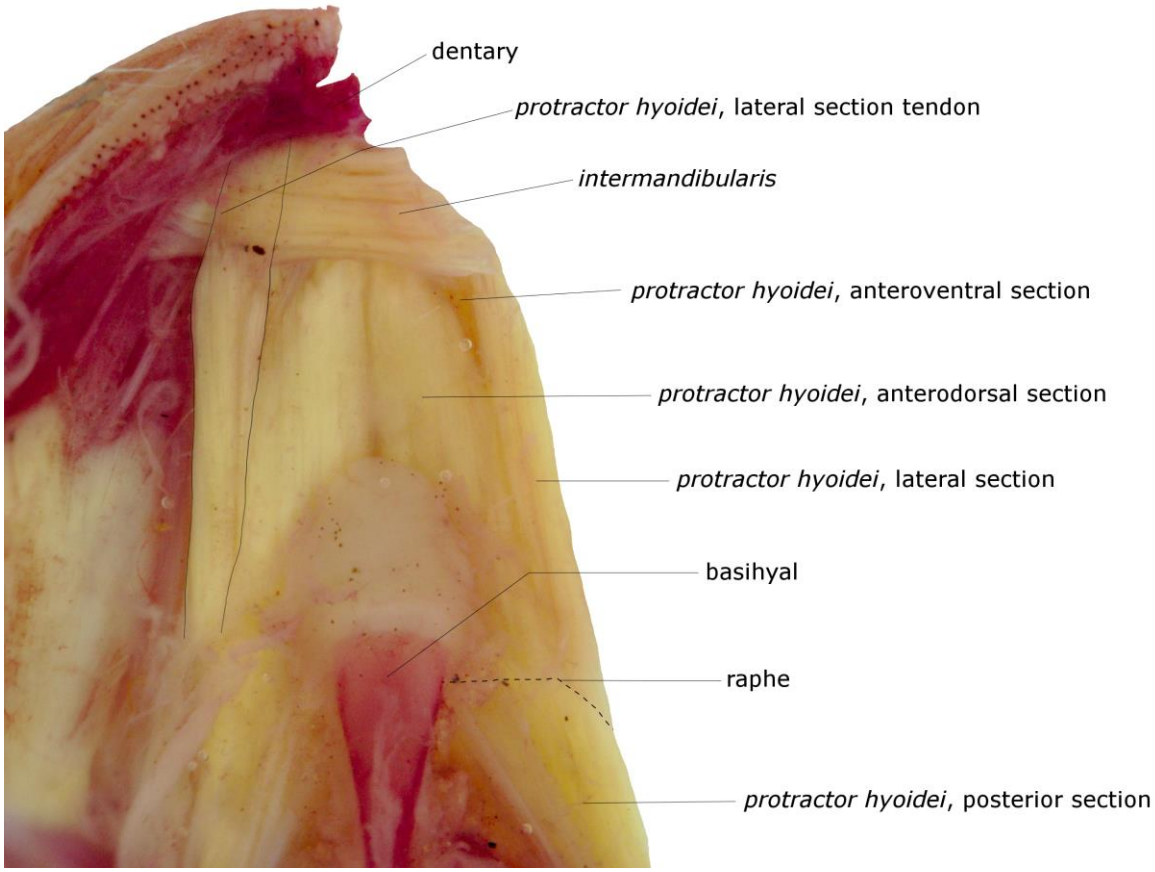

Fig. 7. Dissection stage 4A (see Supplementary File 1 for explanation). Dorsal view of dentary, anterior portion of hyoid arch and associate muscles.

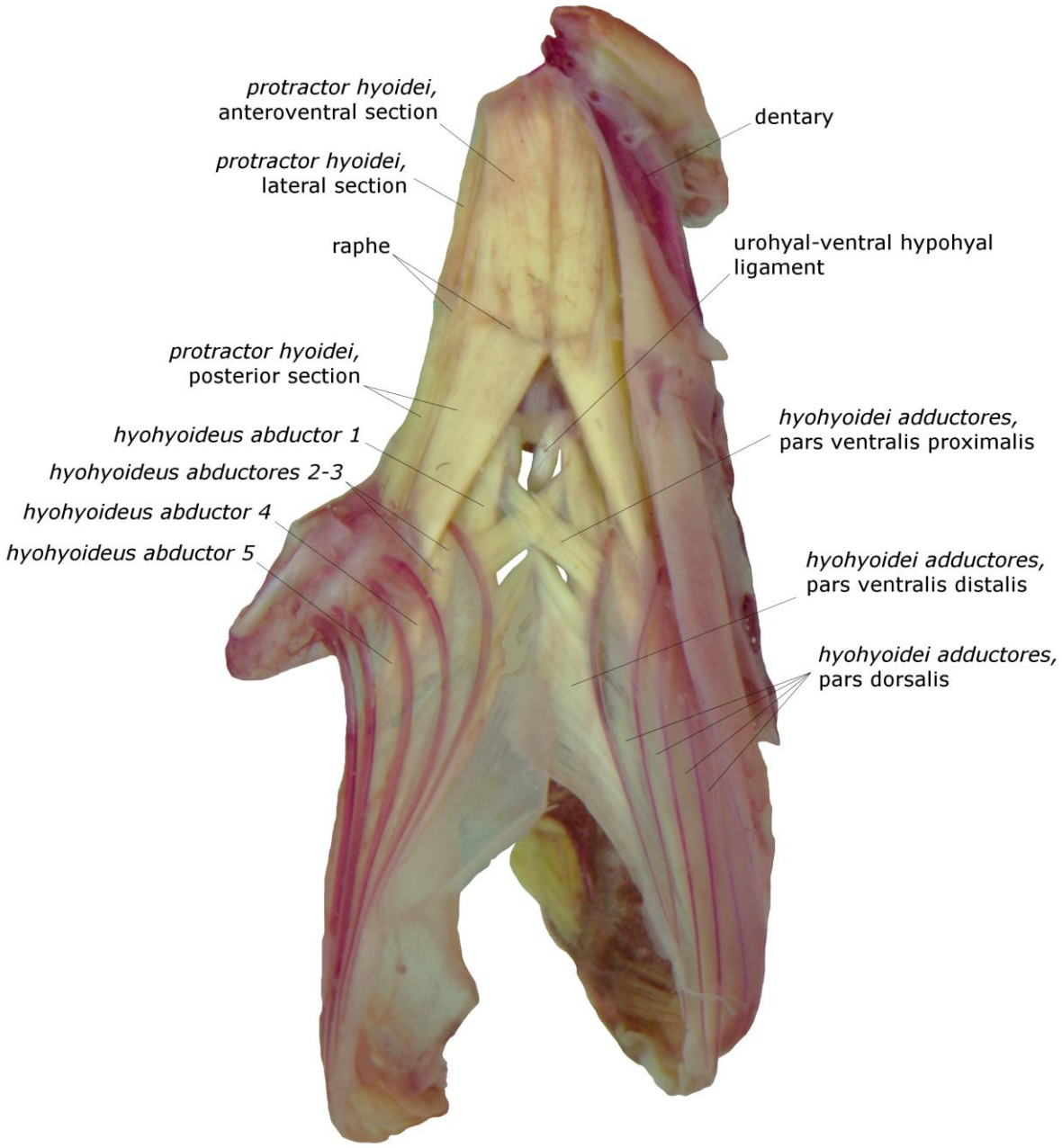

Fig. 8. Dissection stage 4A (see Supplementary File 1 for explanation). Ventral view of hyoid arches, left suspensorium and associated ventral head musculature.

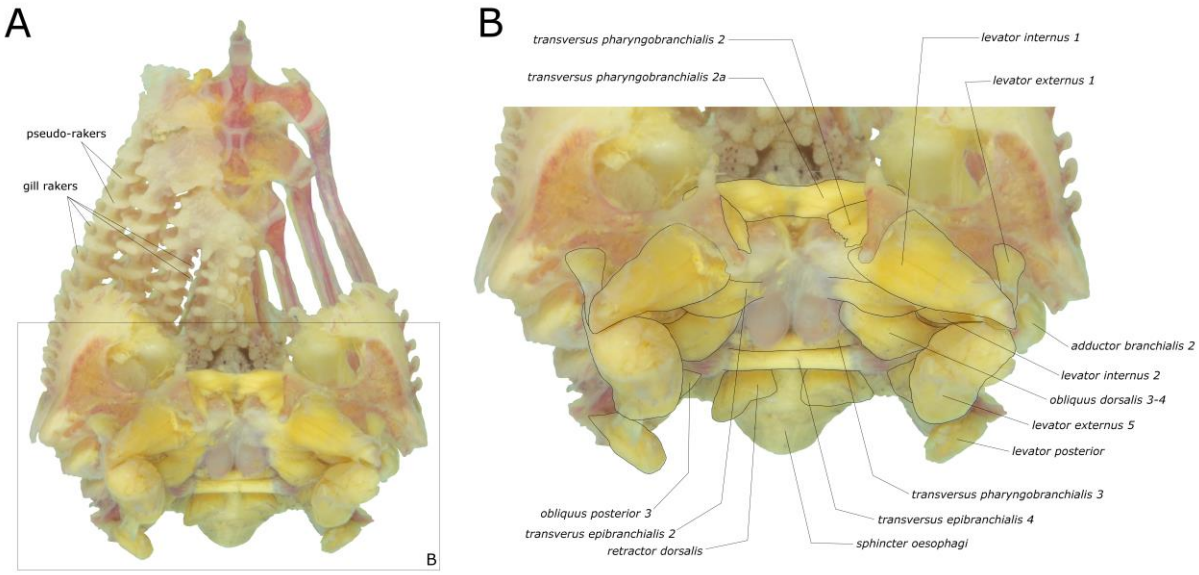

Fig. 9. Dissection stage 4A (see Supplementary File 1 for explanation). (A) Dorsal view of branchial basket and associated musculature. (B) Close-up of the muscles associated with the pharyngobranchials and epibranchials.

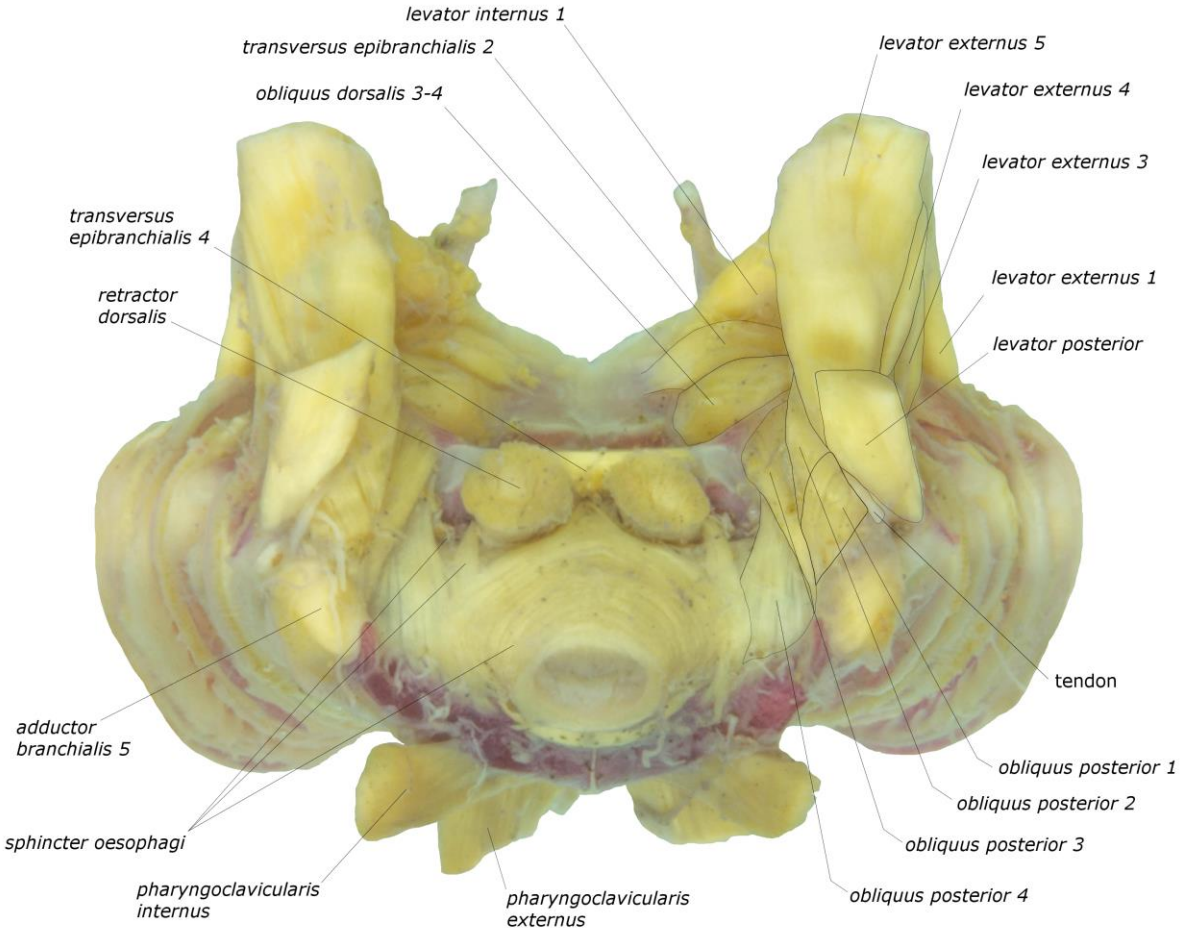

Fig. 10. Dissection stage 4A (see Supplementary File 1 for explanation). Posterior view of branchial basket and associated musculature.

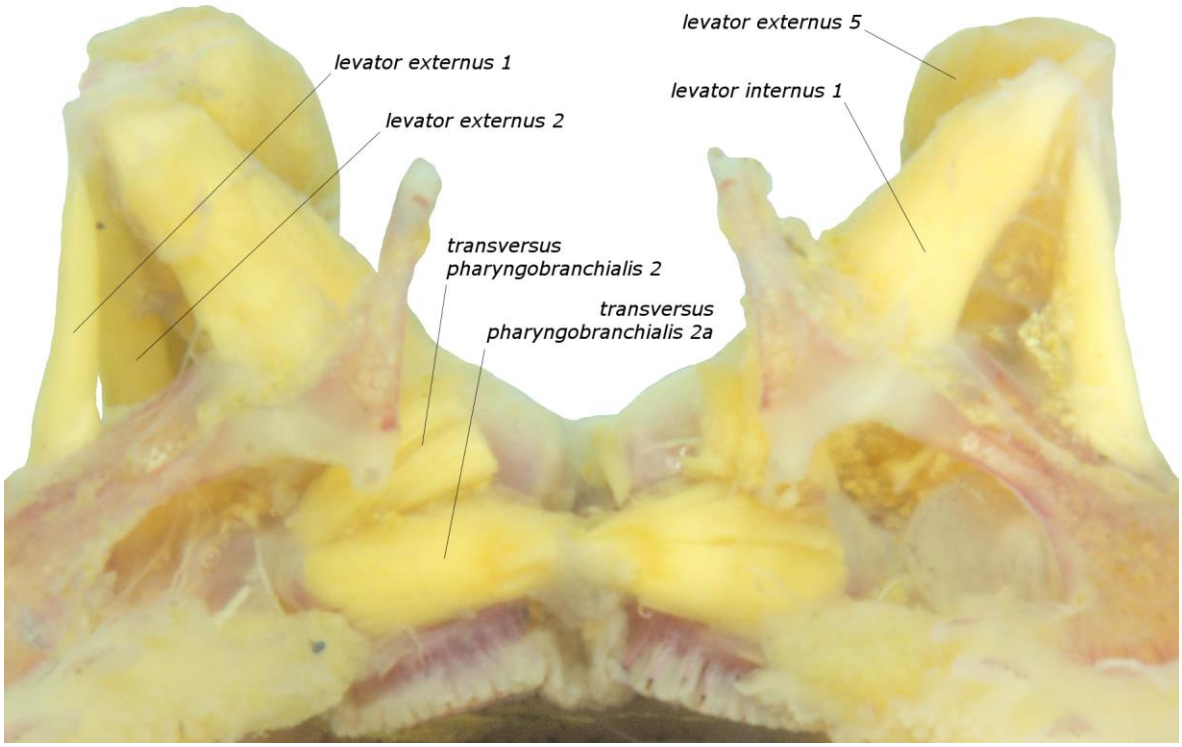

Fig. 11. Dissection stage 4A (see Supplementary File 1 for explanation). Anterior view of dorsal portion of branchial basket and associated musculature.

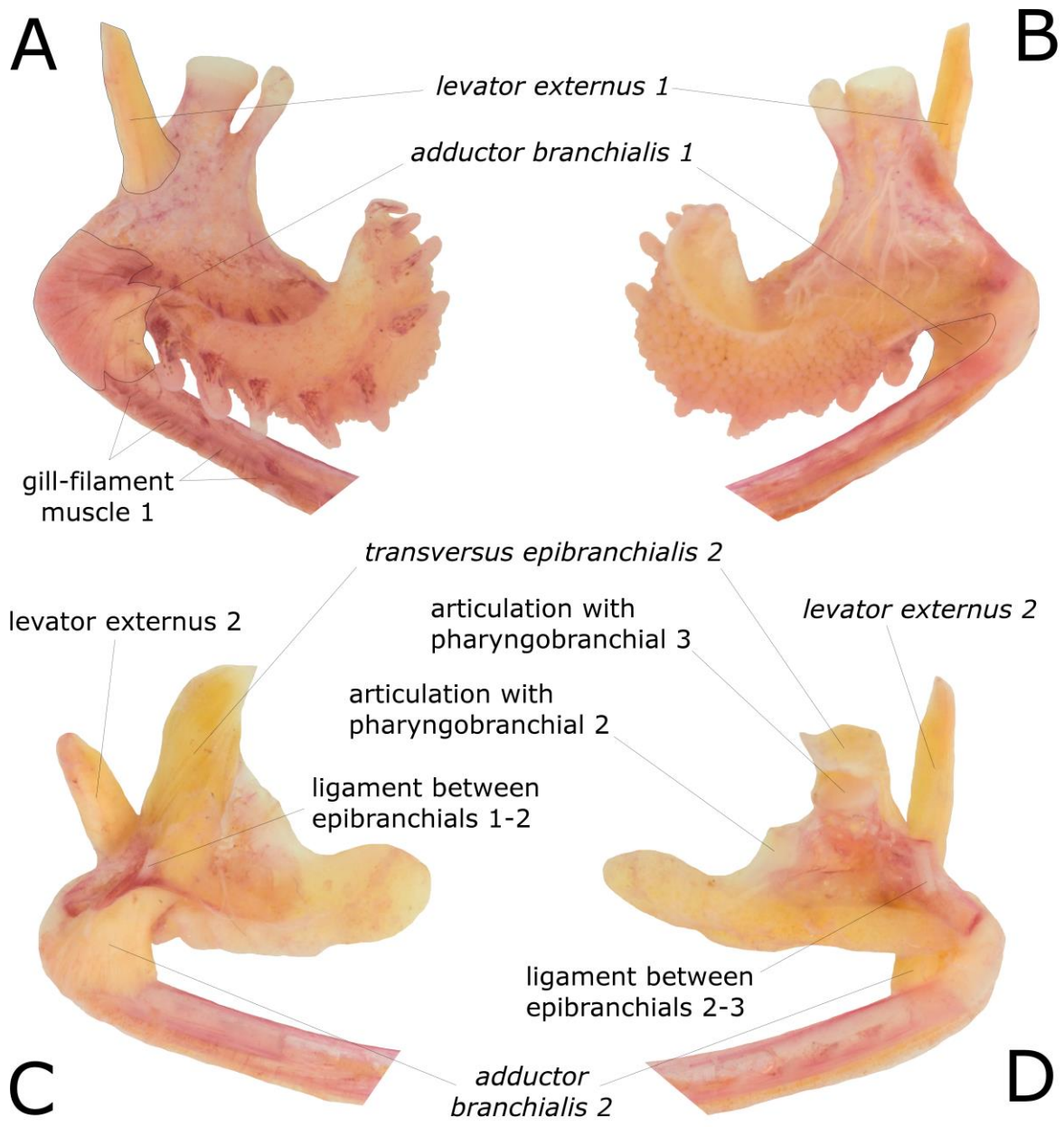

Fig. 12. Dissection stage 6A (see Supplementary File 1 for explanation). Epibranchials 1–2 and associated musculature. (A) Lateral view of epibranchial 1, attached to dorsolateral half of ceratobranchial 1, and associated muscles (anterior to the right). (B) Medial view of epibranchial 1, attached to dorsolateral half of ceratobranchial 1, and associated muscles (anterior to the left). (C) Lateral view of epibranchial 2, attached to dorsolateral half of ceratobranchial 2, and associated muscles (anterior to the right). (D) Medial view of epibranchial 2, attached to dorsolateral half of ceratobranchial 2, and associated muscles (anterior to the left).

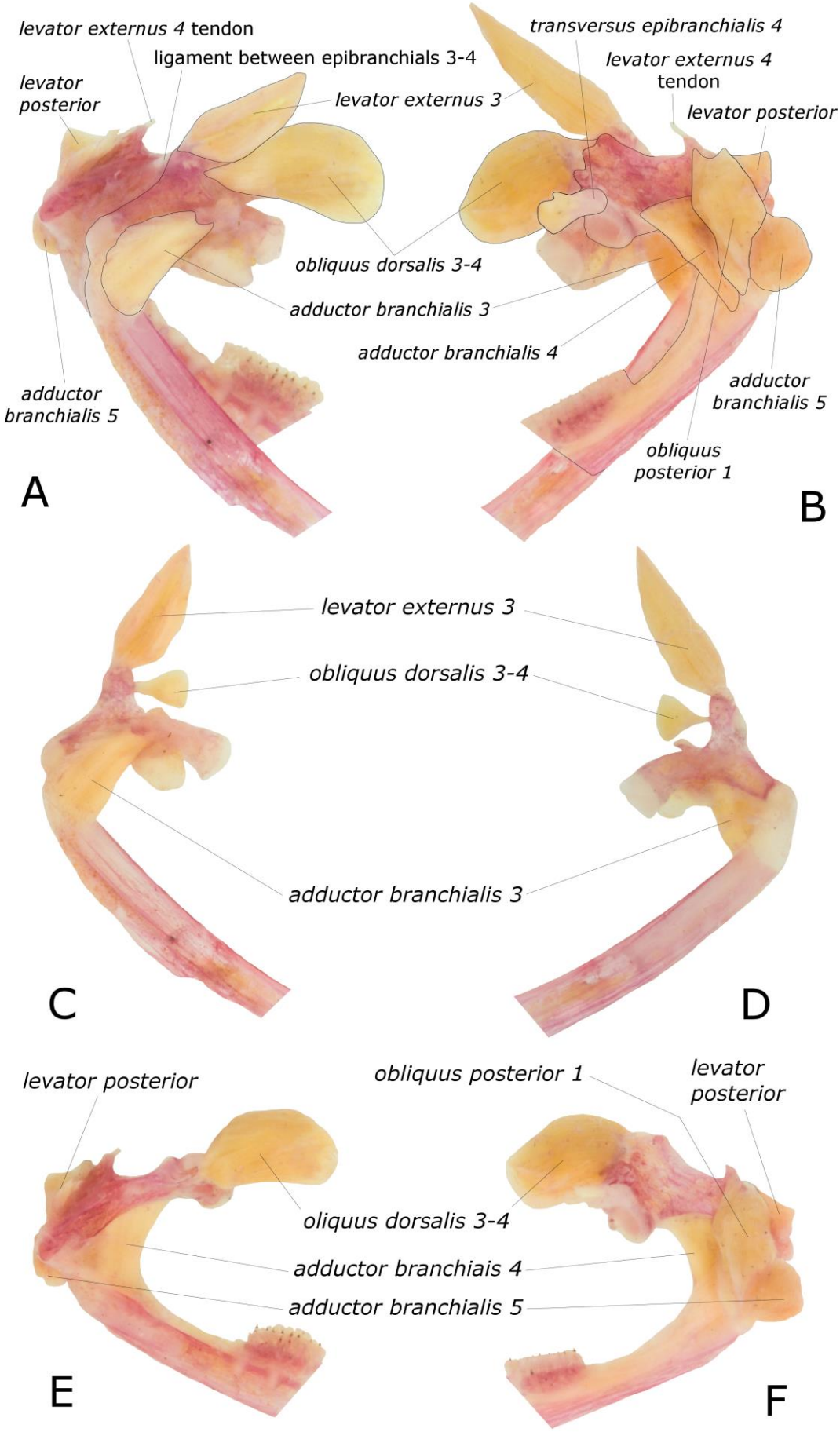
levator externus 4 tendon
ligament between epibranchials 3-4
levator posterior
levator externus 3
obliquus dorsalis 3-4
adductor branchialis 3
adductor branchialis 4
adductor branchialis 5
A
transversus epibranchialis 4
levator externus 4 tendon
levator posterior
adductor branchialis 5
obliquus posterior 1
B
levator externus 3
obliquus dorsalis 3-4
adductor branchialis 3
C
D
levator posterior
oliquus dorsalis 3-4
adductor branchiais 4
adductor branchialis 5
E
obliquus posterior 1
levator posterior
F

Fig. 13. Dissection stage 6A (see Supplementary File 1 for explanation). Epibranchials 3–4 and associated musculature. (A) Lateral view of epibranchials 3–4, attached to dorsolateral halves of ceratobranchials 3–4, and associated muscles (anterior to the right). (B) Medial view of epibranchials 3–4, attached to dorsolateral halves of ceratobranchials 3–4, and associated muscles (anterior to the left). (C) Lateral view of epibranchial 3, attached to dorsolateral half of ceratobranchial 3, and associated muscles (anterior to the right). (D) Medial view of epibranchial 3, attached to dorsolateral half of ceratobranchial 3, and associated muscles (anterior to the left). (E) Lateral view of epibranchial 4, attached to dorsolateral half of ceratobranchial 4, and associated muscles (anterior to the right). (F) Medial view of epibranchial 4, attached to dorsolateral half of ceratobranchial 4, and associated muscles (anterior to the left).

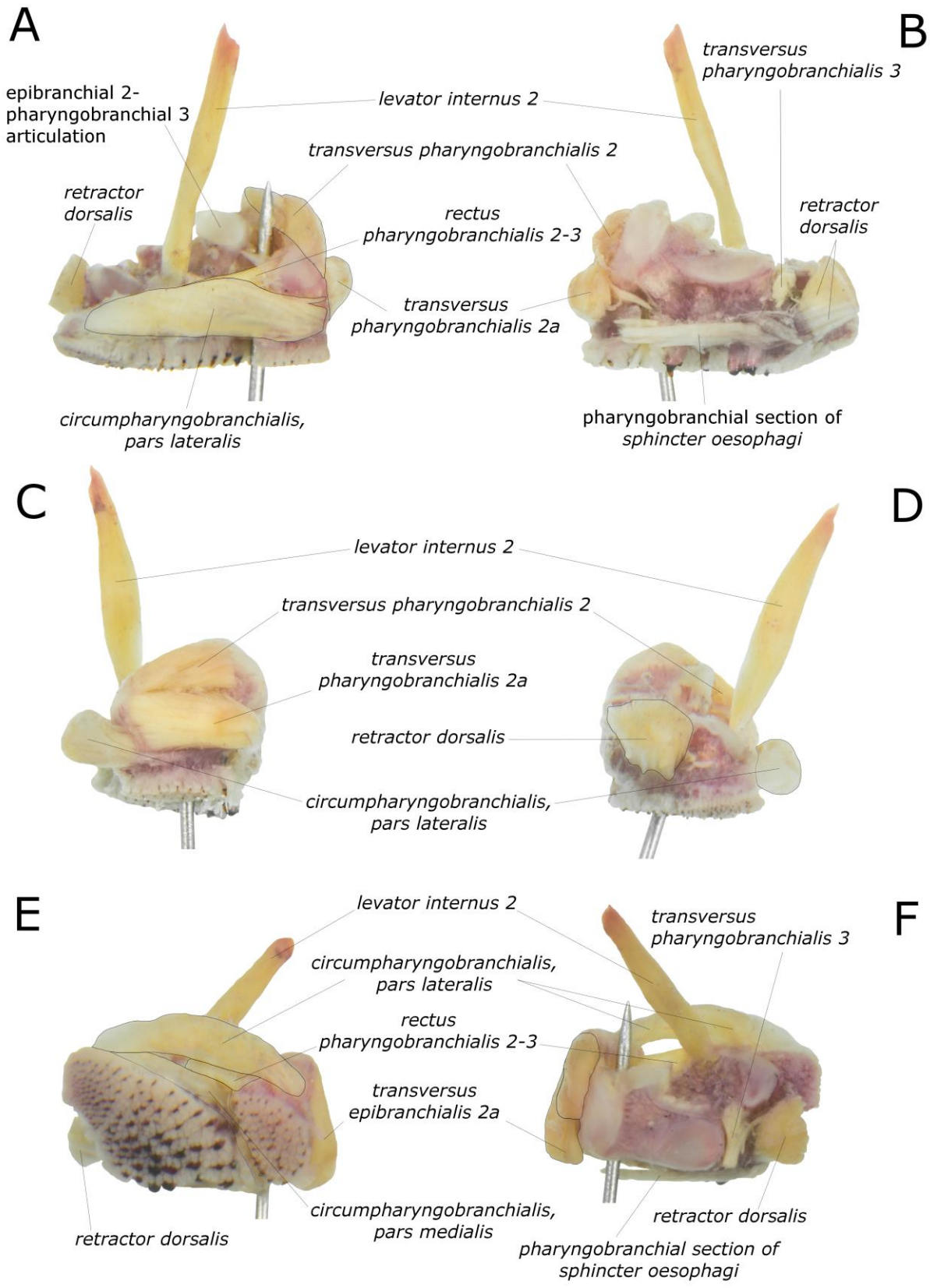

Fig. 14. Dissection stage 5A (see Supplementary File 1 for explanation). Right pharyngobranchials 2–3 and upper tooth-plate 4, with associate musculature. (A) Lateral

view, anterior to the right. (B) Medial view, anterior to the left. (C) Anterior view. (D) Posterior view. (E) Ventral view, anterior to the right. (F) Dorsal view, anterior to the left.

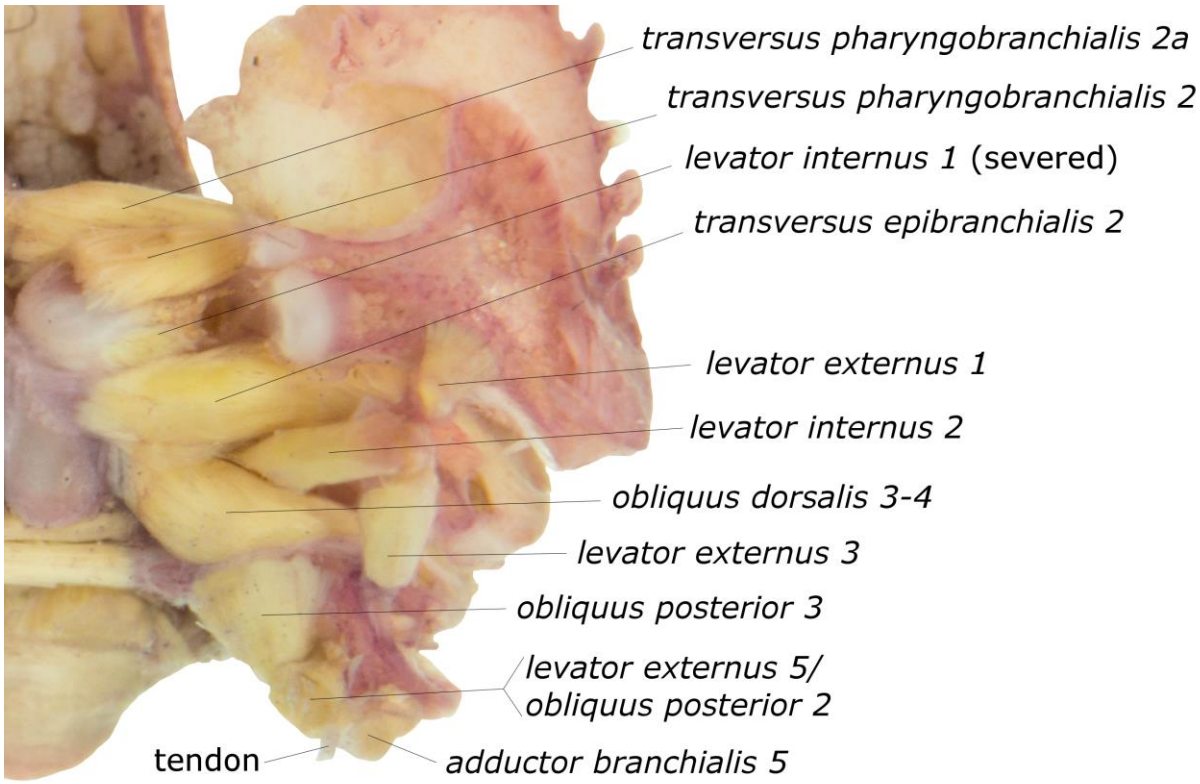

Fig. 15. Dissection stage 4B (see Supplementary File 1 for explanation). Right-side upper portion of the branchial basket (anterior to the top), with associate musculature, evidencing the *transversus epibranchialis 2*, *levator internus 2*, *obliquus dorsalis 3–4* and *obliquus posterior 3*, all of which are partially hidden (in dorsal view) before the extraction of the *levator internus 1* and of the *levator externus 5*.

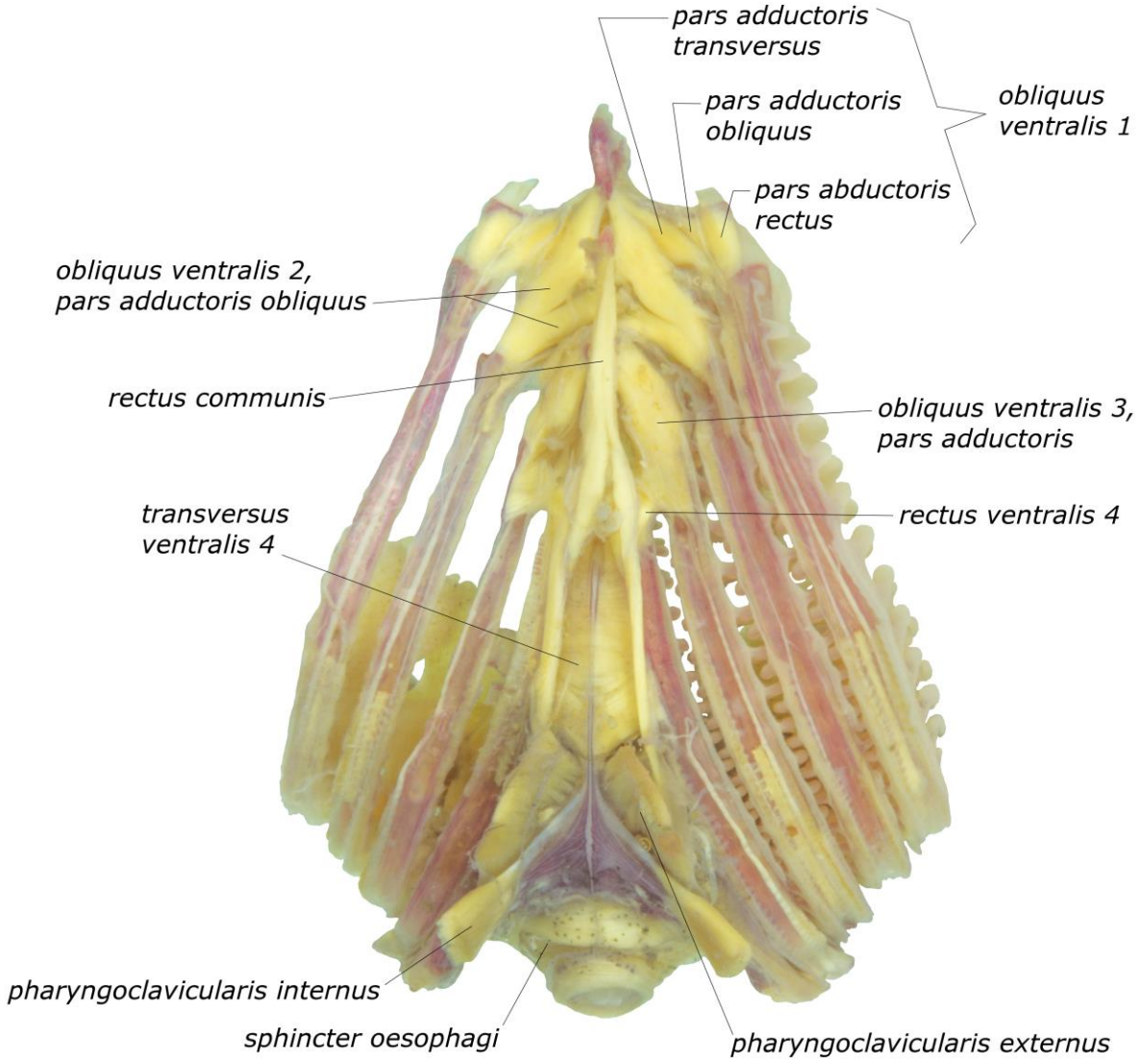

Fig. 16. Dissection stage 4A (see Supplementary File 1 for explanation). Ventral view of branchial basket and associated muscles.

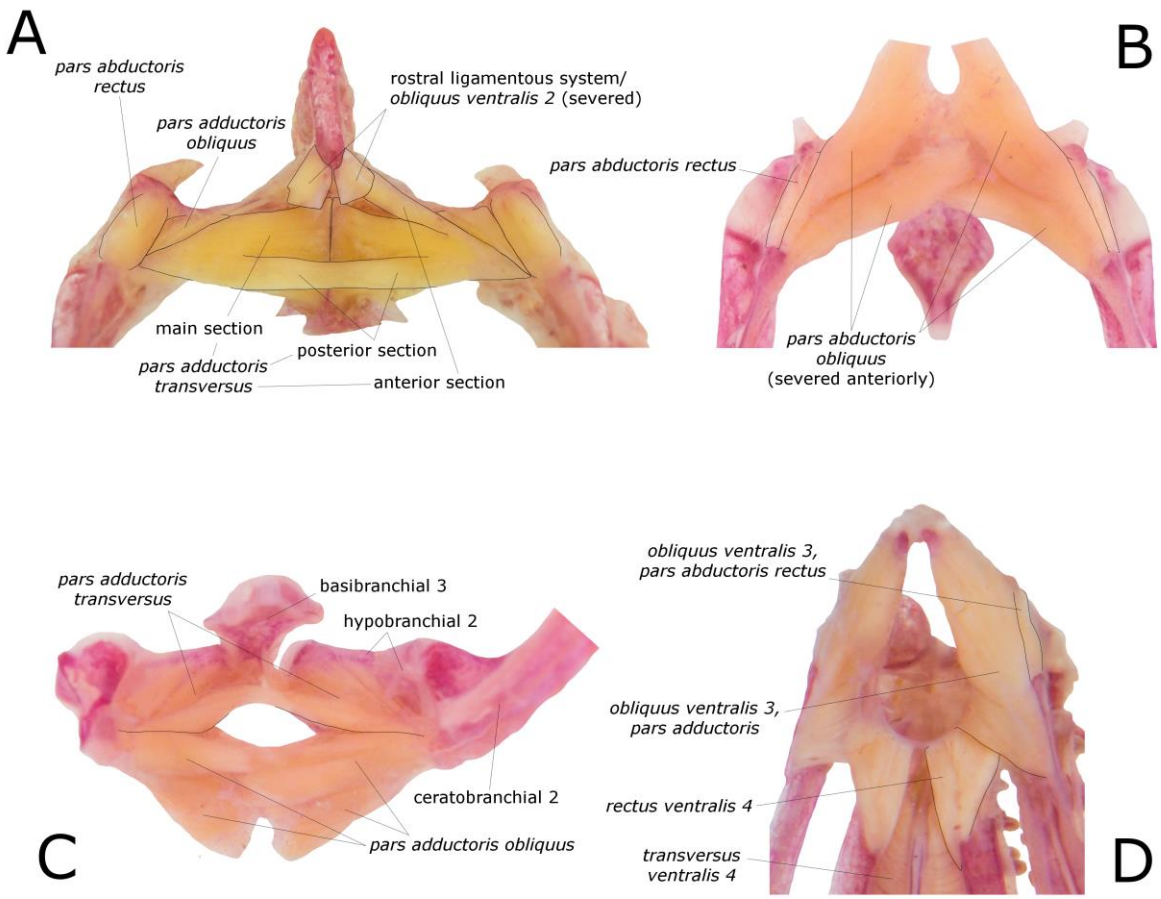

Fig. 17. Dissection stage 6A (see Supplementary File 1 for explanation). Ventral portion of dismembered branchial arches. (A) Ventral view, of basibranchials 1–2, hypobranchials 1, part of ceratobranchials 1 and associated *obliquus ventralis 1* (anterior to the top). (B) Ventral view, of basibranchial 3, hypobranchials 2, part of ceratobranchials 2 and associated *obliquus ventralis 2* (anterior to the top); (C) Same as in (B), but in posterior view. (D) Hypobranchials 3 and part of ceratobranchials 3–5, with associated semi-circular ligamentous system and muscles.

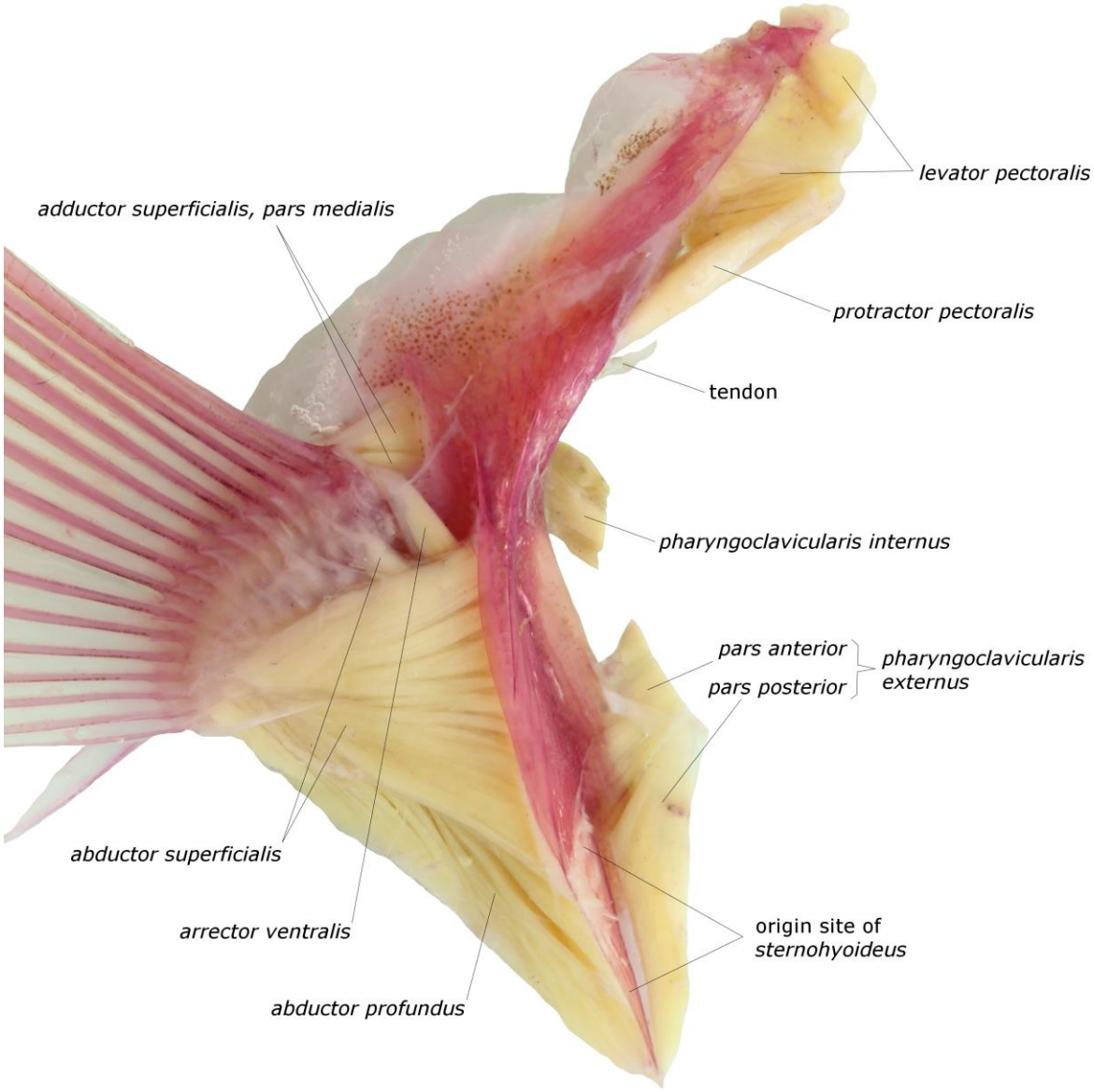

Fig. 18. Dissection stage 6A (see Supplementary File 1 for explanation). Lateral view of right pectoral girdle and associated muscles.

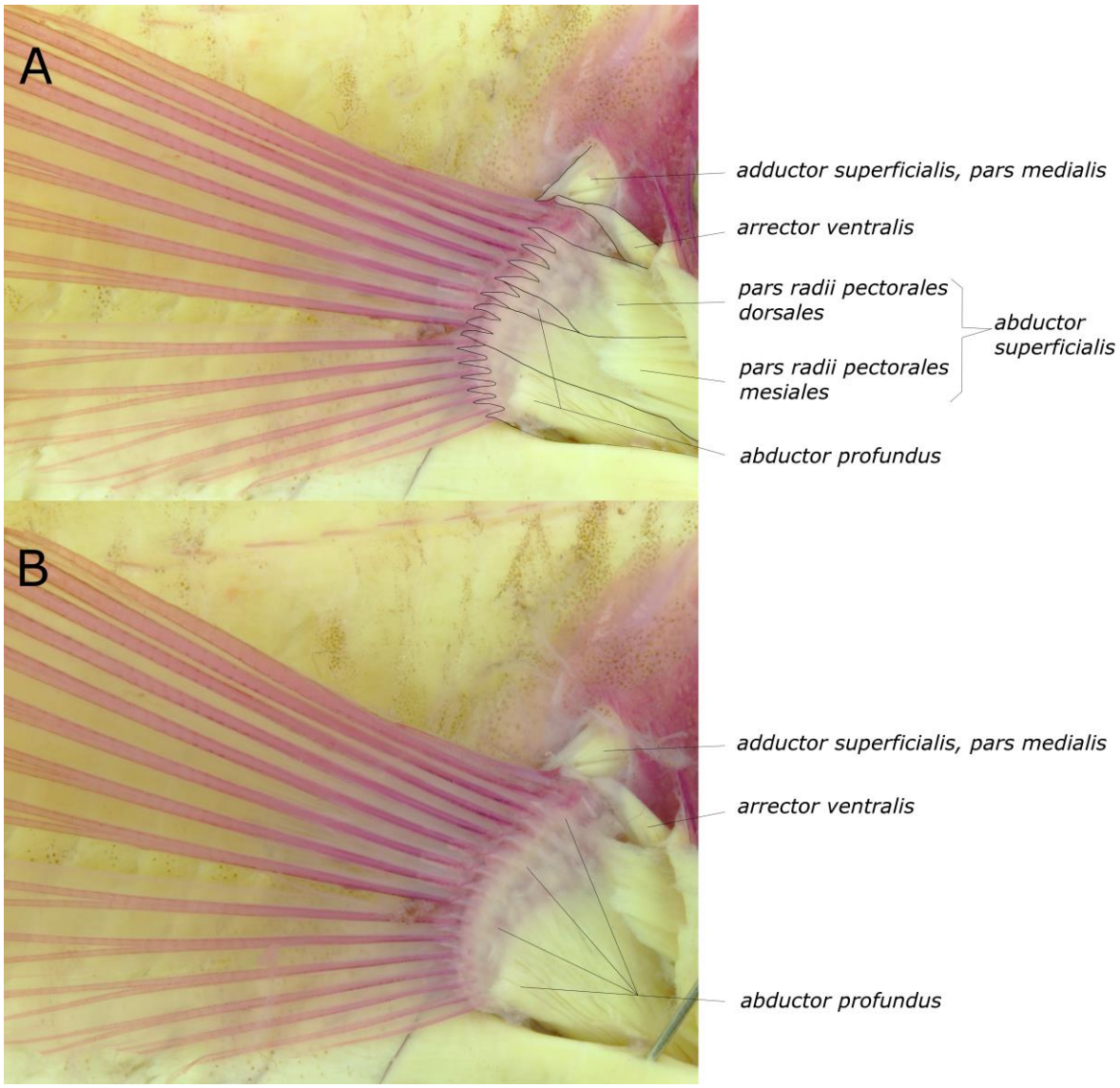

Fig. 19. Dissection stage 5A (see Supplementary File 1 for explanation). Lateral view of right pectoral girdle, evidencing the different muscle layers of *abductor* muscles. (A) *Abductor superficialis*, *pars radii pectorales ventrales* pulled aside. (B) All parts of *abductor superficialis* pulled aside, evidencing *abductor profundus*.

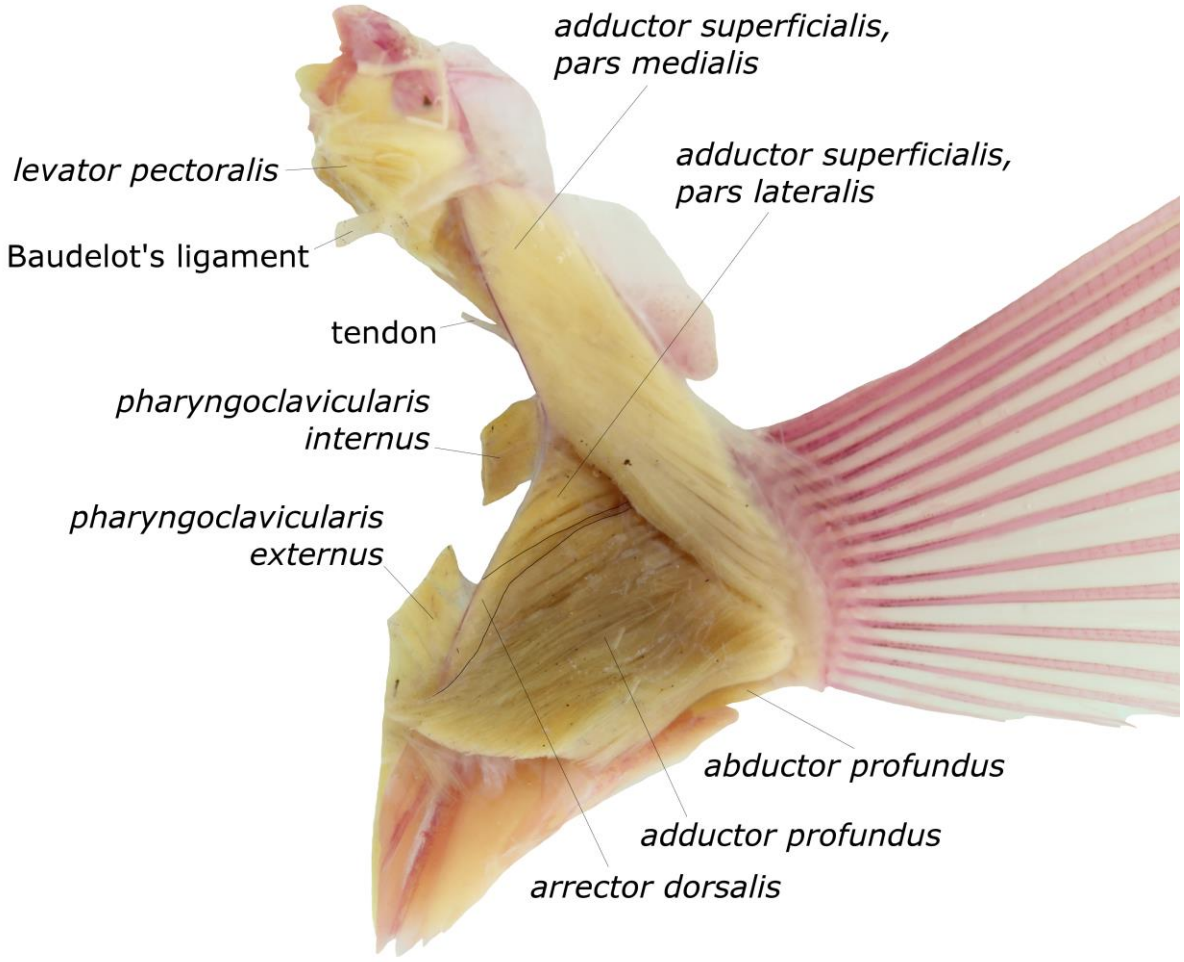

Fig. 20. Dissection stage 6A (see Supplementary File 1 for explanation). Medial view of right pectoral girdle and associated muscles.

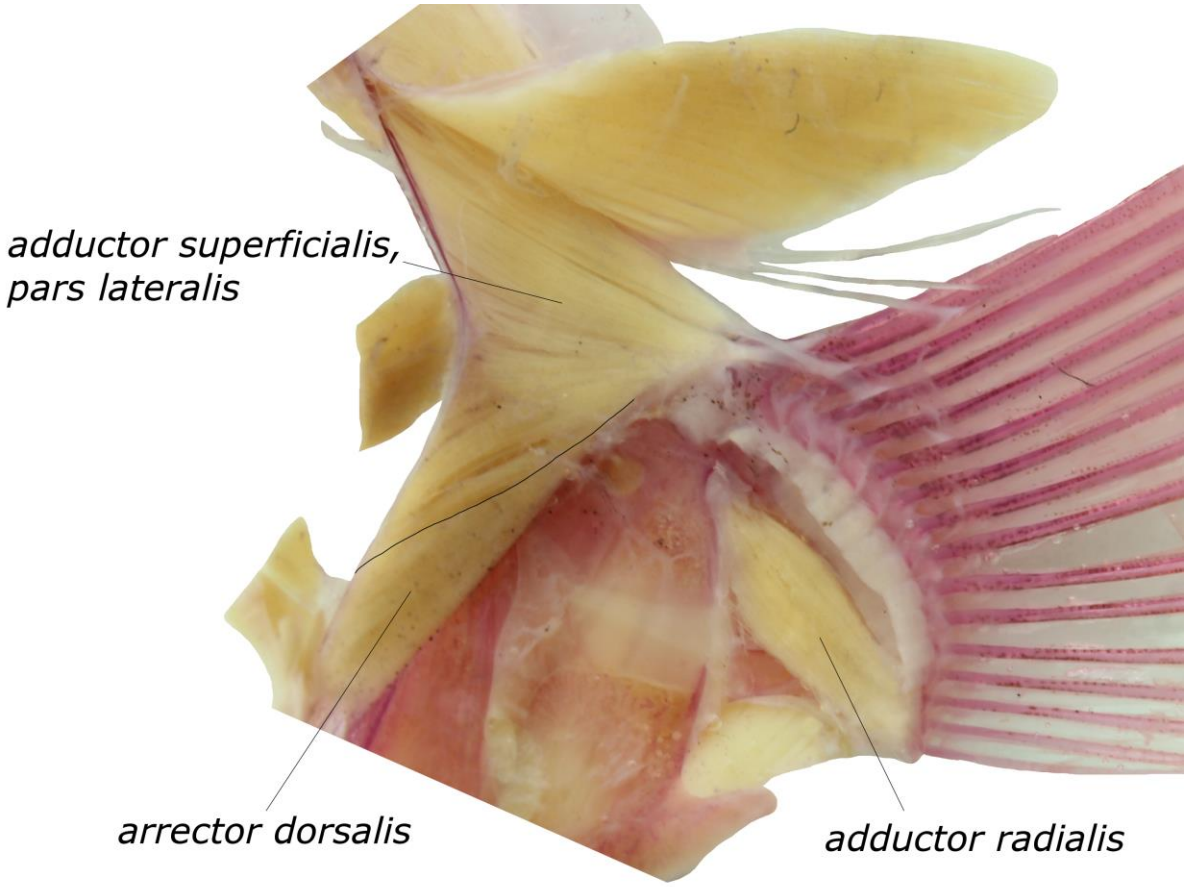

Fig. 21. Dissection stage 6B (see Supplementary File 1 for explanation). Medial view of right pectoral girdle and associated muscles. *Adductor profundus* and *adductor superficialis, pars medialis* pulled aside, evidencing subjacent muscles. Ventral and dorsal portions of pectoral girdle and most of the *adductor superficialis*, *pars medialis* omitted. For unlabelled muscles, compare with Figure 20.

length).

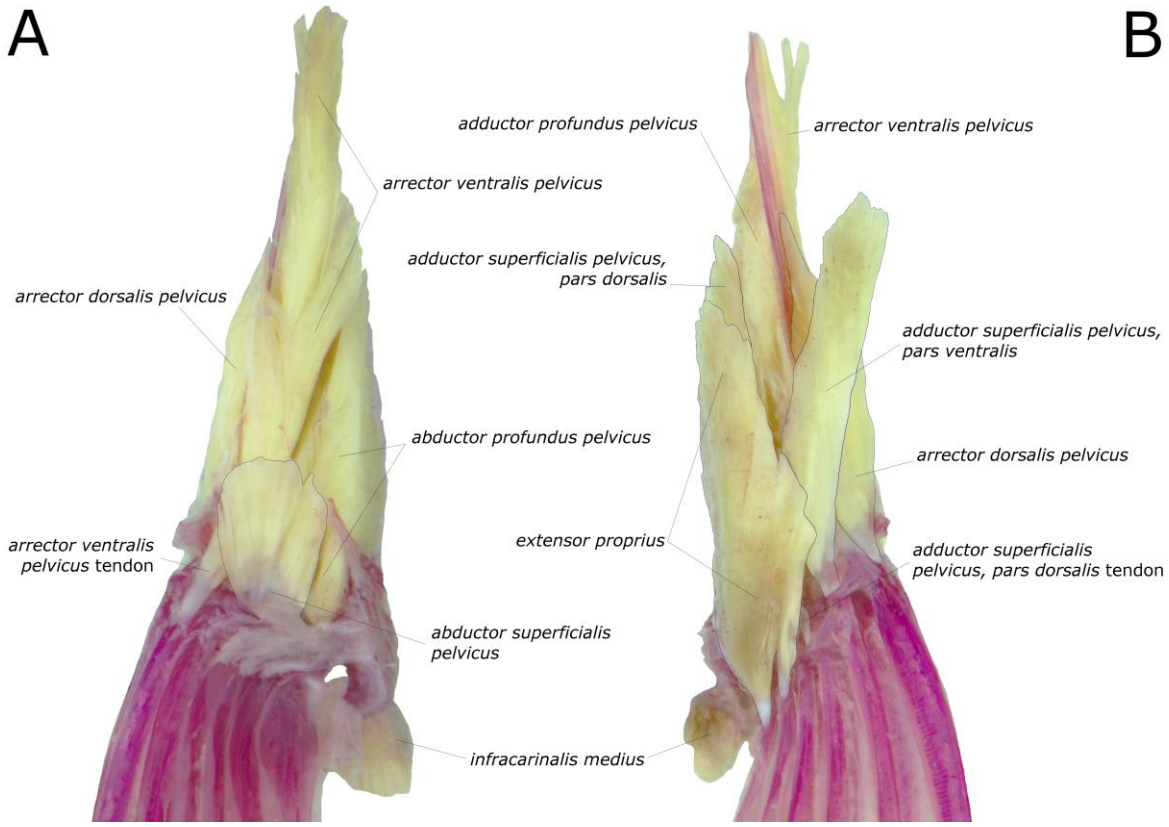

Fig. 22. Dissection stage 6A (see Supplementary File 1 for explanation). Pelvic girdle and associated musculature. (A) Ventral view. (B) Dorsal view. The *adductor superficialis pelvicus*, *pars ventralis*, is laterally displaced, in order to expose the *adductor profundus pelvicus*. Its original position is adjacent to the *pars dorsalis*.

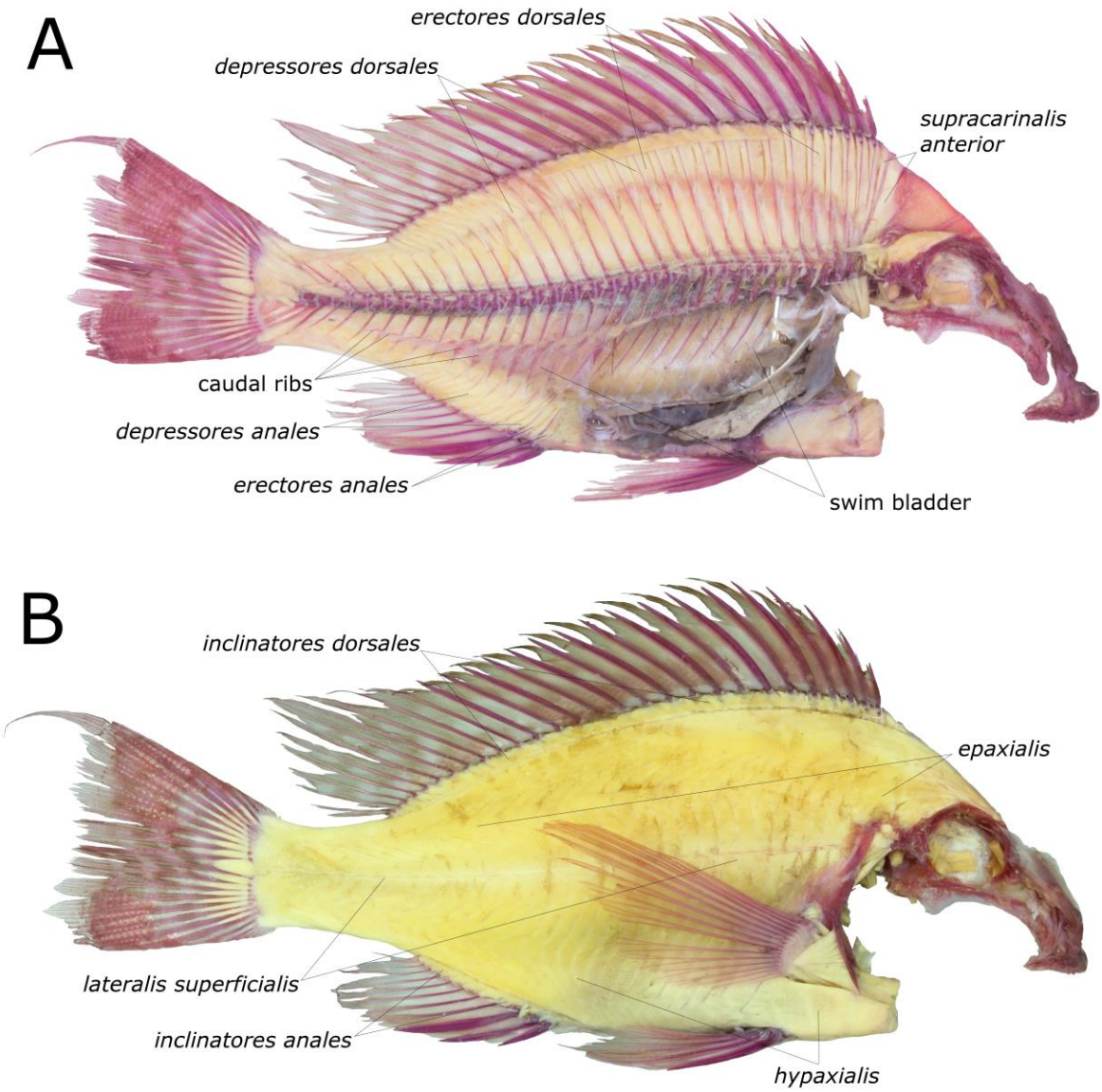

Fig. 23. Lateral view of body musculature. (A) Dissection stage 7 (see Supplementary File 1 for explanation). Notice that there are no specialised muscles associated with caudal swim-bladder extensions. We provide detailed views of muscles associated with vertical fins in Figs. 24–26. (B) Dissection stage 5A. We do not show the limits between the *epaxialis*, *lateralis superficialis* and *hypaxialis* because they are discernible only by the direction of the fibres, under high magnification. See text for details.

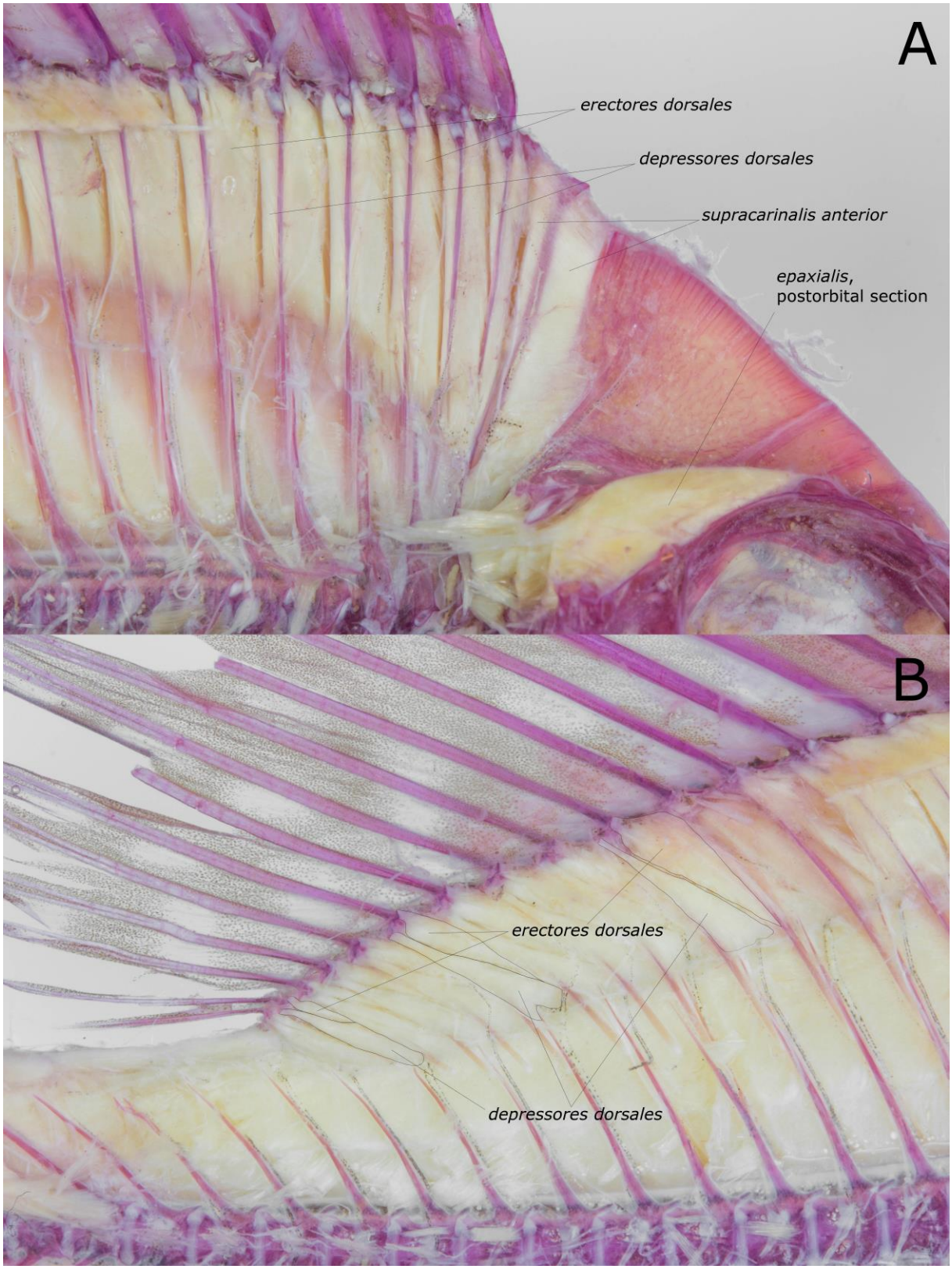

Fig. 24. Dissection stage 5B (see Supplementary File 1 for explanation). Musculature associated with dorsal fin. (A) Detail of the spinous portion of the fin, emphasising the *supracarinalis anterior* and the *erectores* and *depressores dorsales*. Notice that each *erector*

muscle originates from the anterior half of the pterygiophore supporting the spine in which it inserts, with the respective *depressor* muscle originating from the posterior half of the same pterygiophore. (B) Detail of the soft portion of the fin, in which the insertions of both the *erectores* and *depressores* muscles gradually shift to rays supported by more posterior pterygiophores (see text for a more detailed description).

Fig. 25. Dissection stage 5B (see Supplementary File 1 for explanation). Musculature associated with anal fin. Similarly to what we observed in the dorsal fin, an *erector* or *depressor analis* originate from the same pterygiophore that supports the spine it serves (respectively, from the anterior and posterior halves of the pterygiophore). *Erectores* and *depressores* serving soft rays tend to originate from a more anterior pterygiophore, in relation to the rays on which the muscles insert. Notice also the caudal ribs flanking the extensions of the swim bladder, lacking specialised musculature.

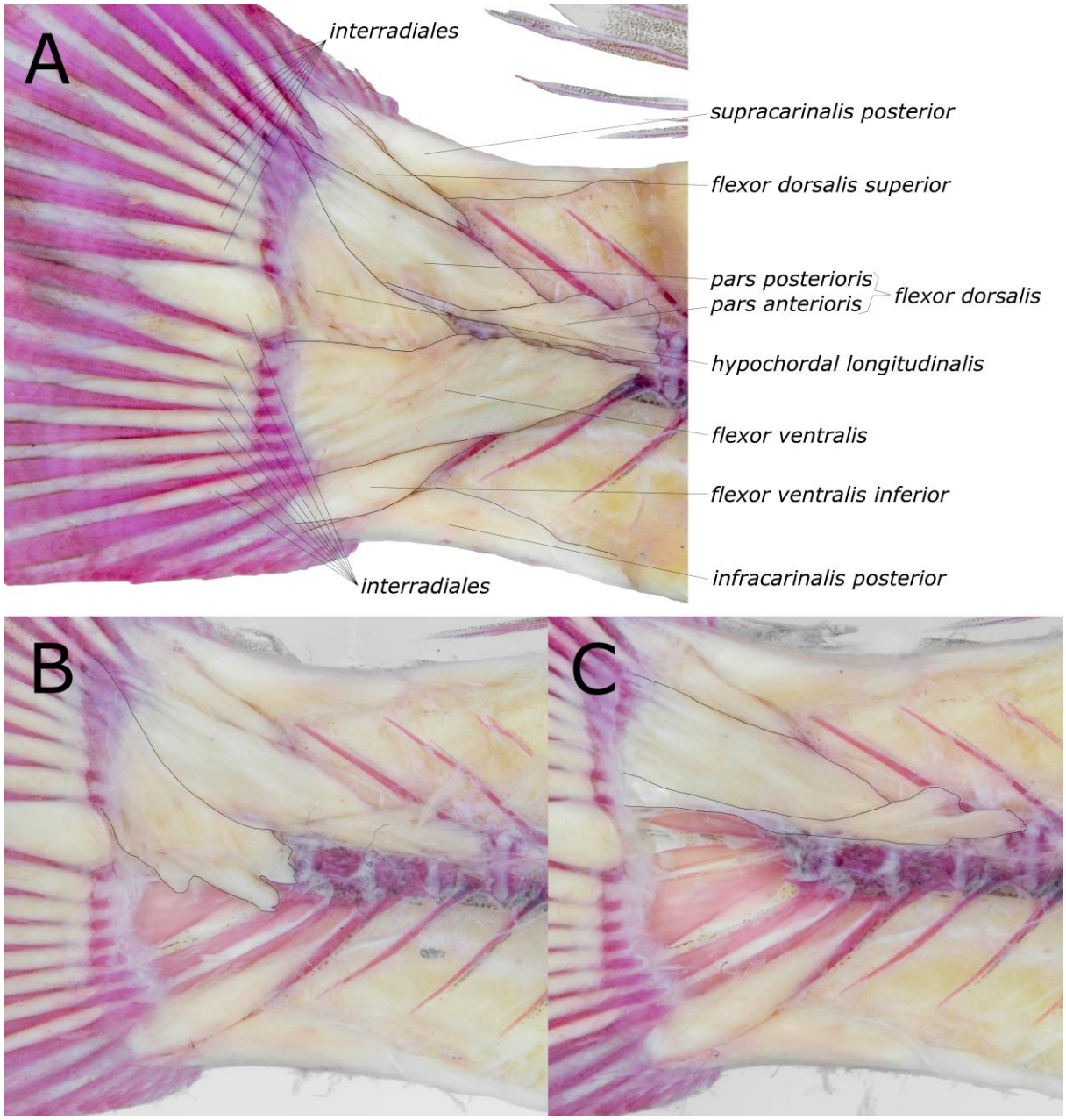

Fig. 26. Dissection stage 5B (see Supplementary File 1 for explanation). Caudal-fin musculature. (A) No associated muscles removed. (B) *Flexor ventralis* removed, exposing the proximal portion of the *hypochordal longitudinalis*. (C) *Flexor ventralis* and *hypochordal longitudinalis* removed, exposing the tendon of *flexor dorsalis*, *pars anterioris*.

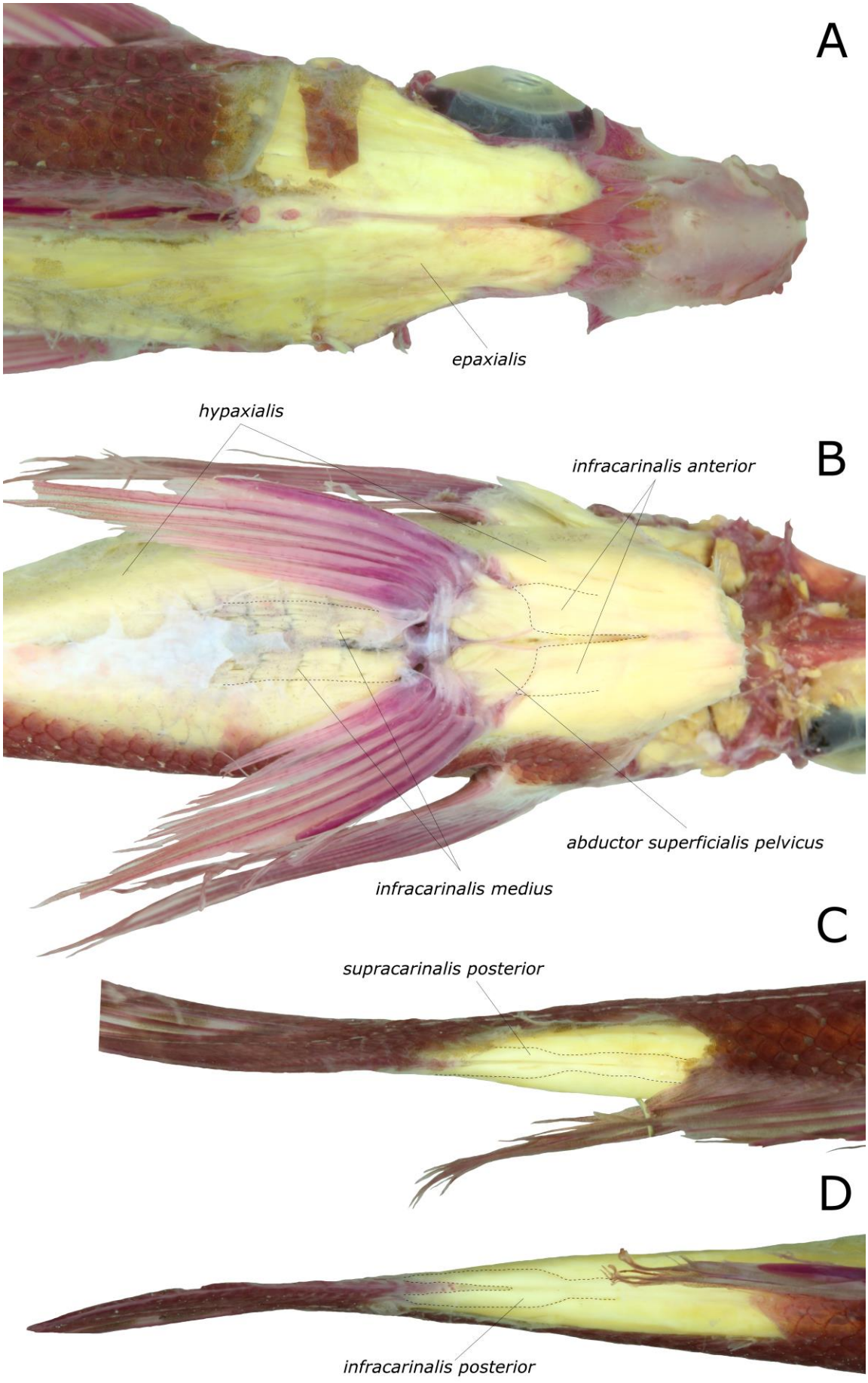
A
epaxialis
hypaxialis
B
infracarinalis anterior
abductor superficialis pelvicus
infracarinalis medius
C
supracarinalis posterior
D
infracarinalis posterior

Fig. 27. Dissection stage 5A (see Supplementary File 1 for explanation). Muscles of the dorsal and ventral portions of the body. (A) Dorsal view of the head and anterior portion of the trunk, evidencing the shape of the insertion site of the *epaxialis* on the neurocranium. (B) Ventral view of the trunk, evidencing the poor distinction between the *hypaxialis* and the *infracarinales anterior* and *medius*. (C) Dorsal view of the caudal peduncle, exposing the *supracarinalis posterior*. (D) Ventral view of the caudal peduncle, exposing the *infracarinalis posterior*.

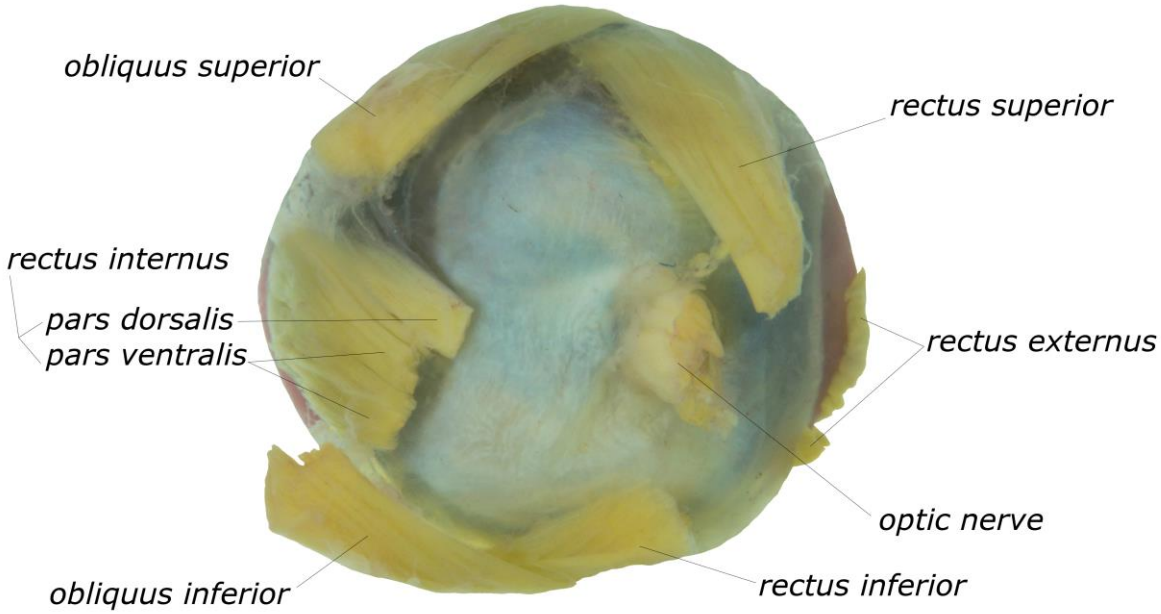

Fig. 28. Dissection stage 2B (see Supplementary File 1 for explanation). Medial view of the eyeball (anterior to the left), showing the distal portions of the ocular muscles and of the optic nerve.

Supplementary File 1 – Protocol for the myological dissection of cichlids

This protocol applies for the dissection of cichlid fishes in general. Of course, we expect most dissection stages to work for a wide variety of Actinopterygii, especially Ovalentariae and Percomorpharia. At each dissection stage, we remove or sever one or more bones. The subdivision of a stage (*e.g.*, 1A, 1B) means that muscles are removed, but not bones, in order to expose a deeper musculature. We recommend that the parts of the fish are photographed at each stage, in order to prevent information loss. In this work, we arbitrarily started the dissection by the right side of the specimen. Regardless of the chosen side, unless stated otherwise, each step only applies to one side of the fish.

STAGE 1A: Head skin and infraorbitals removal. With the scalpel, incise the skin ventral to the lachrymal and continue cutting along the ventral margin of infraorbitals, taking care not to damage the muscles beneath. Carefully remove all infraorbitals, which should detach from the head as a single piece, including the epithelium over the eye (severing the junction between lachrymal and lateral ethmoid may demand some caution). With the tweezers, pull off the remainder of the skin covering the *adductor mandibulae*, *pars malaris* and *rictalis*, as well as the more dorsal *levator arcus palatini*, *dilatator operculi*, *levator operculi* and *levator pectoralis*. Peel the most superficial head bones, the top of the head and the muscles in the gular region. Remove soft structures that are irrelevant to the myological analysis and can interfere with the observation of the muscles, such as nerves and adipose and connective tissues (except those forming tendons and important ligaments).

STAGE 1B: Exposure of *levator arcus palatini* and *adductor mandibulae, pars stegalis*. With the scalpel, detach the *pars malaris* and *rictalis* of the *adductor mandibulae* from its origin in the suspensorium, taking care not to damage the muscle fibres beneath. Hold those sections aside in order to observe the natural the origin of the *pars stegalis* and the insertion of the *levator arcus palatini*.

STAGE 2A. Severing of the lower jaw. With the scalpel, sever the connective tissue attaching the *protractor hyoidei* from the ventral margin of the lower jaw and the *intermandibularis* close to its attachment. Detach the *adductor mandibulae*, *pars stegalis*, from its origin. Holding aside all lateral parts of the *adductor mandibulae* in order to expose the suspensorium, use small, but resistant scissors to cut through the anterior portion of the

interopercle, preopercle, quadrate and ectopterygoid. Remove every connection between maxilla and palatine, vomer, premaxilla and contralateral maxilla. Pull the posterior portion of lower jaw laterally, severing the mandibular symphysis. Remove the epithelium that covers the medial face of the lower jaw, exposing the *pars mandibularis* of the *adductor mandibulae* (do it carefully, because this muscle is usually very delicate). Clean all sorts of tissue that are irrelevant to the analysis.

STAGE 2B. Removal of the eyeball and of the *adductor mandibulae, pars mandibularis*. Pushing the eyeball slightly to the sides, identify the muscles that insert on it and bisect them in a way that some of it remains attached to the insertion site (occasionally it is necessary to remove some soft tissues that cover the muscles, making it difficult to observe them). Sever the optic nerve and pull the eyeball. Clean the orbit, making sure to keep the proximal portions of the muscles in place. Detach the *adductor mandibulae, pars mandibularis* from its insertion site to expose the insertion sites of *pars stegalis* and *malaris* on the lower jaw.

STAGE 3. Suspensorium removal. With the scalpel, sever the connections between the palatine and the neurocranium, and between the hyoid arch and the suspensorium (including opercular series). The detachment of the *hyohyoideus adductor, pars dorsalis*, from the opercular series is necessary. To better observe those attachments, use the other side of the fish later on. With thin scissors, bisect the *adductor operculi* and the *levator operculi* at the middle, leaving the proximal portion attached to the neurocranium and the distal portion attached to the respective insertions. With a scalpel, detach the *dilatator operculi, levator arcus palatini* and *adductor hyomandibulae* from their origin sites. Be careful not to damage other structures while detaching the *adductor hyomandibulae, pars parasphenoidalis hyomandibularis*, which is hard to observe at this point. Sever the articulations between the hyomandibula and the neurocranium, obtaining a single piece consisting of the major portion of the suspensorium, with the distal halves of the *levator operculi, adductor operculi* and *adductor hyomandibulae, pars primordialis* and the entire *dilatator operculi, levator arcus palatini* and *adductor hyomandibulae, pars parasphenoidalis hyomandibularis* and *pterygoidea* attached to it. Remove the integument of the oropharyngeal cavity, as well as other soft tissues that might prevent the clear observation of the muscles attaching to the branchial basket, and of the *levator pectoralis* and *protractor pectoralis*. Be careful not to damage weak tendons and aponeuroses, especially the one joining the *levator externus 5* and

the pectoral girdle, and the ones joining the *pharyngoclavicularis externus* and the branchial basket.

STAGE 4A. Branchial basket removal. This is the most delicate stage of dissection. Some of the connections between the branchial basket and other parts of the body not immediately visible at Stage 3, namely the *retractor dorsalis* and *sphincter oesophagi* muscles and the articulation between the pharyngobranchial 3 and the neurocranium. First, bisect the *levator posterior*, *pharyngoclavicularis internus* and *pharyngoclavicularis externus* at the middle with long, thin scissors. Then, use a scalpel to separate the *levatores externi* and *interni* from their origin sites. Observe if the *transversus pharyngobranchialis 2* attaches to the neurocranium. If it does, sever it close to the origin with small scissors, then use the scalpel to guarantee a complete separation from the neurocranium. This muscle demands some caution to avoid damage. Pull the *levatores* muscle block aside in order to expose the articulation between the pharyngobranchial 3 and the neurocranium. Sever it with a scalpel. Repeat Stage 3 in the other side of the fish, without removing the mandible nor the *adductor mandibulae*, and without detaching the hyoid arch and associated muscles, and then repeat the steps of Stage 4A described so far. At this point, the *sternohyoideus* may be bisected or not. Carefully, pull the entire branchial basket slightly anteriorly in order to expose the distal portion of the *retractor dorsalis* and the *sphincter oesophagi*. Bisect both with thin, but resistant scissors. If the *sternohyoideus* was bisected, the branchial basket is now free. Otherwise, sever the ligament between urohyal and ventral hypohyal and the *rectus communis*, close to its origin. The obtained piece consists of the branchial basket and all associate muscles, attached to the hyoid arches of both sides, with or without the urohyal. Sever the connections between the hyoid arches and the branchial basket.

STAGE 4B. Removal of *levator externus 5* and *levator internus 1*. In order to expose better the *transversus epibranchialis 2*, *levator internus 2*, *obliquus dorsalis 3–4*, and *obliquus posterior 3*, remove the *levator internus 1* from its insertion site and sever the *levator externus 5* close to the raphe shared with *obliquus posterior 2*. To expose the *obliquus posterior 4*, detach the *obliquus posterior 3* from its origin site.

STAGE 5A. Body skin removal and splitting of the upper branchial basket. With a scalpel, carefully separate the body skin from the underlying muscles. This step requires caution, because the *epaxialis*, *lateralis superficialis*, and *hypaxialis* usually attach to the skin

to some extent. Sever the connections between the *sphincter oesophagi* and the pharyngobranchial 3 and upper tooth-plate 4. Then, sever the *transversi pharyngobranchialis 3* and *epibranchialis 4*, and the tissues between the contralateral pharyngobranchials 2–3 and upper tooth-plate 4. Sever the articulations between epibranchials and pharyngobranchials, and the *obliquus dorsalis 3–4*. Detach the *transversus epibranchialis 2* from the connective tissue enveloping the neurocraniad articulation facet of the pharyngobranchial 3. The piece obtained includes pharyngobranchials 2–3, upper tooth-plate 4 and the following associated muscles: *levator externus 2, transversi pharyngobranchiales 2, 2a* and *3, rectus pharyngobranchialis 2–3* and *circumpharyngobranchialis*.

STAGE 5B. Exposure of the *supracarinalis anterior* and of the unpaired-fin musculature. Remove *epaxialis*, *lateralis superficialis* and *hypaxialis* in order to expose the *supracarinalis anterior* and the unpaired-fin musculature. Remove the *inclinatores dorsales* and *anales* in order to expose the distal portion of the *erectores* and *depressores dorsales* and *anales*. Remove the *flexor ventralis* in order to expose the proximal portion of the *hypochordal longitudinalis* and the *flexor dorsalis, pars anterioris*. Then, remove the *hypochordal longitudinalis* in order to expose better the *flexor dorsalis*.

STAGE 6A. Removal of the pectoral and pelvic girdles and of the ribs, and dismemberment of the branchial basket. With thin, but strong scissors, sever the *adductor branchialis 5* and *obliquus posterior 1* close to the insertion. Detach the *obliquus posterior 4* from its origin site. Sever the ceratobranchials 1–4 at the middle, obtaining a piece consisting of the epibranchials and part of the ceratobranchials, with intact *adductores branchiales* and other associate muscles. Sever the ceratobranchial 1 from the opposite side at the middle, the articulation between basibranchials 2–3, the ligaments between hypobranchials 1–2 from both sides and the contralateral attachments of the *obliquus ventralis 2* to the basibranchial 1 (rostral ligamentous system). The resulting piece should include the basibranchials 1–2 and contralateral hypobranchials 1 (articulating with part of contralateral ceratobranchials 1), and the associated *obliquus ventralis 1*. Then, sever the ceratobranchial 2 of the opposite side at the middle, and the articulations of the basibranchial 3 with the contralateral hypobranchials 3 and with the basibranchial 4 cartilage. The resulting piece should include the basibranchial 3 and contralateral hypobranchials 2 (articulating with part of contralateral ceratobranchials 2), and the associated *obliquus ventralis 2*. Detach the *sternohyoideus* from its origin site and the ventral portion of the *hypaxialis* (except the coracoid section) from the anterior face of the

distal post-cleithrum and from the cleithrum. Detach the ventral portion of the pectoral girdle from its antimere and from the pelvic girdle and associate muscles. Sever the dorsal process of the post-temporal close to the base, being careful not to damage the dorsal portion of the *levator pectoralis*, and Baudelot's ligament at its free portion. Pull the pectoral girdle laterally, making the *levator pectoralis* detach from its insertion on the *hypaxialis*. The piece thus obtained consists of the entire pectoral girdle (except the dorsal post-temporal process) and associated muscles (except the *sternohyoideus* and most of the *hypaxialis*, except the coracoid portion). Sever the *infracarinalis medius* close to its attachment to the ischiatic process of the basipterygium. Detach the pelvic muscles (especially the *abductor superficialis pelvicus*) from the surrounding *hypaxialis*/*infracarinalis anterior*. Sever the connections between the basipterygium and its antimere. Remove the ribs with the associated body muscles, exposing the abdominal cavity and the proximal portion of the *retractor dorsalis*.

STAGE 6B. Exposure of pectoral and pelvic deep muscle layers. Expose the deeper layers of the *abductor superficialis* by severing the insertion tendons and pulling aside the more superficial layers. To expose the *arrector ventralis* and the *abductor profundus*, completely remove the *abductor superficialis* from its origin site. Expose the *adductor superficialis, pars lateralis*, and the *adductor profundus*, by severing the insertion tendons of the *adductor superficialis, pars medialis* and pulling it aside. Remove both *adductores superficialis* and *profundus* to expose the *arrector dorsalis* and the *adductor radialis*. Remove the *abductor superficialis pelvicus* to expose *arrector ventralis pelvicus*. Then, remove the latter to expose the *abductor profundus pelvicus*. Remove the *extensor proprius* to expose the *adductor superficialis pelvicus*. Then, remove the latter to expose the *adductor profundus pelvicus*.

STAGE 7. Opening of the myodomes. Remove the bony walls of the anterior and posterior myodomes, exposing the entire length of the eye muscles.

3 BUILDING AN EARTHEATER: MUSCLES AND THE PHYLOGENY OF GEOPHAGINI (CICHLIFORMES: CICHLIDAE: CICHLINAE)

ABSTRACT

Morphology is an important interface between genes and their environment. The way natural selection shapes biological structures reveals their adaptive importance and function. Having a reliable phylogenetic hypothesis on which to trace the evolution of phenotypic characters, we can begin to understand great evolutionary phenomena, such as adaptive radiation. With that purpose, we described for the first time a set of 98 characters observed on the whole head musculature of 23 Neotropical cichlid taxa. We found that myological characters are much more conservative in generalised taxa, while the most specialised genera counted on several synapomorphic characters. Phylogenetic analyses derived from our character matrix mimicked to some degree other morphological hypotheses, especially in clustering dwarf species and winnowers. Otherwise, there is great disagreement between those studies, also when compared with molecular analyses. By mapping the myological characters on a tree found in a recent phylogenetic study including hundreds of exons, we uncovered several characters putatively related to the winnowing behaviour. Some of these correlate with previous osteological specialisations, but others do not. We need further studies in order to confirm the presence or absence of winnowing in some geophagine taxa, and to answer important questions in geophagine evolution, such as how winnowing works in detail or how many times did winnowing evolve within the tribe.

Key words: Adaptive radiation – Evolution – Winnowing - Substrate sifting - Trophic specialisation

3.1 Introduction

Natural selection accounts for the whole morphological diversity observed in any group of organisms. Traits that survived selection are likely to enhance food consumption, evasiveness – survival, in a broader sense – and sexual attractiveness. In many ways, producing abundant offspring tightly depends on feeding success, thus the obvious ties between feeding behaviour and morphology. Fishes rely mostly on the teeth, jaws, gill rakers and other parts of the head to grab, select, crush and swallow food. Thus, we expect the shape of cephalic bones –

especially those that make up the jaws, suspensorium and branchial basket –, as well as the mass, shape and insertion sites of their associated muscles, to correlate with trophic specialization, which lies at the core of adaptive radiations.

Among freshwater fish groups, cichlids underwent multiple, unusually rapid adaptive radiations. The most astonishing of these are the ones that took place in the African rift valley lakes, which resulted in the evolution of hundreds of endemic species with overwhelming morphological diversification and convergence in the last few million years (*e.g.*, Albertson *et al.*, 1999). Nonetheless, Neotropical cichlids have undergone considerable adaptive morphological diversification as well. Among extant taxa, the geophagines had an early diversification burst about 115 Mya, developing markedly divergent body shapes and feeding preferences (López-Fernández *et al*., 2013). Later on, subsequent colonization events of Central America by different heroine clades led to independent radiations in the continent starting less than 50 Mya (Říčan *et al.*, 2013; 2016), which also resulted in very different species, although some present convergent adaptations among themselves and in comparison with geophagines.

In order to elucidate which characters allowed the exploitation of the different niches adopted by cichlids, we must understand how bones and muscles interact during food processing. More than that, we must understand how this mechanism differs among species with distinct specializations. In this sense, an important step is to describe the shape of bones and muscles in a wide variety of taxa. In a series of important papers on the anatomy of *Haplochromis elegans* Trewavas, Barel (1976) and Anker (*e.g.*, 1978; 1986; 1989) contributed a great deal to the knowledge of cichlid morphology. Several osteological descriptions are present in the work of Kullander (*e.g.*, 1983; 1986; 1989), and many characters were described in the several morphological studies dealing with the phylogeny of South American cichlids (*e.g.*, Cichocki, 1976; Kullander, 1998; Landim, 2001, 2006; López-Fernández *et al*., 2005). However, there is little available information on muscles, despite the abundance of osteological characters.

To determine how evolution produced each of the different specialised forms, we also need a well-resolved phylogenetic hypothesis on which to map the observed characters, reconstructing the ancestral character states at each node. Initial hypotheses on the relationships among Neotropical cichlids relied on parsimony analyses of morphological data sets. That approach seems to be flawed mainly because morphological data are intrinsically too scarce to resolve conflicting characters with parsimony, prone to interpretation problems and subject to selection-dependant convergence. If two taxa converged, *e.g.*, towards a similar

feeding preference, it is almost inevitable that they will share independently derived character states. If there are too many convergences, we will need a large number of characters unrelated to this trophic specialisation in order to counterbalance the weight of those characters. Otherwise, the two taxa will falsely attract each other.

Of the aforementioned issues, none seems to affect molecular analyses seriously. Recent methodologies yield tons of information with relatively little effort, which come from the ultimate source of biological diversity, DNA. There are no interpretation problems, since for each site there are four discrete possible characters. Although Castoe *et al*. (2009) reported a case of DNA sequence convergence between snakes and agamid lizards, it is certain that convergence in morphological structures is much more common, because a given phenotype may appear by many different genetic pathways. That does not mean molecular analyses are flawless. Still, if we are trying to map morphological characters along a phylogenetic tree, we should produce this tree from an independent data set. Thus, we believe morphological characters may not yield the best results in phylogenetic analysis, but they are crucial to understand how adaptive radiations work.

In this study, we surveyed the complete cephalic musculature of geophagine cichlids, as well as of members of other tribes in Cichlinae. We described the characters we found, and produced a character matrix from them. From the matrix, we produced morphological phylogenetic analyses, not primarily intended for elucidating the relationships among the taxa analysed. Instead, we hope these analyses will help recognising possible biases intrinsic to morphological characters, *i.e.*, clades repeatedly recovered due to convergence among the taxa included. In a posterior section, we examined which character states are recurrent among winnowers (substrate sifters), and discussed the possible functional importance of those structures. We hope that this study will yield ideas for future hypothesis tests on the function of cichlid muscles.

3.2 Material and methods

3.2.1 Classification

When referring to clades within Cichlinae, we followed the classification of Ilves *et al*. (2017), including the non-standard terms with the suffix ‘ines’: crenicichlines, apistogrammines, guianacarines and crenicaratines (Fig. 1). We cannot use the terms ‘mikrogeophagines’ and ‘geophagines’ with the same meaning as in Ilves *et al*. (2017, Fig. 1):

the first, for representing a paraphyletic group; the second, for its frequent use as a 'vernacular' name for the tribe Geophagini. Thus, we decided to fuse the two groups under the name 'biotodomines', which include *Biotodoma*, the "*Geophagus*" *brasiliensis* species group (an undescribed genus first recognised by Cichocki, 1976, and Kullander, 1998), *Mikrogeophagus*, *Geophagus* (*sensu stricto*), the "*Geophagus*" *steindachneri* species group (another undescribed genus) and *Gymnogeophagus* (Fig. 1).

3.2.2 Myology

Specimens of the 23 taxa analysed are available in Supplementary File 1. We stained the specimens as in the protocol by Datovo & Bockmann (2010), and dissected them following the protocol by Deprá *et al*. (Chapter 1 of this volume, Supplementary File 1). We worked simultaneously on all specimens at each dissection stage, looking for characters, because some structures are necessarily damaged when passing to the next stage. We describe the characters following the sequence of the muscles in which we observed them, as in Deprá *et al*. (Chapter 1 of this volume), but for each character we inform the dissection stage in which it is best observed. Because of the interpretative nature of morphological characters, in some instances it was difficult to establish limits between character states or to decide if we should split some characters or not. We opted for considering under a same character state structures that have a very similar shape. In character 2, for instance, states 1 and 2 are considerably similar to each other, but still distinct, while states 0 and 3 are extremely different. In a few cases (character 1, for instance), it was difficult to interpret the shape of some structures as more than one character and we decided to consider the variation within a single character. In these cases, also, when we coded two taxa as having the same state that means they have a very similar shape for a given structure (in this case, the shape of *adductor mandibulae*, *pars malaris*, as a whole). However, we recognise that some similarities between character states may indicate that the muscle may follow similar evolutionary trends in different taxa (as in character 1, states 2–4).

3.2.3 Phylogenetic analyses

3.2.3.1 Unconstrained analyses

Although we consider molecular data as best suited for phylogenetic analysis, we employed our character matrix to generate two unconstrained analyses, in order to verify the presence of phylogenetic signal in the myological characters and identify possible biases caused by convergence. We ran both analyses (unweighted and weighted) in the TNT 1.5 software (Goloboff *et al*., 2008), as in Supplementary Files 2, 3.

3.2.3.2 Constrained analysis: detecting convergent specialisation by character mapping

One of the goals of the present study is to investigate which characters may improve the fitness of winnowers. However, there is some confusion and a critical lack of information in the literature. First, it is essential to distinguish between two different behaviours that have been treated under the same name. Herein we call 'orobranchial winnowers' fishes that take substrate in the mouth (mainly inorganic, such as sand or mud), expel fine particles through the gills while retaining food particles in the oropharyngeal cavity, and after securing the food within the branchial basket (or swallowing it) expel gross particles back through the mouth. Weller *et al*. (2016) described the external aspect of this behaviour. 'Oral winnowers', on the other hand, is how we call fishes that take substrate in the mouth (mainly organic, such as algae or vegetable debris), shear food items between the pharyngeal jaws in order to separate it from non-edible particles and, after swallowing the food, expel the debris back through the mouth. Drucker & Jensen (1991) described this behaviour in surfperches in detail. Oral winnowing may be a primitive stage towards orobranchial winnowing, because the latter apparently relies heavily on the gill rakers and other branchial structures – such as the epibranchial 1 lobe of some cichlids – in order to separate the edibles from the substrate. On the other hand, oral winnowing (at least in surfperches) does not seem to require any conspicuous morphological specialisation (Drucker & Jensen, 1991).

Another problem is the lack of suitable observational data in the literature regarding the distribution of orobranchial and oral winnowing. For instance, Weller *et al*. (2016, Fig. 6) schematised the distribution of winnowing upon a phylogenetic tree of Geophagini, marking *Biotoecus*, *Crenicichla* and *Dicrossus* as confirmed non-winnowers. Although we are unaware of any example of winnowing in *Crenicichla*, we were able to find footages of aquarium specimens of *Biotoecus* sp. exhibiting this behaviour (possibly of the orobranchial type, because at some points it is possible to distinguish a few small particles passing through the gills). We found no evidence for orobranchial winnowing in *Dicrossus*, but *D. filamentosus* certainly does oral winnowing, which also applies to *Crenicara punctulatum*

(also observed in an aquarium footage). Because the presence of an epibranchial 1 lobe has been associated to winnowing (*e.g.*, López-Fernández *et al*., 2012), we must not rule out the presence of orobranchial winnowing in any taxa presenting that structure. Those include the species of *Apistogramma*, *Crenicara*, *Dicrossus*, *Mazarunia* and *Taeniacara* analysed herein, all of which present a more or less developed lobe (Weller *et al*., 2016, Fig. 6, erroneously suggested that all species of *Dicrossus* and *Mazarunia* lack the structure, while *Acarichthys* and *Biotoecus* possess it).

For our purpose, we will focus our attention on the confirmed orobranchial winnowers, which are those marked in blue in Weller *et al*. (2016, Fig. 6; also confirmed by us in aquarium footages), plus the non-geophagine *Retroculus*. We hope that this way we can filter the most relevant characters, once we expect the morphology of oral winnowers to be more generalised, following the example of surfperches (Drucker & Jensen, 1991). Among the taxa analysed, five clades may have developed orobranchial winnowing independently: Retroculini, biotodomines (of which all members are winnowers), *Guianacara* (guianacarines), *Satanoperca* (apistogrammines) and *Acarichthys* (crenicichlines). Although it is certain that winnowing appeared independently in *Retroculus* and in the geophagines, it is presently unknown where in the geophagine tree this behaviour appeared. Whatever the answer to this question is, we recognise characters as very likely associated to winnowing when it is present in four or five of those lineages, and absent in other taxa. Other characters interpreted as probably linked to winnowing may be present in only two or three winnower lineages, and paralleled in up to one non-winnower lineage.

To better visualise the distribution of the character states, we used the TNT 1.5 software to map the characters on the phylogenetic tree by Ilves *et al*. (2017), so that we can find the most parsimonious polarisation for each character (Supplementary Files 4, 5). We also ran an unweighted and a weighted analysis using the ‘force’ command, to obtain the number of steps required by the aforementioned topology based on our myological characters (Supplementary Files 6, 7).

3.3 Results

3.3.1 Character description

We found 98 characters, distributed as follows: muscles of the cheek, 30; muscles of the ventral surface of the head, 4; muscles serving the dorsal parts of the branchial arches, 32;

muscles serving the ventral parts of the branchial arches, 19; muscles between the pectoral girdle and the skull, hyoid, and branchial arches, 13. We provide the character matrix in Supplementary File 8.

3.3.1.1 Adductor mandibulae

Character 0. Dorsal profile of *pars rictalis*, from origin to insertion (dissection stage 1A). [0] Approximately horizontal (Fig. 2). [1] Slightly ascendant (Fig. 3). [2] Slightly descendant (Fig. 4). [3] Moderately descendant (Fig. 5). [4] Markedly descendant (Fig. 6). [5] Markedly ascendant (Fig. 7).

Mostly correlated with the position of the mouth and mass of the *pars malaris*. In taxa with higher mouth (the most common condition among cichlids), state 0 is frequently present. States 2, 3 and 4 are present in taxa with progressively lower mouths. *Retroculus acherontos*, which also has a low mouth, is a noteworthy exception. However, it has a massive *pars malaris*, as expected for species presenting state 0. The extreme conditions are state 4 (possible synapomorphy of *Satanoperca*) and state 5 (exclusive of *Teleocichla proselytus*).

Character 1. Shape of *pars malaris* (dissection stage 1A). [0] Approximately triangular, slightly deeper proximally, gently tapering towards insertion, then fibres abruptly converging into tendon (Fig. 4). [1] As in state 0, but deeper (Fig. 8). [2] Markedly triangular, deep proximally, strongly descending, with fibres tapering uniformly into tendon (Fig. 9). [3] Approximately triangular, but with sigmoid dorsal profile (accommodating the eyeball), origin very deep and surpassing opercle dorsally (Fig. 2). [4] Origin deep, dorsal profile sigmoid, insertion rectangular (Fig. 10). [5] Rectangular (Fig. 11). [6] As a very elongate triangle, with fibres tapering uniformly towards tendon (Fig. 5). [7] Deep, approximately convex both dorsally and ventrally (Fig. 12).

State 2 is a synapomorphy of *Apistogramma* and *Taeniacara*. State 3 is a synapomorphy of the *Crenicichla* clade. State 4 is present in *Cichla kelberi* and in *Astronotus*. State 5 is present only in *Chaetobranchopsis australis* (possible synapomorphy of Chaetobranchini). State 7 is a possible synapomorphy of *Retroculus*. States 0, 1 and 6 are more generalised. Characteristics considered herein include mainly the depth of *pars malaris* at the origin, the shape of its dorsal profile (*i.e.*, straight, convex or sigmoid), and the shape of

the insertion (*i.e.*, rectangular, pointed or with the fibres abruptly converging into the tendon). Although we chose to consider all this variation within a single character, it probably represents several characters, for which a satisfactory interpretation is problematic.

Character 2. Relative anterior extension of the *pars malaris* and *pars rictalis fibres* (measured along border between the two sections) (dissection stage 1A). [0] *Pars malaris* much shorter (Fig. 7). [1] *Pars malaris* slightly shorter (Figs. 3–6, 8–9). [2] Sections equally long (Fig. 11). [3] *Pars malaris* much longer (Figs. 10, 12).

State 0, which is exclusive of *Teleocichla proselytus* among taxa analysed, is due to the necessity to accommodate the eye anteriorly to the *pars malaris*, given that the latter is massive and the head is shallow, making the eye compete for space with the *adductor mandibulae* (*sensu* Arbour & López-Fernández, 2018). The sigmoid dorsal profile of the *pars malaris* described in character 1, states 3 and 4, has the same importance. State 3 may be synapomorphic for the clade including Cichlini and Retroculini. States 1 and 2 are only slightly different.

Character 3. Degree of separation between anterior portions of *pars malaris* and *pars rictalis* (dissection stage 1A). [0] Both parts close together (Fig. 2). [1] Slightly separated, exposing a small portion of the tendon between *pars malaris* and lower jaw (Figs. 4, 8). [2] widely separated anteriorly, exposing a relatively large portion of the tendon between *pars malaris* and lower jaw (Figs. 5–6).

Character 4. Fibres of the *pars malaris* originating from the lateral face of the preopercular *lateralis* canal (dissection stage 1A). [0] Absent. [1] Located between pores 4 and 5 (Fig. 2). [2] Located between pores 5 and 6 (Fig. 9). [3] Located between pores 4 and 6 (Fig. 7). [4] Located between pores 3 and 6.

Muscles attaching to the external surface of opercular bones are not common in cichlids, probably because they may interfere with the hydrodynamic properties of the head. In comparison, this is common in, *e.g.*, Trichomycteridae (see Datovo & Bockmann, 2010), in which the adaptive advantages of that attachment are obvious. However, in the conditions described in states 1–4, the *adductor mandibulae* only slightly invades the lateral face of the *lateralis* canal, widening the origin of the muscle, but not changing considerably the external

shape of the head. As expected, the only taxa presenting states 1–4 are those in which the *pars malaris* is massive and deep at the origin.

Character 5. Division between origins of *pars malaris* and *pars rictalis* related to preopercular *lateralis* pores (dissection stage 1A). [0] Between pores 4 and 5, much closer to pore 5 (Figs. 4–5). [1] Approximately coinciding with pore 4 (Figs. 2, 10). [2] Approximately in the middle of the distance between pores 4 and 5 (Fig. 13). [3] Between pores 4 and 5, closer to pore 4 (Figs. 3, 8 and 12). [4] Coinciding with pore 5 (Fig. 11). [5] In the middle of the distance between pores 5 and 6 (Fig. 6). [6] Between pores 3 and 4, but slightly ventral to pore 4 (Fig. 7).

State 4 is a possible synapomorphy of Chaetobranchini. State 5 is a possible synapomorphy of *Satanoperca*. State 6 is exclusive of *Teleocichla proselytus*, and correlated with character 0, state 5. States 0–3 are generalised. This character has an interpretation problem, which is that the position of the pores in the *lateralis* canal may evolve independently, so they are not ideal landmarks.

Character 6. *Pars malaris* tendon, in lateral view (dissection stage 1A). [0] Emerging from muscle fibres as a single tendon and bifurcating anteriorly (*e.g.*, Figs 4–5). [1] Emerging from the muscle fibres as two narrowly separated portions (Fig. 6). [2] Emerging from the muscle fibres as two widely separated portions (*e.g.*, Fig. 11).

Although present in a few geophagines, state 2 is probably the ancestral character state in Cichlinae, present in Cichlini, Retroculini, Astronotini and Chaetobranchini, as well as in *Haplochromis elegans* (see Anker, 1978, Fig. 1). We found the intermediate state 1 only in *Satanoperca*.

Character 7. Shape of the tendon between *pars malaris* and maxilla in cross-section (dissection stage 2A). [0] Round. [1] Depressed. [2] Compressed.

Character 8. Anteroventral portion of *pars rictalis* (dissection stage 1A). [0] Not covering the articulation between the quadrate and the anguloarticular. [1] Partially covering the articulation between the quadrate and the anguloarticular.

Character 9. Anteriormost point where *pars rictalis* fibres originate (in lateral view) (dissection stage 1A). [0] Far from articulation between quadrate and anguloarticular (*e.g.*, Figs. 5–6). [1] Close to the articulation between quadrate and anguloarticular (*e.g.*, Figs. 2, 11).

Character 10. Dorsalmost point of the *pars malaris* origin (dissection stage 1A). [0] Well ventral to articulation between hyomandibula and opercle (Figs. 3, 11). [1] Slightly ventral to articulation between hyomandibula and opercle (Fig. 5). [2] On the same horizontal as articulation between hyomandibula and opercle (Figs. 4, 6, 8, 10, 12–13). [3] Slightly dorsal to articulation between hyomandibula and opercle (Fig. 9). [4] Well dorsal to articulation between hyomandibula and opercle (Figs. 2, 7).

Character 11. Inclination of the *pars rictalis* fibres (dissection stage 1A). [0] Dorsalmost fibres extremely descendant; ventralmost fibres approximately horizontal. [1] Dorsalmost fibres markedly descendant; ventralmost fibres approximately horizontal. [2] Dorsalmost fibres slightly descendant; ventralmost fibres moderately ascendant. [3] Dorsalmost fibres horizontal to slightly ascendant; ventralmost fibres slightly to moderately ascendant. [4] All fibres ascendant.

Character 12. Fibres of the *pars rictalis* (dissection stage 1A). [0] Originating from dorsal face of lateral crest of quadrate; crest is entirely visible laterally (*e.g.*, Fig. 6). [1] Originating mostly from dorsal face of lateral crest of quadrate, but posteriorly some fibres originate from the lateral face; crest is partially hidden by muscle fibres when looked in lateral view. [2] Originating largely from lateral face of lateral crest of quadrate; crest is almost completely hidden in lateral view (Fig. 2).

State 2, which is a possible synapomorphy of the *Crenicichla* clade, represents an expansion of the size of the origin site of *pars rictalis*. Thus, it seem to have an adaptive importance similar to character 4, relative to the *pars malaris*.

Character 13. *Pars malaris* (dissection stage 1A). [0] Originating muscularly from suspensorium. [1] Originating, at least dorsally, aponeurotically (Fig. 14). [2] As in state 2, but aponeurosis much smaller.

Character 14. Dorsalmost fibres of *pars malaris* (as seen in lateral view) (dissection stage 1A). [0] Oriented as fibres of the middle portion of the muscle. [1] Ascending from origin to insertion (fibres of the middle portion of the muscle descending).

State 1 is probably a synapomorphy of *Retroculus*.

Character 15. Interface between *pars malaris* and *pars rictalis* (dissection stage 2A). [0] *Pars malaris* with a ventromedial concavity that fits dorsal portion of *pars rictalis*; a ventrolateral projection of the *pars malaris* slightly covers the *pars rictalis* in lateral view. [1] *Pars malaris with* a ventrolateral concavity posteriorly, which fits dorsomedial face of *pars rictalis*; in lateral view, *pars rictalis* covers a large portion of *pars malaris*. [2] Interface between the two parts flat. [3] Both sections concave along their interface. [4] *Pars malaris* concave, *pars rictalis* flat. [5] *Pars malaris* convex; a dorsomedial concavity in the *pars rictalis*, close to its origin, fits the *pars malaris*. [6] A conspicuous ventrolateral concavity in the anterior portion of the *pars malaris*, close to its insertion (related to the fibre twist described in character 14c), fits a conspicuous convexity in the *pars rictalis*. [7] *Pars malaris* anteriorly concave ventrally, posteriorly convex, with *pars rictalis* fitting it. [8] Anterior portion of *pars malaris* concave ventrally, fitting a convexity of *pars rictalis*; posterior portion of both parts concave, but face of *pars malaris* that connects to *pars rictalis* is turned ventrolaterally. [9] *Pars malaris* flat, *pars rictalis* concave.

Character 16. Twist of the pars malaris (dissection stage 2A). [0] Absent (fibres inserting on the tendon, as visible laterally, are all fibres). [1] Outwards (fibres inserting on the tendon, as visible laterally, are those originating in the dorsal portion of the muscle; Fig. 11).

State 1 has independently derived in *Apistogramma borellii*, *Mikrogeophagus ramirezi* and *Chaetobranchopsis australis*.

Character 17. *Pars malaris* tendon (dissection stage 2A). [0] Originating from the medial face of the muscle, next to anterior tip of fibres. [1] Originating from the middle of the medial face of the muscle (Fig. 14).

State 1 is a synapomorphy of *Satanoperca*.

Character 18. Attachment of the *pars mandibularis* fibres to the ventral process of the anguloarticular (dissection stage 2A). [0] Absent; [1] Covering the base of the process; [2] Covering half of the process medially; [3] Completely covering the medial portion of the process; [4] Median portion of the process covered by a posteroventral lobe.

Character 19. *Pars mandibularis* (dissection stage 2A). [0] Reaching about the middle of the dentary (Fig. 14). [1] Reaching a point close to the dentary symphysis (Fig. 15).

State 1 are a clear convergence between the predators *Cichla kelberi* and *Crenicichla britskii*, and may be correlated with the elongation of the lower jaw.

Character 20. Dorsal margin of *pars mandibularis* (dissection stage 2A). [0] Parallel to toothed margin of dentary (Fig. 15). [1] Anteriorly diverging from toothed margin of dentary (Fig. 14).

State 1 is present only in a few winnowers and in *Chaetobranchopsis australis*.

3.3.1.2 Levator arcus palatini

Character 21. Dorsal limit of the *levator arcus palatini* origin (dissection stage 1). [0] On the posterior face of the lateral process of sphenotic (Figs. 4–8). [1] On the tip of the lateral process of sphenotic and on the ventral margin of a posterior ridge of the sphenotic (Fig. 16). [2] On the tip of the lateral process of sphenotic (Fig. 17). [3] On an expansion of the lateral process of sphenotic (Figs. 2, 7, 10–12).

State 2 is exclusive of *Biotoecus opercularis*. State 3 seems to be ancestral in Cichlinae, once it is present in *Retroculus acherontos*, *Cichla kelberi*, *Chaetobranchopsis australis* and in *Haplochromis elegans* (see Anker, 1978, Fig. 1). Paralleled in the *Crenicichla* clade, probably as a consequence of the longitudinal enlargement of the *levator arcus palatini*.

Character 22. Insertion of *levator arcus palatini* (dissection stage 1B). [0] Nested in the *calyx* of the metapterygoid, medial to *pars malaris* and posterior to *pars stegalis* of the *adductor mandibulae* (Deprá *et al*., Chapter 1 of this volume, Fig. 3). [1] Nested deeply

between origins of *pars malaris* and *pars stegalis* (a portion of the *levator arcus palatini* is lateral to the *pars stegalis*; Fig. 18).

State 1 may be related to an increase in the strength of the *levator arcus palatini*.

Character 23. Shape of the insertion of the *levator arcus palatini* (dissection stage 1B). [0] Posteriorly muscular, anteriorly aponeurotic; [1] Entirely muscular.

3.3.1.3 Dilatator operculi

Character 24. *Dilatator operculi* (dissection stage 1A). [0] Anteriorly extending far beyond clst 1 (Figs. 2, 7, 10). [1] Anteriorly extending approximately until vertical through clst 1 (*e.g.*, Figs. 4–6)

State 0 represents a convergence between the predators Cichlini and *Crenicichla* clade. We speculate that the enlargement of the *dilatator operculi* origin may enhance the suction force in those taxa, since this muscle contributes to the expansion of the oropharyngeal cavity. That could be an important adaptation to overpower evasive prey.

Character 25. Origin of *dilatator operculi* (dissection stage 1A). [0] Completely anterior to insertion (Fig. 2). [1] Mostly anterior to insertion, but with a portion immediately dorsal to it (Figs. 9–10, 12, 16–17). [2] With a portion posterior to insertion of the muscle and other portion anterior to it (Figs. 4–6, 8).

Character 26. Lateral overlap between *dilatator operculi* and *levator operculi* (dissection stage 1A). [0] Absent. [1] *Dilatator operculi* slightly overlaps *levator operculi*. [2] *Levator operculi* overlaps *dilatator operculi*. [3] Muscles widely separated proximally. [4] Muscles widely separated distally. [5] *Dilatator operculi* widely overlaps *levator operculi*.

State 5 represents a synapomorphy for Chaetobranchini.

Character 27. Anterior portion of the *dilatator operculi* origin (dissection stage 1A). [0] On the posterior face of the lateral process of sphenotic. [1] On ventral face of ridge between

clst 1 and 2 (Fig. 16). [2] Anteriorly surpassing clst 1, and adjacent to, but not directly on posterior face of the lateral process of sphenotic (Fig. 11).

Only in the Astronotini, Chaetobranchini and Cichlasomatini analysed herein the *dilatator operculi* does not cover the posterior face of the lateral process of sphenotic. State 2, exclusive of *Chaetobranchopsis australis*, differs from state 1 because some of the fibres originate a little anterior to clst 1.

3.3.1.4 Levator operculi

Character 28. Origin of the *levator operculi* (dissection stage 1A). [0] Solely on pterotic, ventral to clst 3 (Figs. 5, 9, 11, 17). [1] Solely on pterotic, ventral to posterior half of *lateralis* canal between clst 2 and 3 (Figs. 10, 12). [2] Solely on bony ridge that lies anteroventrally to clst 3 (Fig. 19). [3] On pterotic, ventral to posteriormost *lateralis* pore, and on lateral face of post-temporal (two portions are present: a main portion and a post-temporal portion; Fig. 6). [4] Solely on pterotic, ventral to clst 3 and on posterior face of bony ridge that lies anteroventrally to clst 3 (*e.g.*, Fig. 2). [5] Solely on pterotic, ventral to *lateralis* canal between clst 2 and 3.

State 0 represents a reduction of the area of the origin of *levator operculi*, and is present in the dwarf species *Biotoecus opercularis* and *Taeniacara candidi*, but also in *Gymnogeophagus balzanii* and *Chaetobranchopsis australis*. State 1 is a possible synapomorphy of Retroculini and Cichlini. State 2 is a synapomorphy of *Dicrossus*. State 3 is a synapomorphy of *Satanoperca*, but also present in an undescribed species of *Teleocichla*. State 5 seems to be exclusive of *Cichlasoma paranaense*. State 4 represents the generalised condition.

Character 29. Relative length of *levator operculi* fibres (dissection stage 1A). [0] Anterior and posterior fibres approximately the same length (Figs. 11, 17). [1] Posterior fibres slightly longer than anterior ones (*e.g.*, Figs, 4, 5). [2] Posterior fibres much longer (*e.g.*, Fig. 6).

Correlates with the shape of the skull. When the insertion of the *levator operculi* is more horizontally aligned with its origin, the posterior fibres tend to be shorter, more similar

to the anterior ones (state 1). This is more common in taxa with deeper heads. In taxa with longer heads, in contrast, state 2 is more common.

3.3.1.5 Protractor hyoidei

Character 30. Posterior reach of *protractor hyoidei* (dissection stage 1A). [0] Anterior to the articulation of branchiostegal ray 2. [1] At level with articulation of branchiostegal ray 2. [2] At level with articulation of branchiostegal ray 3. [3] At level with articulation of branchiostegal ray 4.

3.3.1.6 Hyohyoidei

Character 31. Differentiation of fibres of *hyohyoideus adductor, pars dorsalis,* into *pars preopercularis* (dissection stage 3). [0] Absent. [1] Conspicuous, attached to branchiostegal ray 5. [2] Inconspicuous, attached to branchiostegal ray 1 or 3.

Character 32. Origin of *hyohyoideus abductor 1* (dissection stage 4A). [0] On anteromedial side of the interdigitations between anterior ceratohyal and ventral hypohyal. [1] On connective tissue medial to ventral hypohyal and ventral margin of that bone. [2] On ventral margin of ventral hypohyal.

Character 33. Insertion of *hyohyoideus abductor 2* (dissection stage 4A). [0] On branchiostegal ray 1. [1] On branchiostegal ray 2. [2] On both branchiostegal rays 1 and 2.

3.3.1.7 Levatores externi

Character 34. Degree of separation between the *levatores externi 3–5* (dissection stage 4A). [0] *Levatores externi 4* and *5* united, *levator externus 3* only slightly separate. [1] *Levatores 4* and *5* slightly separate from each other, *levator externus 3* clearly separate. [2] *Levatores externi 3–5* clearly separate. [3] *Levatores externi 4* and *5* united, *levator externus 3* clearly separate.

The use of the name *levator externus 5* for cichlids is a novelty introduced by Deprá *et al*. (Chapter 1 of this volume). We concluded that the use of this name is justified because

there is a thin *levator externus 4* inserting on the uncinate process of epibranchial 4, while the *levator externus 5* inserts on a raphe shared with *obliquus posterior 2*, and ultimately on ceratobranchial 5. However, in some taxa the *levator externus 4* is not clearly separate from *levator externus 5*, except distally. In others, even the *levator externus 3* is not proximally distinct from the *levator externus 4–5* block. The distribution of the character states suggests it is a quite plastic character, or that a more refined analysis could reveal other information (*e.g.*, histological samples).

Character 35. Thickness of the *levator externus 5* (dissection stage 4A). [0] Much thicker than other *levatores externi*. [1] Approximately as thick as other *levatores externi*. [2] Slightly thicker than other *levatores externi*.

State 1 is exclusive of *Chaetobranchopsis australis*. State 2 is exclusive of *Cichla kelberi*. The attachments of the *levator externus 5* suggest that this muscle is important in pressing the ceratobranchial 5 against the upper pharyngeal elements. That makes this muscle important for crushing or cutting small prey. Because *C. australis* is a planktivore, we expect that these functions have lost importance, and the *levator externus 5* has retained only the function of reducing the space between the lower and upper pharyngeal elements.

Character 36. Relative width of *levatores externi 1* and *2* (in lateral view) (dissection stage 3). [0] Both muscles similarly narrow, each of them much narrower than the union of *levatores externi 3–5*. [1] *Levator externus 2* broader than *levator externus 1*, but still narrower than the union of *levatores externi 3–5*. [2] *Levator externus 2* broader than *levator externus 1*, and similar in width to the union of *levatores externi 3–5*.

States 0 and 1 are widespread. State 2 is exclusive of *Crenicichla britskii* among the taxa analysed.

Character 37. Insertion of the *levator externus 2* on epibranchial 2 (dissection stage 3). [0] More posteriorly, on the posterior margin of the bone. [1] More anteriorly, on the middle of the external face of the bone.

Character 38. Shape of the *levator externus 1*. [0] Broadening towards its insertion. [1] Uniformly broad or almost so.

Character 39. Ligament between neurocranium and epibranchial 1, parallel to *levator externus 1* (dissection stage 3). [0] Absent. [1] Present (Fig. 20).

Springer & Johnson (2004:163-164, plate 138) reported an almost identical condition as synapomorphic for Polycentridae, which is curious because Betancur-R. *et al.* (2013) recovered this family as sister to Cichlomorphae (Cichlidae plus Pholidichthyidae).

3.3.1.8 Levatores interni

Character 40. *Levator internus 1* (in anterior view) (dissection stage 4A). [0] Approximately as thick as *levator externus 1* (Fig. 21). [1] Clearly thicker than *levator externus 1* (about twice as thick). [2] Much thicker than the *levator externus 1* (about thrice as thick; Deprá *et al*., Chapter 1 of this volume, Fig. 11). [3] Thinner than *levator externus 1*.

3.3.1.9 Levator posterior

Character 41. *Levator posterior* (dissection stage 4A). [0] Thinner than *adductor operculi*. [1] Approximately as broad as *adductor operculi*. [2] Broader than *adductor operculi*.

3.3.1.10 Obliquus dorsalis 3–4

Character 42. *Obliquus dorsalis 3–4* (dissection stage 4A). [0] Expanded posteromedially, in consequence of the shape of the *transversus epibranchialis 2*, entirely covering dorsally the *transversus pharyngobranchialis3-epibranchialis 4* (Fig. 22). [1] Not expanded posteromedially, entirely exposing the *transversus pharyngobranchialis3-epibranchialis 4* (Deprá *et al*., Chapter 1 of this volume, Fig. 9). [2] Expanded posteromedially, in consequence of the shape of the *transversus epibranchialis 2*, partially covering dorsally the *transversus pharyngobranchialis3-epibranchialis 4* (Fig. 23).

This character represents a convergence between the predator *Cichla kelberi* and the *Crenicichla* clade, but with different character states.

Character 43. Position of the insertion of the *obliquus dorsalis 3–4* relative to the insertion of the *obliquus posterior 3* (dissection stage 4A). [0] Adjacent (the *obliquus dorsalis 3–4* occupies a small portion of the dorsoposterior face of the epibranchial 4). [1] Narrowly separate, leaving a narrow portion of the epibranchial 4 visible. [2] Broadly separate, leaving a broad portion of the epibranchial 4 visible.

Character 44. Origin of *obliquus dorsalis 3–4* (dissection stage 4A). [0] Exclusively from pharyngobranchial 3. [1] From pharyngobranchial 3 and cartilage tip of uncinate process of *epibranchial 2*. [2] From pharyngobranchial 3 and uncinate process of *epibranchial 2*.

3.3.1.11 Obliqui posteriores

Character 45. *Obliquus posterior 3* (dissection stage 4A). [0] Present (Deprá *et al*., Chapter 1 of this volume, Fig. 10). [1] Absent (perhaps, fused to *obliquus posterior 4*; Fig. 24).

Character 46. Distal portion of *obliquus posterior 4* (dissection stage 4A). [0] Clearly distinct from *sphincter oesophagi* (Deprá *et al*., Chapter 1 of this volume, Fig. 10). [1] Fused to *sphincter oesophagi* (Fig. 24).

Character 47. Origin of the *obliquus posterior 4* (dissection stage 4A). [0] Somewhat far from the anterodorsal border of the epibranchial 4, not so coincident whit the origin of the *obliquus posterior 3*. [1] Close to the anterodorsal border of the epibranchial 4, more coincident with the origin of the *obliquus posterior 3*.

Character 48. *Obliquus posterior 1* (dissection stage 4A). [0] Present. [1] Absent.

3.3.1.12 Adductores branchiales

Character 49. *Adductor branchialis 1* (dissection 4A). [0] Much less massive than other *adductores branchiales* (apparently absent in some cases). [1] Slightly less massive than *adductores branchiales 2–3*. [2] Approximately as massive as other *adductores branchiales*.

States 1 and 2, which represent the hypertrophied condition of *adductor branchialis 1*, are mostly present in winnowers (geophagines and *Retroculus*). *Acarichthys heckelii*, a

winnower, presents state 0, which is common to members of crenicichlines. *Guianacara dacrya*, a probable winnower, also presents state 0. Thus, states 1 and 2 clearly correlate with the presence of an epibranchial 1 lobe, well developed or not.

Character 50. *Adductor branchialis 4* (dissection stage 4A). [0] Slightly less massive than *adductores branchiales 2–3*. [1] Approximately as massive as *adductores branchiales 2–3*. [2] More massive than *adductores branchiales 2–3*.

State 2 is exclusive of *Teleocichla proselytus* among taxa examined.

3.3.1.13 Transversi dorsales

Character 51. Relative width, in frontal view, of the *transversus pharyngobranchialis 2* and *transversus pharyngobranchialis 2a* (measured perpendicularly to the long axis of the muscle) (dissection stage 4A). [0] *Transversus pharyngobranchialis 2* is slightly deeper than *transversus pharyngobranchialis 2a*. [1] *Transversus pharyngobranchialis 2* is much deeper than *transversus pharyngobranchialis 2a*. [2] *Transversus pharyngobranchialis 2* is slightly less deep than *transversus pharyngobranchialis 2a*. [3] *Transversus pharyngobranchialis 2* is much less deep than *transversus pharyngobranchialis 2a*.

State 3 is exclusive of *Dicrossus warzeli* among taxa examined.

Character 52. Distal portion of the *transversus pharyngobranchialis 2* (dissection stage 4A). [0] Anterior to the proximal portion of the *transversus pharyngobranchialis 2a*. [1] Dorsal to the proximal portion of the *transversus pharyngobranchialis 2a*. [2] Posterior to the proximal portion of the *transversus pharyngobranchialis 2a*.

State 0 is present only in crenicichlines (but not in *Acarichthys*). State 2 is a possible synapomorphy of *Retroculus*.

Character 53. *Transversus epibranchialis 2* (dissection stage 4A). [0] Greatly developed posteriorly, overlapping dorsally the *obliquus dorsalis 3–4* and the *transversus pharyngobranchialis 3-epibranchialis 4* (Fig. 22). [1] Somewhat developed posteriorly, overlapping about half of the *obliquus dorsalis 3–4* dorsally (Deprá *et al*., Chapter 1 of this

volume, Fig. 9). [2] Somewhat displaced posteriorly by the *transversus pharyngobranchialis 2* and overlapping the medial portion of the *obliquus dorsalis 3–4* (Fig. 25). [3] Not much developed or displaced posteriorly, not overlapping or slightly overlapping the *obliquus dorsalis 3–4* (Fig. 26). [4] Very slightly developed, not touching much of the *obliquus dorsalis 3–4*.

Related to character 42. State 0 is exclusive of *Crenicichla britskii* among taxa analysed. State 1 is typical of geophagines, but also present in *Cichla kelberi*. State 4, which reflects the reduction of the width of *transversus epibranchialis 2* in *Chaetobranchopsis australis*.

Character 54. Origin of the *transversus pharyngobranchialis 2* (dissection stages 3 and 4A). [0] On the neurocranium. [1] On the neurocranium and anterior face of pharyngobranchial 3. [2] On the anterior face of pharyngobranchial 3.

The only taxa to present state 2 are "*Geophagus*" *steindachneri* and *Cichla kelberi*.

Character 55. Medial extension of the *transversus epibranchialis 2* (dissection stage 4A). [0] Reaching much farther than the *obliquus dorsalis 3–4*, extending onto the connective tissue that covers the face of the pharyngobranchial 3 that articulates with the neurocranium (Fig. 26). [1] Reaching somewhat farther than the *obliquus dorsalis 3–4* (Deprá *et al*., Chapter 1 of this volume, Fig. 9). [2] Reaching farther than the *obliquus dorsalis 3–4*, and touching the contralateral muscle, but posteriorly to the articulation face of the pharyngobranchial 3 (Fig. 22). [3] Reaching about as far as the *obliquus dorsalis 3–4* (Fig. 27). [4] The fibres reach about as far as the fibres of *obliquus dorsalis 3–4*, but they end in a tendon that connects to the contralateral muscle.

State 2 is exclusive of *Crenicichla britskii* among taxa analysed, and related to characters 42 and 53.

Character 56. *Transversus pharyngobranchialis 3* and *transversus epibranchialis 4* (dissection stage 4A). [0] Fused to each other or only slightly divided. [1] Clearly divided in an anterior and a posterior section.

State 1 is present in a few taxa, mostly geophagine winnowers, but also in *Cichlasoma paranaense*.

Character 57. Width of the *transversus pharyngobranchialis 3-epibranchialis 4*, along the sagittal axis (dissection stage 4A). [0] Narrow (Fig. 27). [1] Broad.

3.3.1.14 Retractor dorsalis

Character 58. *Retractor dorsalis* (dissection stage 4A). [0] Completely divided in two contralateral portions. [1] Partially divided in two contralateral portions, with ventral portion muscularly united. [2] Partially divided in two contralateral portions, with ventral portion united by a raphe.

State 1 is a possible synapomorphy of Cichlasomatini. State 2 is a possible synapomorphy for *Astronotus*.

Character 59. Width of the *retractor dorsalis* (dissection stage 4A). [0] Narrow, the contralateral muscles widely separate (Fig. 28). [1] Broad, the contralateral muscles close together (Fig. 26).

State 0 is also unique of *Chaetobranchopsis australis*, representing a reduction of the width of a muscle.

Character 60. Transversal section of the distal portion of the *retractor dorsalis* (dissection stage 4A). [0] Flattened in a dorsolateral-ventromedial direction. [1] Dorsoventrally flattened.

3.3.1.15 Circumpharyngobranchialis

Deprá *et al*. (Chapter 1 of this volume) created the name *rectus pharyngobranchialis 2–3* for a muscle most probably derived from the *circumpharyngobranchialis, pars medialis*. We think the muscle deserves its own name because, at least in a few taxa, it is anatomically independent from the *circumpharyngobranchialis*, and probably performs an important adaptive function in food manipulation. Dissecting those muscles is a rather difficult task,

given the fragility of the *circumpharyngobranchialis*, whose fibres are embedded in the connective tissue around the pharyngobranchials.

Character 61. *Rectus pharyngobranchialis 2–3* (a muscle probably derived from *circumpharyngobranchialis, pars medialis,* but originating from anterolateral margin of pharyngobranchial 3, immediately anterior to the insertion of *levator internus 2*, and inserting on posterior face of pharyngobranchial 2) (dissection stage 6A). [0] Present, distinct from *circumpharyngobranchialis* (Deprá *et al*., Chapter 1 of this volume, Fig. 14); [1] Absent; [2] Present, fused to *circumpharyngobranchialis*, *pars medialis*.

Character 62. Insertion of the *rectus pharyngobranchialis 2–3* (dissection stage 6A). [0] Slightly lateral to the middle of posterior face of pharyngobranchial 2. [1] Slightly medial to the middle of posterior face of pharyngobranchial 2. [2] Spanning the posterior face of pharyngobranchial 2 from side to side, close to the teeth. [3] Close to the lateral edge of the posterior face of pharyngobranchial 2.

Character 63. Shape of the *rectus pharyngobranchialis 2–3* (dissection stage 6A). [0] Approximately cylindrical. [1] Depressed, fanning out anteriorly. [2] Uniform in width, but compressed in a dorsomedial-anterolateral way.

Character 64. *Rectus pharyngobranchialis 2–3, pars medialis* (a part that seems to insert on the pharyngobranchial 3 itself) (dissection stage 6A). [0] Absent. [1] Present.

Character 65. Insertion of *circumpharyngobranchialis, pars lateralis* (dissection stage 6A). [0] On anterolateral corner of pharyngobranchial 2. [1] On anteromedial corner of pharyngobranchial 2, almost reaching the insertion of *pars medialis*.

3.3.1.16 Sphincter oesophagi

Character 66. Dorsal extension of the lateral portion of the *sphincter oesophagi*. [0] Long, embracing laterally the *retractor posterior* and attaching extensively to the posterior margin of the upper tooth-plate 4, which is almost entirely hidden. [1] Short, not embracing much of the *retractor posterior* and leaving a large portion of the upper tooth-plate 4 visible. [2] Large,

embracing laterally the *retractor posterior*, but not attaching extensively to the posterior margin of the upper tooth-plate 4, which is almost entirely visible.

3.3.1.17 Obliqui ventrales

To Winterbottom (1974:261), the *obliqui ventrales* "span the joint between the ventral surfaces of the hypobranchial and ceratobranchial elements of the first three branchial arches". Muscles that span between contralateral ceratobranchials would be *transversi ventrales*, and those linking hypobranchials and ceratobranchials of different arches would be *recti ventrales* (Winterbottom, 1974:262-264). We followed Anker (1978) in considering that the first three arches have only *obliqui ventrales*, although parts of those muscles may attach to elements of other arches or span between contralateral ceratobranchials. The reason for that decision is twofold. First, in several taxa the sections originating from different sites are not clearly distinct distally. Second, there are several degrees of development of what we could have called *recti* and *transversi ventrales*, of which our *obliquus ventralis* is the best example. In *Chaetobranchopsis australis*, the *obliquus ventralis 1, pars abductoris rectus* originates from the hyoid arch (character 68), which Winterbottom (1974) would have classified as a *rectus ventralis*. However, in all other taxa this part of *obliquus ventralis 1* originates from the lateral portion of hypobranchial 1. The *pars abductoris transversus* is an even better example, once it may be either absent or originate from basibranchial 2, or span between contralateral ceratobranchials without attaching to a basibranchial, or (in *Satanoperca* sp.) present several sections, running in different directions and linking basibranchials, hypobranchials and ceratobranchials of the first two arches (character 69). Thus, instead of masking this diversity by using different names, we prefer to emphasise that the *obliquus ventralis 1* is an evolutionarily very plastic muscle in cichlids. The *obliquus ventralis 2, pars adductoris obliquus* originates not from the respective hypobranchial but from a ligamentous system, that ultimately attaches to hypobranchial 1 or basibranchial 1 (character 71). In a few taxa, some fibres of the *obliquus ventralis 2* may cross the sagittal plane, while other fibres may reach the basibranchial 1 (character 75). This, too, could be a reason for applying names such as *transversus ventralis 2* or *rectus ventralis 2*, but we prefer to consider those characters under the variation of the *obliquus ventralis 2*.

Character 67. Insertion of the *obliquus ventralis 1, pars abductoris rectus* (dissection stage 4A). [0] On a ventral process at the bony extremity of the ceratobranchial 1. [1] On a

point in the ventral side of the ceratobranchial 1 somewhat distant from the extremity of the bone. [2] As in 1, but more close to the extremity. [3] On the cartilage tip of the ceratobranchial 1.

Character 68. Origin of the *obliquus ventralis 1, pars abductoris rectus* (dissection stage 4A). [0] From the hypobranchial 1. [1] From the dorsal hypohyal.

Character 69. *Obliquus ventralis 1, pars adductoris transversus* (dissection stage 6A). [0] Present, originating from a keel on the ventral side of basibranchial 2, bearing an anterior section and, occasionally, a posterior section (see Deprá *et al*., Chapter 1 of this volume). [1] Absent (Fig. 29). [2] Present, originating from the ventral side of basibranchial 2 (keel present or not), not bearing an anterior nor a posterior section. [3] Present, its fibres freely crossing from one side to the other, originating from the basibranchials 1–2 and from the hypobranchial 1, and inserting on ceratobranchial 1 and hypobranchial 2. [4] Present, originating from the basibranchial 1 and from a ventral keel of basibranchial 2, not bearing an anterior nor a posterior section. [5] Present, originating from a sagittal raphe.

Character 70. *Obliquus ventralis 1, pars adductoris obliquus* (dissection stage 4A). [0] Originating solely from hypobranchial 1, without a transversal section (Deprá *et al*., Chapter 1 of this volume, Fig. 17a). [1] Originating from hypobranchial 1, but also with a transversal section originating from the rostral ligamentous system and from a sagittal raphe (Fig. 29). [2] Originating only from basibranchial 1 (Fig. 30).

Character 71. Anterior origin of the *obliquus ventralis 2, pars adductoris obliquus* (rostral ligamentous system of Anker, 1978:262, Figs. 15-16) (dissection stage 4A). [0] On basibranchial 1 (Deprá *et al*., Chapter 1 of this volume, Fig. 17a). [1] On hypobranchial 1 (Fig. 29). [2] On the anterior portion of basibranchial 2, immediately posterior to basibranchial 1 and medial to hypobranchial 1 (Fig. 31). [3] *Pars adductoris obliquus* absent.

Character 72. Opening of the rostral ligamentous system (anterior attachment of *obliquus ventralis 2, pars adductoris obliquus*) (dissection stage 4A). [0] Small, close to the basibranchial 1 (there is a broad sheet of connective tissue linking the two sides of the ligamentous system, posteriorly to the opening; Deprá *et al*., Chapter 1 of this volume, Fig. 17a). [1] Large (a thin strip of connective tissue links the two sides). [2] Rostral ligamentous

system absent. [3] Small, close to hypobranchial 3 (there is a broad sheet of connective tissue linking the two sides of the ligamentous system, anteriorly to the opening; Fig. 30). [4] Small, only between the tips of the ligamentous system that attach to the contralateral hypobranchials 1. [5] Two openings: a small one between the tips of the ligamentous system that attach to the contralateral hypobranchials 1, and a large slit posterior to it reaching the hypobranchial 3 (Fig. 29).

Character 73. Insertion of *obliquus ventralis 2, pars adductoris obliquus* (dissection stage 6A). [0] On the tip of ceratobranchial 2. [1] On ceratobranchial 2, but far from the tip.

Character 74. Anterior reach of the fibres of the *obliquus ventralis 2, pars adductoris obliquus* (dissection stage 4A). [0] To the anterior end of the rostral ligamentous system. [1] Short from the anterior end of the rostral ligamentous system. [2] Half-way to the anterior end of the rostral ligamentous system. [3] *Pars adductoris obliquus* absent. [4] Fibres are not directed forward, but transversely, so that the *pars adductoris obliquus* has, in fact, an adductor function, bringing the contralateral hypobranchials 2 closer to the sagittal plane.

Character 75. Medial reach of the fibres of the *obliquus ventralis 2, pars adductoris obliquus* (dissection stage 4A). [0] Past the sagittal plane (*i.e.*, fibres attach to both sides of the body; Deprá *et al*., Chapter 1 of this volume, Fig. 17b). [1] Short from the sagittal plane. [2] *Pars adductoris obliquus* absent. [3] On a sagittal raphe, posteriorly to the opening of the rostral ligamentous system. [4] On a sagittal raphe, anteriorly to the opening of the rostral ligamentous system. [5] on a long sagittal raphe.

Character 76. Origin on the *obliquus ventralis 2, pars adductoris transversus* (dissection stage 6A). [0] Reaching the antimere medially. [1] Far from reaching the antimere medially. [2] Short from reaching the antimere medially.

Character 77. Origin of the *obliquus ventralis 3, pars adductoris* (dissection stage 6A). [0] From medial face of hypobranchial 3 and from semi-circular ligamentous system. [1] Only from medial face of hypobranchial 3 (semi-circular ligamentous system absent, or possibly represented by the tendon of *rectus ventralis 4*, but not connecting with the contralateral tendon).

3.3.1.18 Transversus ventralis 4

Character 78. Fibres of the *transversus ventralis 4* (dissection stage 4A). [0] Leaving a long portion of the ceratobranchial 5 keel uncovered (*i.e.*, few fibres cross the keel ventrally; Deprá *et al*., Chapter 1 of this volume, Fig. 16). [1] Covering the ceratobranchial 5 keel, which is nonetheless visible through the fibres (*i.e.*, few fibres crossing the keel ventrally; Fig. 32). [2] Covering the ceratobranchial 5 keel, which cannot be seen through the fibres (*i.e.*, many fibres crossing the keel ventrally; Fig. 31).

Character 79. *Transversus ventralis 4* (dissection stage 4A): [0] Confined to the ceratobranchial 5 keel (Deprá *et al*., Chapter 1 of this volume, Fig. 16). [1] Invading the ceratobranchial 5 main body (Fig. 31).

3.3.1.19 Rectus ventralis 4

Character 80. Attachment of the *rectus ventralis 4* to the ceratobranchial 4 (dissection stage 4A). [0] Mostly on the lateral face of the medioventral crest of ceratobranchial 4, with a small portion on the medial face (anterior to the ceratobranchial 5 keel). [1] On the medial and lateral faces of the medioventral crest of ceratobranchial 4, as well as on the lateral portion of the *transversus ventralis 4* (thus lateral to the ceratobranchial 5 keel). [2] Similar to state 1, but extending much posteriorly, to the vertical through the most anterior ceratobranchial 5 tooth. [3] Similar to state 2, but extending even posteriorly. [4] On the medial face of the body of the bone. [5] On the ventrolateral face of the anterior extremity of the ceratobranchial 4, on the lateral portion of the *transversus ventralis 4*, and on a tendon that is posteriorly confluent with the *rectus communis* tendon (anterior attachment of the *rectus ventralis 4* is the semi-circular ligament).

Character 81. Shape of the *rectus ventralis 4* (dissection stage 4A). [0] Relatively short, triangular, originating from semi-circular ligamentous system. [1] Long, cord-like, originating from hypobranchial 3 via a long tendon. [2] Long, cord-like, originating from hypobranchial 3 via a short tendon, and from the semi-circular ligamentous system; inserting on ceratobranchial 4 by a long tendon.

3.3.1.20 Rectus communis

Character 82. Configuration of the *rectus communis* (dissection stage 4A). [0] Anterior (unpaired) portion entirely muscular, posterior (paired) portion continuously muscular, although with a tendinous portion dorsally that continues to the attachment to the ceratobranchial 5 (Deprá *et al*., Chapter 1 of this volume, Fig. 16). [1] Anterior (unpaired) portion entirely muscular, posterior (paired) portion continuously tendinous, with a bunch of fibres attached ventromedially to the tendon, isolated from fibres of the anterior portion and anterior to the ceratobranchial 5 keel (Fig. 33). [2] With a very long tendon posteriorly, but no bunch of fibres isolated from the anterior portion.

Character 83. Aponeurosis between anterior (unpaired) and posterior (paired) portions of *rectus communis* (dissection stage 4A). [0] Absent. [1] Present.

Character 84. Posterior attachment of the *rectus communis* (dissection stage 4A). [0] To the ceratobranchial 5, by a tendon that attaches immediately posteriorly to the insertion of the *pharyngoclavicularis externus*, and to the lateral face of this muscle by connective tissue. [1] To the ceratobranchial 5, by a tendon that attaches immediately posteriorly to the insertion of the *pharyngoclavicularis externus*, and to the lateral and medial face of this muscle by connective tissue (medially, by a second tendon).

3.3.1.21 Pharyngoclaviculares

Character 85. Proximal portion of *pharyngoclavicularis internus* (dissection stage 3). [0] Partially covered by distal portion of *protractor pectoralis*. [1] Not partially covered by distal portion of *protractor pectoralis*, but close to it (Fig. 34). [2] Partially covering distal portion of *protractor pectoralis*. [3] Not partially covered by distal portion of *protractor pectoralis*, and remote from it (Fig. 35).

Character 86. Relative position of the origins of the *pharyngoclaviculares* and the *sternohyoideus* (dissections stage 3). [0] The *sternohyoideus* overlaps the *pharyngoclavicularis internus* slightly in lateral view or the two muscles are simply juxtaposed, without overlap or they are separate by a small space (Fig. 36). [1] The *pharyngoclavicularis internus* overlaps the *sternohyoideus* in lateral view (Fig. 37). [2] The *sternohyoideus* origin is coincident with the *pharyngoclavicularis externus* origin, and remote

from the *pharyngoclavicularis internus* (Fig. 38). [3] The *sternohyoideus* origin is posterior to the *pharyngoclavicularis externus* origin, but still remote from the *pharyngoclavicularis internus*.

Character 87. Fibres of the *pharyngoclavicularis internus* (dissection stage 4A): [0] Inserting mostly through the anterior tendon, which usually attaches to the anterior keel of the ceratobranchial 5. [1] Inserting mostly through the posterior aponeurosis, which attaches to the body of the ceratobranchial 5. [2] Inserting mostly muscularly on the body of the ceratobranchial 5. [3] Inserting completely through a broad aponeurosis, which is confluent with the *rectus communis* tendon.

Character 88. Insertion of the anterior tendon of the *pharyngoclavicularis internus* (dissection stage 4A). [0] On the ventral keel of the ceratobranchial 5 (Deprá *et al*., Chapter 1 of this volume, Fig. 16). [1] Much posteriorly to the keel of the ceratobranchial 5, on the anterior portion of the body of the bone (Fig. 39). [2] Slightly posterior to the ceratobranchial 5 keel (apparently because of the posterior insertion of the *transversus ventralis 4*; Fig. 30). [3] Tendon absent (Fig. 40).

Character 89. Insertion of the *pharyngoclavicularis internus* (dissection stage 4A). [0] Close to the anterolateral margin of the ceratobranchial 5 (*e.g.*, Figs. 30–33). [1] Close to the ceratobranchial 5 symphysis (Fig. 40).

Character 90. Origin of the *pharyngoclavicularis internus* (dissection stage 3). [0] From the edge of the medial wing of cleithrum. [1] From the lateral wing of cleithrum, close to its angle with medial wing.

Character 91. Posterior reach of the *pharyngoclavicularis externus* insertion (dissection stage 4A). [0] Beyond the posterior end of the insertion of the *pharyngoclavicularis internus*, relatively close to the posterior end of the ceratobranchial 5. [1] At the same vertical though the posterior end of the *pharyngoclavicularis internus* insertion or slightly posterior to it. [2] At the same vertical though the anterior end of the *pharyngoclavicularis internus* insertion (excluding the anterior tendon). [3] At the same vertical though the posterior end of the *pharyngoclavicularis internus* insertion, both close to the posterior end of the ceratobranchial 5.

Character 92. Insertion of the *pharyngoclavicularis externus* (dissection stage 4A). [0] Entirely on the lateroventral face of the ceratobranchial 5. [1] Mainly from the lateroventral face of the ceratobranchial 5, but also from the ventral ridge between the ventral face and the lateral face of the bone.

Character 93. Origin of *pharyngoclavicularis externus* (dissection stage 6A). [0] *Pars anterior* originates from the angle between lateral and medial wings of cleithrum, but *pars posterior* originates closer to the edge of medial wing. [1] Entirely from the angle between lateral and medial wings of cleithrum (the muscle has only one part).

3.3.1.22 Protractor pectoralis

Character 94. Gap between insertions of *protractor pectoralis* and *levator pectoralis* (dissection stage 3). [0] absent (both muscles juxtaposed to one another; *e.g.*, Fig. 38); [1] present (Fig. 41; muscles separated in their insertion, converging towards origin; in *Crenicichla* and *Teleocichla*, the proximal portion of the *pharyngoclavicularis internus* is partially covered by the distal portion of the *protractor pectoralis*, as a consequence of the more dorsal origin of the *pharyngoclavicularis internus*).

3.3.1.23 Levator pectoralis

Character 95. Number of sections of the *levator pectoralis* (dissection stage 3). [0] Two. [1] Three. [2] One.

Character 96. Anterior reach of the *levator pectoralis* origin (dissection stage 4A). [0] At the same vertical though tendinous origin of the *protractor pectoralis*, just posterior to the origin of the *adductor operculi*. [1] Well anterior to the tendinous origin of the *protractor pectoralis*, lateral to the origin of the *adductor operculi*. [2] Slightly anterior to the tendinous origin of the *protractor pectoralis*, lateral to the origin of the *adductor operculi*.

Character 97. *Levator pectoralis* insertion. [0] On cleithrum and post-temporal, dorsally to Baudelot's ligament. [1] On cleithrum and post-temporal, Baudelot's ligament and *hypaxialis*. [2] On cleithrum, post-temporal and *hypaxialis*.

3.3.1.24 Note on rectus externus

Deprá *et al*. (Chapter 1 of this volume) mentioned a remarkable character, *viz*. the *rectus externus* (one of the eye muscles) originating not from within the myodome, but from the first vertebra and basioccipital of *Geophagus sveni*. Presently, we do not have precise information for the state of this character in each of the taxa analysed herein. However, at least *Acarichthys heckelii*, *Satanoperca* sp., *Gymnogeophagus balzanii*, "*G*." *brasiliensis* and *Biotodoma cupido* exhibit a condition similar to that of *G. sveni*. The guianacarines and crenicaratines appear to have an even more posterior origin, although we were unable to define precisely from which vertebra the muscle fibres arise. The posterior opening of the myodome is also present in the *Crenicichla* clade, (possibly) *Biotoecus*, "*G*." *steindachneri*, *Chaetobranchopsis australis*, *Retroculus acherontos* and *Cichla kelberi*, although the origin of the *rectus externus* lies in the basioccipital of those taxa. The closed myodome, which seems to be the normal condition in Actinopterygii in general (Winterbottom, 1974), appears in Cichlasomatini, Astronotini and (possibly) *Apistogramma borellii*.

3.3.2 Phylogenetic analyses

3.3.2.1 Unweighted

We obtained a 524-step tree (Fig. 42). Because the analysis did not recover the clade composed of Cichlini and Retroculini, we rooted the tree in *Retroculus acherontos*. Geophagini resulted paraphyletic, with *Bujurquina vittata*, *Astronotus crassipinnis* and *Cichlasoma paranaense* nested deep within. The analysis recovered a clade largely consistent with the biotodomines, but without *Mikrogeophagus*. In addition, *Satanoperca* nested deep within this clade, which had *Acarichthys heckelii* and *Guianacara dacrya* as successive sister groups. In other words, the orobranchial winnowers (except *Mikrogeophagus*) clustered together. Those taxa appear in our analysis as sister to a clade composed mainly of non-geophagines (*Bujurquina*, *Astronotus* and *Cichlasoma*), but also including *Mazarunia*. The subsequent sister group is made of *Biotoecus* as sister of the *Crenicichla* clade, which is similar to the crenicichlines, without *Acarichthys*. The next nodes lead to a clade including *Mikrogeophagus* and *Apistogramma*; another with *Dicrossus* as sister to *Crenicara* and *Taeniacara*; and the last one, with *Cichla* as sister to *Chaetobranchus*.

Five synapomorphies support the clade including most orobranchial winnowers: 0[2], 11[2], 15[4], 25[2], 56[1]. We recovered character 0[2] as paralleled in *Crenicara punctulatum*, and further derived in a clade including "*Geophagus*" *brasiliensis*, *Gymnogeophagus balzanii*, *Geophagus sveni* and *Satanoperca* sp. Character 11[2] is paralleled in *Cichla kelberi* and *Crenicara punctulatum*, and further derived in a clade including *G. balzanii*, *G. sveni* and *Satanoperca* sp. Character 15[4] is paralleled in *Crenicara punctulatum* and in a clade including "*Geophagus*" *steindachneri*, "*G.*" *brasiliensis*, *G. balzanii*, *G. sveni* and *Satanoperca* sp. Character 25[2] is paralleled in *Mazarunia mazarunii*, and reversed in "*G.*" *steindachneri*. Character 56[1] is paralleled in *Mikrogeophagus ramirezi*, and reversed in "*G.*" *brasiliensis* and *Satanoperca* sp.

Characters 5[0], 31[2], 40[2], 50[0], 83[1], 85[3] and 97[2] support the monophyly of a clade including those orobranchial winnowers, except *Guianacara dacrya*. Character 5[0] is paralleled in *Cichlasoma paranaense*, reversed in "*Geophagus*" *steindachneri*, and further derived in "*G.*" *brasiliensis* and in *Satanoperca* sp. Character 31[2] is paralleled in *Taeniacara candidi*, reversed in a clade including "*G.*" *brasiliensis*, *G. sveni*, *G. balzanii* and *Satanoperca* sp., then reversed back to state 2 in *Satanoperca* sp. Character 40[2] is not paralleled among analysed taxa, but *G. balzanii* and *Satanoperca* sp. present the ancestral state 1. Character 50[0] is paralleled at several nodes, and reversed in "*G.*" *steindachneri* and in *G. sveni*. Character 83[1] is paralleled at several nodes, but not reversed. Character 85[3] is paralleled at several nodes, and reversed only in "*G.*" *steindachneri*. Character 97[2] is paralleled at several nodes, and further derived in a clade including *G. sveni* and *Satanoperca* sp.

The clade including the same taxa, except *Acarichthys heckelii*, encompasses the geophagine orobranchial winnowers bearing an epibranchial 1 lobe. The clade has three synapomorphies: 49[1], 60[1] and 64[0]. Character 49[1] is paralleled at several nodes, further derived in a clade including "*Geophagus*" *brasiliensis*, *Gymnogeophagus balzanii*, *Geophagus sveni* and *Satanoperca* sp., with a reversal to state 1 in *Satanoperca*. Character 60[1] is paralleled at several nodes, but never reversed. Character 64[0], paralleled in the *Crenicichla* clade and in *Astronotus crassipinnis*, is reversed in *Satanoperca* sp.

Excepting *Biotodoma cupido*, four synapomorphies support the resulting clade: 15[8], 30[0], 51[2] and 65[1]. Character 15[8] is further derived in *Geophagus sveni* and in *Satanoperca* sp. Character 30[0] is paralleled at several nodes, but never reversed. Character 51[2] is apparently ancestral to Cichlinae, and further derived in "*Geophagus*" *brasiliensis*

and *Satanoperca* sp. Character 65[1] is paralleled only in the orobranchial winnower *Retroculus acherontos*, but reversed in the clade including *G. sveni* and *Satanoperca* sp.

The clade including "*Geophagus*" *brasiliensis*, *Gymnogeophagus balzanii*, *Geophagus sveni* and *Satanoperca* sp. relies on four synapomorphies: 31[0], 49[2], 74[0] and 78[0]. Character 31[0] is a reversal to a state that would be synapomorphic to a clade including *Geophagus*-like winnowers and the clade including *Bujurquina*, *Mazarunia*, *Cichlasoma* and *Astronotus*. Further reversed to state 2 in *Satanoperca* sp. Character 49[2] is unique to this clade, and further reversed to state 1 in *Satanoperca* sp. Character 74[0], which is present in other clades, is also further reversed to state 1 in *Satanoperca* sp. Character 78[0], paralleled at two nodes, is further derived in *G. balzanii* to state 1 (paralleled at several nodes).

Characters 1[6], 3[2], 11[1], 80[1] and 91[1] support a clade including *Gymnogeophagus balzanii*, *Geophagus sveni* and *Satanoperca* sp. Character 1[6] is paralleled in *Mikrogeophagus ramirezi*. Character 3[2] is paralleled in *Mazarunia mazarunii* and *Biotodoma cupido*. Characters 11[1] and 80[1] are further uniquely derived in *Satanoperca* sp. (state 0 in both cases). Character 91[1] is paralleled at several nodes.

Finally, characters 20[1], 65[1], 76[0] and 97[1] support the sisterhood between *Geophagus* (*sensu stricto*) and *Satanoperca*. Character 20[1] is paralleled at several nodes. Character 65[0] represents a reversal to the most common state. Character 76[0] is paralleled at two nodes. Character 97[1] seems unique to *Geophagus* and *Satanoperca*.

The bootstrap values supporting each clade in the unweighted analysis are extremely low. Except for the *Crenicichla* clade, which has a bootstrap value of 92, the highest support is that of the clade composed of *Cichla kelberi* and *Chaetobranchopsis australis* (28). Among geophagines, the highest value is 18 (for the clade composed of *Biotoecus* plus the *Crenicichla* clade) and 15 (for the clade composed of *Geophagus sveni* and *Satanoperca* sp. and for the clade composed of the preceding one plus *Gymnogeophagus balzanii*). These low bootstrap values may result from the fact that the characters analysed are not very numerous, and highly discordant among themselves.

3.3.2.2 Weighted

The weighted analysis, too, failed to recognise the sisterhood between Cichlini and Retroculini, forcing us to arbitrarily elect *Retroculus acherontos* as the outgroup. We obtained a tree with a best score of 453.11429 (Figs. 43). This time, only a clade uniting *Bujurquina* and *Cichlasoma*, deeply nested within Geophagini, rendered the tribe paraphyletic. There is,

again, a clade including the orobranchial winnowers, except *Mikrogeophagus*, but this time including *Crenicara* too. Sister to this clade is one including *Mazarunia* as sister to the cichlasomatines *Bujurquina* and *Cichlasoma*. The subsequent sister group is roughly similar to the clade formed by apistogrammines plus crenicichlines. It includes to clades: one encompasses the *Crenicichla* clade and its successive outgroups, *Biotoecus* and *Taeniacara*; the other encompasses *Dicrossus* as sister to *Mikrogeophagus* plus *Apistogramma*. The most basal node leads to a clade encompassing *Astronotus* as sister to *Cichla* plus *Chaetobranchopsis*.

Four synapomorphies support the clade including orobranchial winnowers: 0[2], 11[2] and 15[4], as in the unweighted analysis; and 94[0]. The weighted analysis recovered character 0[2] as unparalleled, reversed only in "*Geophagus*" *brasiliensis*, and further derived in *Satanoperca* sp. and in the clade encompassing *Geophagus sveni* and *Gymnogeophagus balzanii* (in both cases, unparalleled). Character 11[2], paralleled only in *Cichla kelberi*, is also further derived in *Satanoperca* sp. and in the clade encompassing *G. sveni* and *G. balzanii* (in both cases, unparalleled). Character 15[4], also unparalleled, is further derived into state 8 at several nodes, and into other states in *Satanoperca* sp. and *G. sveni*. Character 94[0] is unreversed, but paralleled in three other clades.

The clade including orobranchial winnowers divides into a clade including *Guianacara* as sister to *Crenicara* and "*Geophagus*" *brasiliensis*, and another clade including the remaining taxa. Two characters support the first clade: 43[1], 75[4]. Character 43[1] is paralleled at several nodes, being present in *Geophagus* and *Satanoperca*. Character 75[4] is paralleled only in *Mazarunia*.

Characters 31[2], 36[0] and 88[0] support the second clade, encompassing *Biotodoma* and *Acarichthys* as sister to "*Geophagus*" *steindachneri*, *Satanoperca* sp., *Geophagus sveni* and *Gymnogeophagus balzanii*. Character 31[2] is paralleled only in *Taeniacara*, but reversed in the clade including *G. sveni* and *G. balzanii*. Character 36[0] is paralleled at several nodes, including the winnower *Retroculus acherontos*. Character 88[0] is paralleled in the winnowers "*G.*" *brasiliensis* and *Retroculus acherontos*, and in the probable winnower *Apistogramma borellii*. Characters 13[1], 15[8] and 72[0] support the clade including "*G.*" *steindachneri*, *Satanoperca* sp., *G. sveni* and *G. balzanii*. Character 13[1] is unparalleled and unreversed. State 2, which we consider as intermediate between states 0 and 1, appear in *Acarichthys heckelii* and in *Guianacara dacrya* (we ran the analysis considering all characters as non-additive). Character 15[8] is paralleled in a few taxa and further derived in

Satanoperca sp. and in *G. sveni*. Character 72[0] is paralleled in *Mikrogeophagus ramirezi*, and posteriorly derived in *Satanoperca* sp.

Characters 1[6] and 3[2] support the clade including *Satanoperca*, *Geophagus* and *Gymnogeophagus*. Character 1[6] is paralleled only in *Mikrogeophagus ramirezi*. Character 3[2] is paralleled in *Mazarunia mazarunii* and in *Biotodoma cupido*.

3.3.2.3 Constrained analysis, convergence and function

The constrained analysis served three purposes. First, to compare the minimum tree length necessary to reach the topology in Fig. 1 (based on Ilves *et al*., 2017) and the shortest trees obtained in our unconstrained analyses (unweighted and weighted). Second, to present a solution to the polytomies present in the aforementioned hypothesis. Third, to map the myological character states on the topology in Fig. 1 in order to determine their evolutionary history (regarding the molecular analysis as closest to the true phylogeny of the group) and identify characters that probably converged in taxa with similar feeding adaptations.

The weighted constrained analysis yielded a tree with a score of 463.77500 (Figs. 44). This is only 2.3% 'worse' than the unconstrained weighted analysis. However, even under the constraints, the tree obtained in the weighted analysis does not correspond perfectly to Fig. 1, which probably contributed to lower the score. The unweighted constrained analysis, which succeeded in reaching the expected topology, resulted in a 585-step tree 11.6 % 'worse' than the unweighted unconstrained tree (Fig. 45). As well as the weighted analysis, the unweighted one recovered *Geophagus* (*sensu stricto*) and *Gymnogeophagus* as sister groups, resolving the polytomy among those two taxa and the "*Geophagus*" *steindachneri* complex (Ilves *et al*., 2017). This group remained in an unsolved polytomy with *Biotodoma* and the clade formed by *Mikrogeophagus* and the "*G.*" *brasiliensis* complex. Other, unexpected polytomies appeared in the unweighted analysis, resulting from the lack of synapomorphies. The first includes guianacarines; the clade composed of apistogrammines and crenicichlines; and the clade composed of crenicaratines and biotodomines (thus failing to find support to the sisterhood between guianacarines and the clade composed of apistogrammines and crenicichlines). The second includes Astronotini; Cichlasomatini; and the clade composed of Chaetobranchini and Geophagini (thus failing to find support to the sisterhood of Astronotini and the clade composed of Chaetobranchini and Geophagini).

The third purpose of the constrained analysis, *i.e.*, to map the myological character states on the topology in Fig. 1, allowed us to recognise characters that are putatively

convergent among orobranchial winnowers. Character states independently derived between organisms with similar dietary preferences frequently give us insights on the function of the respective structures. Although having a similar diet does not mean that the adaptations will be the same, there is a probability that convergent solutions will appear. In the following paragraphs, we list the characters that appear to have converged among orobranchial winnowers, and discuss their possible functional relevance.

We interpret characters 0 (states 2–4), 11 (states 0–2) and 13 (states 1–2) as the most likely to represent specialisations for orobranchial winnowing. Character 0 reflects the degree to which the origin of *adductor mandibulae, pars rictalis*, is elevated, making its dorsal profile more inclined and longer. States 2–4 represent successively more intense inclination degrees of the *pars rictalis* dorsal profile. Those states are present in the four geophagine lineages of confirmed orobranchial winnowers, and state 2 (slightest inclination) is also present in *Crenicara punctulatum*, which is herein considered as an oral winnower. Character 11 describes the inclination of the fibres of the *pars rictalis*, and not of its dorsal profile, but is nonetheless largely redundant to character 0, except that among the states common in orobranchial winnowers (0–2) state 2 (which represents the slightest inclination) is present also in *Cichla*.

Character 13 describes the nature of the *pars malaris* origin (tendinous our muscular). States 1 and 2, which are only slightly different, are present in each of the lineages of geophagine orobranchial winnowers, and not in any other taxon analysed. In most cichlids analysed herein, the fibres originate muscularly on a large area. This is viable because the competition for headspace among *pars malaris*, *pars rictalis* and *levator arcus palatini* is negligible. In the taxa presenting states 1 and 2, on the other hand, there is little room for the insertion of *levator arcus palatini*. This muscle has to be very narrow along the longitudinal axis of the fish, because of the small distance between the sphenotic and the posterior margin of the hyomandibula, and because of the forward inclination of the lower part of the hyomandibula. In addition, those geophagine orobranchial winnowers have compressed heads, meaning that the available area for muscular insertion in the suspensorium (mainly hyomandibula) is short along the transversal axis too. Because of the elevation of the origin site of *pars rictalis*, the *pars malaris* has to be inclined in those taxa. If the dorsal fibres of *pars malaris* extended posteriorly in a straight line along the dorsal profile of the muscle, originating muscularly, their projected origin would lay in the neurocranium. That is a clear evidence of why the aponeurotic origin of the *pars malaris* represents a solution for avoiding competition for space with *levator arcus palatini*.

Thus, we hypothesise character 13 to have developed, in part, in consequence of character 0, with the extreme condition 13[1] being present in the same taxa as the extreme conditions 0[3–4]. The importance of those characters as adaptations to the winnower life style perhaps reside in the fact that longer fibres contract faster than shorter ones in absolute terms. The winnowing process relies heavily in the creation of pressure waves pushing the water back and forth through the oropharyngeal cavity (Drucker & Jensen, 1991; Weller *et al.*, 2016). This movement is performed by rapidly repeating a cycle with two phases: (1) expansion of the oral cavity as a result of the abduction of the suspensorium and protraction of the premaxillae; (2) compression of the oral cavity as a result of the adduction of the suspensorium and retraction of the premaxillae. Thus, it seems that the strength of the muscles involved (proportional to their cross sections) can be compromised in exchange of a rapid movement.

Because the *adductor mandibulae*, *pars malaris* retracts the premaxilla (Drucker & Jensen, 1991), it seems logical that a longer *pars malaris* would provide faster retraction, and faster winnowing cycles. The longer fibres of the dorsal portion of *pars rictalis* may also contribute to this movement, once the elevation of the lower jaw also contributes to the retraction of the premaxilla, because the bones connect to each other at the rictus. Ultimately, we conclude that these characters evolved in response to the evolution of the skeleton. The horizontal preopercular arm is short in geophagine orobranchial winnowers, so if the *pars rictalis* fibres were horizontal they would be inevitably short. Additionally, as mentioned before, the slender shape of the *levator arcus palatini* is a consequence of the approximation between the verticals through the posterior margins of the sphenotic and of the hyomandibula.

The skull, in turn, seems to have evolved towards a complex of morphological properties that have already been associated to winnowers in the literature (*e.g.*, Arbour & López-Fernández, 2013; Říčan *et al.*, 2016). The anterior inclination of the lower portion of the hyomandibula carries the whole suspensorium forward, including the articulation of the lower jaw. It also compensates the postorbital reduction of the head, permitting the elongation of the ceratobranchials, thus enlarging the area through which the sediment is sifted. The growth of the vomer, in the shape of a curved ‘beak’, brings the premaxilla ventrally, forming an elongate snout, with a low mouth and a vertically enlarged oral cavity, which accommodates a large volume of substrate and water.

Characters 25[2] and 88[0] are present in four lineages of orobranchial winnowers, but the reconstruction of their ancestral states is ambiguous at some nodes, meaning that those characters may represent convergences or retention of ancestral character states. In either

case, the fact that they are absent from non-winnowers supports the hypothesis that they improve winnowing or correlate with characters that do so. The insertion of the *dilatator operculi* positioned about the vertical through the middle of its origin (character 25[2]) may have appeared only once, at the base of Geophagini. Alternatively, it can be simultaneously a synapomorphy of biotodomines and of the clade including guianacarines, apistogrammines and crenicichlines, or it may have appeared up to four times independently. The only taxon presenting state 2, which is not a confirmed winnower, is *Mazarunia mazarunii*.

The shape of the *dilatator operculi* relates to the aforementioned change in the shape of the skull in geophagine orobranchial winnowers. As usual for most taxa analysed, the posterior end of the *dilatator operculi* insertion reaches clst 3 or close to it. However, in most other taxa, clst 3 lies about dorsal to the insertion of *dilatator operculi*, or even anterior to it. The anterior inclination of the suspensorium in geophagine orobranchial winnowers carried the insertion of the muscle anteriorly. Thus, there is probably no direct selection towards character 25[2], but rather an indirect selection mediated by the shape of the skull.

The more anterior insertion of the anterior tendon of the *pharyngoclavicularis internus* (character 88[0]), as inferred by the character reconstruction based on parsimony, appeared at least three times independently: in *Retroculus*, in biotodomines and in the clade including apistogrammines and crenicichlines. Alternatively, it may have appeared independently in apistogrammines and crenicichlines. The function of the *pharyngoclavicularis internus* is to swing the ceratobranchial 5 (lower pharyngeal jaw) posteriorly. The topology of the muscle suggests that a more anterior insertion may allow a wider rotation of the ceratobranchial 5 around a transversal axis. Liem (1986) and Drucker & Jensen (1991) showed the importance of the relative movement between the upper and lower pharyngeal jaws to the shearing mechanism of the embiotocid oral winnowers (surfperches). However, there is no direct evidence of shearing in orobranchial winnowers.

An alternative hypothesis to explain the importance of this character relies on another putative function of the *pharyngoclavicularis internus*. The *rectus communis* (= *pharyngohyoideus* of early studies, *e.g*., Liem, 1986) is an antagonist of *pharyngoclavicularis internus*, swinging the lower pharyngeal jaw forward. However, this seems to depend on whether the urohyal is protracted or not (which is a function of *protractor hyoidei*). If the urohyal retracts (by action of *sternohyoideus*), the *rectus communis* may assume the function of bending the basibranchial bar, which would result in the relative movement between ceratobranchials. That movement would imply the separation or approximation between the

gill rakers. A more anterior insertion of the *pharyngoclavicularis internus* may turn it synergetic with *sternohyoideus* when the basibranchial bar is arched.

The separate *transversus pharyngobranchialis 3* and *transversus epibranchialis 4* (character 56[1]) evolved four times independently: one in biotodomines (reversed only in "*Geophagus*" *brasiliensis*), one in *Guianacara*, one in *Acarichthys* and one in the non-winnower *Cichlasoma*. The anatomic separation of the two muscles possibly gives them an independence of contraction that might provide a more refined control to the movement of pharyngobranchial 3 and epibranchial 4. The anatomic topology suggests that the *transversus pharyngobranchialis* is probably an antagonist of the *circumpharyngobranchialis*, both muscles likely promoting the rotation of the pharyngobranchial 3 around a vertical axis. The *circumpharyngobranchialis* would contribute to pull the posterior portion of the upper pharyngeal jaws laterally (*i.e.*, away from each other), while the *transversus pharyngobranchialis 3* would pull them together. Although *transversus epibranchialis 4* may, of course, act synergeticallly with *pharyngobranchialis 3*, it is possible that an independent movement is advantageous in some circumstances.

Character 69 is, perhaps, the most interesting character that seems to have converged among geophagine orobranchial winnowers. States 0, 3, 4 and 5 are quite different from one another, but all have in common the widening of the origin site of *obliquus ventralis 1, pars adductoris transversus*. Additionally, muscle's architecture in each state suggests it has the function of depressing the lateral portion of hypobranchial, while adducting the ceratobranchial 1 (towards the sagittal plane). We believe that the fine control of the movement of ceratobranchials 1 and 2 is relevant to orobranchial winnowing because the fish ejects sediment through the space between those bones. The interlocked gill rakers that line up each ceratobranchial delimit this space. In fact, one can deduce that gill rakers are necessary to separate small food items from sediment particles. Thus, the distance between the gill rakers and the way they interlock (more or less tightly) probably selects the size of the particles that can pass through the gills. However, to keep the ceratobranchials apart at a constant distance while hydraulic forces act upon them may require a specialised ventral gill-arch musculature, thus the modifications of *obliquus ventralis 1*.

Characters 1[6], 40[2], 65[1], 66[1] and 97[1] each appear only in two clades of orobranchial winnowers, but in no other taxa, and we consider them as possible adaptations towards winnowing too. The *adductor mandibulae, pars malaris*, shaped as a very elongate triangle (character 1[6]), clearly correlates with characters 0, 11 and 13, which we discuss above. The hypertrophy of *levator internus 1* (character 40[2]) may relate to its function as a

protractor of the upper pharyngeal jaw, essential to shearing the prey (Liem, 1986:314). However, it remains unclear if shearing is as important in orobranchial winnowers as in surfperches. Additionally, the hypertrophy of the muscle implies an increased cross-section and therefore more strength, which may enhance the efficiency of the fish in manipulating certain types of food that are not necessarily exclusive to winnowers.

Another interesting character is the hypertrophy of the *adductor branchialis 1* (character 49, states 1 and 2). Its distribution is the same as that of the epibranchial 1 lobe, even when the latter is rudimentary (*Crenicara*, *Dicrossus*, *Mazarunia* and *Taeniacara*). State 2, representing the maximum hypertrophy, is present only in the taxa with the most developed lobes, except in *Satanoperca*. The morphology of the lobe makes it clear that its function is not to provide a wider site for attachment of the *adductor branchialis 1*. Rather, adducting the lobe, which seems to be important to winnowing, may require strength when water flux tends to abduct it. In taxa presenting a well-developed lobe, it seems that its function is to isolate the anterior and posterior portions of the branchial basket. We hypothesise that, in a first stage, the fish pushes the mixture of water, sediment and food through the gill rakers on the anterior half of ceratobranchials 1–4, while adducting the lobe and occluding the upper and lower pharyngeal jaws. This would result in the expulsion of fine sediment through the gills, and in the retention of food and gross sediment within the mouth. Subsequently, the fish would open the space between the pharyngeal jaws and abduct the lobe only enough to let the food inside the pharyngeal cavity proper, leaving the gross sediment particles in the oral cavity. Then, the fish would grab the food between the jaws and between the gill rakers along the posterior halves of ceratobranchials 1–4, expelling water through the mouth in order to get rid of the gross particles. Once undesired particles are out of the mouth, the fish can use pressure waves to pull the food back and forth, accommodating it where it can swallow them.

3.4 Discussion

3.4.1 Congruence between topologies

It is a long observed fact that morphological phylogenetic analyses frequently disagree among themselves at important points. The same is true when comparing morphological and molecular analyses. The phylogenetic relationships in the Cichlinae and, in particular, of the Geophagini, have been subject to important controversies. Some of these are the relationships of *Crenicichla* and *Retroculus* and the monophyly of a clade including geophagines bearing

an epibranchial 1 lobe. To Cichocki (1976), *Crenicichla* diverged from other Cichlinae quite early, at the very base of the clade. On the other hand, he recovered *Retroculus* deeply nested within the geophagines, which would include only the genera possessing an epibranchial 1 lobe. *Biotoecus* curiously appeared in a clade with *Acaronia* and *Chaetobranchus*, diverging immediately after *Crenicichla*. *Acarichthys* and *Crenicara* appear in a polytomy including the geophagines, *Astronotus* and numerous cichlasomatine terminal taxa.

Kullander (1998) notably found the composition of Geophagini to be quite similar to our present understanding of the tribe. An important divergence, however, is the hypothesised sisterhood between *Crenicichla* and *Cichla*, diverging from Neotropical cichlids close to the base of the tree. The internal arrangement of the geophagine taxa also differs a bit from the hypothesis by Ilves *et al*. (2017). Kullander found a clade similar to biotodomines, but including all lobed Geophagini (*i.e.*, also includes *Apistogramma* and *Satanoperca*). The remaining geophagines known to be orobranchial winnowers, *Acarichthys* and *Guianacara*, which do not have an epibranchial 1 lobe, nested together, as sister to a clade including dwarf geophagines, *Biotoecus* and crenicaratines. He also hypothesised *Retroculus* to have diverged prior to the clade formed by *Cichla* and *Crenicichla*.

Landim (2001) found neither *Crenicichla* nor *Retroculus* to be closely related to Geophagini. Within the tribe, she found two clades. One includes all orobranchial winnowers, with *Acarichthys* and *Guianacara* nested deep within, and *Mikrogeophagus* as sister to all other orobranchial winnowers. The other clade includes all dwarf geophagines, except *Mikrogeophagus*.

López-Fernández *et al*. (2005) presented the first morphological analysis to find *Crenicichla* within the Geophagini, but as sister to all other members of the tribe, instead of deeply nested within it. Interestingly, their morphological data alone was also able to recover the sisterhood between *Retroculus* and *Cichla*, confirmed later on by Ilves *et al*. (2017). The analysis by López-Fernández *et al*. (2005) differed from that of Cichocki (1976) and Kullander (1998) in finding a clade including the known geophagine orobranchial winnowers (except *Mikrogeophagus*, which they recovered as sister to a clade containing all the other dwarf geophagines), instead of grouping the taxa bearing an epibranchial 1 lobe.

Landim (2006) found *Retroculus* within Geophagini, as sister to all remaining members of the tribe. The clade including all geophagines, except *Retroculus*, included a clade with all dwarf geophagines, with *Crenicichla* nested deep within. The successive sister groups of this dwarf clade are the geophagine orobranchial winnowers.

In sum, previous morphological analyses tended to group taxa according to three putative biases: orobranchial winnowing, presence of an epibranchial 1 lobe and miniaturisation. That could explain why geophagines occasionally 'attracted' *Retroculus* and not *Crenicichla*. Our unweighted analysis presented the same biases, with two clades of dwarf geophagines closer to the base of the tree; a large clade including all taxa known to be orobranchial winnowers (except the dwarf *Mikrogeophagus*); and, within that clade, another one with taxa presenting a well-developed epibranchial 1 lobe. The analysis recovered *Crenicichla* and *Teleocichla* deep within the geophagines, recognising their close relationship to *Biotoecus*. The lobed geophagines did not attract *Retroculus*; otherwise, they would appear closer to the base of the tree. However, *Astronotus* and the cichlasomatines nested within the geophagines, an unexpected result.

In the weighted analysis, there was a greater attraction between dwarf cichlids, which clustered together in a single clade (except *Crenicara*), also including *Crenicichla* and *Teleocichla*. The analysis also found a clade including all known geophagine orobranchial winnowers, along with *Crenicara*. However, there is a considerable mixture between taxa with and without an epibranchial 1 lobe (see the position of *Acarichthys* and *Guianacara*). The weighted analysis, too, recovered the cichlasomatines among the geophagines. Concatenating our data with the morphological data by López-Fernández *et al*. (2005), with a resultant matrix of 238 characters, we obtained a tree in which the geophagines split into two clades. The first clade includes all orobranchial winnowers, except *Mikrogeophagus* (thus, largely overlapping with biotodomines, but including *Acarichthys*, *Guianacara* and *Satanoperca*). The other clade includes all dwarf geophagines, plus the *Crenicichla* clade and, at the base, *Mazarunia* as sister to *Bujurquina*. In fact, within the dwarf clade there is a group similar to the union of apistogrammines and crenicichlines, but lacking *Satanoperca* and *Acarichthys*, respectively.

All that considered, we conclude that, even with growing character matrices encompassing different data sources (muscles, bones, scales *etc*.), morphological analyses repeatedly resulted in topologies dominated by three aforementioned biases (winnowers, lobe-bearers and dwarves), with very low support for each node. Therefore, we believe that the obvious differences between the topologies derived from morphological and molecular studies make it a useless effort to produce 'total evidence' studies (*i.e.*, concatenating morphological and molecular matrices).

3.4.2 Adaptive characters

As observed by Drucker & Jensen (1991) for surfperches, we noticed that the putative oral winnowers analysed have a more generalised morphology, when compared to orobranchial winnowers. However, even the characters thought to be adaptations to orobranchial winnowing are heterogeneously distributed among fishes with that behaviour. Some of them seem to have reversed in members of biotodomines, which is evidence for their plasticity. Most of these characters are absent in *Retroculus*, which suggests that the Retroculini and Geophagini may have acquired different specialisations, or that *Retroculus*, despite being an orobranchial winnower, is less specialised than geophagines. The second hypothesis seems to be correct, because none of the character states unique to *Retroculus* (1[7], 14[1], 52[2] and 71[2]) reveal a function clearly related to winnowing.

Nonetheless, when compared to *Cichla*, its sister group, *Retroculus* clearly shows a few osteological changes in the same direction as the geophagines. The distance between the posterior margin of the sphenotic and the posterior margin of hyomandibula is shorter, the ventral portion of the suspensorium is somewhat inclined anteriorly, the clst 2 lies well ventral to clst 3, the vomer is long and arched, the mouth lies low in the head and the oral cavity is relatively deep. According to the analysis by López-Fernández *et al*. (2013), the lineage that gave rise to the Retroculini diverged from Cichlini a few million years after the Geophagini started to diversify. Perhaps the Retroculini were not efficient enough as orobranchial winnowers to compete with geophagines, and the clade remained restricted to a few species distributed in a relatively small area. In contrast, according to Říčan *et al.* (2016, Fig. 20) the Central American Heroini developed at least three clades of winnowers (*Cribroheros, Darienheros* and *Throrichthys*), in the absence of geophagine competitors. That reasoning, however, depends on whether orobranchial winnowing in geophagines developed several times (biotodomines, *Acarichthys*, *Guianacara* and *Satanoperca*) or only once, at the base of the geophagine tree. In the first scenario, orobranchial winnowing appeared four times within Geophagini: (1) in biotodomines, (2) in *Guianacara*, (3) in *Satanoperca* and (4) in *Acarichthys*. An alternative hypothesis is that the adaptations present in Geophagini appeared at the base of the clade, and posteriorly reversed in non-orobranchial winnowers. That hypothesis is about as likely as admitting four independent origins of orobranchial winnowing, because there are five clades in which that behaviour is unreported: (1) crenicaratines, (2) *Mazarunia*, (3) *Apistogramma* plus *Taeniacara*, (4) *Biotoecus* and (5) *Crenicichla* clade.

The presence of an epibranchial 1 lobe in all five subgroups of Geophagini (*i.e.*, those shown in Fig. 1) is a strong evidence that this structure appeared in a common ancestor of all members of the tribe, although the degree of development of the lobe is different among the taxa. However, even if we assume that this hypothesis is true, it is premature to consider it as proof that the ancestor of all geophagines was an orobranchial winnower for the following reasons. First, the adaptive importance of the lobe in oral and orobranchial winnowing was never studied, thus we cannot assume that only orobranchial winnowers take adaptive advantage of it. Second, *Acarichthys* and *Guianacara* (two orobranchial winnowers) lack the lobe, while *Crenicara* and *Dicrossus* (putative oral winnowers) have a rudimentary one, which poses the question: if the lobe has an important adaptive role in orobranchial winnowers, why is it absent in *Acarichthys* and *Guianacara*? Third, as stated before, our knowledge about the distribution of winnowing in geophagines is incomplete. If we can gather a substantial amount of observational data on this behaviour, perhaps some of the taxa believed to be oral winnowers will reveal to be orobranchial winnowers. Likewise, the frequency by which each species relies on that behaviour to feed may explain why some are morphologically more specialised than others.

Besides determining which species frequently resort to winnowing when foraging, there is a need for understanding in more detail how orobranchial winnowing happens. Cineradiography and electromyography, as performed by Drucker & Jensen (1991), could give us insight on how the fish separates food from substrate. However, we would need more accurate images, showing the movements of the whole branchial basket, and readings from the activity of different muscles, such as the *adductor branchialis 1* and the *obliquus ventralis 1*, both hypothesised herein to be important in orobranchial winnowing.

3.5 Conclusion

Our study succeeded in finding a number of myological characters never described before in cichlids. Ecologically specialised forms, such as *Satanoperca* and *Chaetobranchopsis*, for instance, revealed a much higher amount of synapomorphies, when compared to generalised forms. Our phylogenetic analyses disagree largely from the molecular study of Ilves *et al*. (2017), as do all other morphological analyses. Given that all morphological analyses disagree largely among themselves too, but with repeating patterns, we conclude that they suffer from biases related to miniaturisation and feeding specialisation. We believe this is an intrinsic problem of morphological phylogenetic analyses because convergence towards ecological

specialisations is very common in phenotypic characters (and not in molecular ones). Therefore, we recommend that phylogeneticists focus their attention in improving the techniques employed to recover phylogenies from molecular data in order to obtain more reliable hypotheses of relationships. If this is accomplished, morphology will become increasingly important as a means of understanding important phenomena in evolution, such as adaptive radiation. By mapping our myological characters on the tree by Ilves *et al*. (2017), we were able to detect several characters probably related to a specialisation towards orobranchial winnowing. Although some of them seem to be inevitable consequences of osteological changes, others appear to be unrelated to them. More studies will be necessary to determine how many times in geophagine evolution orobranchial winnowing and morphological characters related to this behaviour came to existence.

REFERENCES

Albertson RC, Markert JA, Danley PD, Kocher TD. 1999. Phylogeny of a rapidly evolving clade: The cichlid fishes of Lake Malawi, East Africa. *Proceedings of the National Academy of Sciences* 96: 5107–5110.

Anker GC. 1978. The morphology of the head-muscles of a generalized *Haplochromis* species: *H. elegans* Trewavas 1933 (Pisces, Cichlidae). *Netherlands Journal of Zoology* 28: 234–271.

Anker GC. 1986. The morphology of joints and ligaments in the head of a generalized *Haplochromis* species: *H. elegans* Trewavas 1933 (Teleostei, Cichlidae). I. The infraorbital apparatus and the suspensorial apparatus. *Netherlands Journal of Zoology* 36: 498–530.

Anker GC. 1989. The morphology of joints and ligaments in the head of a generalized *Haplochromis* species: *H. elegans* Trewavas 1933 (Teleostei, Cichlidae). III. The hyoid and the branchiostegal apparatus, the branchial apparatus and the shoulder girdle apparatus. *Netherlands Journal of Zoology* 39: 1–40.

Arbour JH, López-Fernández H. 2013. Ecological variation in South American geophagine cichlids arose during an early burst of adaptive morphological and functional evolution. *Proceedings of the Royal Society B* 280: 20130849.

Arbour J, López-Fernández H. 2018. Intrinsic constraints on the diversification of Neotropical cichlid *adductor mandibulae* size. *The Anatomical Record* 301: 216–226.

Barel CDN, Witte F, van Oijen MJP. 1976. The shape of the skeletal elements in the head of a generalized *Haplochromis* species: *H. elegans* Trewavas 1933 (Pisces, Cichlidae). *Netherlands Journal of Zoology* 26: 163–265.

Betancur-R. R, Broughton RE, Wiley RO, Carpenter K, López JA, Li C, *et al*. 2013. The tree of life and a new classification of bony fishes. *PLoS Currents Tree of Life*.

Castoe TA, Jason de Koning AP, Hyun-Min Kim, Wanjun Gu, Noonan BP, Naylor G, Zhi J. Jiang, Parkinson CL, Pollock DD. 2009. Evidence for an ancient adaptive episode of convergent molecular evolution. *Proceedings of the National Academy of Sciences* 106: 8986–8991.

Cichocki FP. 1976. Cladistic history of cichlid fishes and reproductive strategies of the American genera *Acarichthys*, *Biotodoma* and *Geophagus*. Unpublished D. Phil. Thesis, The University of Michigan.

Datovo A, Bockmann FA. 2010. Dorsolateral head muscles of the catfish families Nematogenyidae and Trichomycteridae (Siluriformes: Loricarioidei): comparative anatomy and phylogenetic analysis. *Neotropical Ichthyology* 8: 193–246.

Drucker EG, Jensen JS. 1991. Functional analysis of a specialized prey processing behavior: winnowing by surfperches (Teleostei: Embiotocidae). *Journal of Morphology* 210: 267–287.

Goloboff PA, Farris JS, Nixon KC. 2008. TNT, a free program for phylogenetic analysis. *Cladistics* 24: 774–786.

Ilves KL, Torti D, López-Fernández H. 2017. Exon-based phylogenomics strengthens the phylogeny of Neotropical cichlids and identifies remaining conflicting clades (Cichliformes: Cichlidae: Cichlinae). *Molecular Phylogenetics and Evolution* 118: 232–243.

Kullander SO. 1983. *A review of the South American cichlid genus* Cichlasoma. Stockholm: Swedish Museum of Natural History.

Kullander SO. 1986. *Cichlid fishes of the Amazon River drainage of Peru*. Stockholm: Swedish Museum of Natural History.

Kullander SO. 1989. *Biotoecus* Eigenmann and Kennedy (Teleostei: Cichlidae): description of a new species from the Orinoco basin and revised generic diagnosis. *Journal of Natural History* 23: 225–260.

Kullander SO. 1998. A phylogeny and classification of the South American Cichlidae (Teleostei: Perciformes). In: Malabarba LR, Reis RE, Vari RP, Lucena ZM, Lucena CAS, eds. *Phylogeny and classification of Neotropical fishes*. Porto Alegre: Edipucrs, 461–498.

Landim MI. 2001. Relações filogenéticas na subfamília Geophaginae Haseman (Perciformes, Cichlidae). Unpublished Masters dissertation, Universidade Federal do Rio de Janeiro.

Landim MIPF. 2006. Relações filogenéticas na família Cichlidae Bonaparte, 1840 (Teleostei: Perciformes). Unpublished D. Phil. Thesis, Universidade de São Paulo.

Liem KF. 1986. The pharyngeal jaw apparatus of the Embiotocidae (Teleostei): a functional and evolutionary perspective. *Copeia* 1986: 311–323.

López-Fernández H, Arbour JH, Winemiller KO, Honeycutt RL. 2013. Testing for ancient adaptive radiations in Neotropical cichlid fishes. *Evolution* 67: 1321–1337.

López-Fernández H, Honeycutt RL, Stiassny MLJ, Winemiller KO. 2005. Morphology, molecules, and character congruence in the phylogeny of South American geophagine cichlids (Perciformes, Labroidei). *Zoologica Scripta*, 34: 627–651.

López-Fernández H, Winemiller KO, Montaña C, Honeycutt RL. 2012. Diet-morphology correlations in the radiation of South American geophagine cichlids (Perciformes: Cichlidae: Cichlinae). *PLoS One* 7: e33997.

Říčan O, Piálek L, Dragová K, Novák J. 2016. Diversity and evolution of the Middle American cichlid fishes (Teleostei: Cichlidae) with revised classification. *Vertebrate Zoology* 66: 1–102.

Říčan O, Piálek L, Zardoya R, Doadrio I, Zrzavý. 2013. Biogeography of the Mesoamerican Cichlidae (Teleostei: Heroini): colonization through the GAARlandia land bridge and early diversification. *Journal of Biogeography* 40: 579–593.

Springer VG, Johnson GD. 2004. Study of the dorsal gill-arch musculature of the teleostome fishes, with special reference to the Actinopterygii. *Bulletin of the Biological Society of Washington* 11: 1–260.

Weller HI, McMahan CD, Westneat MW. 2016. Dirt-sifting devilfish: winnowing in the geophagine cichlid *Satanoperca daemon* and evolutionary implications. *Zoomorphology* 136: 45–59.

Winterbottom R. 1974. A descriptive synonymy of the striated muscles of the Teleostei. *Proceedings of the Academy of Natural Sciences of Philadelphia* 125: 225–317.

FIGURE LEGENDS

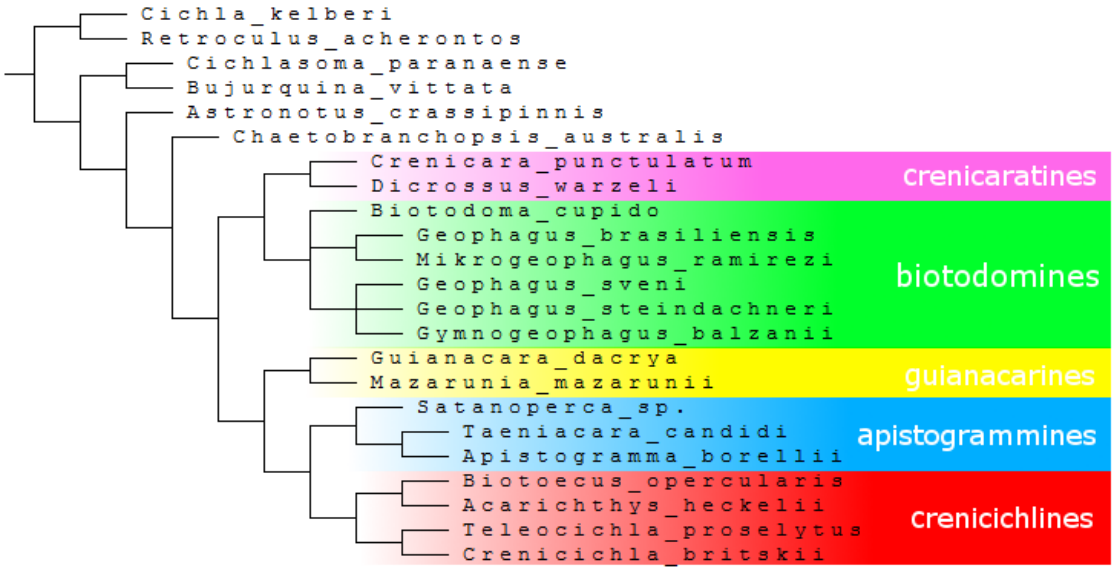

Fig. 1. Taxa analysed herein arranged in a topology following Ilves *et al*. (2017), in which polytomies represent collapsed clades with low support. Shaded clades represent the five subgroups recognised within Geophagini. The biotodomines correspond to the union of the geophagines and mikrogeophagines *sensu* Ilves *et al*. (2017, Fig. 1).

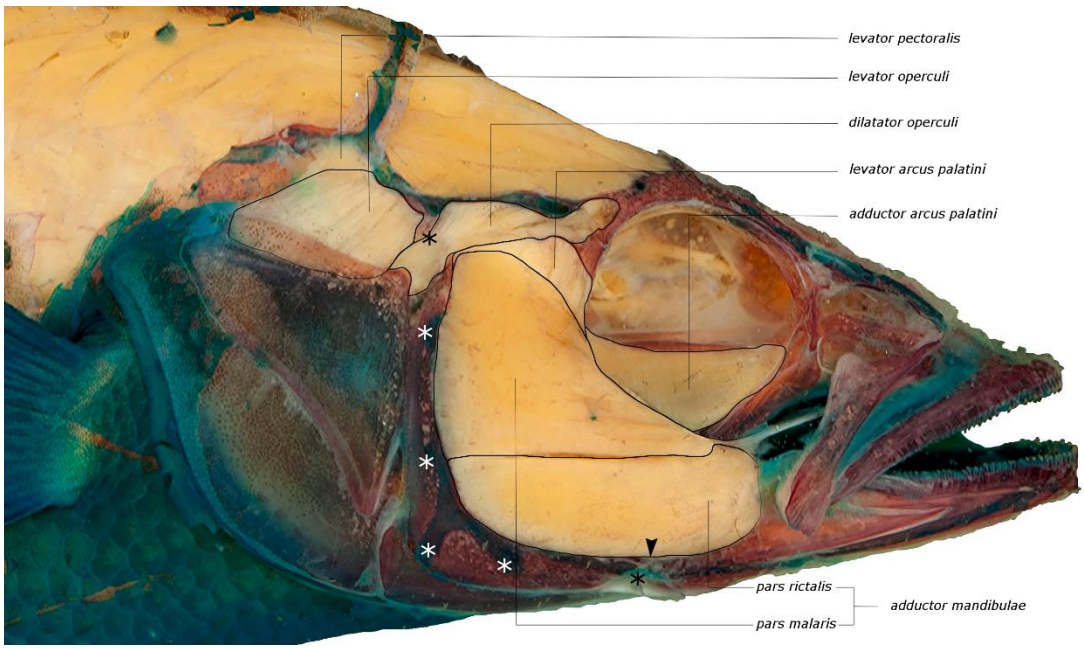

Fig. 2. Lateral view of the head of *Crenicichla britskii* (dissection stage 1A), evidencing the muscles of the cheek.

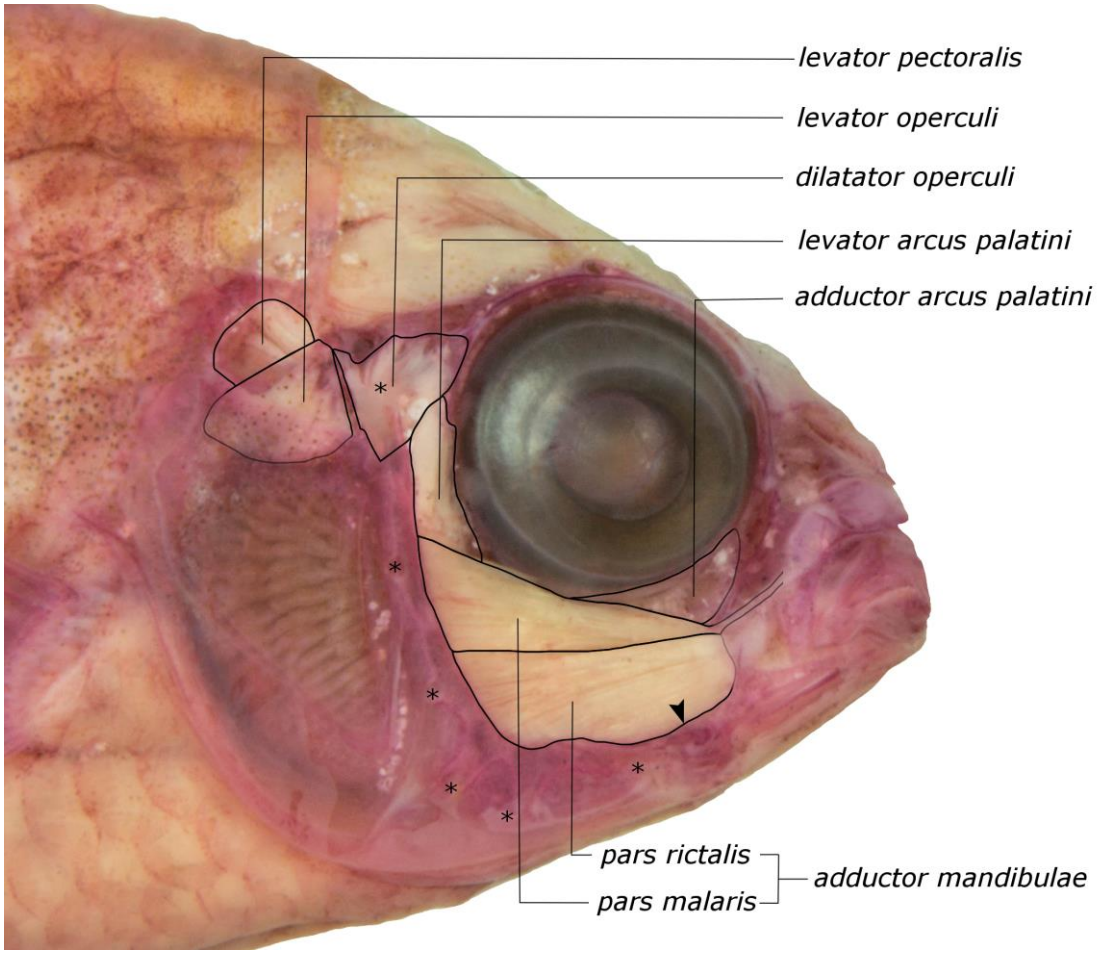

Fig. 3. Lateral view of the head of *Mikrogeophagus ramirezi* (dissection stage 1A), evidencing the muscles of the cheek.

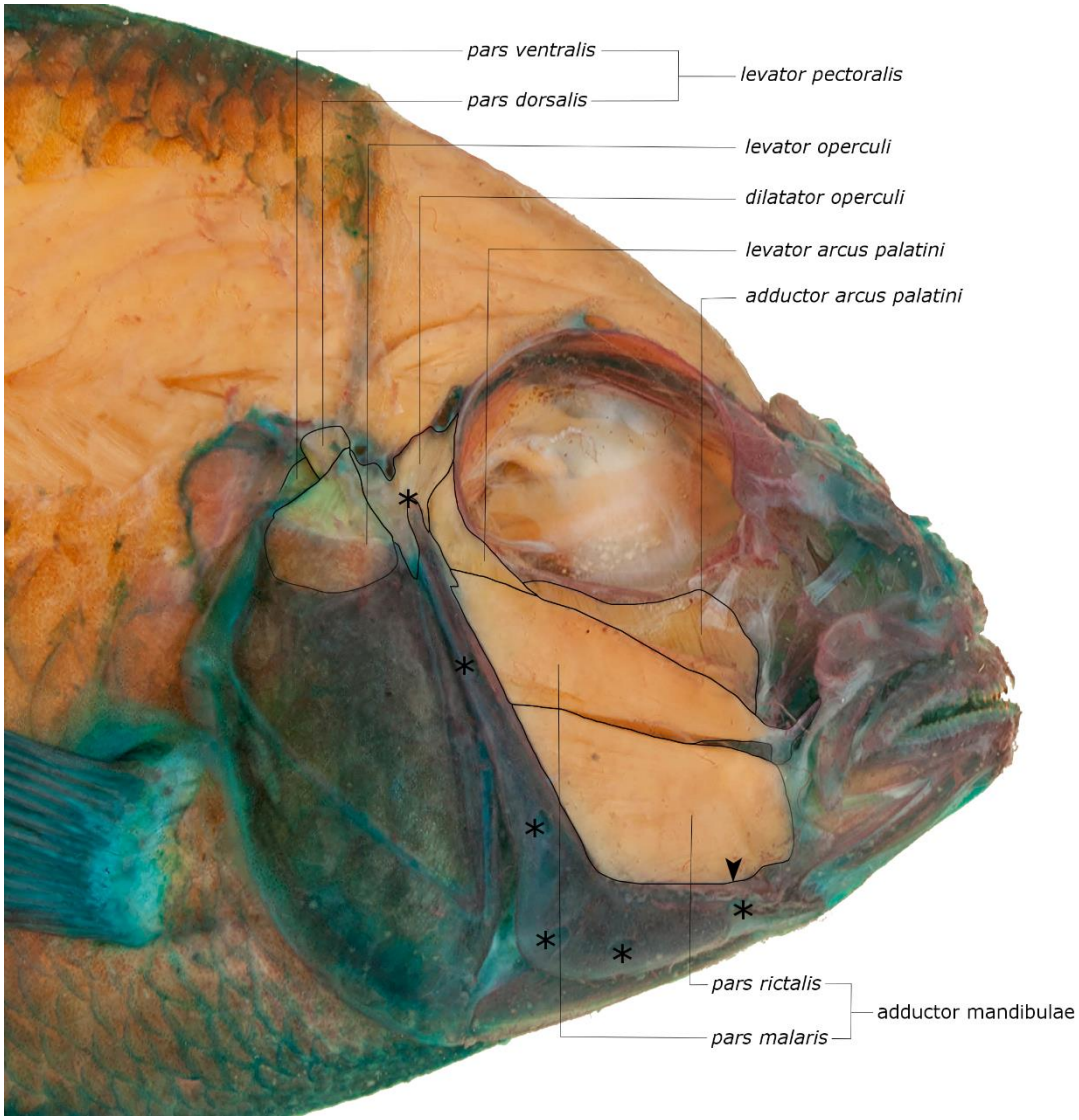

Fig. 4. Lateral view of the head of *Acarichthys heckelii* (dissection stage 1A), evidencing the muscles of the cheek.

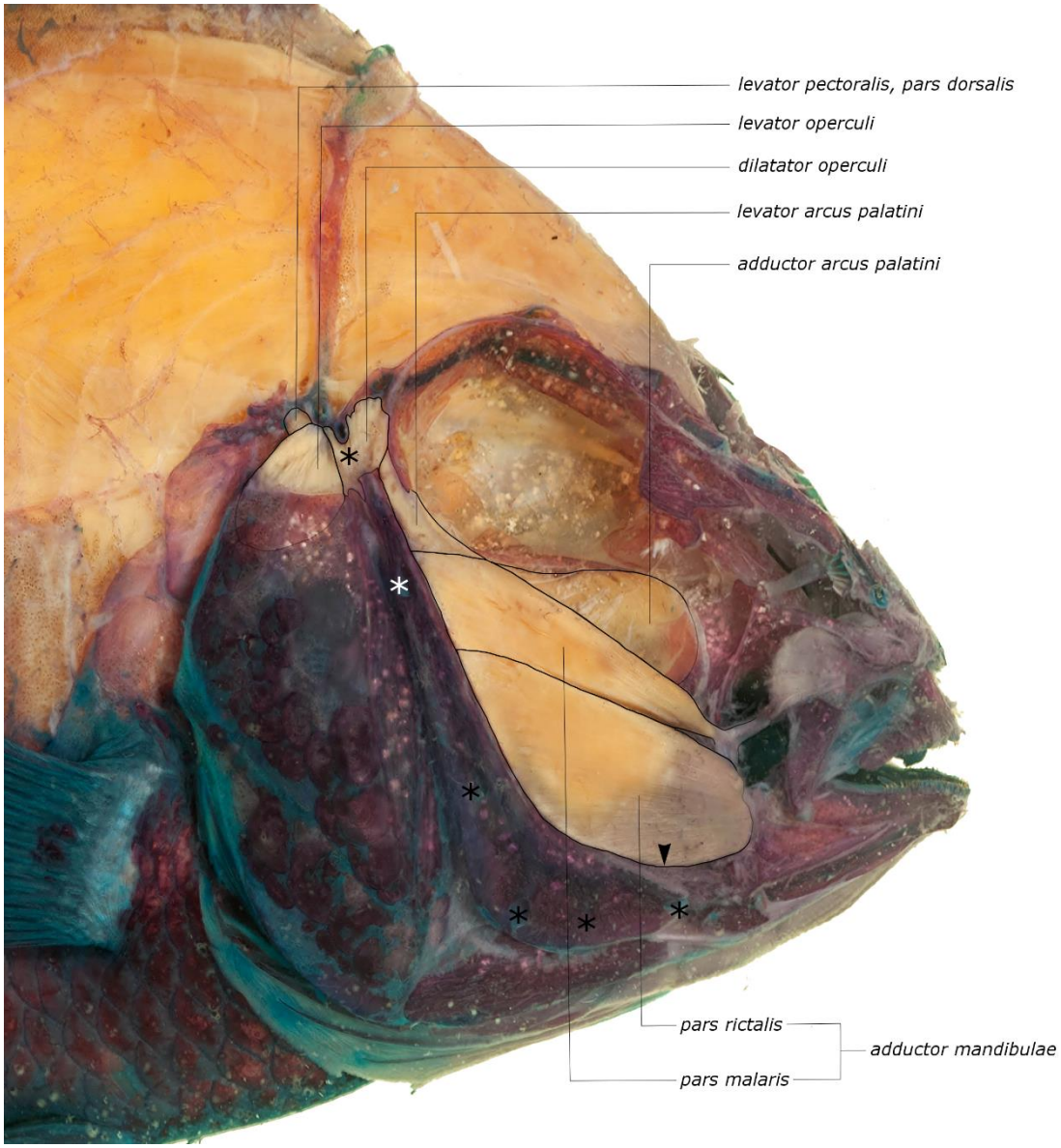

Fig. 5. Lateral view of the head of *Gymnogeophagus balzanii* (dissection stage 1A), evidencing the muscles of the cheek.

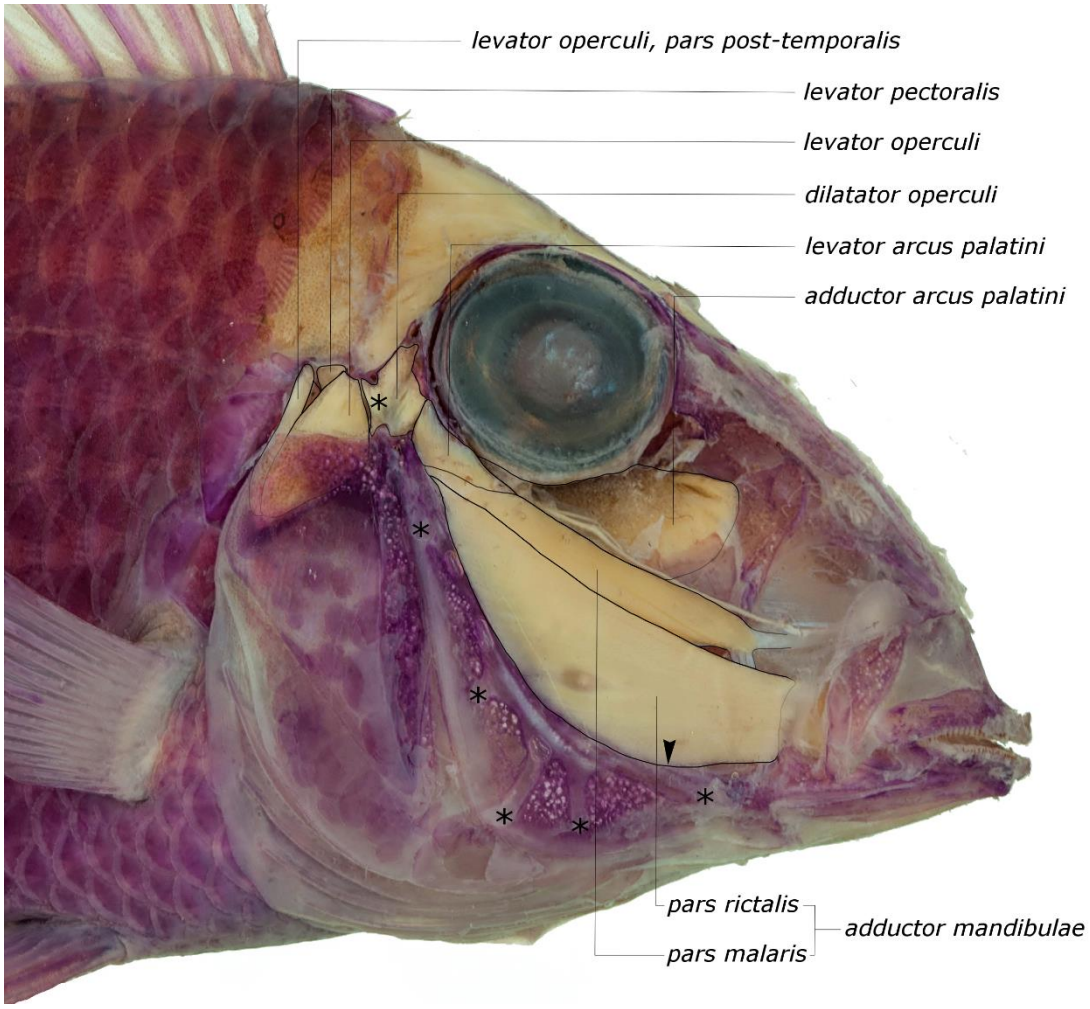

Fig. 6. Lateral view of the head of *Satanoperca* sp. (dissection stage 1A), evidencing the muscles of the cheek.

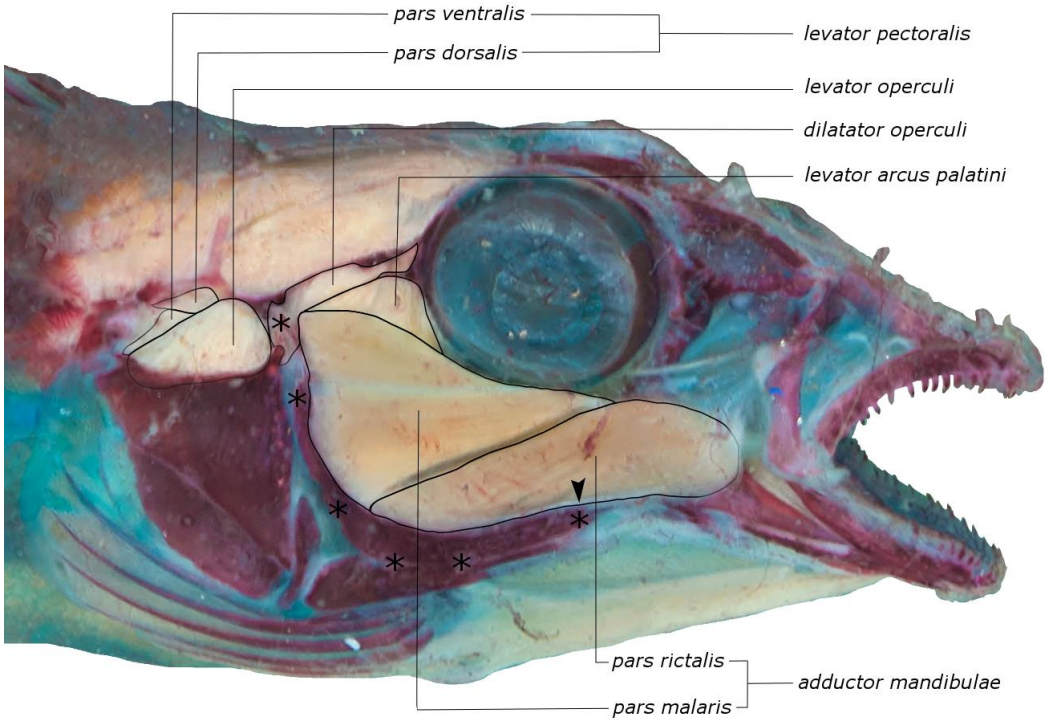

Fig. 7. Lateral view of the head of *Teleocichla proselytus* (dissection stage 1A), evidencing the muscles of the cheek.

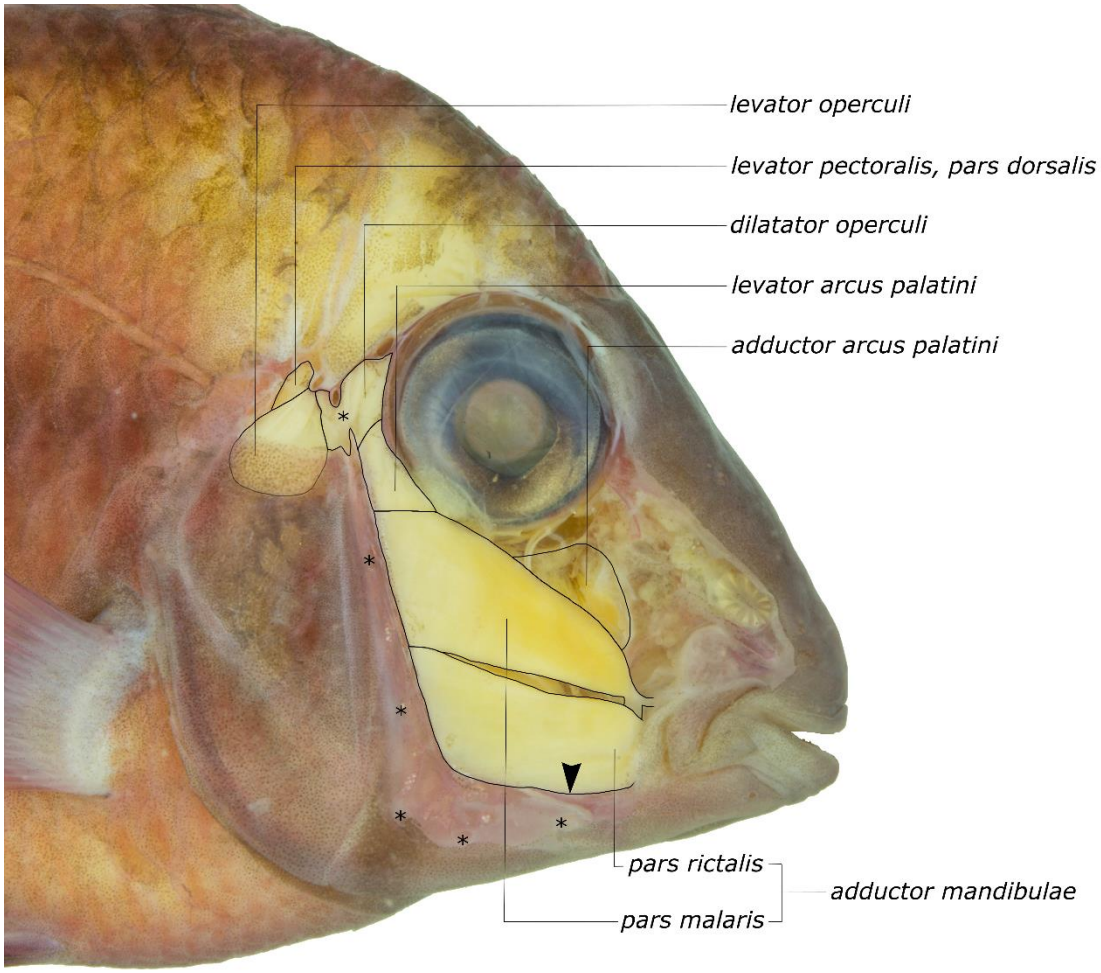

Fig. 8. Lateral view of the head of *Guianacara dacrya* (dissection stage 1A), evidencing the muscles of the cheek.

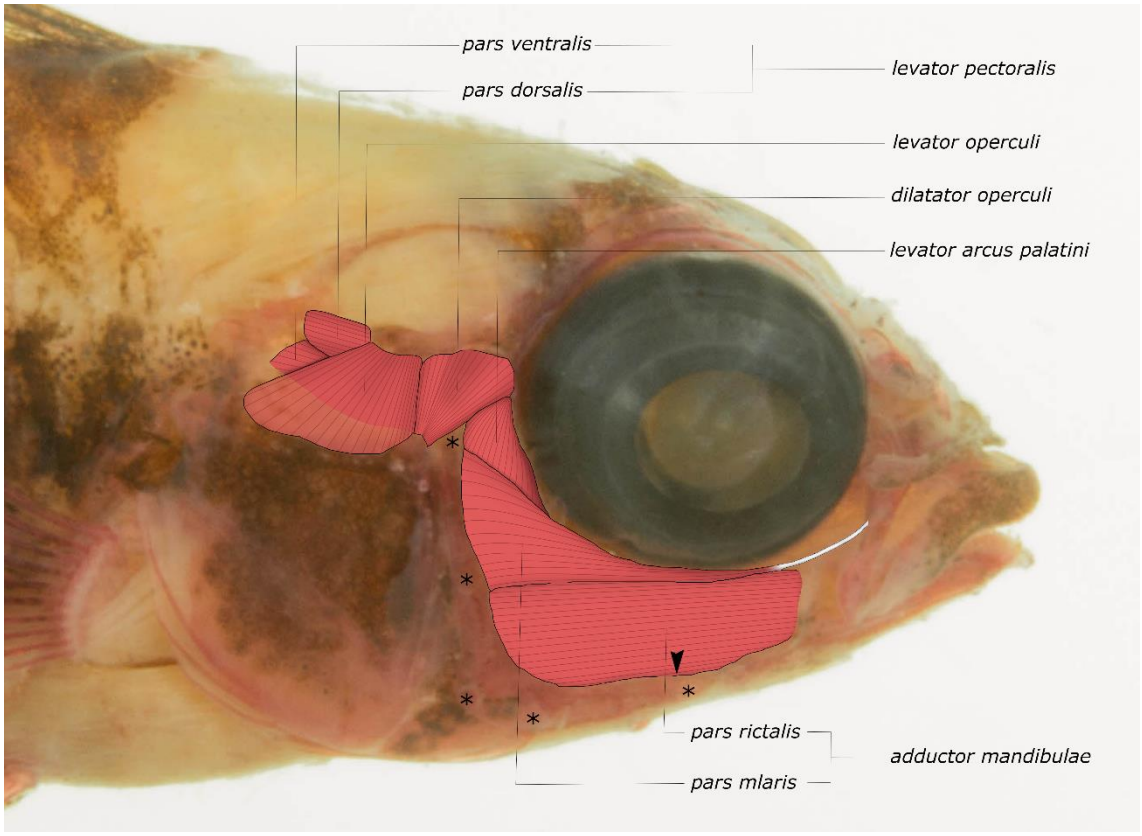

Fig. 9. Lateral view of the head of *Taeniacara candidi* (dissection stage 1A), evidencing the muscles of the cheek.

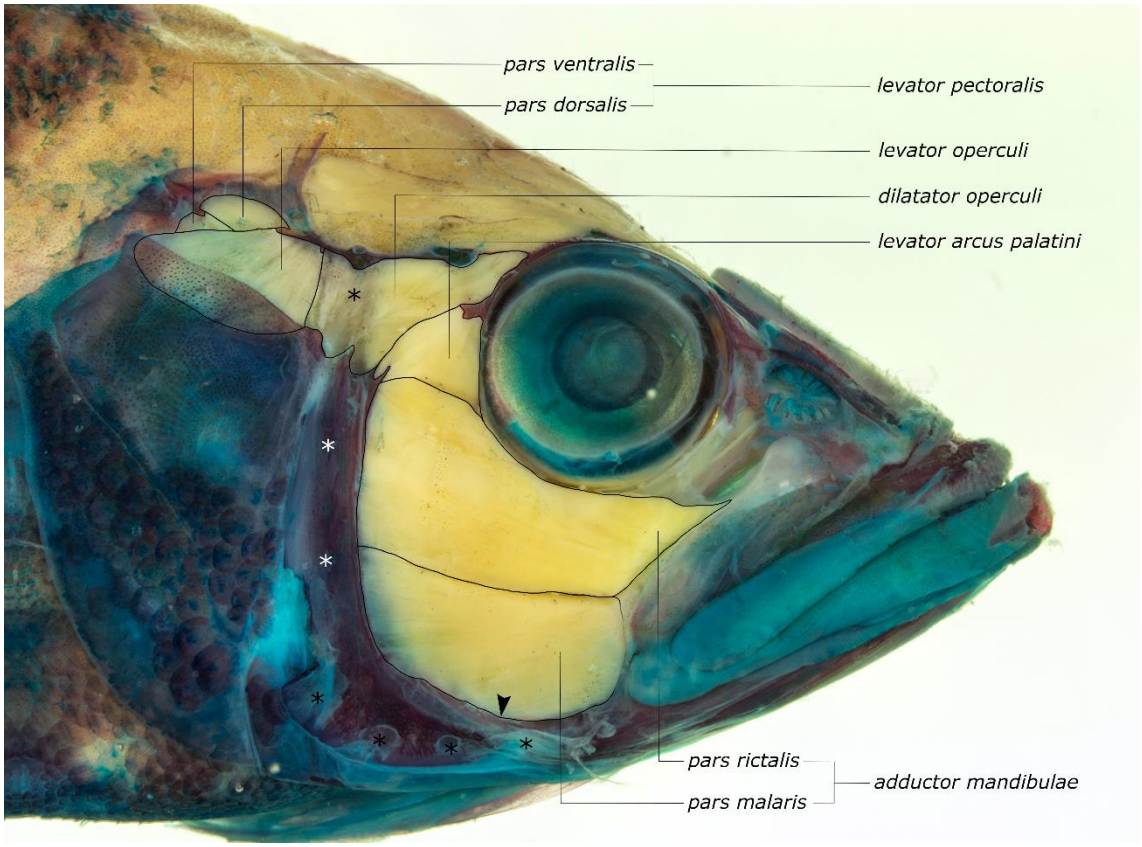

Fig. 10. Lateral view of the head of *Cichla kelberi* (dissection stage 1A), evidencing the muscles of the cheek.

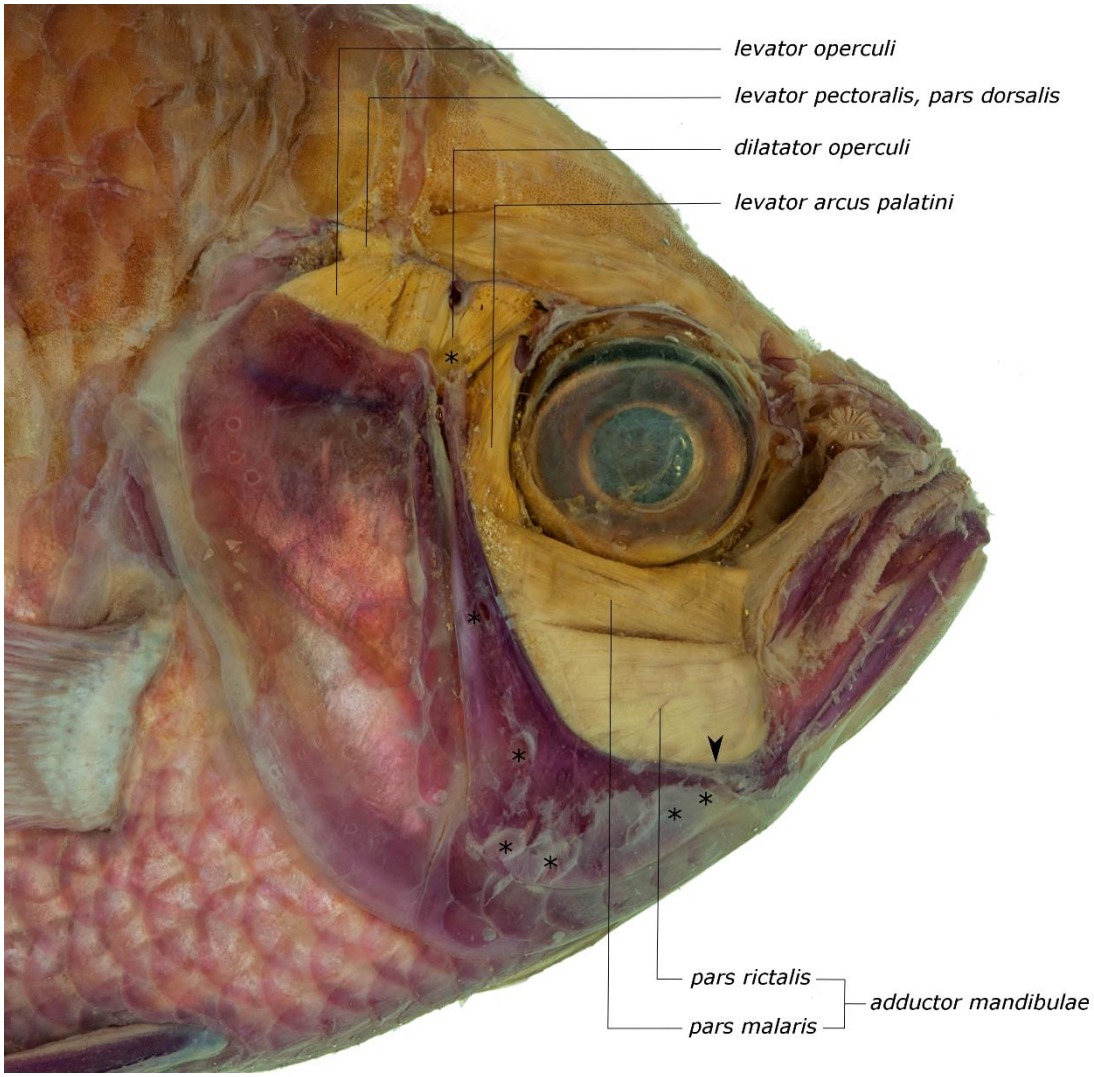

Fig. 11. Lateral view of the head of *Chaetobranchopsis australis* (dissection stage 1A), evidencing the muscles of the cheek.

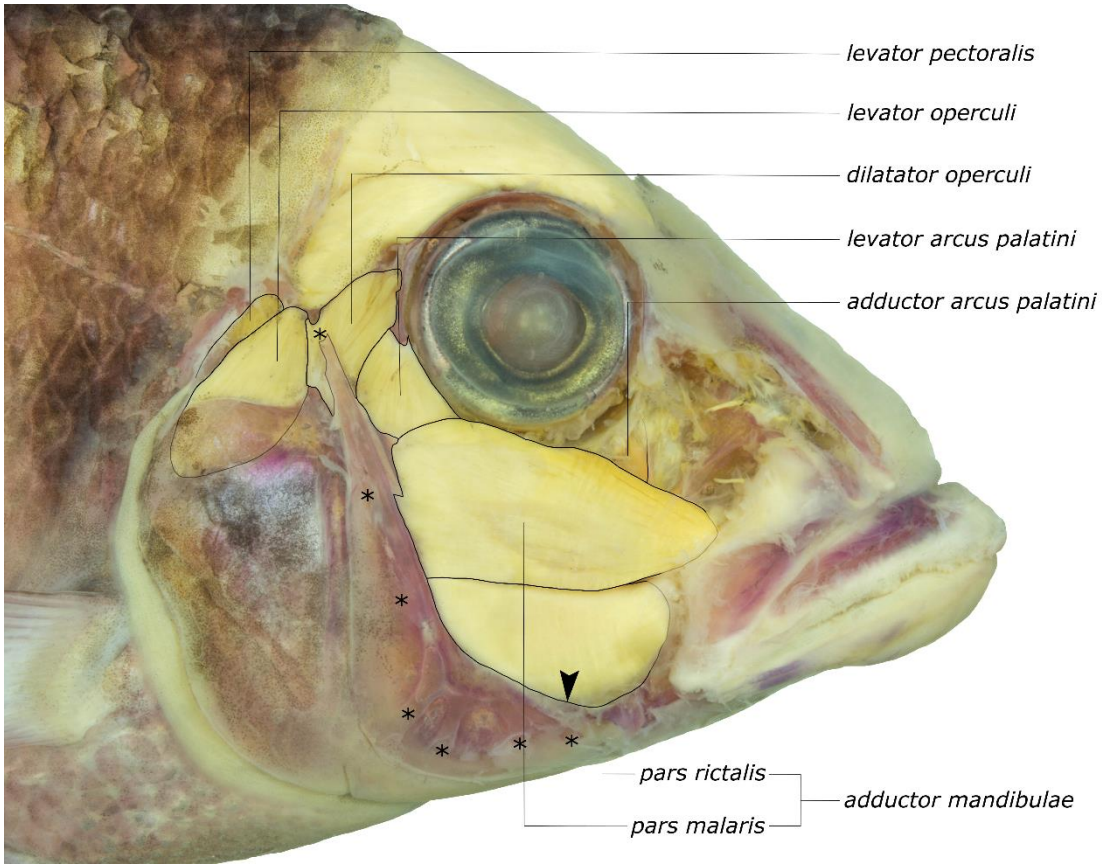

Fig. 12. Lateral view of the head of *Retroculus acherontos* (dissection stage 1A), evidencing the muscles of the cheek.

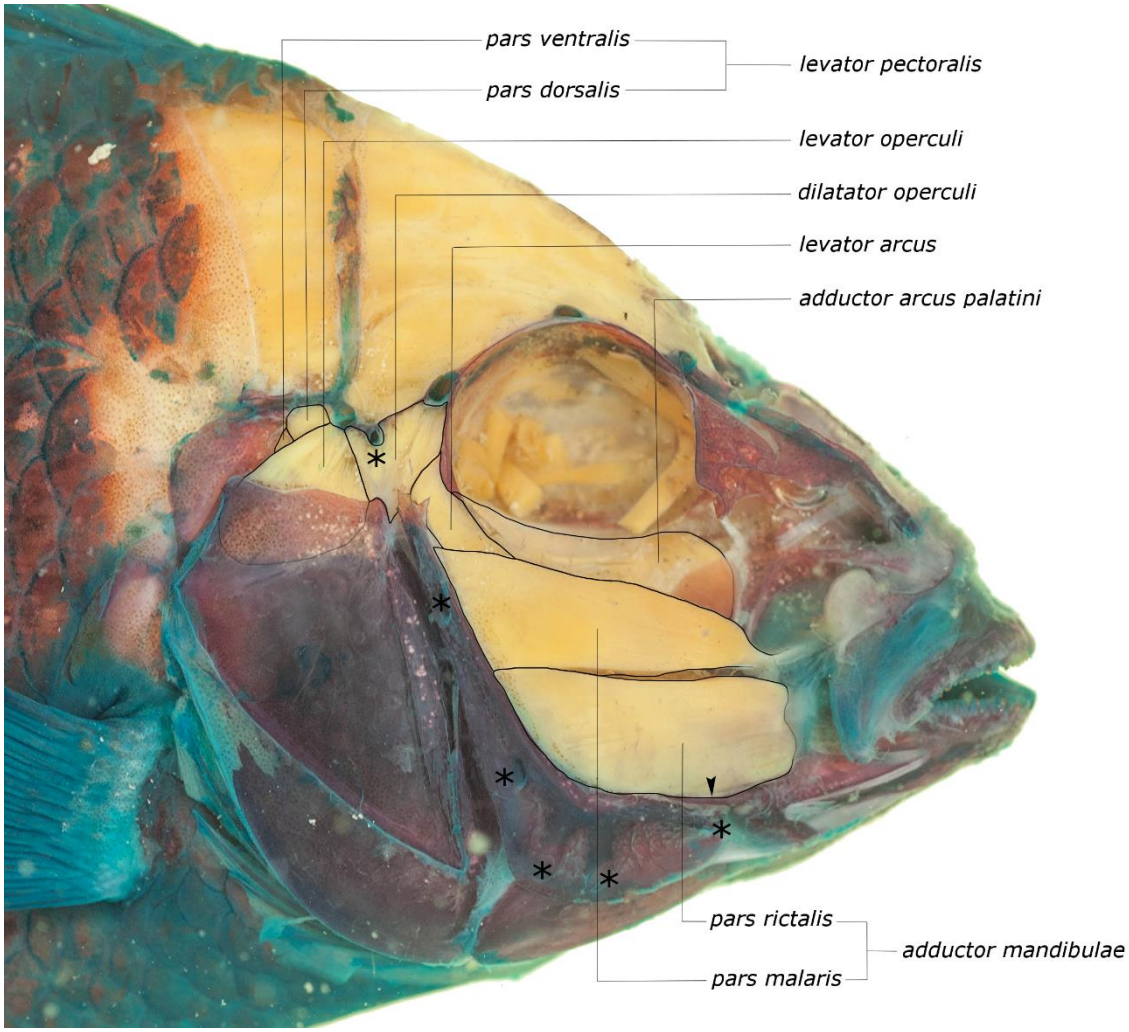

Fig. 13. Lateral view of the head of **"***Geophagus*" *brasiliensis* (dissection stage 1A), evidencing the muscles of the cheek.

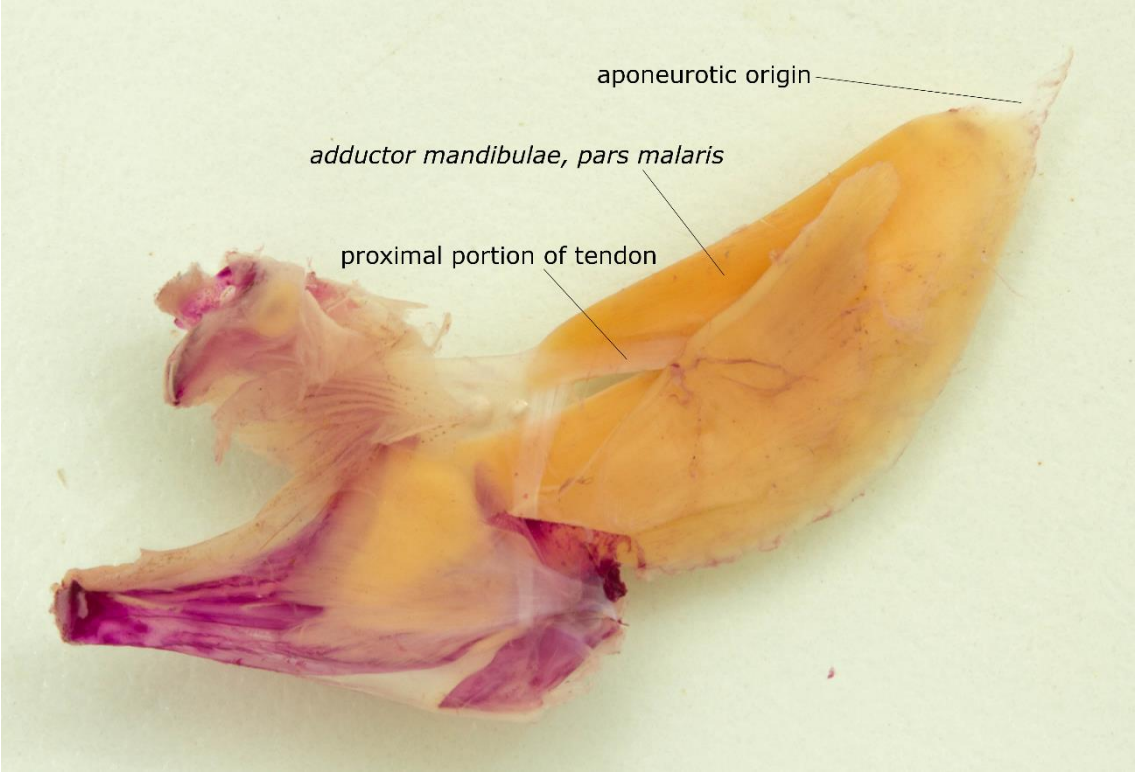

Fig. 14. Medial view of right lower jaw and maxilla, with associated *adductor mandibulae*, of *Satanoperca* sp. (dissection stage 2A).

Fig. 15. Medial view of right lower jaw and maxilla, with associated *adductor mandibulae*, of *Crenicichla britskii* (dissection stage 2A).

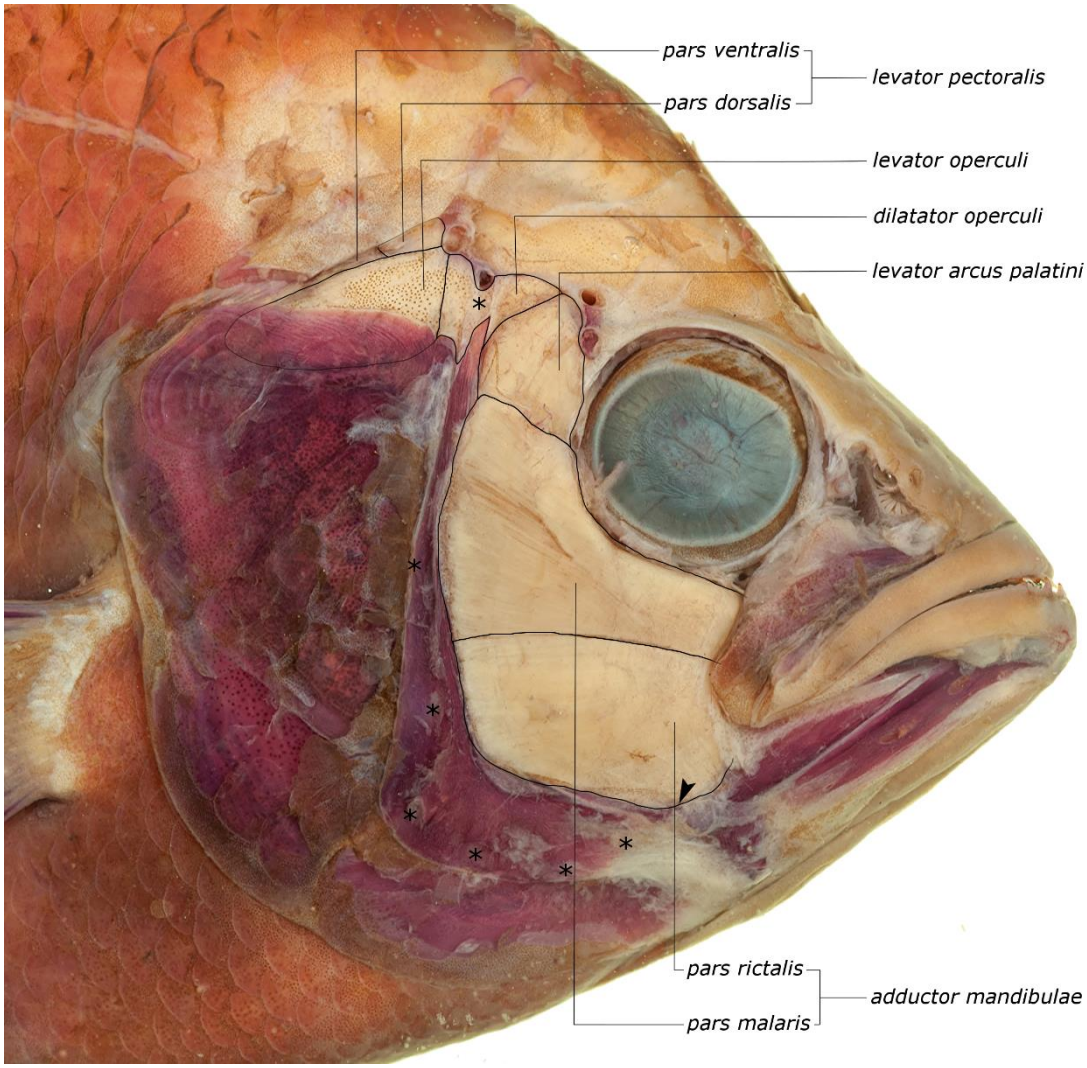

Fig. 16. Lateral view of the head of *Astronotus crassipinnis* (dissection stage 1A), evidencing the muscles of the cheek.

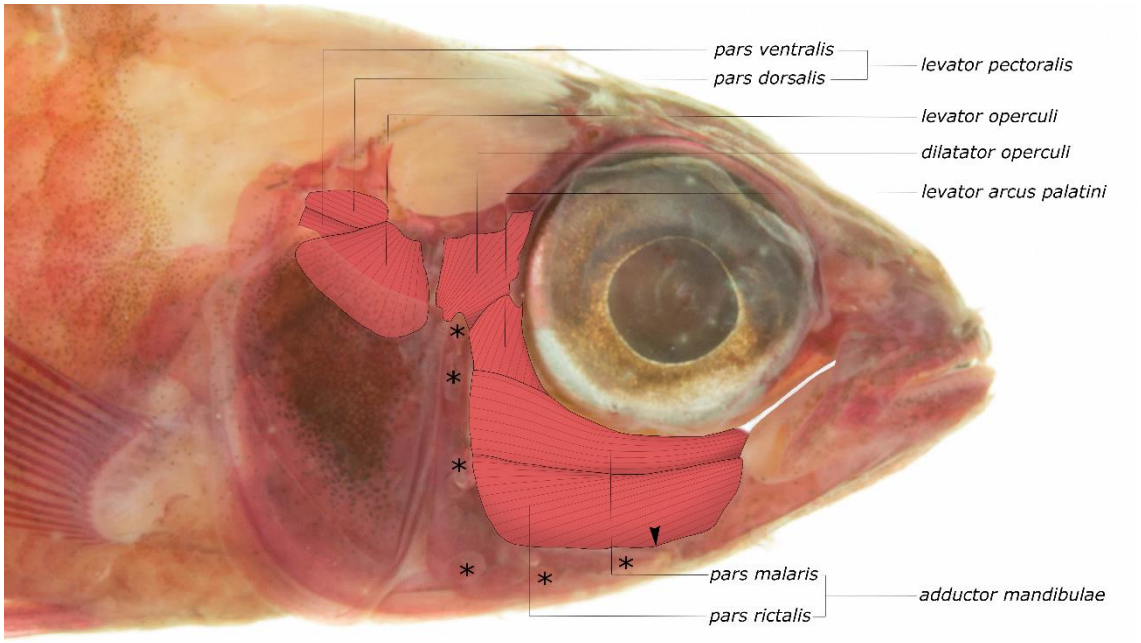

Fig. 17. Lateral view of the head of *Biotoecus opercularis* (dissection stage 1A), evidencing the muscles of the cheek.

Fig. 18. Lateral view of the head of *Crenicichla britskii* (dissection stage 1B), evidencing the insertion of the *levator arcus palatini*.

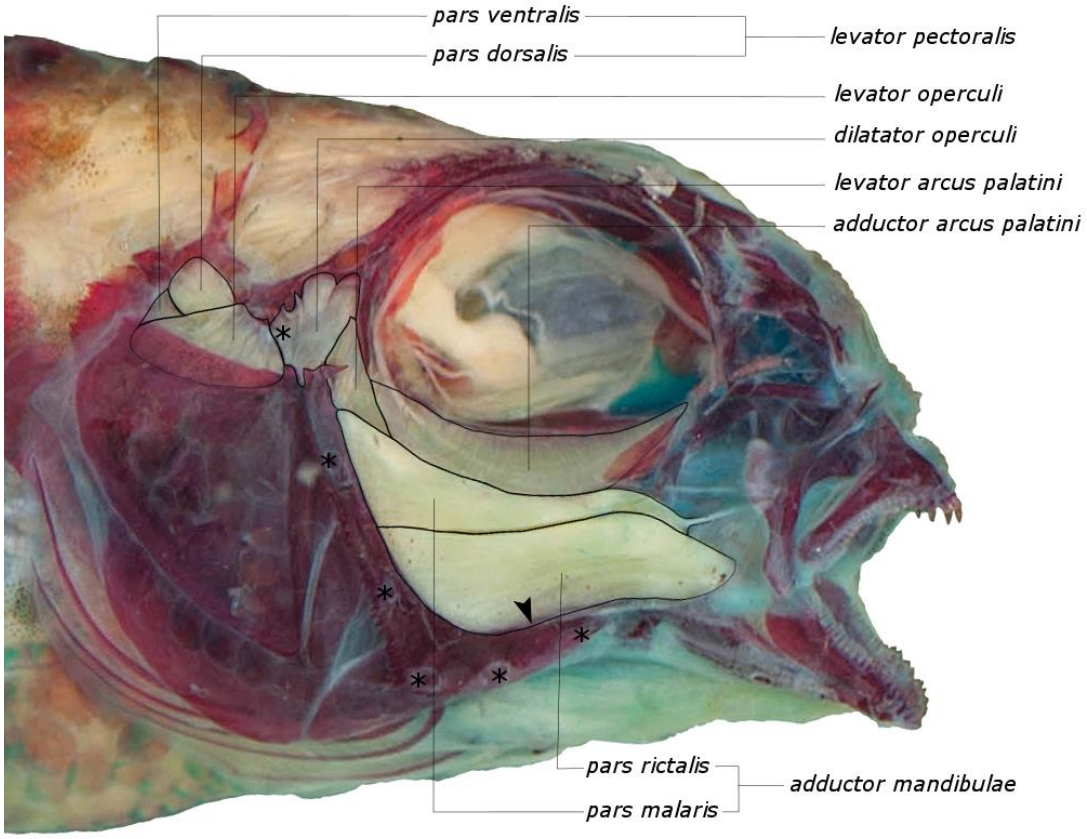

Fig. 19. Lateral view of the head of *Dicrossus warzeli* (dissection stage 1A), evidencing the muscles of the cheek.

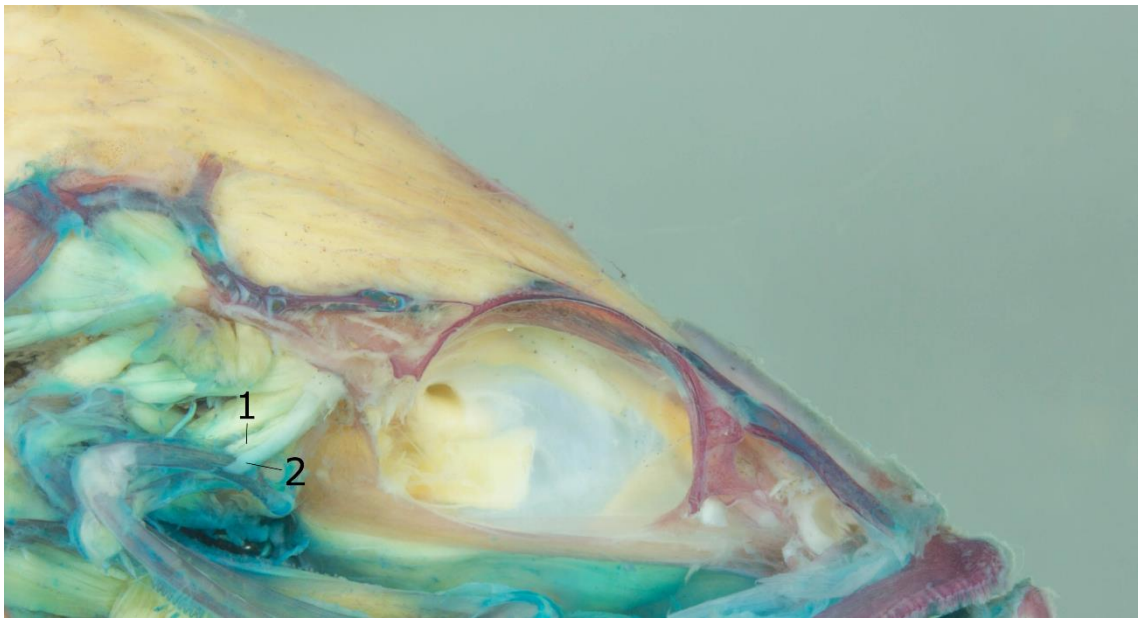

Fig. 20. Lateral view of the head of *Cichla kelberi* (dissection stage 3), evidencing (1) the *levator externus 1* and (2) the ligament parallel to it (character 39[1]).

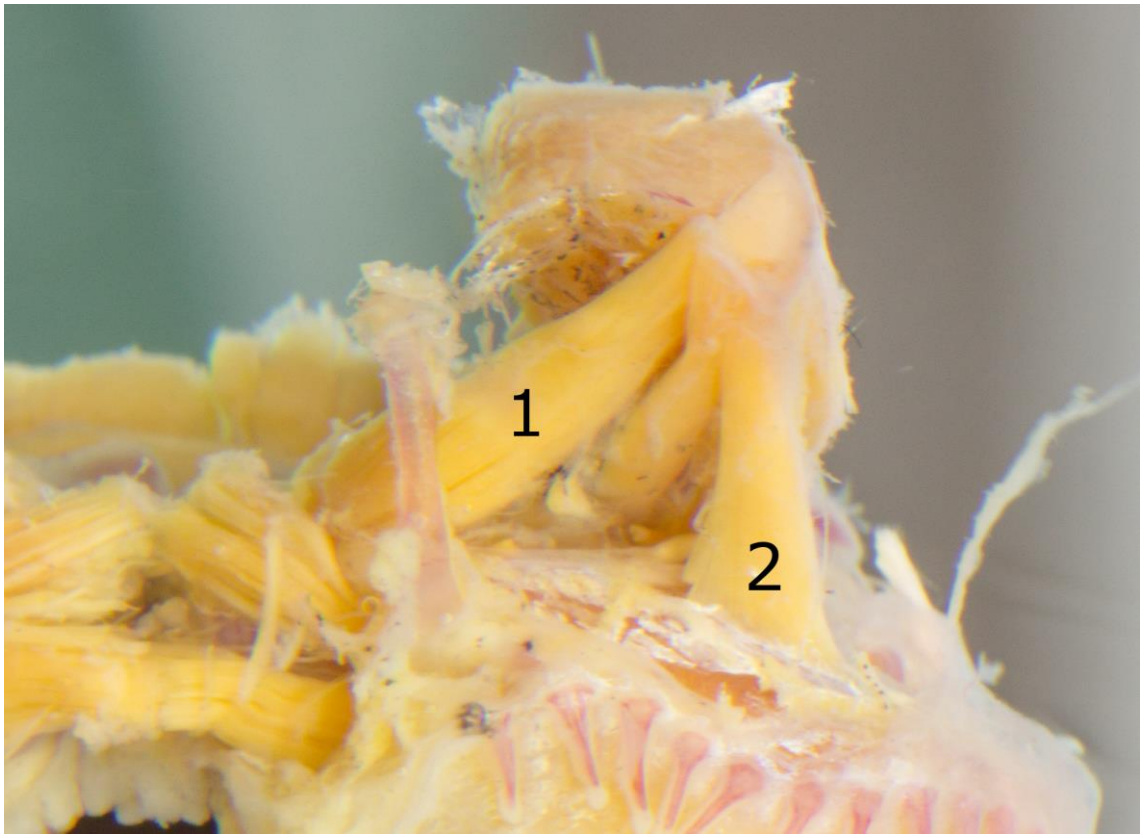

Fig. 21. Anterior view of dorsal portion of branchial basket and associated muscles of *Retroculus acherontos* (dissection stage 4A; left side), evidencing the similar thickness of (1) *levator internus 1* and (2) *levator externus 1* (Character 40[0]).

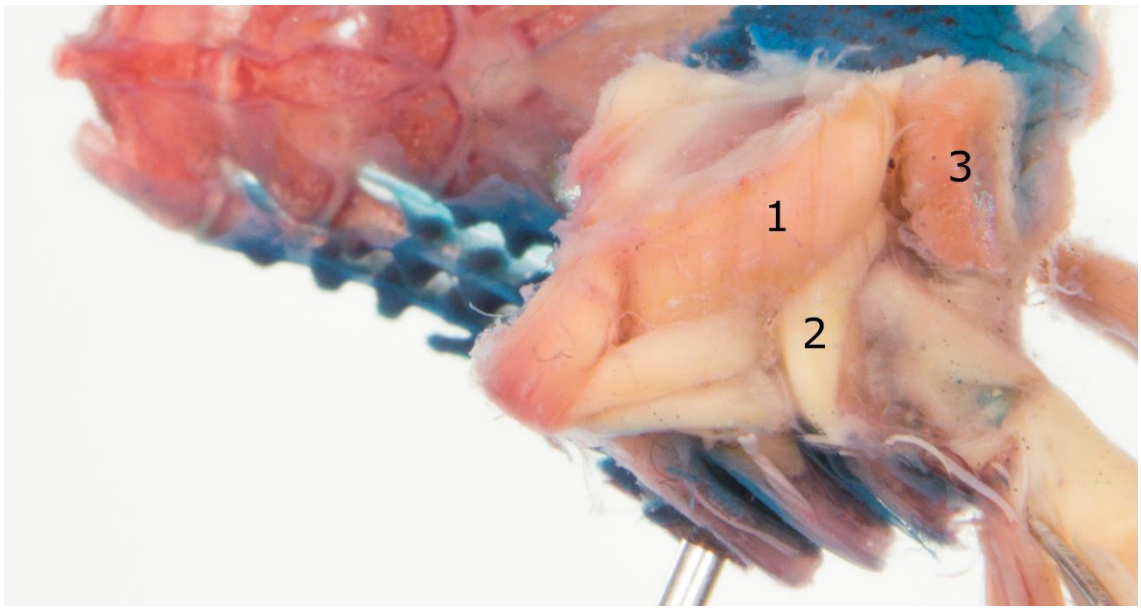

Fig. 22. Dorsal view of branchial basket and associated muscles of *Crenicichla britskii* (dissection stage 4A; left side), evidencing the shape of (1) *transversus epibranchialis 2*, (2) *obliquus dorsalis 3–4* and (3) *retractor dorsalis*. *Levator internus 5* pulled aside.

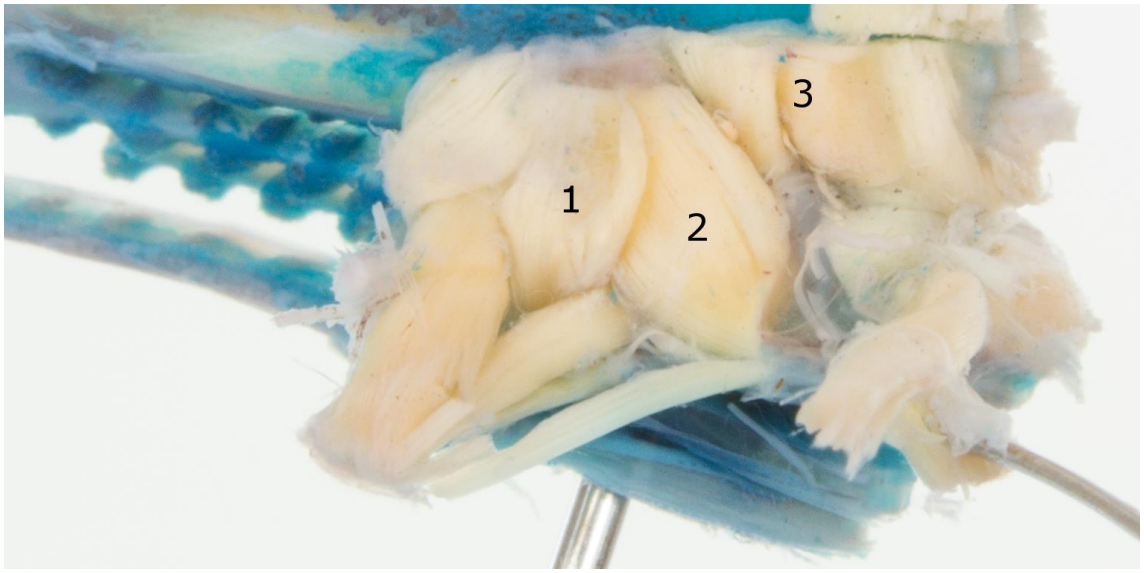

Fig. 23. Dorsal view of branchial basket and associated muscles of *Cichla kelberi* (dissection stage 4A; left side), evidencing the shape of (1) *transversus epibranchialis 2*, (2) *obliquus dorsalis 3–4* and (3) *retractor dorsalis*. *Levator internus 5* pulled aside.

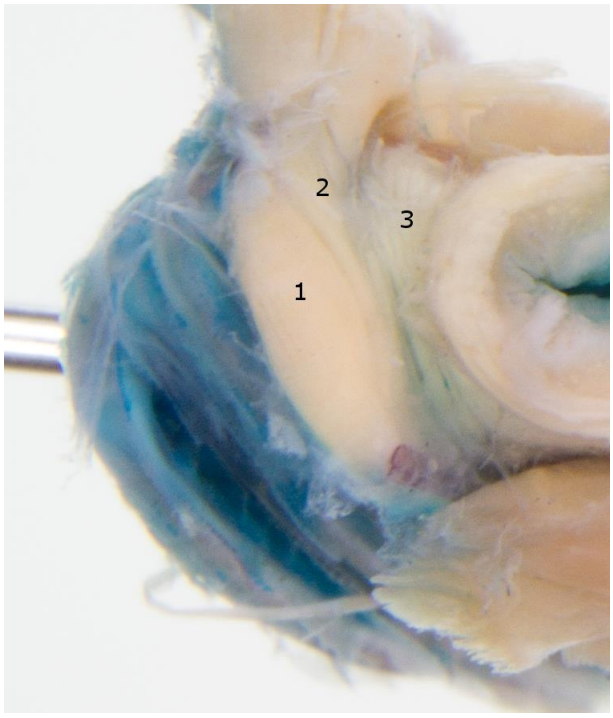

Fig. 24. Posterior view of branchial basket and associated muscles of *Cichla kelberi* (dissection stage 4A; left side), evidencing the shape of (1) *adductor branchialis 5*; (2) *obliquus posterior 2* and (3) *obliquus posterior 4*.

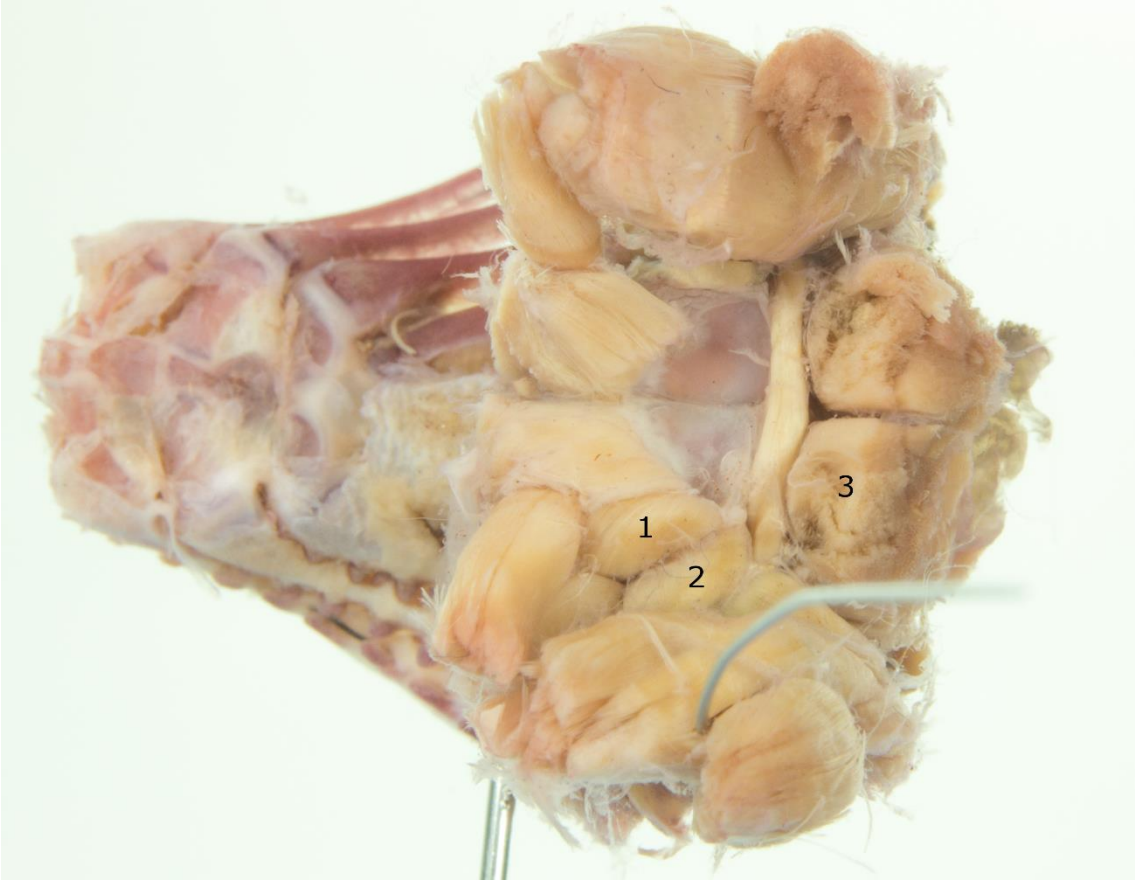

Fig. 25. Dorsal view of branchial basket and associated muscles of *Astronotus crassipinnis* (dissection stage 4A), evidencing the shape of (1) *transversus epibranchialis 2*, (2) *obliquus dorsalis 3–4* and (3) *retractor dorsalis*. *Levator internus 5* pulled aside.

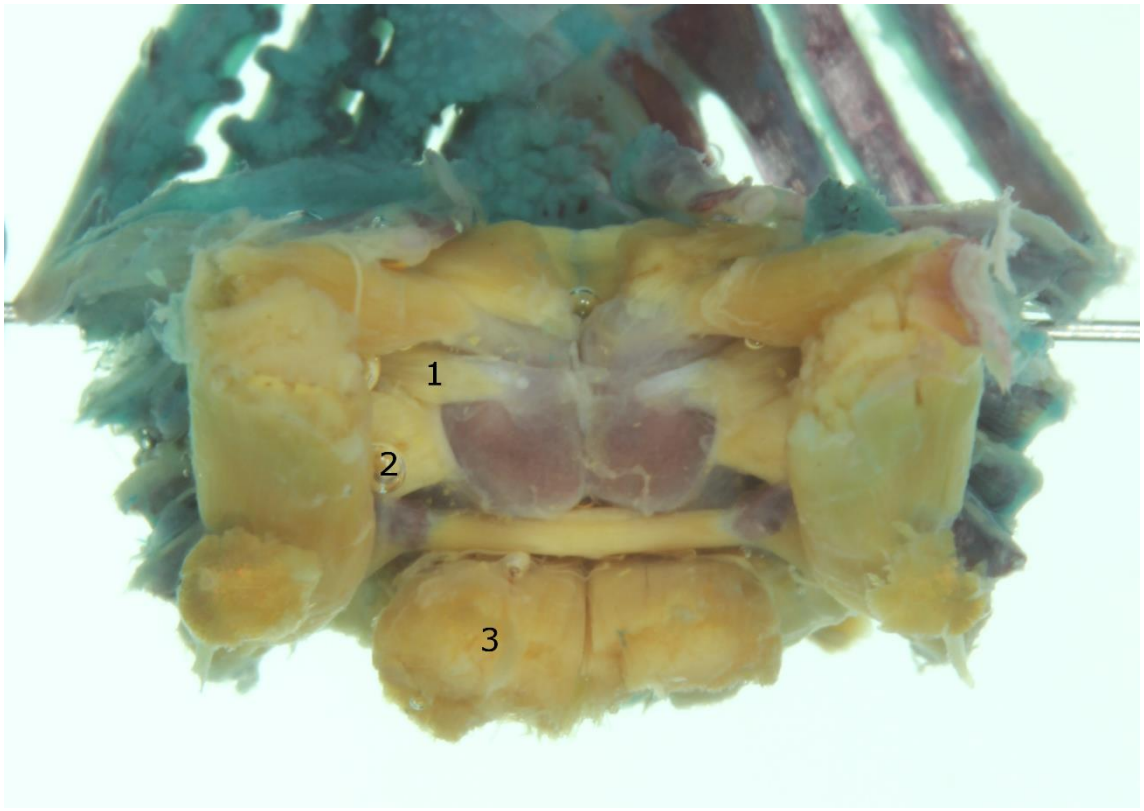

Fig. 26. Dorsal view of branchial basket and associated muscles of *Cichlasoma paranaense* (dissection stage 4A), evidencing the shape of (1) *transversus epibranchialis 2*, (2) *obliquus dorsalis 3–4* and (3) *retractor dorsalis*. *Levator internus 5* pulled aside.

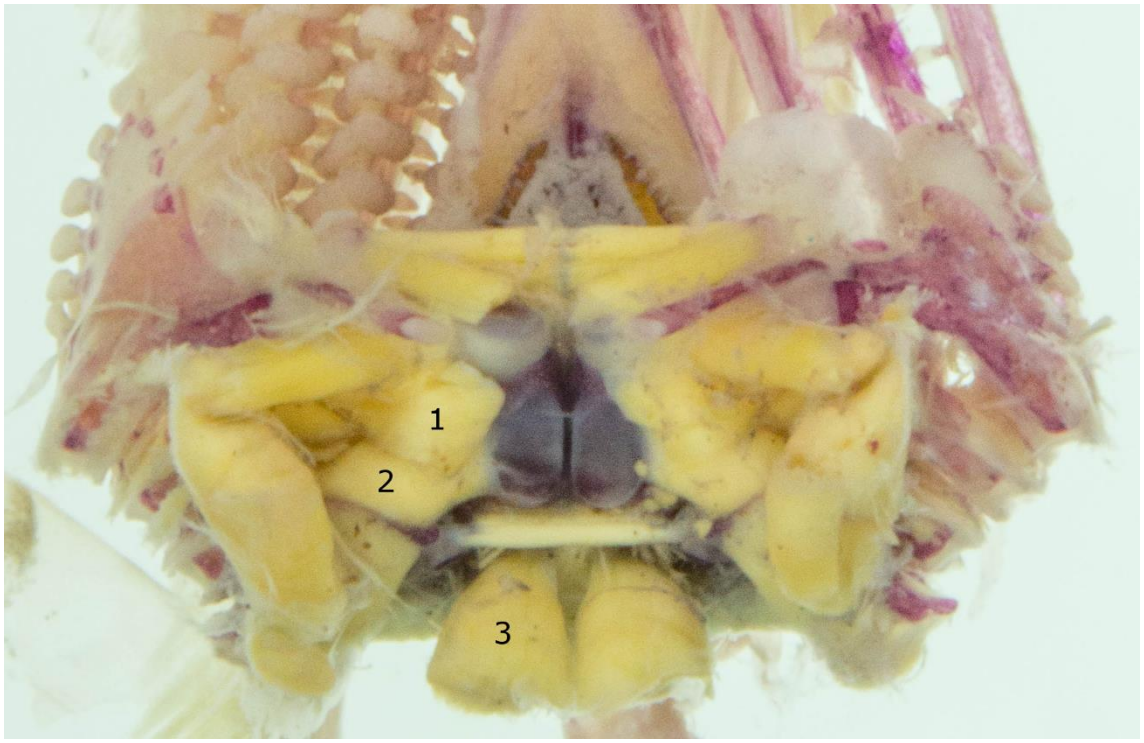

Fig. 27. Dorsal view of branchial basket and associated muscles of *Satanoperca* sp. (dissection stage 4A), evidencing the shape of (1) *transversus epibranchialis 2*, (2) *obliquus dorsalis 3–4* and (3) *retractor dorsalis*. *Levator internus 5* pulled aside.

Fig 28. Dorsal view of branchial basket and associated muscles of *Chaetobranchopsis australis* (dissection stage 4A), evidencing the thin, separate *retractores dorsales* (dashed lines; character 59[0]).

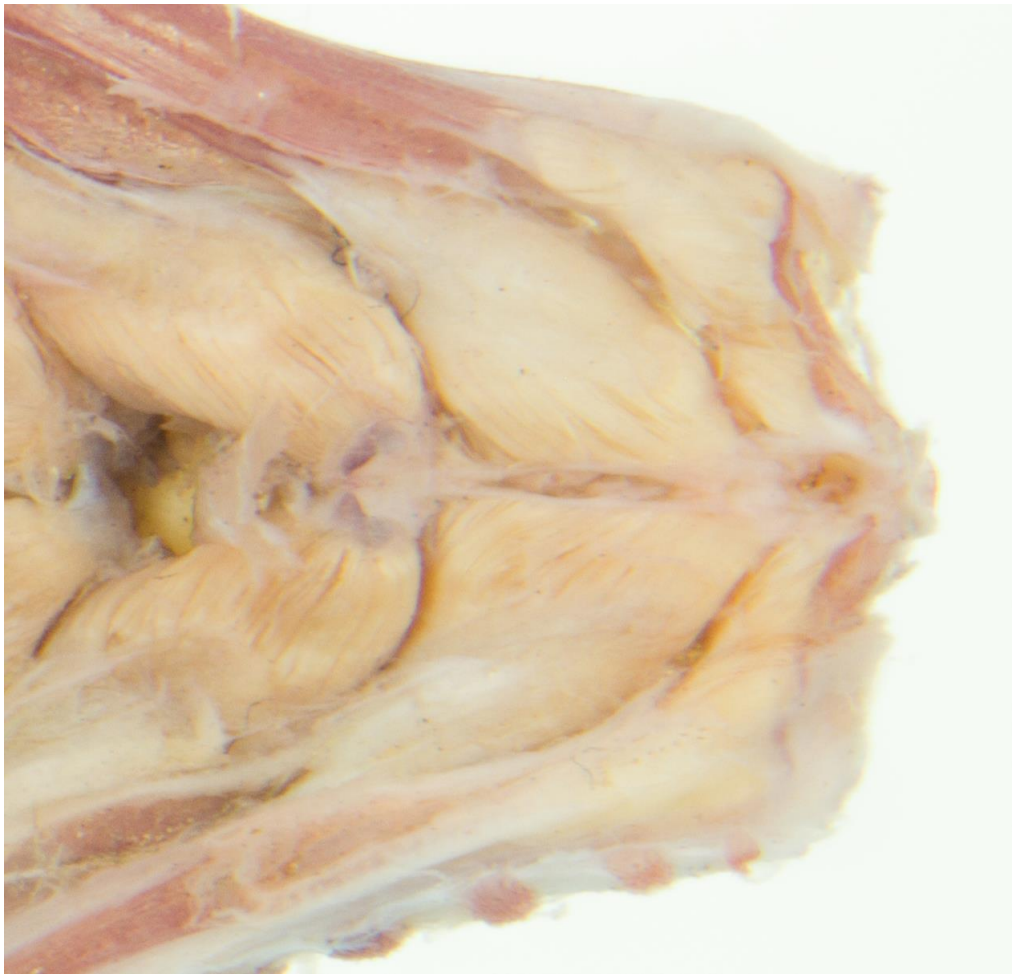

Fig. 29. Ventral view of branchial basket and associated muscles of *Astronotus crassipinnis* (dissection stage 4A).

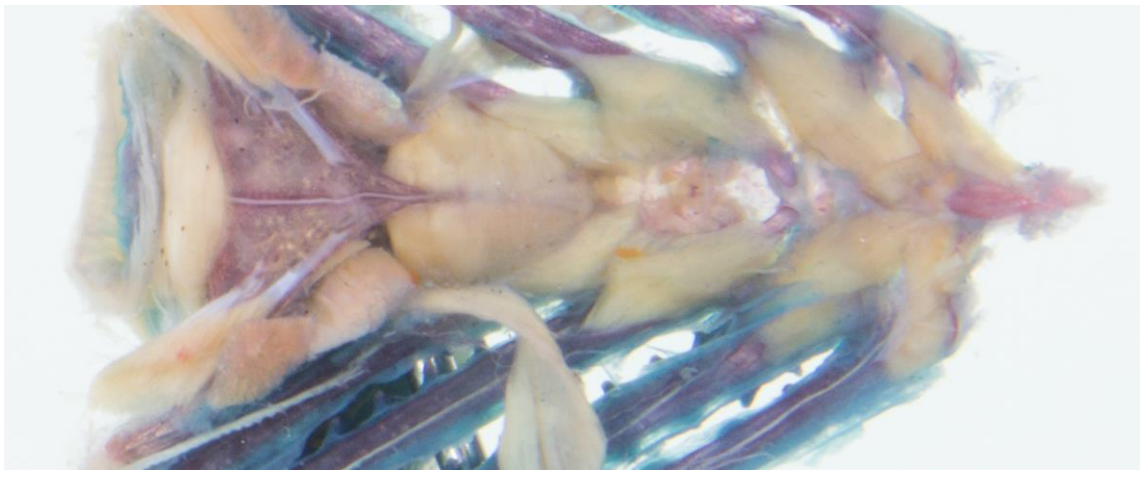

Fig. 30. Ventral view of branchial basket and associated muscles of *Bujurquina vittata* (dissection stage 4A). *Rectus communis* pulled aside.

Fig. 31. Ventral view of branchial basket and associated muscles of *Retroculus acherontos* (dissection stage 4A). *Rectus communis* pulled aside.

Fig. 32. Ventral view of branchial basket and associated muscles of *Gymnogeophagus balzanii* (dissection stage 4A).

Fig. 33. Ventral view of branchial basket and associated muscles of *Satanoperca* sp. (dissection stage 4A).

Fig. 34. Lateral view of the head of *Guianacara dacrya* (dissection stage 3), evidencing the proximity between *protractor pectoralis* and *pharyngoclavicularis internus*.

Fig. 35. Lateral view of the head of *Cichlasoma paranaense* (dissection stage 3), evidencing the wide distance between *protractor pectoralis* and *pharyngoclavicularis internus*.

Fig. 36. Lateral view of the head of *Teleocichla proselytus* (dissection stage 3), evidencing the relative position of the *sternohyoideus* and *pharyngoclaviculares*.

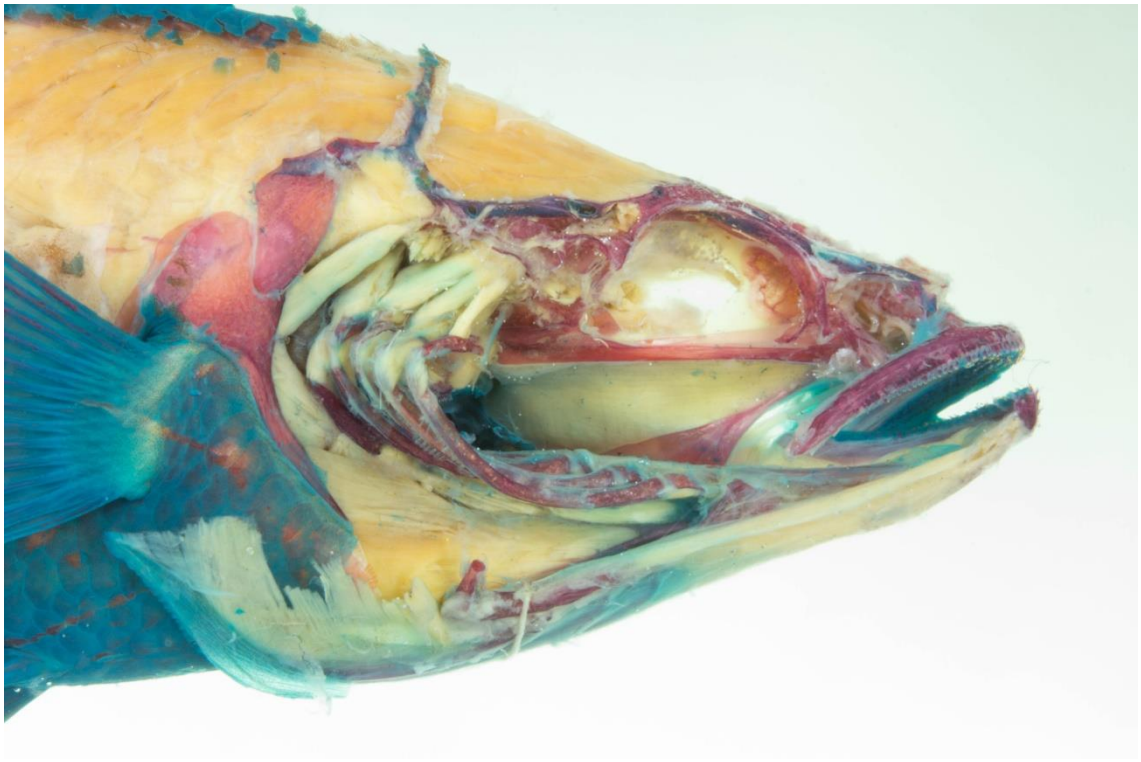

Fig. 37. Lateral view of the head of *Crenicichla britskii* (dissection stage 3), evidencing the relative position of the *sternohyoideus* and *pharyngoclaviculares*.

Fig. 38. Lateral view of the head of *Satanoperca* sp. (dissection stage 3), evidencing the relative position of the *sternohyoideus* and *pharyngoclaviculares*.

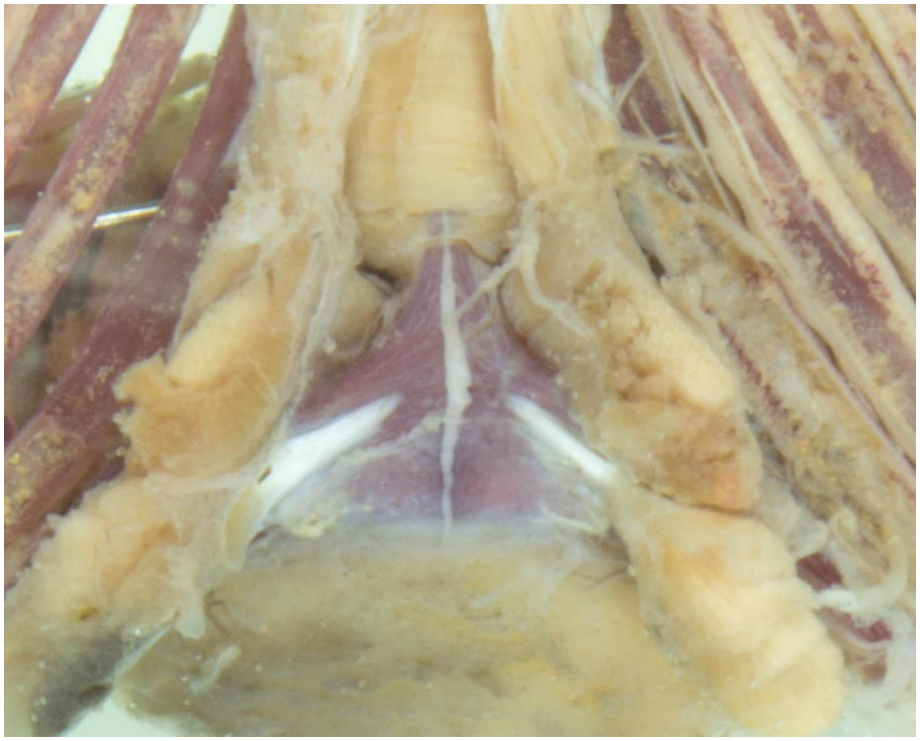

Fig. 39. Ventral view of branchial basket and associated muscles of *Astronotus crassipinnis* (dissection stage 4A), evidencing the more posterior insertion of the *pharyngoclavicularis internus* tendon.

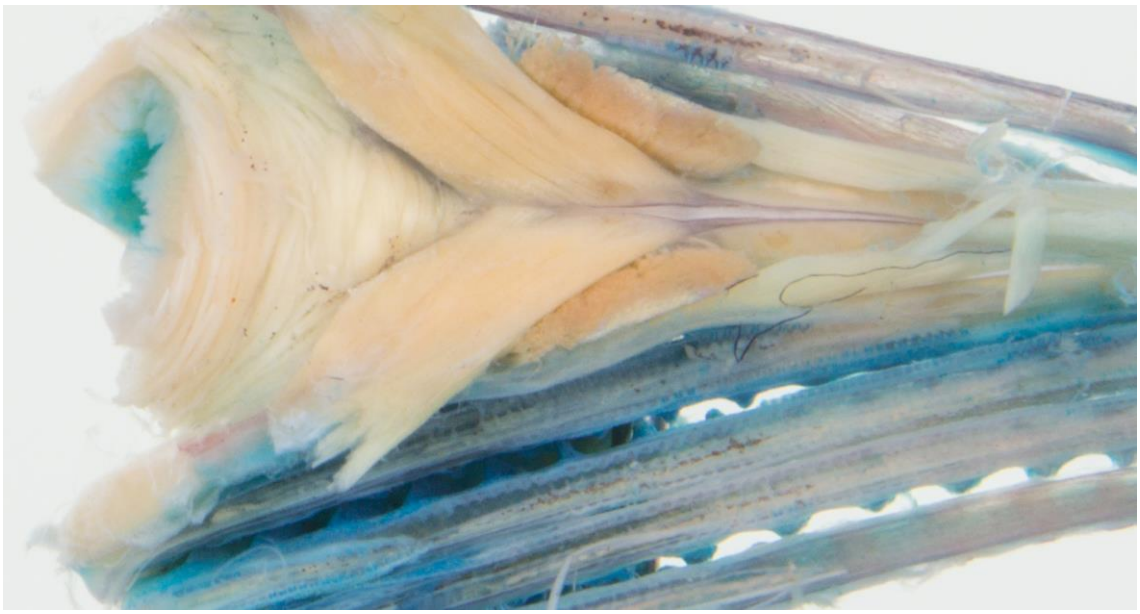

Fig. 40. Ventral view of branchial basket and associated muscles of *Cichla kelberi* (dissection stage 4A), evidencing shape and insertion site of the *pharyngoclavicularis internus*.

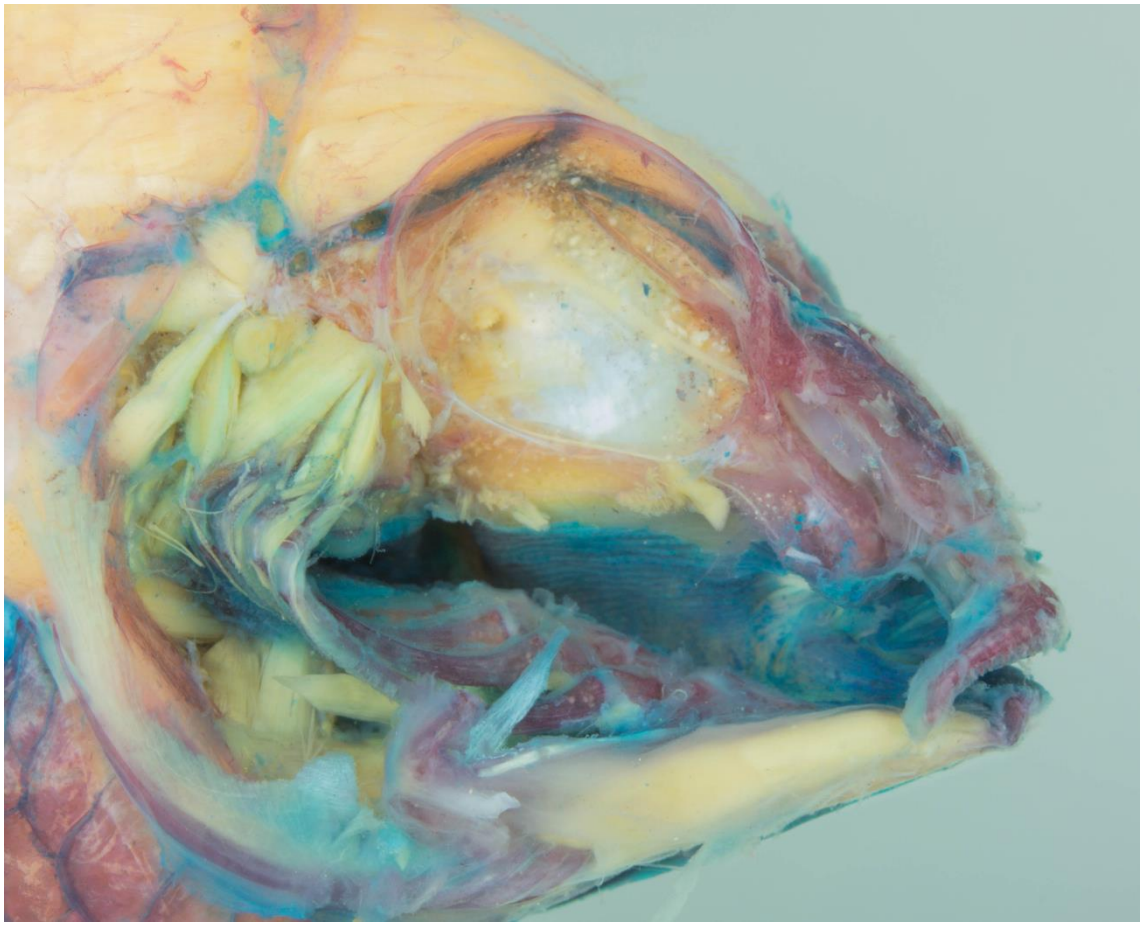

Fig. 41. Lateral view of the head of *Bujurquina vittata* (dissection stage 3), evidencing the gap between the distal portions of *levator pectoralis* and *protractor pectoralis*.

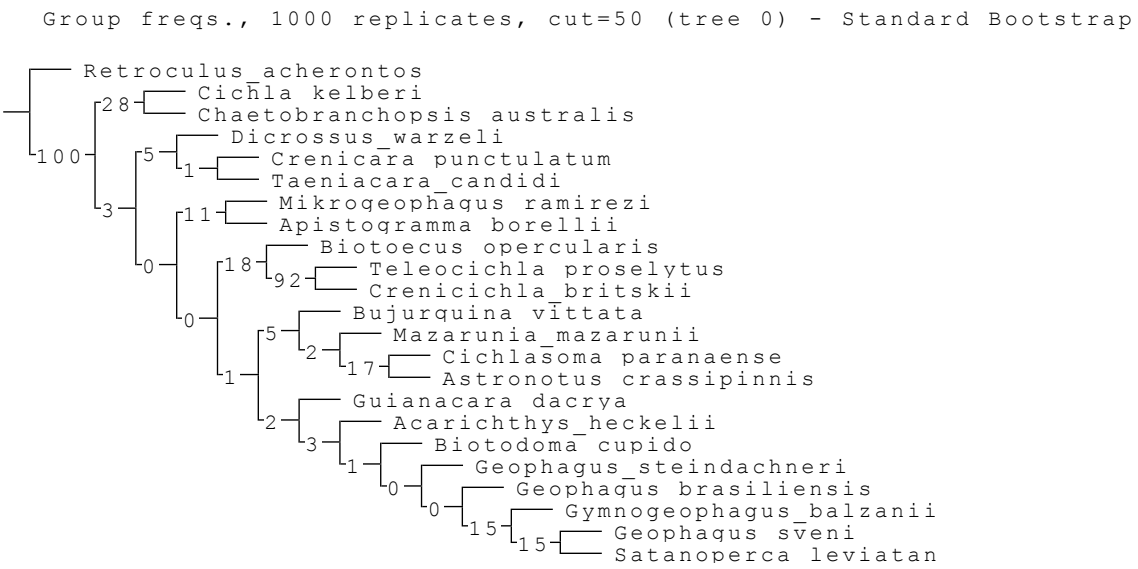

Fig. 42. Tree resulting from the unconstrained, unweighted analysis. Numbers at the base of branches represent bootstrap values.

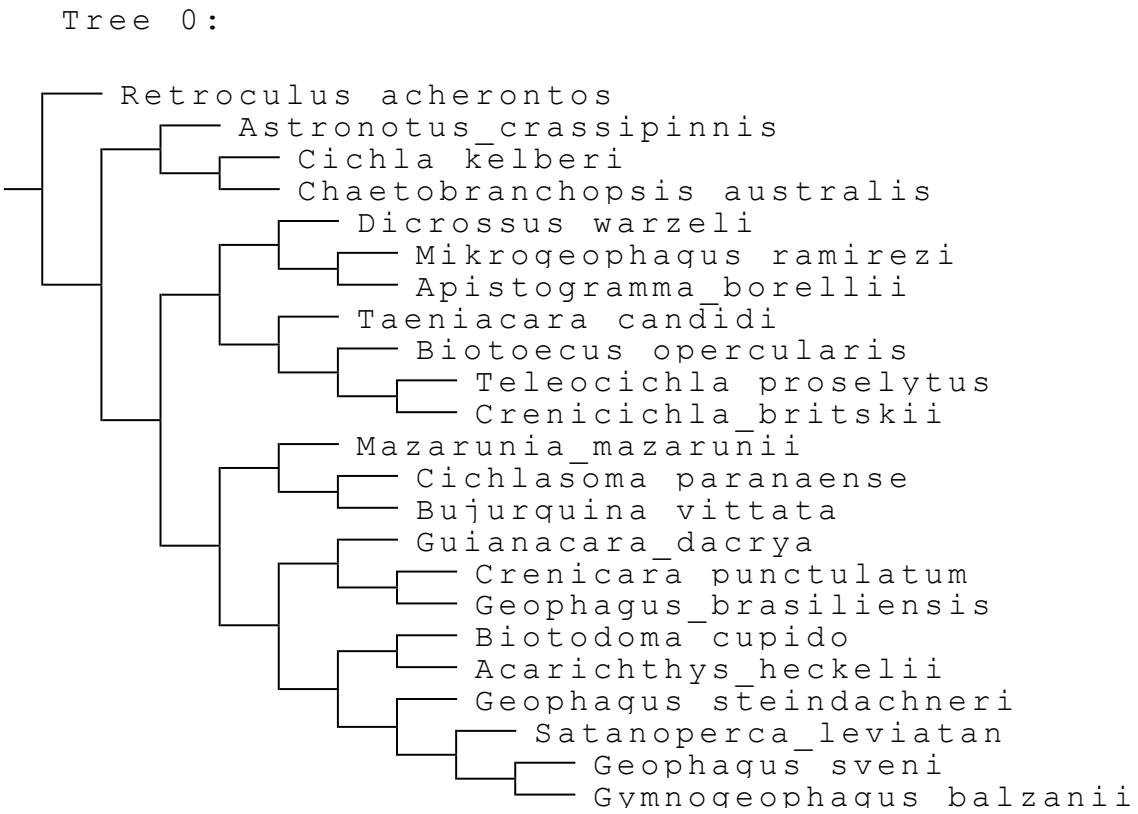

Fig. 43. Tree resulting from the unconstrained, weighted analysis.

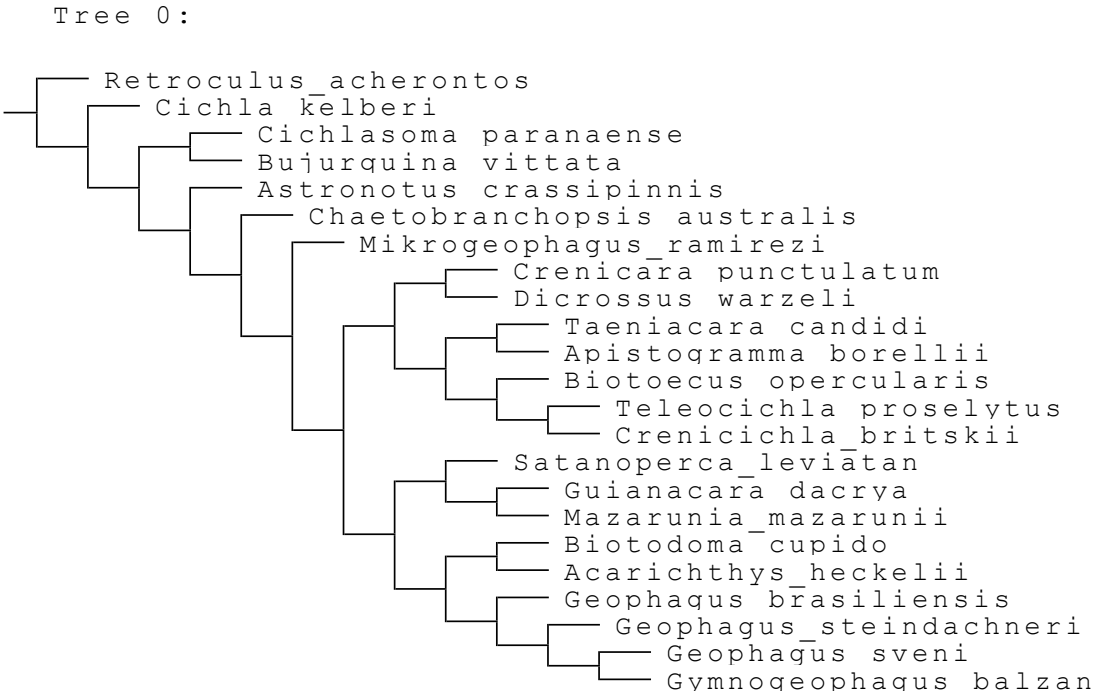

Fig. 44. Tree resulting from the constrained, weighted analysis.

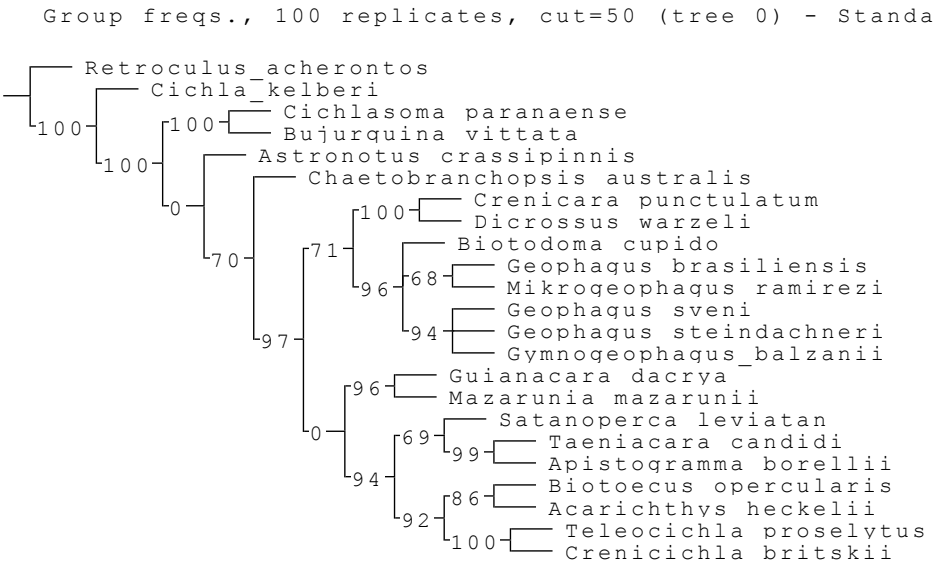

Fig. 45. Tree resulting from the constrained, unweighted analysis. Numbers at the base of branches represent bootstrap values.

SUPPLEMENTARY MATERIAL CAPTIONS

Supplementary File 1. List of material examined.

Supplementary File 2. TNT file containing the script for the unconstrained, unweighted analysis.

Supplementary File 3. TNT file containing the script for the unconstrained, weighted analysis.

Supplementary File 4. TNT file containing the script for character mapping.

Supplementary File 5. Document containing character mapping cladograms for all of the characters analysed herein.

Supplementary File 6. TNT file containing the script for the constrained, unweighted analysis.

Supplementary File 7. TNT file containing the script for the constrained, weighted analysis.

Supplementary File 8. Spreadsheet containing the character matrix.

SUPPLEMENTARY FILE 1

Geophagini

Acarichthys heckelii. NUP 4892, 2 ex.
Apistogramma borellii. NUP 4267, 2 ex.
Biotodoma cupido. NUP 13014, 1 ex.
Biotoecus opercularis. UFRO-I 6070, 1 ex.
Crenicara punctulatum. UFRO-I 12763, 1 ex.
Crenicichla britskii. NUP 7953, 2 ex.
Dicrossus warzeli. MZUSP 25423, 1 ex.
"*Geophagus*" *brasiliensis*. NUP 3717, 2 ex.
"*Geophagus*" *steindachneri*. LBP 18635, 1 ex.
Geophagus sveni. NUP uncatalogued, 1 ex.
Guianacara dacrya. ROM 96095, 2ex.
Gymnogeophagus balzanii. NUP 3035, 1 ex.
Mazarunia mazarunii. ROM 89586, 2 ex.
Mikrogeophagus ramirezi. MZUSP 96547, 1 ex.
Satanoperca sp. NUP 13017, 1 ex.
Taeniacara candidi. UFRO-I 20710, 1 ex.
Teleocichla proselytus. MZUSP 22017, 1 ex.

Astronotini

Astronotus crassipinnis. NUP 1464, 1 ex.

Chaetobranchini

Chaetobranchopsis australis. NUP 209, 1 ex.

Cichlasomatini

Bujurquina vittata. NUP 179, 2 ex.
Cichlasoma paranaense. NUP 1936, 2 ex.

Cichlini

Cichla kelberi. NUP 628, 1 ex.

Retroculini

Retroculus acherontos. NUP uncatalogued, 1 ex.

SUPPLEMENTARY FILE 8

	0	1	2	3	4	5	6	7	8	9	10	11	12	13	14	15	16	17	18	19	20	21	22	23	24	25	26	27	28	29	30	31	32	33	34	35	36	37	38	39	40
Crenicichla_britskii@Cichlinae	0	3	1	0	1	1	0	1	1	1	4	3	2	0	0	3	0	0	3	1	0	3	1	0	0	0	2	0	4	2	1	1	1	1	0	0	2	0	1	0	0
Teleocichla_proselytus@Cichli	5	3	0	0	3	6	0	1	1	1	4	4	2	0	0	7	0	0	2	0	0	3	1	0	0	0	3	0	4	2	1	1	1	1	0	-	0	0	0	0	0
Acarichthys_heckelii@Cichlinae	2	0	1	1	0	0	0	0	0	0	2	2	0	2	0	4	0	0	2	0	0	0	0	1	1	2	0	0	4	1	1	2	0	2	1	0	0	0	0	0	2
Biotoecus_opercularis@Cichli	0	0	2	0	0	1	0	1	0	0	1	3	0	0	0	0	0	0	0	0	1	2	1	1	1	1	3	0	0	0	1	?	1	1	1	0	1	0	0	0	0
Apistogramma_borellii@Cichl	1	2	1	0	3	3	0	1	0	1	2	3	0	0	0	6	1	0	2	0	1	0	1	1	1	1	0	0	4	2	1	1	2	1	0	0	0	1	1	0	0
Taeniacara_candidi@Cichlinae	0	2	1	0	2	1	2	1	0	0	3	3	0	0	0	3	0	0	0	0	0	0	1	0	1	1	0	0	0	1	0	2	?	?	1	0	1	1	1	0	1
Satanoperca_sp.@Cichlinae_c	4	6	1	2	0	5	1	2	0	0	2	0	0	1	0	1	0	1	1	0	1	0	0	1	1	2	0	0	3	2	0	2	1	2	[01]	0	0	0	0	0	1
Mazarunia_mazarunii@Cichli	1	1	2	2	0	3	0	0	0	0	1	3	1	0	0	0	0	0	1	0	0	0	0	1	1	2	1	0	4	1	1	0	1	2	3	0	1	0	0	0	1
Guianacara_dacrya@Cichlinae	2	1	1	1	0	3	0	0	0	0	2	2	0	2	0	4	0	0	1	0	1	0	0	1	1	2	0	0	4	1	2	0	1	0	1	0	1	0	0	0	1
Gymnogeophagus_balzanii@	3	6	1	2	0	0	0	0	0	0	1	1	0	1	0	8	0	0	1	0	0	0	0	1	1	2	0	0	0	1	0	0	1	2	2	0	0	0	0	0	1
Geophagus_steindachneri@Ci	2	0	1	1	0	3	2	0	1	0	2	2	1	1	0	8	0	0	1	0	0	0	0	1	1	1	3	0	4	2	0	2	1	2	1	0	0	0	1	0	2
*Geophagus_sveni@Cichlinae_*	3	6	1	2	0	0	0	0	0	0	2	1	0	1	0	5	0	0	1	0	1	0	0	1	1	2	0	0	4	1	0	0	0	0	2	0	0	0	0	0	2
Mikrogeophagus_ramirezi@C	1	6	1	0	0	3	0	0	0	0	0	3	0	0	0	2	1	0	2	0	1	0	0	1	1	1	0	0	4	1	0	?	2	2	2	0	1	0	1	0	1
Geophagus_brasiliensis@Cich	0	0	1	1	0	2	0	0	0	0	2	2	0	0	0	8	0	0	1	0	0	0	0	1	1	2	1	0	4	1	0	0	1	1	1	0	1	0	1	0	2
Biotodoma_cupido@Cichlinae	2	0	1	2	0	0	0	0	0	0	1	2	0	0	0	4	0	0	1	0	1	0	0	0	1	2	0	0	4	1	1	2	1	1	0	0	0	1	0	0	2
*Dicrossus_warzeli@Cichlinae_*	0	0	1	0	0	2	2	0	0	0	1	3	1	0	0	5	0	0	2	0	0	0	0	1	1	1	0	0	2	2	1	?	2	?	3	0	0	1	1	0	1
Crenicara_punctulatum@Cich	2	0	1	1	0	2	2	1	0	0	1	2	0	0	0	4	0	0	2	0	0	0	0	1	1	1	0	0	4	1	0	?	0	1	3	0	1	1	0	0	0
Chaetobranchopsis_australis@	0	5	2	0	0	4	2	1	1	1	0	3	0	0	0	9	1	0	2	0	1	3	0	1	1	1	5	2	0	0	2	1	1	?	0	1	0	1	0	0	3
Astronotus_crassipinnis@Cich	0	4	2	0	2	2	2	1	0	1	1	3	1	0	0	3	0	0	1	0	0	1	0	1	1	1	0	1	4	2	2	0	1	2	2	0	1	0	0	0	1
Bujurquina_vittata@Cichlinae	0	1	1	1	0	3	0	0	0	0	2	3	1	0	0	2	0	0	1	0	0	0	1	1	1	1	1	1	4	1	3	?	2	0	3	0	0	1	0	0	1
Cichlasoma_paranaense@Cici	0	0	2	0	0	0	0	0	0	0	1	3	1	0	0	8	0	0	1	0	0	0	0	0	1	1	1	1	5	2	2	?	1	2	3	0	1	1	0	0	1
Retroculus_acherontos@Cichli	0	7	3	0	0	3	2	0	0	0	2	3	0	0	1	0	0	0	0	0	0	3	0	1	1	1	0	0	1	2	0	0	2	?	0	0	0	0	0	0	0
Cichla_kelberi@Cichlinae_cla	0	4	3	0	0	1	2	1	0	0	2	2	2	0	0	0	0	0	0	4	1	0	3	0	1	0	1	0	0	1	2	0	?	1	1	0	2	1	0	0	1	1

41	42	43	44	45	46	47	48	49	50	51	52	53	54	55	56	57	58	59	60	61	62	63	64	65	66	67	68	69	70	71	72	73	74	75	76	77	78	79	80	81	82	83	84	85	86	87	88	89	90	91	92	93	94	95	96	97
1	0	2	0	0	0	1	1	0	1	1	0	0	1	2	0	0	0	1	1	0	1	2	0	0	0	3	0	2	0	1	1	0	2	1	0	0	2	1	2	0	0	0	0	1	1	[12]	2	0	1	0	1	1	0	0	2	0
2	0	2	1	1	1	0	1	0	2	1	0	1	0	3	0	0	0	1	0	2	0	2	0	0	0	3	0	2	0	3	2	0	3	2	2	0	2	1	3	0	2	0	0	1	0	2	3	0	1	3	0	1	1	2	0	0
0	1	0	1	0	0	0	0	0	0	1	1	1	1	1	1	0	0	1	1	2	?	1	1	0	0	0	0	2	0	0	3	0	1	1	2	0	2	0	2	0	0	1	0	3	3	1	0	0	0	2	0	0	0	0	2	2
0	1	2	-	-	-	-	-	0	1	1	0	1	0	3	0	0	0	1	1	?	?	?	?	?	?	0	0	2	0	0	1	0	2	1	1	0	1	1	1	0	2	0	0	3	3	0	2	0	0	2	0	1	0	0	1	2
0	1	0	2	0	0	1	-	1	0	0	1	1	1	3	0	0	0	1	1	1	-	-	-	0	0	0	0	2	0	0	1	0	0	1	1	0	2	0	1	0	0	0	0	1	3	0	0	0	0	2	0	1	1	0	2	-
2	1	1	-	-	-	-	-	1	1	2	1	1	1	1	0	0	0	1	1	?	?	?	?	?	?	?	0	2	0	0	1	0	0	1	?	0	2	1	2	0	0	0	0	2	3	2	3	0	0	2	0	1	1	0	0	0
0	1	1	0	0	0	0	-	1	0	0	1	1	0	3	0	0	0	1	0	0	2	1	1	0	1	0	0	3	0	0	1	0	1	1	0	0	0	0	0	0	1	1	0	3	2	0	0	0	0	1	0	0	0	0	0	1
1	1	1	0	0	1	0	0	1	0	1	1	1	1	0	?	?	0	1	1	2	?	?	1	0	2	0	0	2	0	0	3	0	1	4	1	0	2	0	3	0	0	0	0	1	3	0	2	0	0	1	0	0	1	0	0	0	0
1	1	1	0	0	0	0	0	0	1	1	1	1	1	0	1	0	0	1	1	0	0	0	1	0	1	0	0	4	0	0	3	0	1	4	1	0	2	1	2	0	0	0	0	1	2	2	3	0	0	2	1	0	0	0	0	0
0	1	0	0	0	0	0	0	2	0	2	1	1	3	1	0	0	1	0	0	0	0	0	0	1	0	0	0	2	0	0	0	0	0	3	1	0	1	0	1	0	0	1	0	3	2	0	0	0	0	1	0	0	0	0	1	2
0	1	0	0	0	0	0	0	1	1	2	1	1	2	1	1	0	0	1	0	0	0	0	0	1	0	0	0	2	0	0	0	0	0	1	1	1	0	2	0	2	0	0	1	0	1	2	1	0	0	0	2	0	0	0	0	2
0	1	1	0	0	0	-	0	2	1	2	1	1	1	1	1	0	0	1	0	0	0	0	0	0	2	0	0	0	0	0	0	0	0	0	0	0	0	0	1	0	0	1	0	3	3	1	0	0	0	1	0	0	0	0	0	1
0	1	2	-	-	-	-	-	1	0	1	1	1	1	3	1	0	0	1	0	?	?	?	?	?	0	0	0	2	0	0	0	0	0	3	?	0	0	0	1	0	0	1	0	1	3	0	2	0	0	2	0	0	1	1	2	2
1	1	1	0	0	0	0	0	0	2	0	0	1	1	1	1	0	0	1	0	0	0	0	0	1	0	0	0	2	0	0	3	0	0	4	1	0	0	0	2	0	0	1	0	3	3	0	0	0	0	2	0	0	0	0	0	2
0	1	0	0	0	0	0	0	1	0	1	1	1	?	3	1	0	0	1	0	0	0	0	0	0	0	0	0	4	0	0	3	0	1	1	1	0	1	0	2	0	0	1	0	3	3	0	0	0	0	1	0	0	0	1	0	2
?	1	2	0	0	0	0	1	1	1	3	1	1	0	1	0	0	0	1	1	1	-	-	-	0	?	0	0	5	0	0	1	0	0	1	0	0	2	1	3	0	0	0	0	3	3	2	3	0	0	2	[01]	0	1	0	2	0
0	1	1	-	-	-	-	-	1	0	0	1	3	0	1	0	1	0	1	1	1	-	-	-	0	0	0	0	2	0	0	3	0	0	4	0	0	1	1	2	0	0	?	0	3	3	1	3	0	0	1	1	0	0	0	2	2
0	1	1	2	0	1	1	0	0	1	2	1	4	0	4	0	1	0	0	0	0	3	0	?	?	0	1	1	1	0	1	4	1	4	5	1	0	0	0	5	2	2	1	1	1	2	3	3	0	0	1	0	0	0	0	2	2
?	1	0	0	0	0	0	0	0	1	1	1	2	1	1	0	0	2	1	1	0	0	1	0	0	0	1	0	1	1	1	5	0	1	1	1	0	2	0	3	0	0	1	0	1	0	2	0	0	2	1	0	0	2	0	0
0	1	0	1	0	0	0	0	0	1	1	1	3	1	3	0	0	1	1	1	1	0	1	0	1	2	0	0	2	2	0	3	0	1	1	1	0	2	0	2	0	0	0	0	3	3	0	0	0	0	1	1	0	0	0	0	0
1	1	0	1	0	1	1	0	1	1	2	2	3	1	0	0	0	0	1	1	1	-	-	-	1	0	2	0	2	0	2	1	0	1	1	1	1	0	2	1	2	0	0	0	0	1	3	0	0	0	0	1	0	0	1	2	0	0
0	2	2	1	1	1	1	0	0	1	0	1	1	2	3	0	1	0	1	1	1	-	-	-	0	0	1	0	1	0	1	1	0	1	1	1	1	0	0	4	1	0	1	0	3	0	2	3	1	1	1	0	1	0	2	2	0